Validation of the Numerical Wave Models SWAN and HISWA at Norderney

Caroline Gautier
July 1996

TU Delft
Technische Universiteit Delft

Faculty of Civil Engineering
Section Fluid Mechanics

Coastal Research Station
Norderney, Germany

Section Fluid Mechanics
Faculty of Civil Engineering
Delft University of Technology
The Netherlands

Coastal Research Station
of the Lower Saxonian
State Board for Ecology
Norderney, Germany

Validation of the Numerical Wave Models SWAN and HISWA at Norderney

Master Thesis by: Caroline Gautier

Supervisors: Prof. dr. ir. J.A. Battjes
Dr. ir. L.H. Holthuijsen
Dipl.-Ing. R. Kaiser

July 1996

Preface

This report is my master thesis for graduating at Delft University of Technology, faculty of Civil Engineering, section Fluid Mechanics. Part of the work I did in Germany at the Coastal Research Station Norderney, part of it at Delft University.

Many people I owe thanks; First of all my supervisors prof. dr. ir. J.A. Battjes and dr. ir. L.H. Holthuijsen of Delft University, and Dipl.-Ing. Ralf Kaiser of the Coastal Research Station. The Coastal Research Station offered me good facilities to carry out my research, which I am very grateful for. Although no supervisors, but of great help were also SWAN-experts ir. Roeland Ris and dr. ir. N. Booij. Without the help and computer advises of Detlef, Bas and Azarja I would never have been able to produce this report. Finally I would like to thank my friends, especially Frank, for the support they gave me during my study.

Caroline Gautier
Delft, July 1996

Abstract

In coastal engineering waves often play a dominant role. To predict the wave behaviour in coastal regions numerical wave propagation models have been developed. This study deals with the verification of two models against measurements in the field, namely HISWA and SWAN. The second generation model HISWA has already proven to perform well for both engineering and research purposes. The third generation model SWAN is a new model, still under development. Also made by Delft University of Technology, SWAN is more or less the improved sequel to HISWA.

Both models are based on the action density balance, which is made stationary to reduce the required computer capacity. They simulate wave growth and decay accounting for wind input, bottom friction, depth limited wave breaking, and whitecapping. The main differences between the models are the fact that SWAN is spectral both in frequencies and in directions, whilst in HISWA the frequencies are parametric. Secondly, the numerical scheme in SWAN for the wave propagation is unconditionally stable and encompasses waves from all directions (360°). In HISWA the directional sector wherein wave propagation is considered is limited to a maximum of 120° to obtain stability. Furthermore - being third generation - SWAN allows the spectrum to develop without any a priori constraints.

During the measuring campaign, which was carried out by the Coastal Research Station Norderney, in the winter of 1995-1996, nine Waverider buoys recorded wave data. These buoys were located in the Norderneyer Seegat, a Wadden Sea area.

Two cases have been simulated with SWAN and HISWA: one during high tide and one during low tide. I varied several parameters to examine the influence on the wave heights. These variations concern wind input formulation, wind speed, nonlinear wave wave interactions, friction, breaking, whitecapping, water level and incoming wave height. With reference to these research runs a set of input parameters is composed with which the models perform best in the area of this research.

Both models turn out to have a good performance indicator (>90%). It has been found that the wave heights are to a large extent determined by the wind and by breaking. The wave height of the incoming wave at the seaward boundary of the computational domain is of minor importance. In equal circumstances, SWAN tends to calculate higher wave heights than HISWA. It appeared from this study that SWAN performs slightly better than HISWA and is therefore a suitable tool for wave prediction in a Wadden Sea area.

Table of Contents

Chapter 1

Introduction

...in which the scope of the study is presented. Furthermore this first chapter deals with wind waves and wave models in general to supply the reader with some background information.

In coastal engineering waves often play a dominant role. To predict the wave behaviour in coastal regions numerical wave propagation models have been developed. This study deals with the validation of two models against measurements in the field, namely HISWA and SWAN. HISWA has already proven to perform well for both engineering and research purposes (Vogel *et al*, 1988). SWAN is a new model, still under development. Made by the same institute, SWAN is more or less the improved sequel to HISWA.

In this first chapter I will give the scope of the study, including the objective and my work approach. Also I will provide the reader with some background information on wind waves and wave models.

§ 1.1 Scope of the Study

During the last years HISWA has generated useful results in wave hindcasting (den Adel *et al.*, 1990 and Niemeyer *et al.*, 1992). Still, not in all situations the results were satisfying. For instance, a situation where swell and local wind waves are present, coming from different directions, cannot be simulated properly with HISWA. In such a case better results are expected from SWAN, because of - among other things - SWAN's ability to take wave energy coming from all directions into account. Although the implementation of SWAN has not been finished

yet, it survived many tests, both in laboratories and in the "field"(Ris *et al.* (1994) and Otta *et al.* (1995)). To get a reliable and complete picture of the performance of the model more test cases are always useful. This justifies this study. Before I come to the objective of the study, I'll give brief descriptions on SWAN, HISWA, and the area where the measuring took place. The measuring campaign lasted from November '95 till February '96.

§ 1.1.1 SWAN

The model SWAN (an acronym for simulation of waves in near shore areas) is a numerical model to obtain estimates of wave parameters in coastal areas, lakes and estuaries from given stationary wind-, bottom-, and current conditions. The model is based on the action balance equation (or energy balance in the absence of currents) with sources and sinks. The model simulates wave growth and decay, explicitly accounting for wind input, bottom friction, depth-limited wave breaking, and white capping. SWAN is fully spectral and it is a third generation model (no a priori spectral constraints). Wave propagation is not along wave rays but across a grid.

(source: SWAN user manual)

The computations are made with SWAN version 20.63.

§ 1.1.2 HISWA

HISWA (an acronym for hindcast shallow water waves) is a numerical wave model for coastal areas, lakes and estuaries. It uses stationary wind-, bottom-, and current conditions as input. HISWA is based on the notion of a spectral action balance. In HISWA the spectrum is discrete spectral only in the directions, it is parametric in the frequencies. HISWA computes the variation of the wave energy and the mean wave frequency by integrating the local effects of wind, bottom and currents while propagating with these quantities at the group velocity of the mean frequency across a grid. It's called a second generation model, because of its parametrized frequencies.

(source: HISWA user manual)

The computations are made with HISWA version 110.56.

§ 1.1.3 Measurement Area

The area where the measurements took place is situated around the "Norderneyer Seegat". This tidal channel lies between the East Frisian islands of Juist (westerly) and Norderney (easterly) in Germany, so partly in the North Sea and partly in the Wadden Sea (fig.1.1). On the northern side the Wadden Sea is sheltered by a chain of islands with deep channels between them. North of the inlets lie - more or less from one island to the other - sandbanks ("Riffbogen") on which most waves coming from the North Sea, break. This sandbank is not only a buffer for the exchange of sediment between North Sea and Wadden Sea, but also for the littoral east-west transport from one island to the other. South of the islands lies a complex system of gullies and flats that become partly dry during low tide. In the research area the gullies are branches from the Norderneyer Seegat and the Busetief. Coming from the North Sea and meeting the Wadden Sea, the

Norderneyer Seegat divides in several gullies and channels of which the Norderneyer Riffgat (to the east) is the deepest (±10m). Further away from the Seegat the gullies are smaller, and the flats bigger and higher. The Norderneyer Seegat has considerable influence on the wave direction. Offshore generated waves have therefore a rather uniform direction in the inlet which is more or less independent of their initial offshore propagation (Niemeyer, 1986). The bottom position is liable to changes. Not only does the morphology affect the waves, also the waves affect the morphology. So it is recommended to use a bottom file coming from recent measurements when using a wave model.

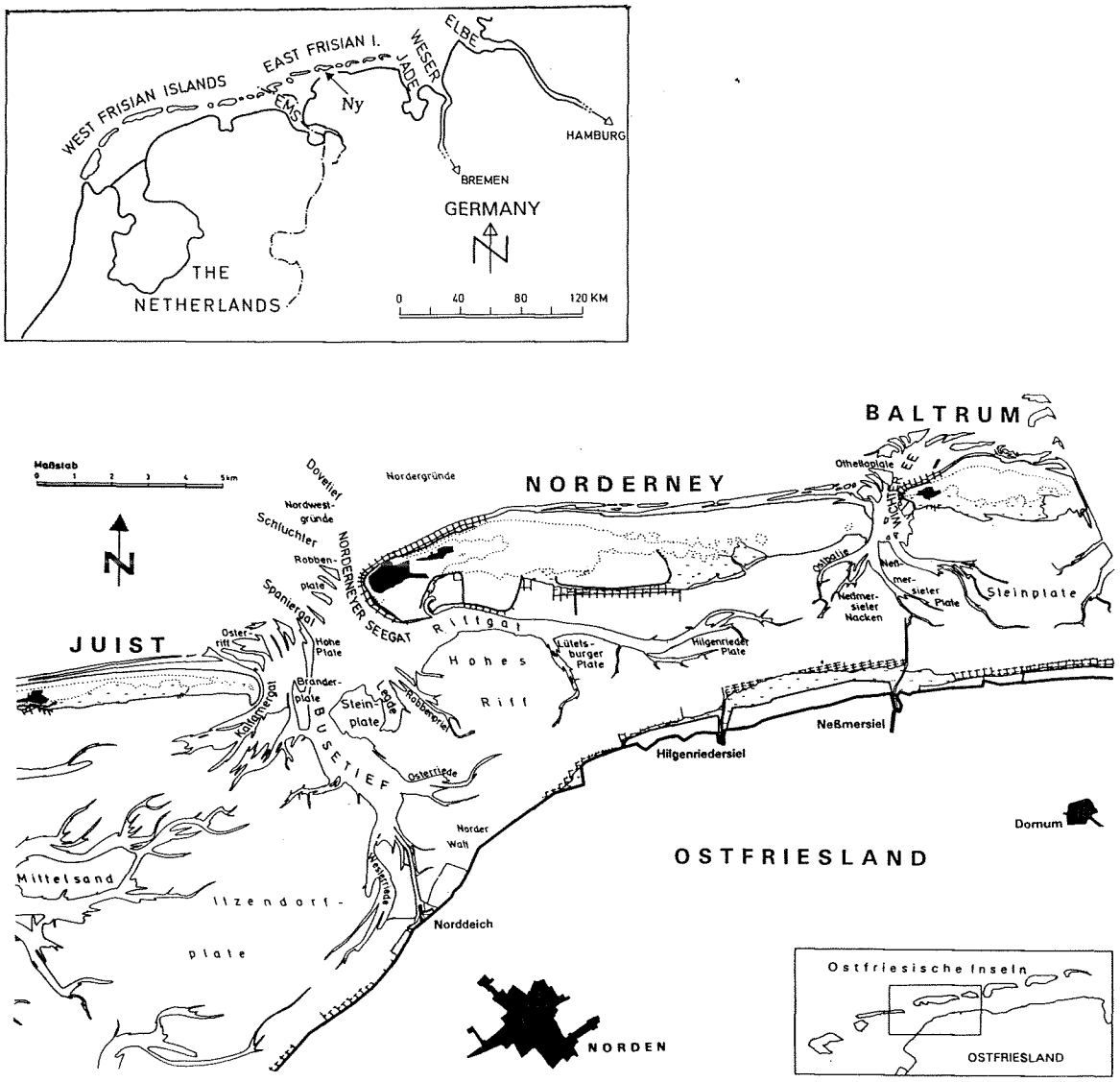

Fig. 1.1 measurement area (Ny in upper picture stands for Norderney)

§ 1.1.4 Objectives

The main objective of the study is to examine the applicability of the wave models SWAN and HISWA to a Wadden Sea area. This will be done by comparing the models results with each other and with field measurements which were carried out by the Coastal Research Station at Norderney. To meet this objective I formulate two sub-objectives:
- Determine the values of the input parameters with which the models function best in the research area.
- Examine the sensitivity of the models to the input parameters to find out how important it is to use the optimal values of the various input parameters.

Besides these objectives I would like to:
- Examine the performance of SWAN and HISWA against each other.
- Make proposals to extend and improve SWAN and HISWA, if necessary.

There is special interest in the wave prediction at the south coast of Norderney because there are plans for dike improvement there. It has to be stressed that value judgements concerning wave attack on the dike are beyond the scope of this study.

§ 1.1.5 Approach

During the winter of '95-'96 a measuring campaign took place around the Norderneyer Seegat, in which nine Waverider buoys recorded wave data. Two 'storm'events that occurred in November are simulated in SWAN and HISWA; one during high tide (case 1) and one during low tide (case 2).
By doing sensitivity tests on computational grid and frequency domain and by using default values where possible I came up with a standard run for each of the two research cases. On the basis of these standard runs I systematically changed one parameter each time. Within SWAN I examined the influence of:

- wind input formulation (1st, 2nd, 3rd generation)
- nonlinear interactions (quadruplets and triads)
- uniform wind versus variable wind, and change in wind speed
- friction
- breaking coefficient for shallow water (γ)
- white capping
- water level
- incoming wave

Within HISWA I examined the influence of:

- uniform wind versus variable wind, and change in wind speed
- friction
- shallow water breaking
- deep water breaking
- water level
- incoming wave

Both with SWAN and with HISWA approximately 16 runs were carried out for each of the two research cases (high tide and low tide). The output that is presented in this report consists of significant wave height and wave period at the buoy locations. Besides this SWAN produced spectral output. The one dimensional wave spectrum coming from SWAN for the position of each buoy and the observed spectrum are presented. For each research run I calculated the absolute error in significant wave height (Hs_{model} - $Hs_{observed}$) per buoy and for all buoys together (= overall absolute error). Also the relative error (=absolute error divided by observed wave height) is calculated for each buoy and for all buoys together. I judge the performance of the different research runs by the overall absolute error. The run with the smallest is considered best.Finally after comparing the models with the observations, SWAN and HISWA are compared with each other. The 'performance indicator' is used to give an objective judgement.
Fig. 1.2 shows the work approach in a scheme.

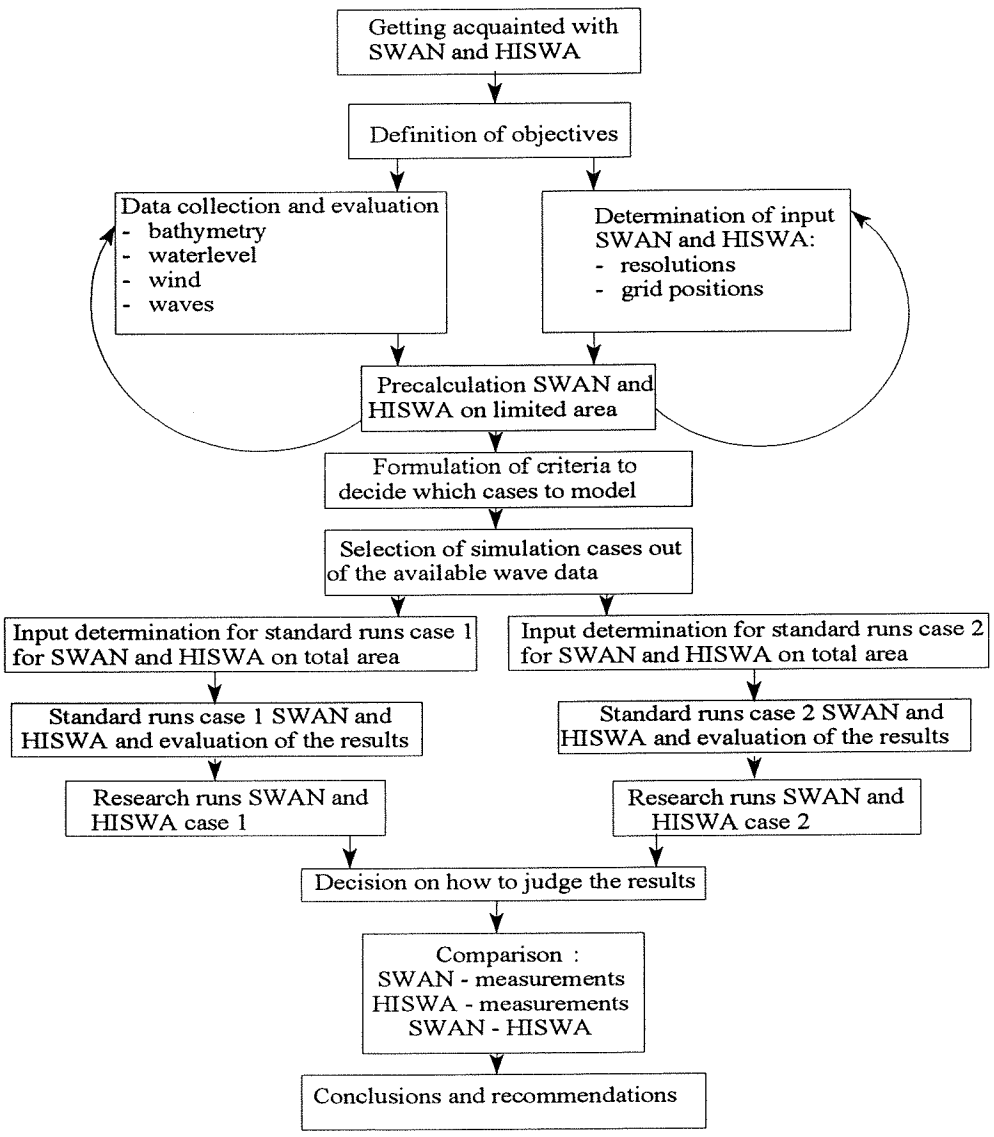

Fig. 1.2 approach scheme

§ 1.1.6 The Set Up of the Report

The set up for the rest of this report is as follows: In chapter 2 I will describe the wave models SWAN and HISWA. Chapter 3 deals with the data both for the model input and for the comparison material. Chapter 3 also lists the cases which are modelled. The actual calculations and their results from SWAN and HISWA for the high tide situation are subject of chapter 4, followed by remarks per research run. The same for the low tide situation can be found in chapter 5. In chapter 6 the models are compared with each other. In the last chapter I will give conclusions and recommendations. A schematized reproduction of the set up of the report follows now:

1.	INTRODUCTION	what do I examine? how did I examine it? some information on wind waves and wave models
2.	WAVE MODELLING	which tools do I use for the modelling? which things play an important role?
3.	DATA & TEST CASES	which data do I use? where do the data come from? which situations will I model?
4.	RESULTS CASE 1 (HIGH TIDE)	SWAN model input SWAN model output & analysis HISWA model input HISWA model output & analysis
5.	RESULTS CASE 2 (LOW TIDE)	SWAN model input SWAN model output & analysis HISWA model input HISWA model output & analysis
6.	COMPARISON SWAN and HISWA	what are the similarities and what are the differences between SWAN and HISWA and how come?
7.	CONCLUSIONS	what can be concluded from this study? how to improve the models and possible future studies?

§ 1.2 Wind Waves

The irregularly fluctuating sea surface in the presence of wind waves seems very difficult to catch in mathematical equations. Due to the turbulent character of the wind the surface never looks the same. A deterministic description is not suitable, but the wind waves can be described with the help of statistics, as a stochastic process.

Wave records representing a series of wave observations at a given point show a wide range of amplitudes, periods, and propagation directions. Harmonic analysis or Fourier analysis is frequently applied to such data to extract meaningful information. This is done by decomposing the time series into harmonic components, each having a particular frequency and amplitude. Harmonic analysis is based on the relationship between a time series (a wave record for instance) and the sum of harmonic component waves.

$$\eta(t) = \Sigma\ a_i \cos(2\pi f_i t + \alpha_i)$$

$\eta(t)$: the instantaneous surface elevation
a_i : the amplitude of the i^{th} cosine component
f_i : the frequency of the i^{th} cosine component
α_i : the phase of the i^{th} cosine component
t : time

Wave energy is proportional to wave amplitude squared, and the results of the time series analysis (wave amplitudes and frequencies) are generally expressed as an energy spectrum. A spectrum is a plot of spectral density $E(f_i)$, which is proportional to wave energy, and frequency. Under actual sea conditions waves are not long-crested and do not all travel in the same direction. For such two-dimensional or short-crested waves a more complicated time series analysis is required, that accounts for both time and space variations of wave elevations. The resulting directional spectrum distributes energy density across both frequency and direction of propagation. The total energy E in a given sea state is calculated by summing the contributions from each spectral component across all frequencies and directions (the volume under the 2D spectrum, or the area below the 1D spectrum).
It should be noted that the total spectral energy has the dimensions of length squared (L^2), because the constant ρg used in the definition of component energy E_i
Some main wave characteristics can easily be derived from the spectrum. They can be expressed in terms of moments of $E(f)$ denoted by m_n. The n^{th} moment of the spectrum is

$$m_n = \int_0^\infty f^n E(f) df \qquad n = 0,1,2,...$$

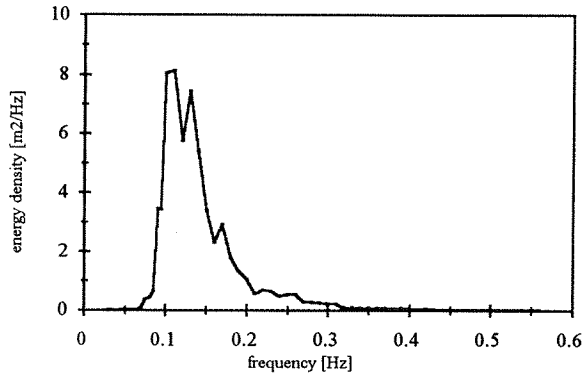

Fig. 1.3 one dimensional energy density spectrum

- The significant wave height $H_s = 4\sqrt{m_0}$
- The mean wave height $\mu_H = \sqrt{(2\pi m_0)}$
- The root mean square wave height $H_{rms} = 2\sqrt{(2m_0)}$

Also wave periods can be found from the spectrum.
- The 'zero-downcrossing wave period', that is the mean time interval between consecutive zero-down crossings is $T_0 = \sqrt{(m_0/m_2)}$.
- $T_{m01} = m_0/m_1$
- The peak period is the period at which the spectrum has its maximum energy: $T_p = 1/f_m$. (f_m is the frequency where the energy is maximum)

§ 1.3 Wave Models

The aim of using wave propagation models is to estimate near shore wave conditions from offshore available wave data, by considering the processes which might influence the waves. Mainly because the allied forces needed wave forecasts for landing operations in the second world war, the methods of wave prediction became to concentrate more on practical applicability since the 1940's. The first operational predictions were based on the work of Sverdrup and Munk (1946). On the basis of empirical data they expressed dimensionless wave parameters (wave height $\tilde{H} = gH/U^2$ and period $\tilde{T} = gT/U$) in terms of dimensionless wind parameters (fetch $\tilde{F} = gF/U^2$ and duration $\tilde{t} = gt/U$). Although their theory lacks thorough foundations the idea of expressing dimensionless wave parameters in wind parameters is still useful (for instance Young and Verhagen, 1996).

An important advance in the study after wind waves was the introduction of the energy density spectrum (Barber and Ursell (1948)), which did already have a function in electrical engineering and acoustics. Neumann (1953) indicated how the spectrum develops as a function of fetch or wind duration, and that the spectrum in fully developed wind sea has a standard form. Pierson, Neumann and James discovered that if this spectrum is cut off at the low frequency side it approximates the non full-grown sea. So dependent on wind velocity, fetch and duration the

spectrum could be predicted in a standard wind field. Several publications followed, of which Pierson's and Moscowitz' (1964) description of the spectrum on full-grown wind sea and the JONSWAP-spectrum of Hasselman *et al.* (1973) on growing wind sea are still very useful.

The above mentioned prediction methods are useful for a standard wind field. Considering the sea surface as the superposition of many independent wave components, the prediction can also be made for all the components separately. For a standard wind field this is not necessary because it is easy enough just to use some parameter relations. In the case of a wind field that varies in time and place, and if also the bottom and coast have arbitrary shapes, it is wise to compute the energy density per spectral component.

The method is based on drawing up the energy balance for each wave component separately, while travelling with the component's group velocity along its wave ray. Energy received from the wind is added, and energy lost, to bottom dissipation for instance, is subtracted from the amount of energy that was already present. Doing so on regular time steps one can calculate the development of the amount of energy for each wave component. This can be expressed by the energy balance equation:

$$\frac{dE(f,\theta)}{dt} = S(f,\theta)$$

The left hand side is the increase per unit time of the energy density of wave component (f,θ), moving with the group velocity of this component. The right hand side is the source term, the sum of all external processes removing wave energy from or introducing wave energy into the system. The source term also includes the nonlinear wave-wave interactions. The difference between first and second generation models can be found in these nonlinear interactions which are neglected in the first generation, and are described in a parametrized form in the second.

In a certain point the energy density $E(f,\theta)$ can be calculated as function of time by integrating the above mentioned equation, with given initial conditions. Making this calculation for many locations at various points of time, the wave field can be predicted in terms of place and time.

This "wave-ray method" often results in chaotic wave patterns that are hard to interpret. To overcome this problem, and to allow an efficient representation of the random short-crested character of the waves with their generation and dissipation, models have been developed which are formulated on a regular grid. For wave computations in oceans and shelf seas these grid formulated models are quite common. It is not so easy to use these deep water models - after including some shallow water effects - in coastal areas. First, coastal areas usually need many more gridpoints than ocean areas to describe them properly. Second, to satisfy the Courant stability criterion of the numerical finite difference schemes, the time step must be very small. Fulfilment of these two requirements demands high computational efforts which make the models impractical in coastal regions. For this reason a model has been developed that is computationally feasible and still has as much the basic characteristics of oceanic models as possible: the second generation model HISWA (Holthuijsen *et al.*,1989). This was done by removing time as an

independent variable, and by limiting the degrees of freedom of the wave spectrum. The result is a fairly successful model, but it has some imperfections: The propagation is limited to a directional sector of about 120°, multi modal wave fields cannot be accommodated (wind sea and swell for instance), and the computational grid has to be oriented in the mean wave direction, which is operationally inconvenient.
These measures were forced by the available computer capacity at that time and by the available knowledge of the spectral development of waves in very shallow water. Developments on both points have led to the development of the fully spectral model SWAN. Because of a different numerical scheme the propagation is unconditionally stable. It is a third generation model which means - according to Komen *et al* (1994) - that it is *" a full spectral model with an explicit representation for the physical processes relevant for wave evolution and which gives a full two-dimensional description of the sea state"*.

Chapter 2

Wave Modelling

... in which a description of the used models is given.

HISWA and SWAN are both numerical wave propagation models, developed at Delft University of Technology. HISWA (2nd generation) came out in 1988, SWAN (3rd generation) some 7 years later in 1995; it is more or less the sequel to HISWA. The main differences are the fact that SWAN is spectral both in frequencies and in directions, whilst in HISWA the frequencies are parametric. Secondly the numerical scheme in SWAN for the wave propagation is unconditionally stable and encompasses waves from all directions (360°). In HISWA the directional sector wherein wave propagating is considered is limited to a maximum of 120° to obtain stability. Furthermore - being third generation - SWAN allows the spectrum to develop without any a priori constraints.

§ 2.1 gives the action balance equation on which both models are based. How SWAN deals with this equation is subject of § 2.2, whilst HISWA will be described in § 2.3. For a full description of the models I refer to the SWAN user manual (Ris *et al*, 1996) and for HISWA to 'A prediction model for stationary, short-crested waves in shallow water with ambient currents' (Holthuijsen *et al.*, 1989).

§ 2.1 Principle of the Models

HISWA and SWAN are numerical wave propagation models to simulate random, short-crested sea conditions. The elevation of the sea surface is considered as the sum of an infinite number of sinusoidal wave components, each with a different wave number, wave period, wave height and direction. Both models are based on the spectral action balance which in the absence of a mean

current reduces to an energy balance. The energy balance approach implies that for each spectral wave component of the wave field the rate of energy change is equal to the net effect per unit time of wind growth, bottom-induced dissipation etc. Action density N equals the energy density divided by the relative frequency, $N = E/\sigma$. Unlike energy, action is also conserved in the presence of a current. The spectral action balance equation (Whitham, 1974) is given by :

$$\frac{\partial}{\partial t}N(\sigma,\theta) + \nabla_x[(\underline{c}_g + \underline{u})N(\sigma,\theta)] + \frac{\partial}{\partial\sigma}[c_\sigma N(\sigma,\theta)] + \frac{\partial}{\partial\theta}[c_\theta N(\sigma,\theta)] = \frac{S(\sigma,\theta)}{\sigma} \qquad (2.1)$$

The first term in the left-hand side is the rate of change of action density in time, the second term is the rectilinear propagation of action in geographic x,y-space. The third term represents the shifting of the relative frequency due to currents and variations in depth. The fourth term describes the propagation in θ-space (depth and current induced refraction). From the linear theory the propagation velocities in geographical space, frequency space and in the spectral direction can be obtained:

$$\underline{c}_g + \underline{U} = \frac{d\underline{x}}{dt} = \frac{1}{2}\left(1 + \frac{2kh}{\sinh 2kh}\right)\frac{\sigma\underline{k}}{k^2} + \underline{U} \qquad (2.2)$$

$$c_\sigma = \frac{d\sigma}{dt} = \frac{\partial\sigma}{\partial h}\left(\frac{\partial h}{\partial t} + \underline{U}\,\nabla h\right) - \underline{c}_g\underline{k}\frac{\partial\underline{U}}{\partial s} \qquad (2.3)$$

$$c_\theta = \frac{d\theta}{dt} = -\frac{1}{k}\left(\frac{\partial\sigma}{\partial h}\frac{\partial h}{\partial m} + \underline{k}\,\frac{\partial\underline{U}}{\partial m}\right) \qquad (2.4)$$

$\underline{c}_g$ is the group velocity of the waves, s is the space coordinate in the propagation direction θ and m is a coordinate perpendicular to s. h stands for depth, $\underline{U}$ is the current velocity vector and $\underline{k}$ the wave number vector (magnitude k, direction θ). σ is the relative frequency, defined as:
$\sigma=\omega-\underline{k}\cdot\underline{U}$
The term $S(\sigma,\theta)$ is the source function representing the growth of wave energy by wind, the wave energy transfer by nonlinear wave-wave interactions (quadruplets and triads) and the decay of wave energy by bottom friction, whitecapping and depth induced wave breaking.

$$S(\sigma,\theta) = S_{in}(\sigma,\theta) + S_{nl}(\sigma,\theta) + S_{ds}(\sigma,\theta) \qquad (2.5)$$

The action density balance equation is a partial differential equation of the first order with independent variables: time t, the two horizontal coordinates (x,y), the frequency (σ) and the direction of propagation normal to the crest (θ). The dependent variable is the action density $N(\sigma,\theta,x,y,t)$.

An Eularian approach is used to solve the action balance; energy propagates not along rays but

across a grid covering the area. The wave models HISWA and SWAN compute the variation in action density by integrating the local effects of wind, bottom and currents while propagating with these quantities at the group velocity across a grid in the area of interest. Both in HISWA and in SWAN a simplification to reduce the required computer capacity is introduced: The independent variable time has been removed from the balance equation, thus making it stationary. This is acceptable for most coastal wave models since the residence time of the waves is usually far less than the time scale of variations of the wave boundary condition, the current, the tide, or the wind. The way HISWA and SWAN deal with the stationary action balance is fairly different from each other.

§ 2.2 SWAN

§ 2.2.1 Theory of SWAN

The basic spectrum in SWAN is a full action density spectrum, represented by a discrete number of finite bandwidth bins in frequency and direction. The frequency σ is logarithmically distributed, to make the nonlinear transfer (quadruplets and triads) scale with frequency. The following effects are implemented in the source term, using third generation formulations, mainly based on the WAM model (Komen *et al.*,1994) (one of the first 3rd generation models for the simulation of ocean waves):
- generation of wave energy by wind
- dissipation of wave energy by bottom friction
- dissipation of wave energy by whitecapping
- dissipation of wave energy by surf breaking
- redistribution of wave energy over the spectrum by nonlinear wave-wave interactions (both three wave-wave interactions and four wave-wave interactions)
- refraction by bottom and current variations
- wave-current interactions (wave blocking, reflection)

- WIND

The only source from which waves gain energy is the wind input. In SWAN the growth rate of a wave component is described by $S(\sigma,\theta) = A + B \cdot E(\sigma,\theta)$ in which A describes the linear growth rate and B the exponential. The linear growth term is small and is only relevant for the first stage of the wave growth on an initially calm sea. It is used in SWAN mainly to ensure energy growth if no initial wave energy is present. The linear wind growth was first described by Phillips, in 1957. The wind field is thought to be the sum of Fourier components with frequencies f and wave vector $\underline{k}$. Turbulent pressure forces will generate wave components on the water surface with the same wave number as the wind pressure components. Some of these wind pressure components fulfill the dispersion relation of the water waves, so that energy can be transported from the by wind generated pressure field to the wave field. Because the influence of the water waves on the wind field is neglected, the energy input is stationary. The theory for the exponential wave growth comes from Miles. Considering the water wave components seperatly - they do not affect each other - Miles assumes a time averaged logarithmic wind profile above one such wave component. The wave height is small yet. As the wave height increases (for instance via Phillips'

mechanism) it will disturb the logarithmic wind profile, causing a varying wind pressure field on the water surface. At the weather-side of the wave top a relative overpressure will arise, where energy is transported from the wind field to the water. More energy can be transported as the wave height is bigger. The energy transfer is proportional to the energy density, and the energy density increases exponentially as time proceeds. The wind input takes place on the high frequency side of the spectrum.
For the linear wind growth term one formulation for the first and second generation mode is available and one for the third generation. Concerning the exponential wind growth term the third generation has two options, and the first and second generation mode one formulation. The third genration wind input formulations distinguish in the interaction between the wind and the waves. In the first parameterization, a modified expression from the original formulation of Snyder *et al.* (1981), the exponential wind input term is - among many other things- a function of the friction velocity, u_*. This parameterization is taken from WAM cycle 3. The second parameterization is that of Janssen (1989, 1991), as used in WAM cycle 4. Janssen derived a wind input formulation explicitly accounting for the interaction between the wind and the waves. Possible changes in the wind profile with the evolution of the waves are taken into account by considering boundary layer effects and the roughness length of the sea surface. Now, the wind input term is a function of $(u_*/c)^2$, and - among others - the Miles constant β. The Miles constant depends - among others - on z_e, the effective roughness length due to the total stress, i.e. the sum of a turbulent part and a wave induced part. z_e can be determined by means of:

$$z_e = \frac{z_0}{\sqrt{1 - \tau_\omega/\tau}} \tag{2.6}$$

where τ is the total wave stress $\tau = u_*^2 \cdot \rho_a$ and z_0 is given by a Charnock-like relation:

$$z_0 = \alpha_{ch} \frac{u_*^2}{g} \tag{2.7}$$

The wave stress τ_ω is obtained by integrating the input source term: $\tau_\omega = \rho_\omega \int\int \sigma S_{in,\sigma}(\sigma,\theta)\, d\sigma d\theta$. The friction velocity u_* is defined as the square root of the ratio of the surface stress τ caused by the wind and the air density ρ_a. Expressing u_* in U_{10} (he wind velocity at 10m height) leads (according to Wu, 1982) to:

$$u_* = U_{10}\sqrt{(0.8 + 0.065\, U_{10})10^{-3}} \qquad , u_* \text{ and } U_{10} \text{ in m/s}$$

- BOTTOM FRICTION
In water of finite depth waves are influenced by the shear stress at the bottom, resulting in an energy dissipation. In SWAN there are three different formulations available to describe the energy dissipation due to bottom friction: Hasselman *et al.* 1973, derived from the JONSWAP experiment, Putnam and Johnson, 1949, using both a friction coefficient for the waves and for the current, and Madsen *et al.*, 1988 in which the user can choose a roughness length scale of the

bottom. These formulations can all be expressed as:

$$S_{ds,b}(\sigma,\theta) = -C_{bottom} \frac{\sigma^2}{g^2 \sinh^2(kh)} E(\sigma,\theta) \qquad (2.8)$$

They distinguish in the way C_{bottom} is represented. The bottom friction influences mainly the low frequency waves.

- WHTECAPPING

The whitecapping dissipation source term represents the process by which energy is lost through deep water wave breaking in the high frequency portion of the spectrum. Whitecapping occurs when the waves become too steep (H_{max} / L $\geq$0.1). For the first and second generation mode there is no explicit formulation for the whitecpaping dissipation, but it is included in the wind input formulaton. The wind input terminates when the spectral density per frequency interval has achieved the value of the Pierson-Moskowitz spectrum (1964) limit. For the first generation mode of SWAN the spectral scale parameter α_{PM} of the Pierson-Moskowitz spectrum is 0.0081. For the second generation mode α_{PM} depends on the wave energy of the wind sea part of the spectrum, and is never lower than 0.0081. The dependency of α_{PM} on the total wave energy in the second generation permits an overshoot in the wave spectrum. 'Overshoot' is the excess of energy at the high frequency side of the non full grown spectrum above the maximum amount of energy for these frequencies in the full grown spectrum.
In the third generation mode two whitecapping formulations are available in SWAN: Komen *et al.*, 1984 (as in WAM cycle 3) and Janssen, 1991 (as in WAM cycle 4).

- SURF BREAKING

When the water becomes very shallow compared to the wave height (H_{max} /h $\geq$0.5) the waves will break. In SWAN a spectral version of the Battjes and Janssen (1978) wave breaking model is used. SWAN distributes the depth induced dissipation over the frequencies without affecting the shape of the spectrum.

- NONLINEAR WAVE-WAVE INTERACTIONS

In most wave models the sea surface is treated as a superposition of many different wave components. In a linear theory these wave components do not interact with each other, therefore all higher order terms are neglected. In reality if some wave components become (nearly) resonant, energy is redistributed in the spectrum. If a set of four waves fulfils the resonance conditions: $\underline{k}_1 + \underline{k}_2 = \underline{k}_3 + \underline{k}_4$ and $\omega_1 + \omega_2 = \omega_3 + \omega_4$, then they can exchange energy. These so called quadruplets can occur in deep and intermediate water. In very shallow water triad interactions become dominant. The resonance conditions which must be fulfilled before energy can be redistributed concern $\underline{k}_1 + \underline{k}_2$ and $\underline{k}_1 - \underline{k}_2$. The triad wave- wave interactions are modelled in such a way that part of the energy belonging to a frequency 'f' is pumped to a frequency '2f', resulting in a second peak. Fig. 2.1 shows the effect of the triads and the quadruplets.

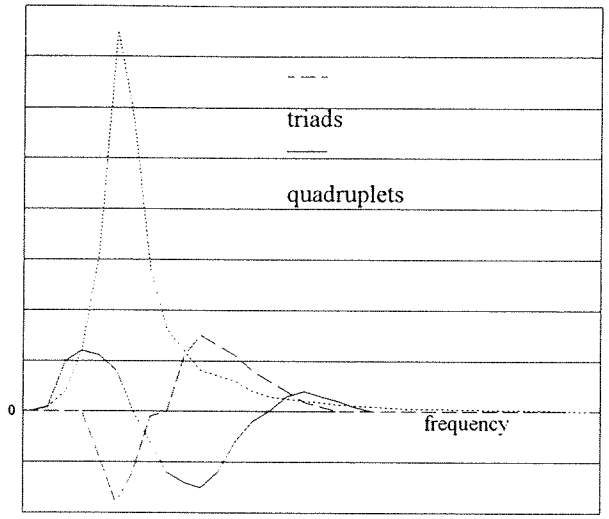

Fig. 2.1 effect of triads and quadruplets on the wave spectrum

§ 2.2.2 Numerical Procedure in SWAN

The action balance equation to be solved in SWAN is:

$$\nabla_x \cdot [(\underline{c}_g + \underline{U}) N] + \frac{\partial}{\partial\sigma}[c_\sigma N] + \frac{\partial}{\partial\theta}[c_\theta N] = \frac{S}{\sigma} \qquad (2.9)$$

-Propagation of action in geographical space
If no current is present the wave energy propagates in the same direction as the wave crest. In this case also the absolute magnitude of the propagation velocities of energy (c_x,c_y) is equal to the group velocity (c_{gx},c_{gy}). SWAN computes the variations of energy density by integrating the local effects which are included in the source terms while propagating with these quantities with the group velocity across a grid in the area of interest. For every grid point the action density is calculated using the source terms and the results from the upwave grid points. In the case of a current the propagation velocities of energy are no longer equal to the group velocities of the waves, but become: $c_x=c_{gx}+U_x$ and $c_y=c_{gy}+U_y$.
The way in which SWAN propagates through the geographic space is a forward marching scheme in a sequence of four 90° sectors (quadrants). In the first quadrant the state in a grid point (x_i,y_j) is determined by its up-wave grid points (x_{i-1},y_j) and (x_i,y_{j-1}). Waves from the directions in the 90° directional interval between the lines $x=x_i$ and $y=y_j$ are propagated with this scheme over the entire geographic region. This is the first sweep.

By rotating the stencil over 90° the second quadrant is propagated. After two more rotations one can be sure that waves from all directions are accounted for. The scheme is unconditionally stable. In the presence of refraction, wave action can shift from one quadrant

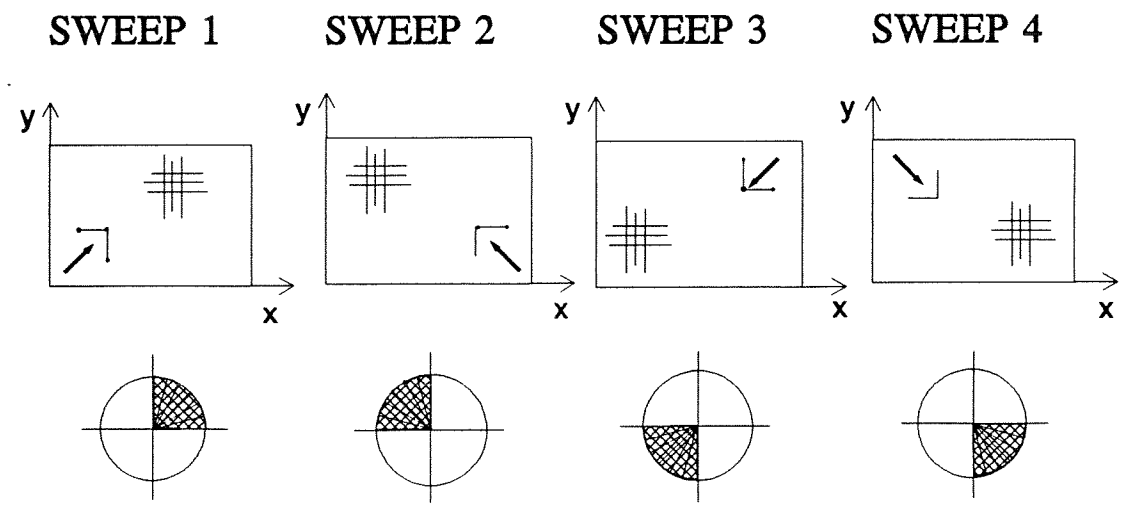

Fig. 2.2 numerical scheme for wave propagation in geographical space in SWAN *(source: Ris et al., 1995)*

to another. SWAN takes this into account by repeating the computations with converging results (iterative four-sweep technique (Holthuijsen *et al.*,1993)).

-Propagation of action in spectral space
Only when a current is present action propagates in spectral space along the frequencies with propagation velocity c_σ. Propagation of action in directional space with propagation velocity c_θ takes place when gradients in depths occur or when a current is present.

After the action density has been calculated in all grid points some energy related wave parameters can easily be found out of the energy spectrum, for instance the significant wave height

$$H_{sig} = 4\sqrt{\int\int E(\sigma,\theta)\,d\sigma d\theta} \qquad (2.10)$$

and the mean absolute wave period

$$T_{m01} = 2\pi \left(\frac{\int\int \omega E(\sigma,\theta)\,d\sigma d\theta}{\int\int E(\sigma,\theta)\,d\sigma d\theta} \right)^{-1} \qquad (2.11)$$

§ 2.3 HISWA

§ 2.3.1 Theory of HISWA

In HISWA the spectrum is discrete spectral only in the directions; it is parametric in the frequencies. As a result the third term of eq. 2.1 is skipped, and the action density is presented as $N(\theta) = \int N(\omega,\theta)d\omega$, in which ω is the absolute frequency. In each spectral direction two quantities are propagated: a frequency-integrated energy density and a mean frequency. Both

quantities vary across the geographic area. The computations are carried out for each wave component separately on the basis of two evolution equations:
- an evolution equation for the zeroth-order moment of the frequency-integrated directional action density for each spectral direction:

$$\frac{\partial}{\partial x}(c_x^* N_0) + \frac{\partial}{\partial y}(c_y^* N_0) + \frac{\partial}{\partial \theta}(c_\theta^* N_0) = T_0 \qquad (2.12)$$

- an evolution equation for the first-order moment of the frequency-integrated directional action density for each spectral direction:

$$\frac{\partial}{\partial x}(c_x^{**} N_1) + \frac{\partial}{\partial y}(c_y^{**} N_1) + \frac{\partial}{\partial \theta}(c_\theta^{**} N_1) = T_1 \qquad (2.13)$$

The left hand side of these equations represents propagation of the waves where c_x^*, c_y^* and c_θ^* are the propagation speeds of action in x-, y-, and θ-space respectively. Similarly, c_x^{**}, c_y^{**} and c_θ^{**} are the propagation speeds of the mean frequency in x-, y-, and θ-space. The propagation speeds c_x and c_y (in both equations) represent rectilinear propagation (including shoaling) whereas c_θ (in both equations) represents refraction. N_0 and N_1 are the zero- and first-order moments of the action density spectrum in each spectral direction. The effect of generation and dissipation on N_0 and N_1 is represented by the source terms T_0 and T_1, representing the effects of wave generation and dissipation. T_0 and T_1 can be expressed in terms of the source functions of wave energy (S_E) and the mean frequency of the spectrum (S_ω). The following effects are implemented, using second generation formulations:
- generation of wave energy by wind
- dissipation of wave energy by bottom friction
- dissipation of wave energy by whitecapping
- dissipation of wave energy by surf breaking
- dissipation due to vegetation
- refraction by bottom and current variations
- wave-current interactions

- WIND
The wind induced development of the wave energy and the mean frequency are considered for each spectral wave direction separately and independently from other spectral directions. The formulations are taken from empirical information.

- BOTTOM DISSIPATION
In shallow water some wave energy is dissipated by bottom friction. The formulation according to Putnam and Johnson (1949) is used. The mean wave frequency per spectral wave direction is

affected by bottom friction in HISWA assuming that the wave energy dissipation due to bottom friction affects only the energy at low frequencies.

- WHITECAPPING AND SURF BREAKING
In HISWA the expression of Battjes and Janssen (1978) is used to compute the dissipation due to breaking. The maximum wave height is the smallest value of ($\gamma_{shallow}$ · depth) and (γ_{deep} / k). The γ's can be chosen by the user. The mean frequency is not affected in HISWA in the case of steepness induced breaking (whitecapping). The surf breaking affects only the energy at low frequencies, resulting in a change in mean frequency.

§ 2.3.2 Numerical Procedure in HISWA

The evolution equations for $N_0(\theta)$ and $N_1(\theta)$, eq. 2.12 and 2.13 are partial differential equations of first order with the horizontal coordinates x and y and the spectral direction θ as independent variables. The state in a point in (x,y,θ)-space, thus the values of N_0 and N_1 is determined by the state upwave from this point (upwave according to c_x, c_y, and c_θ).The computations start at the upwave boundary at the plane x=0 in (x,y,θ)-space where the values of N_0 and φ (and consequently also of c_{0x}, c_{0y}, and $c_{0\theta}$) are given for all locations along this boundary and for all spectral directions. The computations proceed step-wise, in a direction roughly parallel to the main wave direction (x in fig.2.3). As a consequence only waves can be represented in the model which make an angle of less than 90° with the computational direction. Moreover, stability conditions for the computation schemes in x,y-space and in θ-space restrict this angle further. Depending on the mesh size the total directional sector is therefore less than 120°.

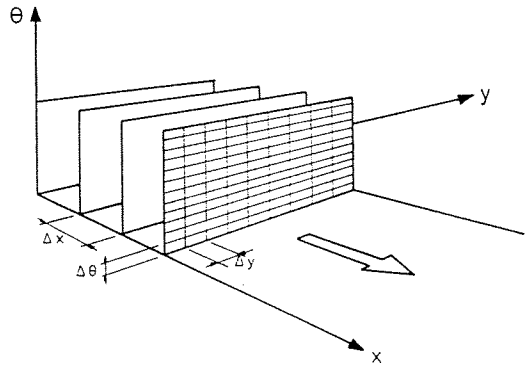

Fig. 2.3 method of HISWA's stepwise computation in mean wave direction *(source: Holthuijsen et al, 1989)*

Several (wave related) variables can be given as output. During output the quantities σ, k, c_g are calculated from $\omega(\theta)$. Significant wave height and mean period are defined as follows:

$$H_s = 4\sqrt{\int \sigma(\theta)\, N(\theta)\, d\theta} \qquad (2.14)$$

$$T_{mo1} = \frac{2\pi}{1.09}\frac{\int N/\omega d\theta}{\int N d\theta} \tag{2.15}$$

Chapter 3

Data & Test Cases

...in which it is explained which data are used and where they come from. Also a selection is made of cases to be modelled.

To enable a model to function well one should provide it with all data which are relevant to simulate the desired aspect of the real world. In the case of simulating short waves in nearshore areas the model needs information on the water depths, the incoming waves, the currents, and the wind. This chapter describes the measurements of these items. Concerning the wave measurements, one buoy provides the model with boundary values, eight others serve to supply data to be compared with the calculations.
§ 3.1 deals successively with the data on bottom, water levels, wind and waves. § 3.2 gives the criteria to select the test cases, and finally these selected cases are given.

§ 3.1 The Measurements

To determine locally defined items like the positions of the buoys and origins of computational and bottom grids, use is made of the Gauss-Krüger coordinate system. This system is divided in five zones of which the middle-meridian is respectively 3°, 6°, 9°, 12° and 15°. The east (X) coordinate of the middle meridian is chosen to be 500.000,00. In front of this east coordinate a number is placed which marks the zone. The X-coordinate of the origin of the bottom coordinate system that is used here is 2.562.744. This means that this spot lies in zone 2; 62.744 metre east of the 6° meridian. The north (Y) coordinate is counted from the equator. So the origin of the bottom coordinate system (of which the Y-coordinate is 5.942.803) lies nearly 6000km north of the equator.

§ 3.1.1 The Bottom

The data for the bathometry which were used in this research cover an area of about 25*21 km^2. The origin of the bottom coordinate system is given in Gauss-Krüger coordinates, being 2562744; 5942803. The bottom data came partly from measurements taken in august 1995, and partly from 1990. Each dot in fig.3.1 represents a measuring point where in august 1995 the position of the bottom elevations was determined with echo sounding. The distance between two points varies from about 50 to 200 metre. These measurements were carried out by the Bundesamt für Seeschiffahrt und Hydrographie. At the Coastal Research Station Norderney this set of data was transformed with the help of Arcinfo into a bottom file with a regular grid size of 80x80 m^2. Because the measurements of 1995 did not cover the full area where the wave measurements took place, it was combined with the older bottom data from 1990, to obtain one bottom file for the whole area. The measurements that were taken in 1990 were done by BWK (Bundeswasserstrassenkarten der Wasser- und Schiffahrtsdirektion Nord-West, Aurich), and covers a larger area. The step size between the measuring points is somewhat larger, varying roughly between 200 and 300 metre. By hand the depth contour lines were drawn, and finally the computer also gave it a regular grid size of 80 x 80 m^2. So the resolution of the bottom file that is used as input for SWAN and HISWA is at some places finer than the resolution with which was measured. This can result in some interpolation errors. On the other hand, a coarser bottomgrid would mean a loss of information at places where the measuring resolution was high.

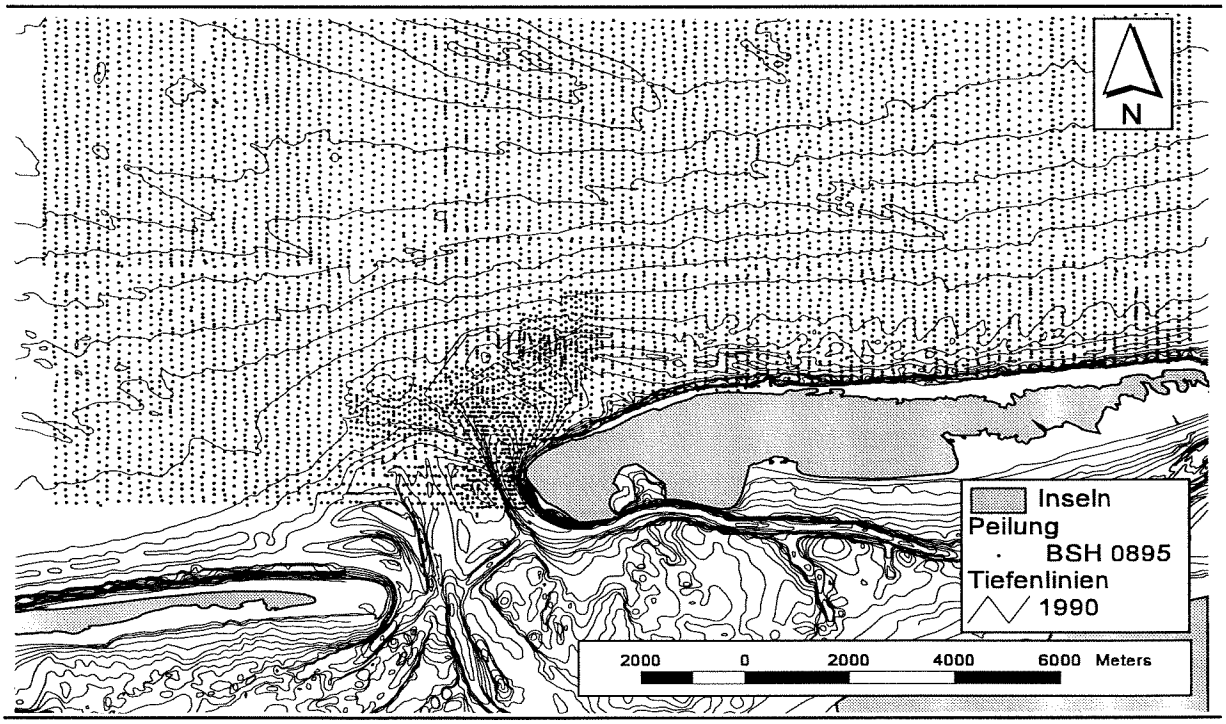

Fig. 3.1 bottom measurements and depth contour lines *(source: Niemeyer et al. 1996)*

§ 3.1.2 The Water Levels

Curves of the changing water levels are continuously drawn by the tide gauge at the Norderneyer Riffgat (see appendix B and fig.3.2). The difference between the mean high water and the mean low water there is 2.4 metre. The water level is mainly determined by the astronomical tide, but also the wind set up can have some influence. During extreme storm surges an additional 3m above the mean high water is observed. Furthermore waves may cause wave set up and wave set down resulting in lower water levels outside the surf zone and higher water levels near the coast. For the calculations a constant (in time) and uniform (over the area) water level is assumed. The first assumption is allowed as the time needed for the waves to travel from the deep buoy to the main land is small compared to the tidal period (see appendix B). The uniformity of the water level is imposed because of lack of data about water levels at several places, and because SWAN can read just uniform water levels. (In later versions also non-uniform water levels are possible.) On the North Sea wind set up can have some influence on the water level but there the depths are so big that a mere 10 cm from wind and wave set up (see appendix B) will not have much influence on the waves, and can be neglected. For the area were the measurements took place uniformity is not unrealistic.

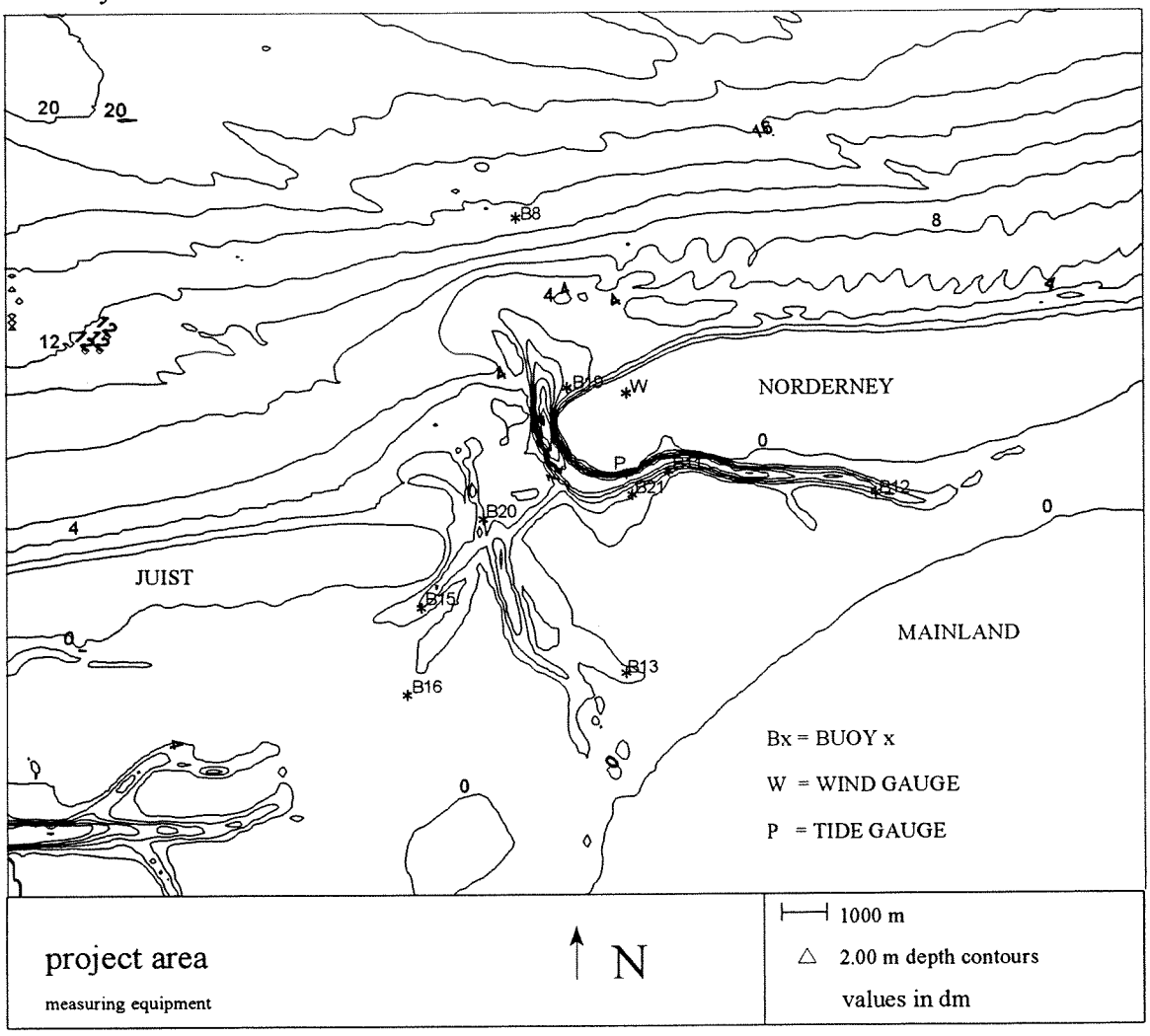

Fig. 3.2 position of the measuring equipment

§ 3.1.3 The Wind

For the calculations both stationary uniform wind fields and a stationary non-uniform wind field (referring to as varying wind field) are used. The data for the uniform wind field (velocity and direction) came from the *Wetterwarte Norderney*, and was measured near the northern coast (see fig 3.2), 23.9 metre above N.N. I converted this in u_{10} , the wind velocity 10 metre above the sea surface, using the logarithmic wind profile:

$$u(z) = \frac{u_*}{\kappa} \ln \frac{z}{z_0}$$

in which $u(z)$ is the wind velocity on height z
u_* is the friction velocity
κ is the Von Karman constant = 0.4
z_0 is the surface roughness parameter, on open water $z_0 \approx$ 0.00025m

The values are the mean for one hour.
Data on a varying wind field was available for only one situation (17.11.95, high tide). The file that describes this varying wind field comes from the See Wetteramt, Hamburg, Germany. It was made with the programm MKW (German abbreviation for mass-consistent windfield). This model needs information about the topography over land, the roughness over the whole area of research and one or more reference values for the windspeed. The initialization is based on the logarithmic wind profile and responds to changes in roughness in development of an internal boundary layer. Finally the constraint of mass-consistence will be satisfied by an optimization technique. The model is time independent and stratification is not considered. Data on the roughness over land came from the Coastal Research Station Norderney. The roughness over sea was estimated with the help of the Charnock relation. First a parametrization of the friction velocity is determined, being only a function of windspeed $u_*^2 = C_d \cdot U_{10}$, C_d being the drag coefficient and u_{10} the wind speed 10m above the sea surface. If the friction velocity is known, the roughness length can be estimated using the Charnock relation:

$$z_0 = \alpha_{ch} \frac{u_*^2}{g}$$

in which α_{ch} is the dimensionless Charnock constant
g is the gravity acceleration

This scheme has to be repeated until wind field and roughness length are in balance (high windspeed gives higher roughness gives lower windspeed...etc.)

§ 3.1.4 The Waves

The wave measurements used for this research came from nine waverider buoys. The Waverider is a buoy which, following the movements of the water surface, measures waves by measuring the vertical acceleration of the buoy. This vertical acceleration is the second derivative of the vertical elevation of the water surface. The discrepancy between vertical movement of the Waverider and the movement of the sea surface is small. Four of the nine buoys are so called 'directional waveriders'. The directional Waverider is a spherical (⌀ 0.9m) buoy which determines wave height and wave direction. The direction measurement is based on the translational principle which means that horizontal motions instead of wave slopes are measured. As a consequence the measurement is independent of buoy roll motions and therefore a relatively small spherical buoy can be used. From the accelerations measured in the x and y directions of the moving 'buoy reference frame' the accelerations along the fixed horizontal, north and west axis are calculated. All three accelerations (vertical, north and west) are digitally integrated with a high frequency cut-off at 0.6Hz to get filtered displacements. Finally every 90 minutes Fast Fourier Transforms of 8 series of 256 data points (200s) are summed to give 16 degrees of freedom on 1600 seconds of data. The frequency resolution is 0.005Hz for $0.025Hz<f<0.1Hz$, and 0.01Hz for $0.1Hz<f<0.59Hz$. The energy density spectrum is calculated on board. The other five buoys give the water surface fluctuations as output and some wave statistics for every 20 minutes concerning wave heights and periods. The spectrum is not calculated inside the buoy, but this is done later with a separate programme using the records of the surface fluctuations. The frequency resolution used is 0.023Hz, whilst the domain stretches from 0Hz to 2.9251Hz. The frequency resolution and domain of the Waverider buoy is equal to that of the directional Waverider. The buoys are provided with an fm-transmitter, sending the wave data to the coast.

A more thorough description of the buoys can be found in appendix A.

The measuring campaign was planned to take place from November 1995 until February 1996. This period was chosen because in the winter season stronger wind resulting in higher waves can be expected. Unfortunately the winter season of '95/'96 provided us not with strong winds but with very low temperatures and lots of ice in the Wadden Sea. To protect the buoys against damage done by the ice they had to be taken out of the sea on December 19th, and could not be put back before the end of February 1996. Moreover not all buoys functioned all the time. The period for which data from all buoys together is available is November 16th till December 19th. Figure 3.2 shows where the buoys are situated. To provide the models with good boundary conditions a directional waverider is used in deep water (depth$\approx$13m), about 4 km off shore. Going from there with the main wave direction to the Norderneyer coast gives the spot where the second directional buoy can be found. The third one lies right between Norderney and Juist, where the bathometry is quite complicated. The fourth directional Waverider is located in the tidal channel south of Norderney. Here the direction of the waves changes considerably; the waves follow the shape of the Norderneyer Riffgat. The rest of the buoys are in the Wadden Sea. The table below shows the position of the buoys and the depths at the position.

buoy	8	19	20	21	11	12	13	15	16
X[1]	74045m	75224m	73269m	76601m	77445m	82114m	76460m	71901m	71592m
Y[2]	57907m	54153m	51277m	51794m	52323m	51778m	47785m	49324m	47350m
depth[3]	-13.06m	-6.93m	-4.51m	-4.64m	-6.26m	-4.01m	-2.83m	-4.24m	-1.94m
type[4]	DWR	DWR	DWR	DWR	WR	WR	WR	WR	WR

Table 3.1 the wave buoys
1) X+2.500.000 in Gauss Krüger coordinates
2) Y+5.900.000 in Gauss Krüger coordinates
3) against N.N. (= Normalnull = N.A.P.)
4) DWR=Directional Waverider WR=Waverider

§ 3.2 Selected Situations

Because of lack of severe winds during the short period for which wave data were available the criteria to select the measurements could not be too rigid. The criteria I used are:
1) I want the incoming waves at buoy 8 to be higher than 2m, and preferably higher than 3m, otherwise the waves on the Wadden Sea will be too small to measure and model properly.
2) I want both a two-peaked spectrum, and a 'well shaped' one peaked spectrum.
3) Because of lack of current data I was forced to take measurements close to the turn of the tide.
4) I want both high tide cases and low tide cases

Table 3.2 shows the input parameters of three selected cases. The wave parameters that are mentioned come from the measurements from buoy 8

I will use the cases 1 (high water) and 2 (low water) to examine the influence of several parameters within SWAN and HISWA. With the results of these two cases I will use case 3 for hindcasting. This means that I will not vary the parameters, but use the values that have proven to be suitable in case 1 and 2.

case	date 1995	time	water level [m]	wind speed u_{10} [m/s]	wind direction	wave height Hs [m]	mean period Tz [s]
1	17.11	04:58	+1.42	8	NNW	2.98	6.35
2	16.11	22:58	-0.07	13	NW	2.84	6.15
3	19.11	07:59	+1.75	14	NNW	3.46	6.56

Table 3.2 selected cases to model

Of the selected situations not all measured wave data are well received. Buoy 20 shows no proper spectrum on November 17th at 05:41. Instead of an energy density spectrum over 64 frequency intervals a spectrum is created over only 27 frequency intervals. Information about the 37 intermediate frequencies is not available. The difference in time between this missing spectrum and either the preceding or the following one is too big to use these spectra instead of the missing one.

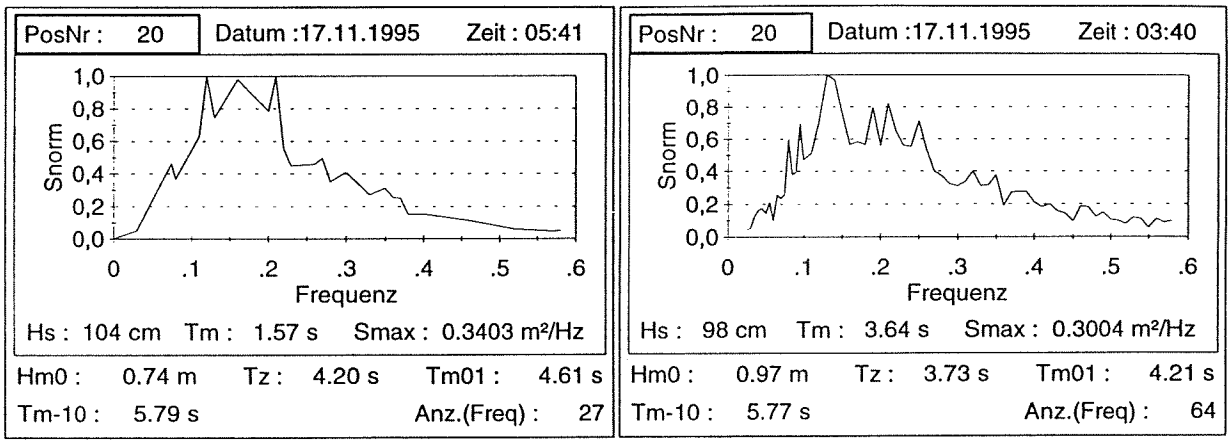

Fig 3.3 energy density spectra of buoy20 over 27 frequency intervals and over (the proper) 64 frequency intervals

The output of buoy 15 seems to be unrealistic. The two peaks are too high to be true. A more or less similar shape as the spectrum of buoy 16 is expected but that is certainly not the case (see fig.3.4). The significant wave height (determined directly by the buoy) seems to be right so I will only refrain from the spectrum and still use the observed significant wave height. Unfortunately this fault happens in both case 1 and 2. For the reasons given above, the spectra of buoy 20 case 1 and buoy 15 case 1 and 2 are not presented further in this report.

The observed wave heights for case 1 and case 2 are listed in appendix C. Approximately every 90 minutes the directional Waveriders send the spectrum - calculated over 1600 seconds (≈ 26 min) - to shore. The other Waveriders calculate the wave parameters every 20 minutes. The tables in appendix C also present the succeeding (and for some buoys the preceding) observed wave heights to get an idea of the differences in wave height over 90 minutes, respectively 20 min. Because the directional Waveriders are not equally scaled in time the points of time do not exactly match. Although the differences in time are so small that the waves can still be considered to be stationary, this might be a source of errors. Especially buoy 19 shows in case 2 a considerable change; from 1.15m to 1.78m. The incoming wave that was measured at 22:58 at buoy 8 reaches buoy 19 roughly some 8 minutes later, at 23:06. This is 20 minutes after 22:46 and 70 minutes before 00:16. So it is well possible that at that time the significant wave height is more than 1.15m. Still, this 1.15m is used to compare the by SWAN and HISWA calculated wave heights with.

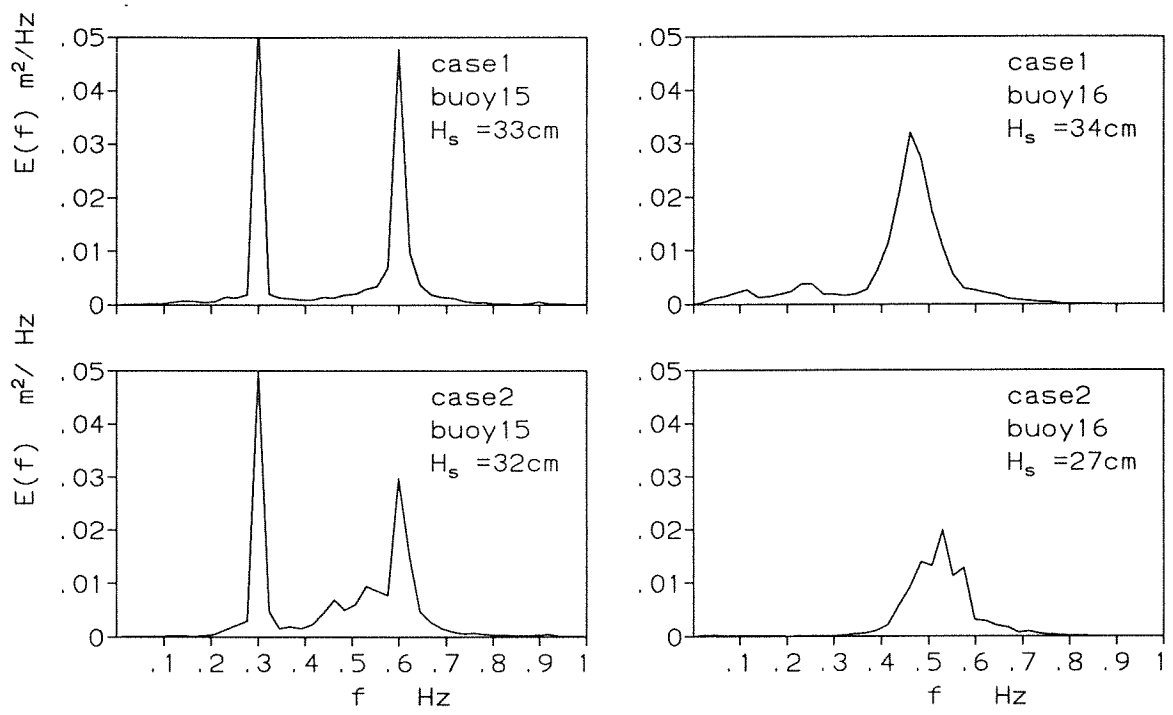

Fig 3.4 energy density spectra of buoy15 with unrealistically sharp peaks compared with buoy16

Chapter 4

Results Case 1 (high tide)

...in which the actual modelling is reported for the high tide case. The input for both SWAN and HISWA is given, and the results are presented and analysed.

Case 1 is the situation on November 17th 1995, at 4:58am. The significant wave height at that time at the position of buoy 8 is 2.98m. The North-Eastern wind blows with a speed of u_{10}=8m/s. It is high tide so the tidal currents are expected to be small.
I varied several parameters in SWAN and HISWA to examine the influence on the wave heights and the one dimensional spectrum (for SWAN only). § 4.1 deals with SWAN. First the standard run, next the research runs. HISWA is the subject of § 4.2, also with standard run and research runs. The different runs have a three-character code. The first letter refers to SWAN (s) or HISWA (h). The second character refers to the case. In chapter 4 only case 1 can be found and in chapter 5 case 2. The last character refers to the different runs (see table 4.1 and table 4.12). The results of the research runs are handled as follows: In SWAN the 1D-spectra are produced (see appendix F). The computed significant wave height is compared with the measured significant wave height. Per buoy the absolute error is calculated and the relative error. Per research run these absolute errors are added and the relative errors too. The run with the smallest absolute error is considered best.

§ 4.1 SWAN Results Case 1 (high tide)

§ 4.1.1 SWAN Standard Run

The model options are described in detail in the SWAN user manual (Ris *et al.*, 1995). The model input I used for the test cases will be given now. First I will describe the options that are the same for all the situations I selected.

- computational grid

  The origin of the computational grid is situated at (2566389 ; 5955613). The X-axis is rotated 197° anti-clockwise from the north (see fig. 4.1). The reason for this is the fact that HISWA needs the X-axis in the direction of the main wave direction. To use as many similarities as possible for SWAN and HISWA, I use this rotated grid in both models. In X-direction the area covers 159 meshes of 70 m each and in Y-direction 160 meshes of 95 m, giving an area of 11,13 x 15,20 km^2. This is justified in appendix D

- spectral directions

  The spectral directions cover the full circle, so wave energy coming from all directions is taken into account. The resolution in θ-space is 10°.

- frequency intervals

  The σ-space between the lowest frequency (=1/highest period = 1/22s = 0.045Hz) and the highest frequency (=1/lowest period = 1/0.9s = 1.11Hz) is logarithmically distributed in 24 meshes. This is justified in appendix E

- boundary

  The incoming waves are given along the seaward side of the computational grid, by reading spectral data coming from buoy 8. This file contains for each 64 frequency steps (ranging from 0.025 - 0.58 Hz) the energy density (in m^2/Hz), the average wave direction and the directional spreading. The incoming wave is assumed to be uniform along the seaward boundary of the computational domain. This is very likely since the water is quite deep there (±14m), the bottom contour lines go parallel with the Y-axis, and there is nothing at open sea which points to the contrary.

- numerical options

  I enforce the programme to continue calculating until in 98% of the wet gridpoints either:

  1) the relative increment becomes smaller than 0.02 (this means ($|Hs_2 - Hs_1| / Hs_1 < 0.02$) and ($|Tm_2 - Tm_1| / Tm_1 < 0.02$) between two succeeding iterations in a wet gridpoint), or

  2) the absolute increment in Hs between two succeeding iterations is smaller than 0.02m ($|Hs_2 - Hs_1| < 0.02$m) and the absolute accuracy in mean wave period is smaller than 0.2s ($|Tm_2 - Tm_1| < 0.2$s).

  In spectral θ-direction I add some diffusion by choosing cdd=0.5. The value cdd=0 corresponds to an implicit central difference scheme with the largest accuracy, cdd=1 corresponds to an implicit upwind difference scheme. This scheme is more diffusive, and it is preferred if strong gradients in θ-direction can be expected, as by strong currents and steep bottom slopes.

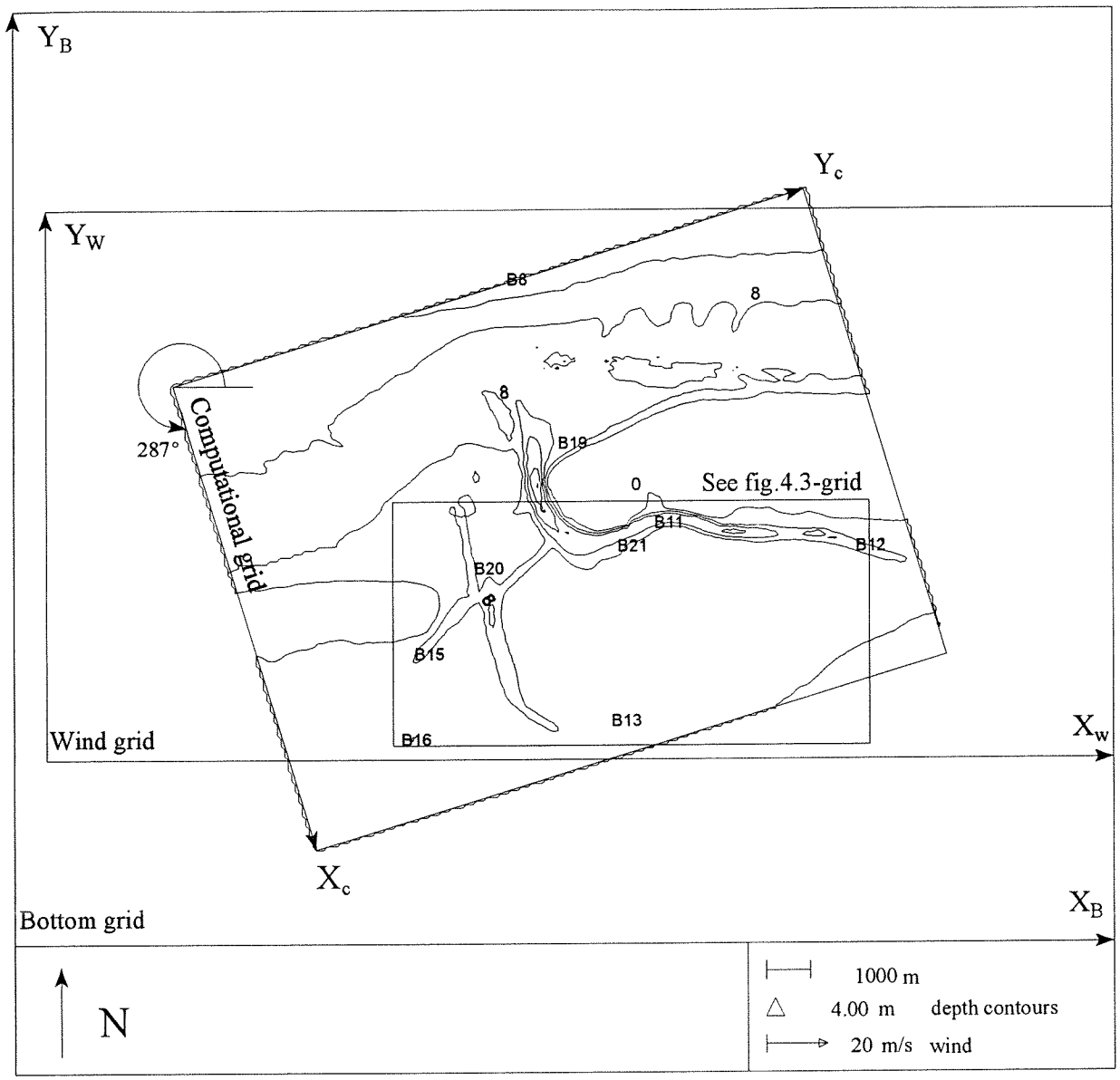

Fig. 4.1 grids in SWAN and HISWA

Starting from a standard run I will vary several parameters to find out how the model approximates the measurements best and to examine the influence of the parameters. The standard run uses default options where possible (see SWAN user manual). The results of the standard run, concerning significant wave height and wave direction are presented in fig. 4.2. Fig 4.3 shows the significant wave height and the period on the southern part of the computational domain.

In fig. 4.4 the observed and the calculated spectra are presented. When examining the spectra it is important to realise the difference in scale of the spectral density. To illustrate this, the observed spectra are presented in two ways. In fig. 4.4a they have such a scale that all plots have roughly the same height on the page. In fig. 4.4b all observed spectra are plotted together on one linear scale to show the huge decrease in wave energy from buoy 8 to the Wadden Sea buoys. The energy at the peak frequency of buoy 16 is less than one hundredth of the energy at the peak

frequency of buoy 8. The decay of the waves as they propagate from the North Sea to the Wadden Sea is shown in fig. 4.5, where the significant wave height and the mean period of the standard run and the observations is plotted for the respective stations.

Standard run s1a, Case 1 (17.11.95 04:58)
- water level: 1.42m above N.N. (high tide)
- wind: u_{10}=8m/s, direction 292° (wind vector points 292° anti-clockwise from eastern direction)
- quadruplets: on (default)
- bottom friction: JONSWAP, Γ=0.067m^2/s^3 (default).
- breaking: γ=0.80 (default) α=1.0 (default)
  γ is the coefficient determining how big waves may grow before depth induced breaking occurs. The maximum individual wave height is H_{max}= γ·depth.
  α is a coefficient determining the rate of dissipation.
- wind input formulation: third generation, sny3 (default), with all default values
  sny3 indicates a third generation wind input model according to Cavalari and Malanotte-Rizzoli, 1981 and Snyder *et al.*, 1981 and Komen *et al.*, 1984.
- whitecapping: Komen (default), with all default values

The coefficients for which default values are used concern the rate of dissipation (equals 2.36e-5) and a value indicating the wave steepness for the Pierson Moskowitz spectrum (α_{PM}=3.02e-3). The whitecapping dissipation rate is proportional to the square of the mean wave steepness divided by α_{PM}.

SWAN standard run case 1 (s1a) fig. 4.3

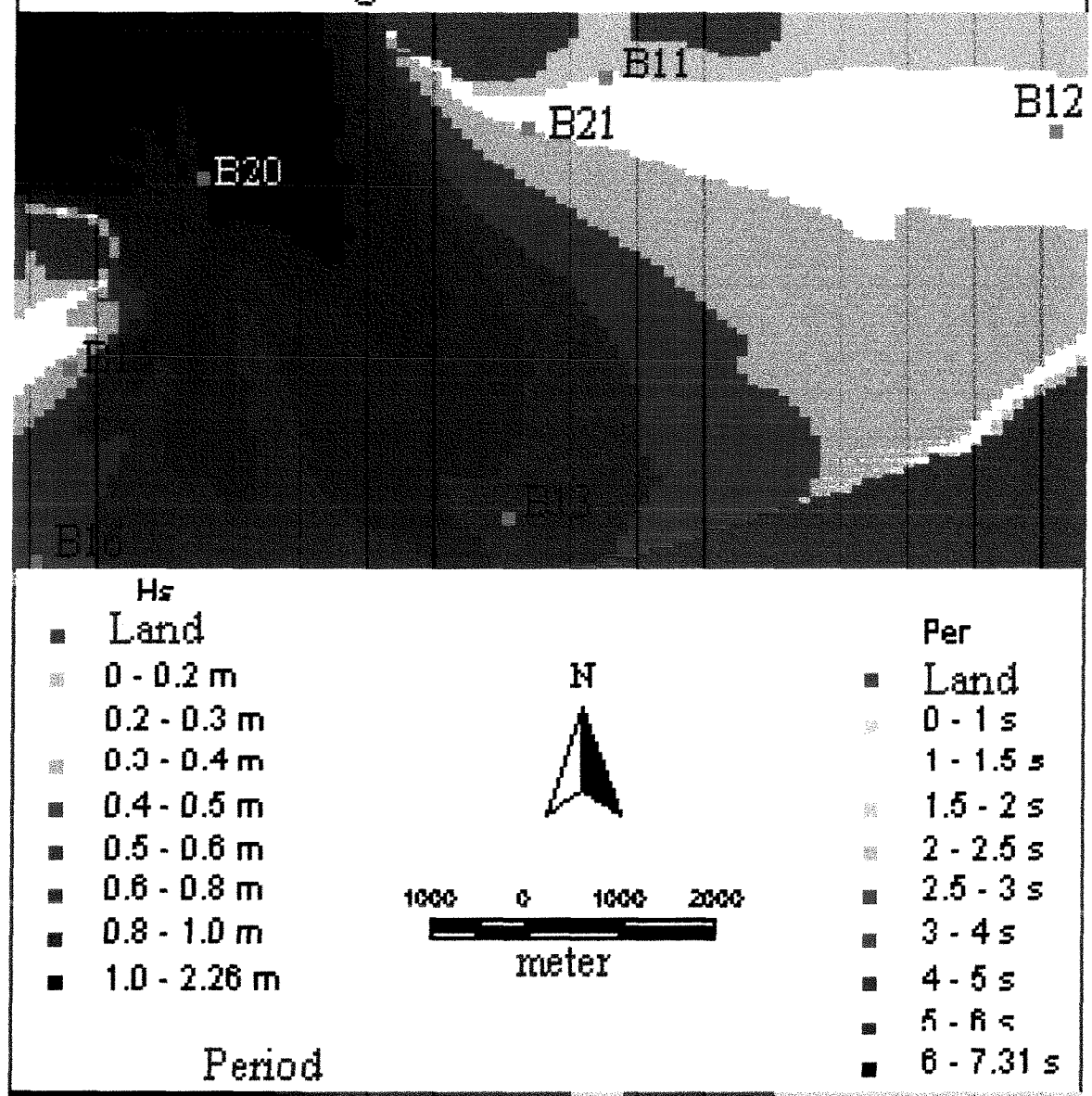

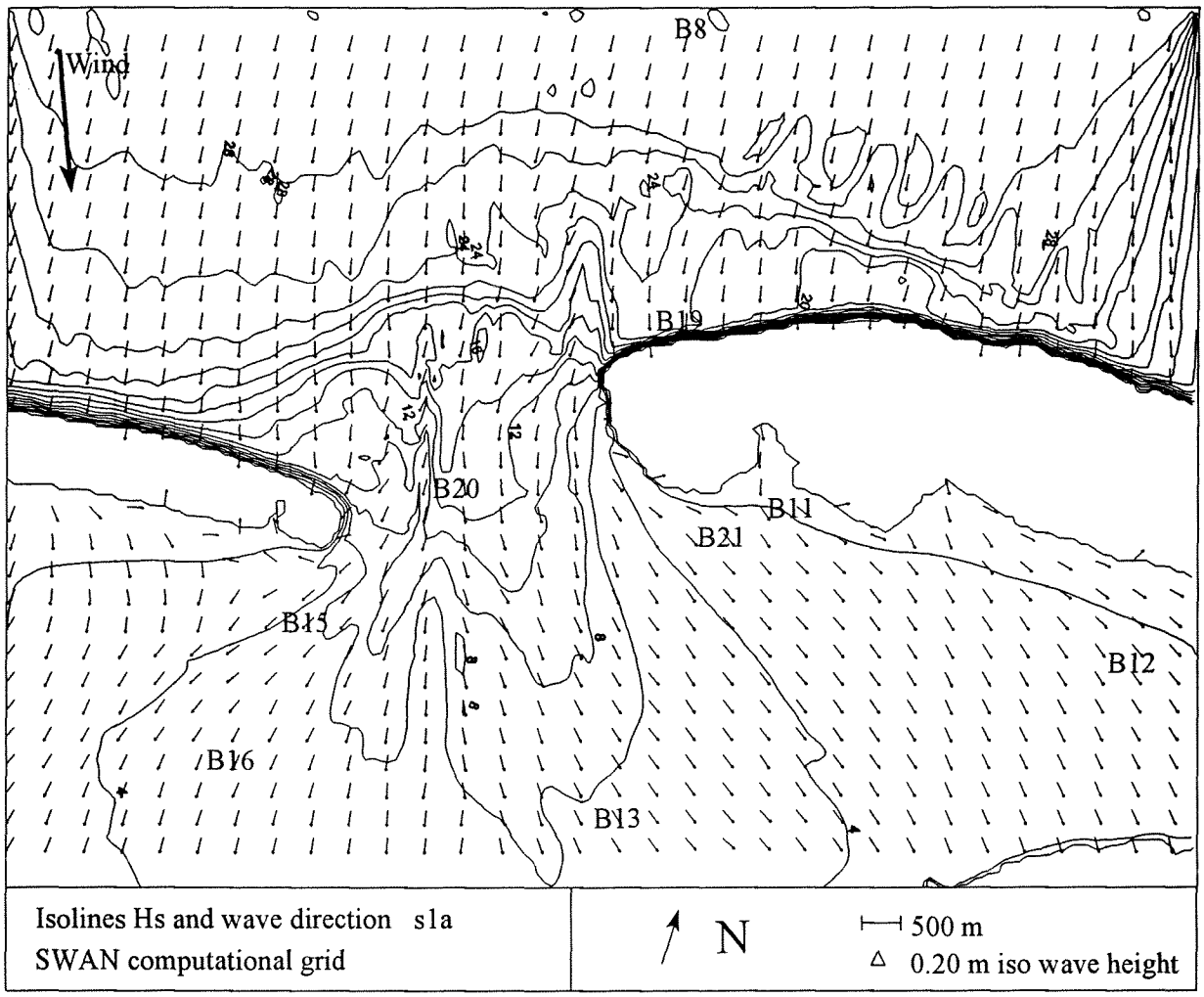

Fig 4.2 SWAN results case 1: iso wave height lines and wave direction on compgrid (values in dm)

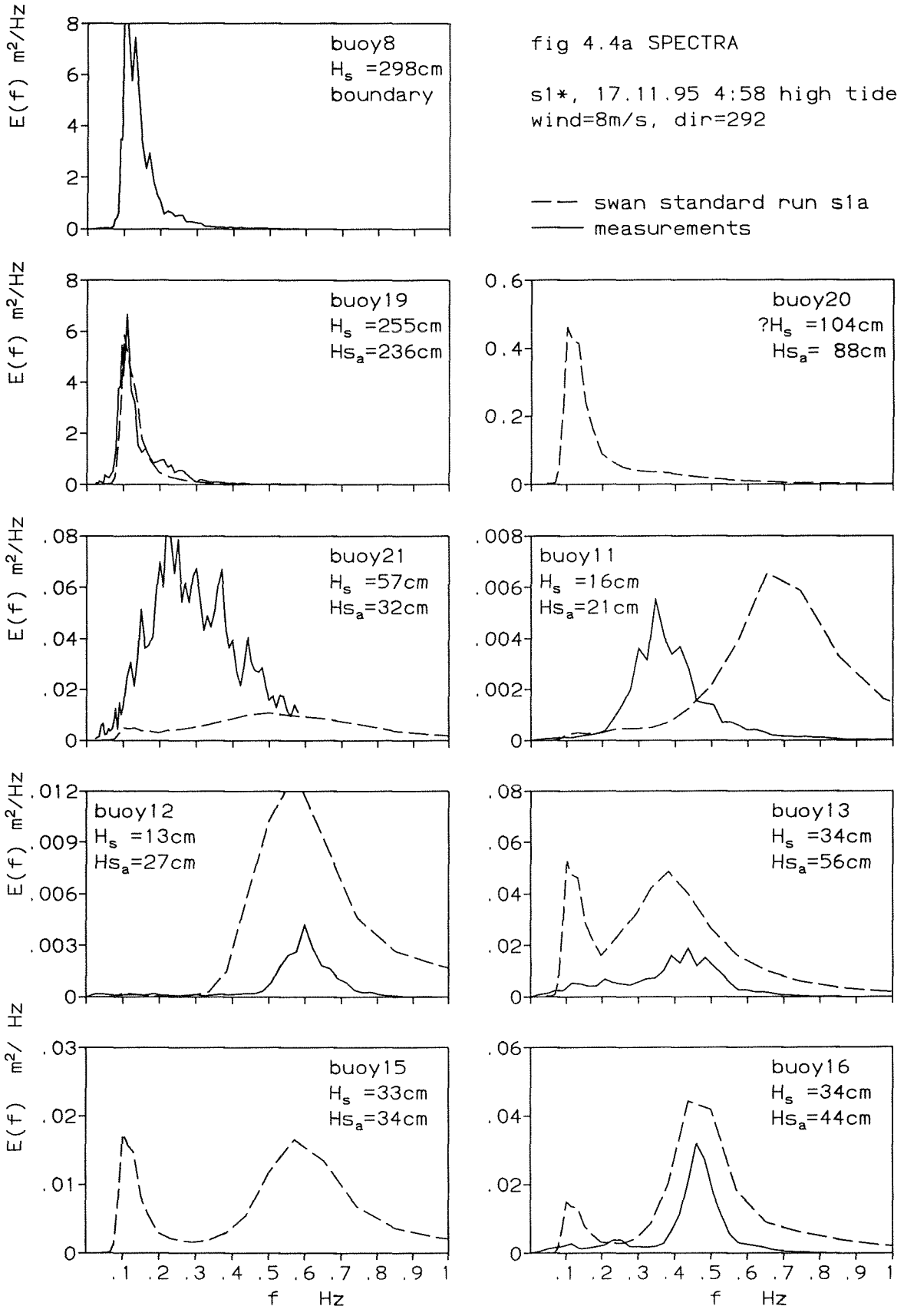
E(f) m²/Hz
buoy8
Hs =298cm
boundary
fig 4.4a SPECTRA
s1*, 17.11.95 4:58 high tide
wind=8m/s, dir=292
swan standard run s1a
measurements
buoy19
Hs =255cm
Hsa=236cm
buoy20
?Hs =104cm
Hsa= 88cm
buoy21
Hs =57cm
Hsa=32cm
buoy11
Hs =16cm
Hsa=21cm
buoy12
Hs =13cm
Hsa=27cm
buoy13
Hs =34cm
Hsa=56cm
buoy15
Hs =33cm
Hsa=34cm
buoy16
Hs =34cm
Hsa=44cm
f Hz

fig 4.4b SPECTRA

s1*, 17.11.95 4:58 high tide
wind=8m/s, dir=292

in decreasing order:
—— buoy 8, 19, 20, 11,
12, 13 and 16

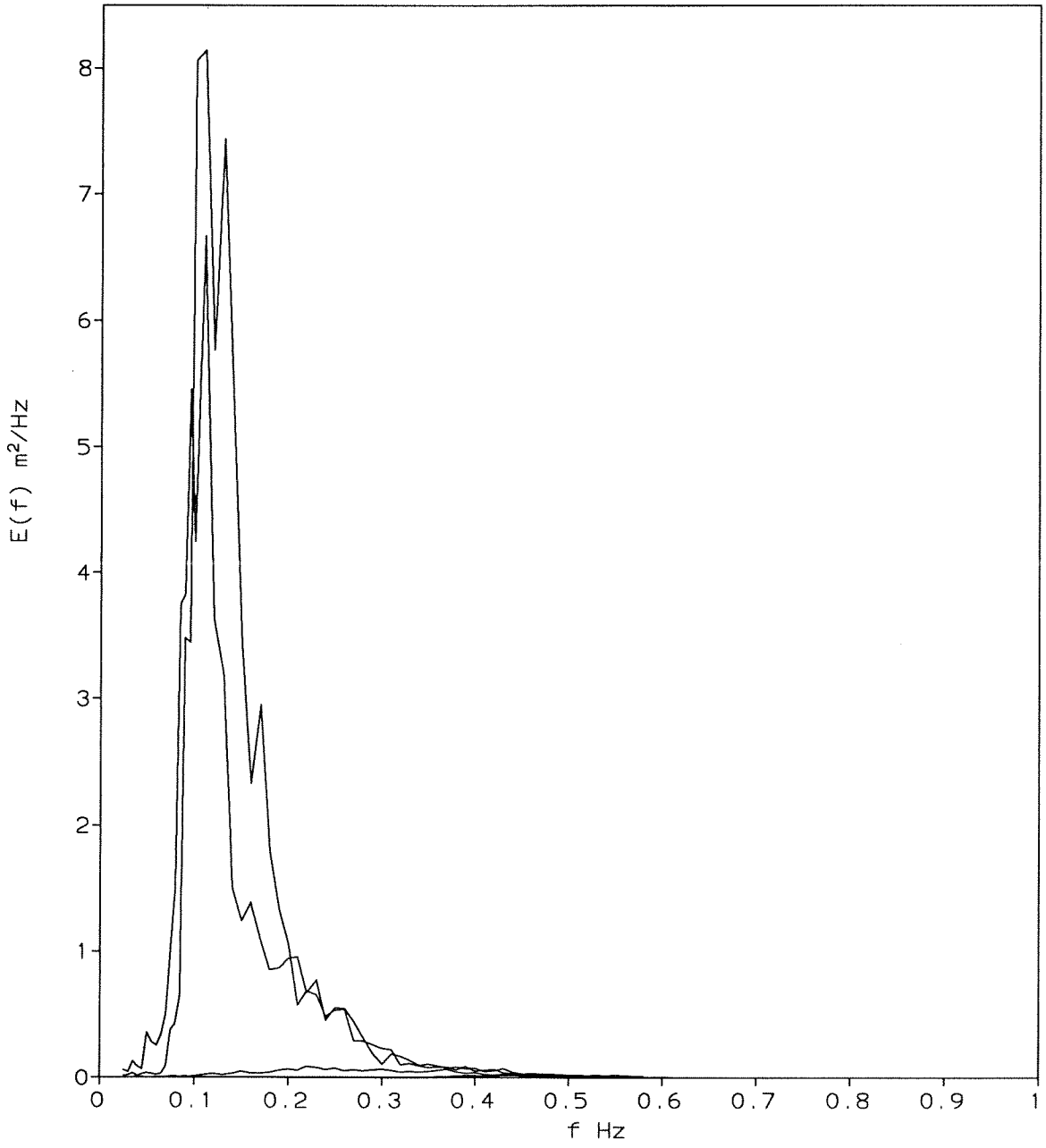

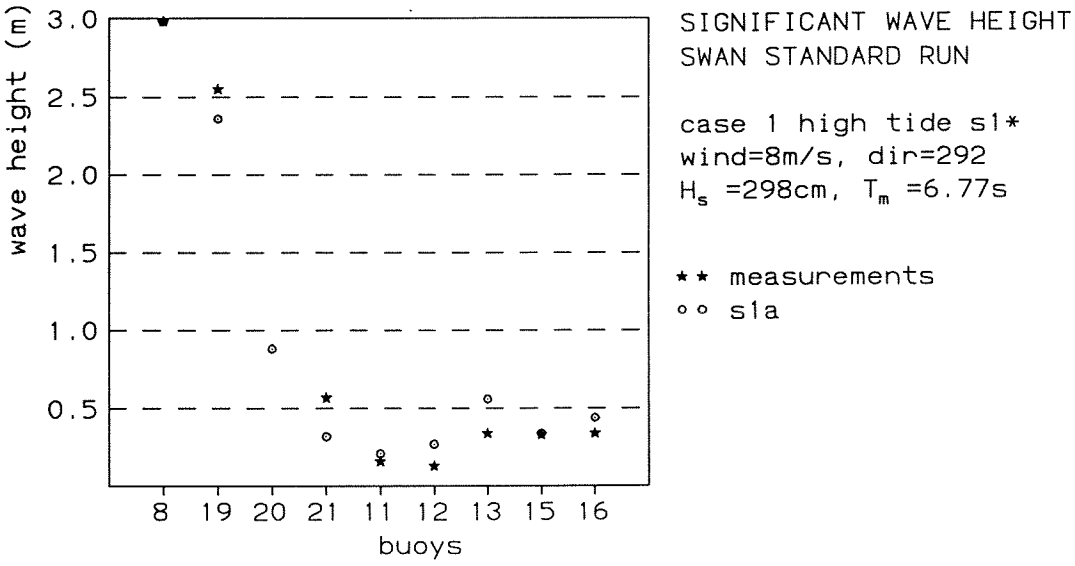

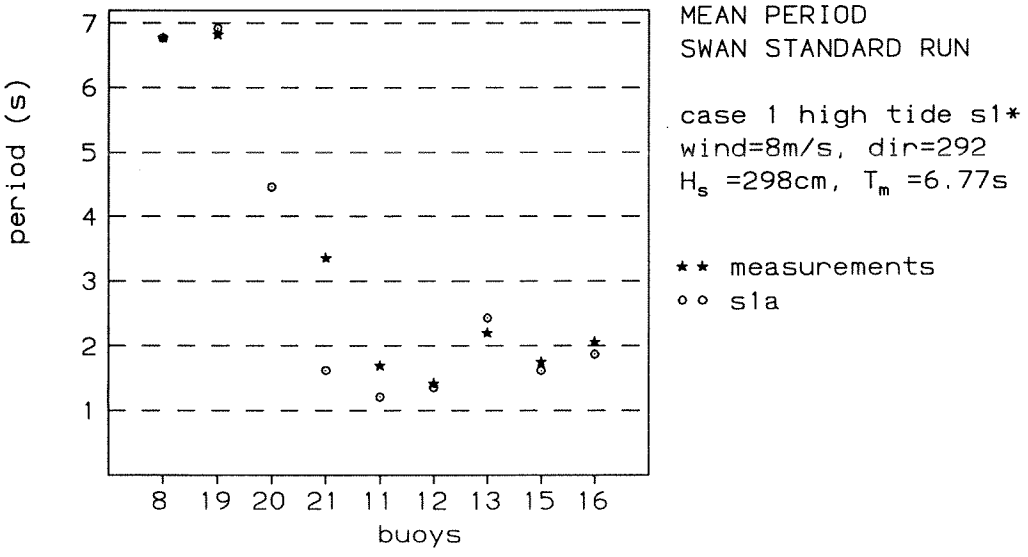

Fig 4.5 significant wave height and period case 1

§ 4.1.2 SWAN Research Runs

On the basis of the standard run as described in the previous paragraph a number of research runs is composed. In each research run one input parameter is changed (sometimes this leads to one or two additional changes) to find out its influence on the calculated results. The 16 research runs are not aimed at completeness. Besides the dissipation processes like friction, breaking and whitecapping I examine the results of a change in wind input (non-uniform wind field, different velocity, and wind on only part of the area). Also the influence of the incoming wave and the water level is looked at.

run	generation	wind [m/s] [°]	triads	friction	γ break	whitecapp.	w.level [m]	incoming wave
s1a	3rd (sny)	8 292	OFF	JONSWAP	0.80	Komen	1.42	100%
s1b	2nd	8 292	OFF	JONSWAP	0.80	OFF	1.42	100%
s1c	1st	8 292	OFF	JONSWAP	0.80	OFF	1.42	100%
s1d	3rd (sny)	varying	OFF	JONSWAP	0.80	Komen	1.42	100%
s1e	3rd (sny)	0 0	OFF	JONSWAP	0.80	Komen	1.42	100%
s1f	3rd (sny)	6 292	OFF	JONSWAP	0.80	Komen	1.42	100%
s1g	3rd (sny)	left part only	OFF	JONSWAP	0.80	Komen	1.42	100%
s1h	3rd (sny)	8 292	ON	JONSWAP	0.80	Komen	1.42	100%
s1i	3rd (sny)	8 292	OFF	OFF	0.80	Komen	1.42	100%
s1j	3rd (sny)	8 292	OFF	P&J	0.80	Komen	1.42	100%
s1k	3rd (sny)	8 292	OFF	Madsen	0.80	Komen	1.42	100%
s1l	3rd (sny)	8 292	OFF	JONSWAP	0.95	Komen	1.42	100%
s1m	3rd (sny)	8 292	OFF	JONSWAP	0.73	Komen	1.42	100%
s1n	3rd (sny)	8 292	OFF	JONSWAP	OFF	Komen	1.42	100%
s1o	3rd (jans)	8 292	OFF	JONSWAP	0.80	Janssen	1.42	100%
s1p	3rd (sny)	8 292	OFF	JONSWAP	0.80	Komen	0.42	100%
s1q	3rd (sny)	8 292	OFF	JONSWAP	0.80	Komen	1.42	75%

Table 4.1 SWAN runs case 1

Table 4.1 gives an overview of the different SWAN runs I made. The results can be found in table 4.2 (significant wave heights), table 4.3 (mean period), and in the figures on the following pages. The one dimensional spectra can be found in appendix F.
In this paragraph I will take a closer look at the variations by examining the influence of the different parameters.

run	buoy 19	buoy 20	buoy 21	buoy 11	buoy 12	buoy 13	buoy 15	buoy 16
meas.	2.55	1.04?	0.57	0.16	0.13	0.34	0.33	0.34
s1a	2.36	0.88	0.32	0.21	0.27	0.56	0.34	0.44
s1b	2.39	0.99	0.36	0.19	0.24	0.71	0.30	0.41
s1c	2.33	0.98	0.30	0.13	0.17	0.68	0.19	0.32
s1d	2.36	0.89	0.29	0.19	0.25	0.57	0.34	0.45
s1e	2.38	0.79	0.12	0.03	0.03	0.28	0.15	0.15
s1f	2.31	0.85	0.25	0.17	0.21	0.45	0.27	0.36
s1g	2.36	0.88	0.24	0.11	0.09	0.46	0.34	0.44
s1h	2.40	1.16	0.38	0.23	0.27	0.60	0.36	0.46
s1i	2.57	1.04	0.33	0.22	0.39	0.78	0.40	0.58
s1j	2.31	0.88	0.32	0.21	0.32	0.62	0.36	0.49
s1k	2.11	0.77	0.31	0.21	0.27	0.48	0.31	0.40
s1l	2.53	1.02	0.33	0.22	0.27	0.59	0.34	0.46
s1m	2.23	0.82	0.31	0.21	0.26	0.54	0.33	0.44
s1n	2.81	1.64	0.39	0.24	0.27	0.70	0.44	0.54
s1o	2.34	0.83	0.26	0.18	0.21	0.47	0.31	0.38
s1p	2.00	0.59	0.28	0.19	0.20	0.40	0.26	0.33
s1q	2.11	0.88	0.32	0.21	0.27	0.56	0.33	0.44

Table 4.2 SWAN results case 1; significant wave height in metre

The measurements of buoy 20 and buoy 15 are not fully reliable. Instead of an energy spectrum over 64 frequency steps buoy 20 generated a spectrum over only 27 frequencies. Information about all intermediate frequencies is not available. For this reason the measured spectrum for buoy 20 is not drawn in the spectra figures of § 4.1.2.
The spectrum coming from buoy 15 looks not fully reliable either. Looking at their positions, I would expect a more or less similar spectral shape as for buoy 16. This is certainly not the case, buoy 15 has two unrealistically high peaks. However, the value of the significant wave height seems to be plausible.

run	buoy 19	buoy 20	buoy 21	buoy 11	buoy 12	buoy 13	buoy 15	buoy 16
meas.	6.85	?	3.35	1.69	1.42	2.20	1.75	2.06
s1a	6.92	4.46	1.62	1.21	1.36	2.43	1.62	1.87
s1b	6.77	4.45	2.17	1.19	1.42	3.13	1.95	2.23
s1c	6.67	4.44	2.42	1.34	1.45	3.38	1.76	2.32
s1d	6.90	4.40	1.60	1.16	1.31	2.42	1.64	1.88
s1e	7.41	6.84	3.63	2.66	1.61	5.70	6.11	5.61
s1f	7.06	4.95	1.57	1.10	1.27	2.43	1.65	1.77
s1g	6.94	4.47	2.06	1.50	1.53	2.85	1.62	1.87
s1h	5.09	3.36	1.86	1.30	1.37	2.45	1.71	1.91
s1i	7.12	5.31	1.72	1.22	1.84	3.61	2.02	2.50
s1j	6.86	4.47	1.63	1.22	1.55	2.70	1.70	2.05
s1k	6.63	3.76	1.61	1.21	1.37	2.09	1.50	1.75
s1l	6.87	4.85	1.71	1.23	1.39	2.63	1.73	1.95
s1m	6.90	4.25	1.59	1.20	1.36	2.36	1.58	1.84
s1n	7.12	6.49	1.85	1.30	1.35	3.20	2.07	2.21
s1o	7.62	5.08	1.55	1.19	1.31	2.46	1.60	1.85
s1p	6.79	3.03	1.48	1.12	1.18	1.83	1.38	1.55
s1q	6.61	4.27	1.67	1.21	1.38	2.46	1.63	1.88

Table 4.3. SWAN results case 1; mean period* in second

*) Note that the mean period calculated by SWAN, and by buoys 8, 19 and 21 is T_{01}, whilst the mean period calculated by buoys 11, 12, 13, 15 and 16 is T_{02}. For a narrow spectrum there is hardly any difference between these two. On the Wadden Sea where much energy is present in the higher frequencies T_{01} and T_{02} differ too much to compare them properly.

- INFLUENCE GENERATION

SWAN can run as a first, second or third generation model. This refers to the kind of wind growth model that is used. In first generation wave models each spectral component evolves essentially independently of all other components until it approaches its limiting saturation level. So the nonlinear wave wave interactions are not accounted for and no "overshoot"occurs. The second generation models do take the nonlinear interactions into account, but in a highly parametrized form. In the third generation mode the spectrum can "develop" freely, without any parametrized restrictions. Note that the standard case s1a computes no triads. The results of these runs can be

found in fig. 4.6 and the wave spectra in the appendix, fig. F-1.

In fig F-1, buoy 13 shows the influence of the quadruplets, dividing the energy in two peaks, whereas the first and second generation runs show respectively one and 'almost' two peaks. Except for buoys 20 and 13, the first generation comes out with the smallest waves. Although the Hs from the first generation comes closest to the measured Hs - looking at the relative errors -, the shape of the measured spectra is best approximated by the third generation run. Moreover, the third generation has the smallest absolute error and is therefor considered best.

	buoy19	buoy21	buoy11	buoy12	buoy13	buoy15	buoy16	SUM
meas. Hs	2.55	0.57	0.16	0.13	0.34	0.33	0.34	
3rd gen Δ abs	-0.19	-0.25	+0.05	+0.14	+0.22	+0.01	+0.10	0.96
Δ %	7.45	43.9	31.3	107.7	64.7	3.03	29.4	287.4
2nd gen Δ abs	-0.16	-0.21	+0.03	+0.11	+0.37	-0.03	+0.07	0.98
Δ %	6.27	36.8	18.8	84.6	108.8	9.09	20.6	285.0
1st gen. Δ abs	-0.22	-0.27	-0.03	+0.04	+0.34	-0.14	-0.02	1.06
Δ %	8.63	47.4	18.8	30.8	100	42.0	5.88	253.4

Table 4.4 influence generation on Hs. measurements and absolute errors (Δ abs = SWAN - measurement) in metre

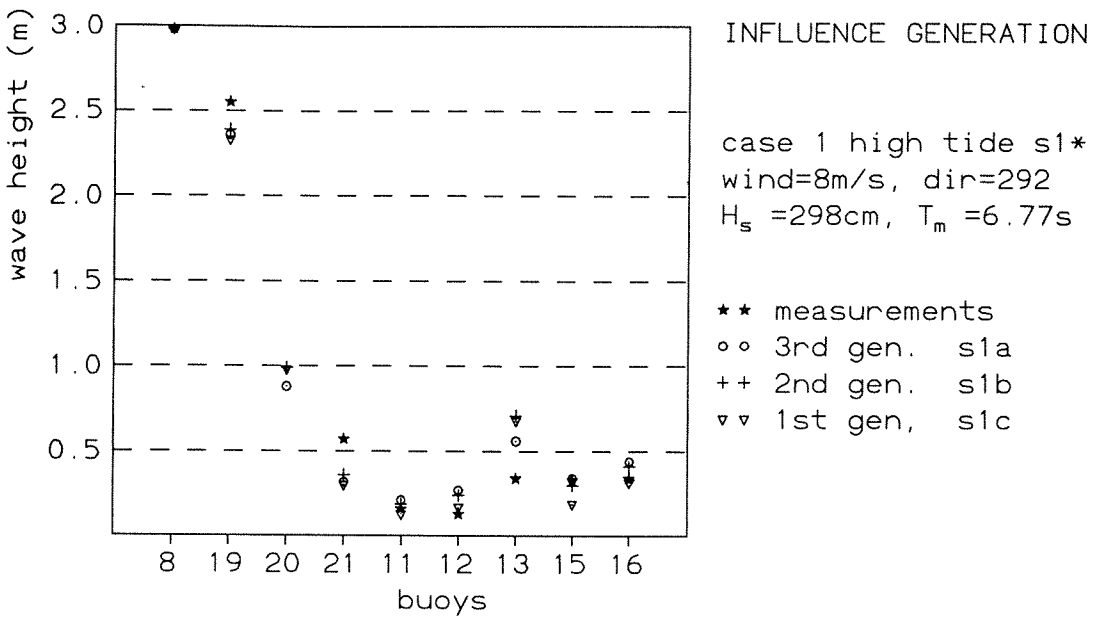

Fig. 4.6 influence generation on significant wave height

- INFLUENCE WIND

Fig. 4.8, fig. 4.9 and fig. F-2 and F-3 of appendix F show the results of SWAN calculations with various wind velocities. The varying wind comes from a wind model that takes into account that under the lee of the islands the wind velocity is less than on open sea. According to this model the wind velocity right behind the islands (buoys 11 and 12) is 6m/s, instead of the uniform 8m/s. This explains the smaller wave heights at buoys 21, 11 and 12 for case s1d compared with case s1a, although the differences are only small.

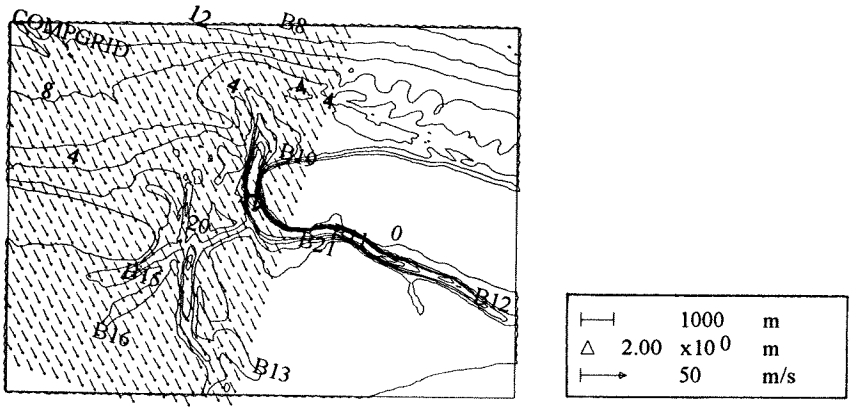

Fig. 4.7 position wind grid for run s1g, h1e, s2f and h2d

In case no wind would blow all the available wave energy came from the North Sea. This is clearly noticeable in the spectra from buoys 13, 15 and 16 (see fig. F-2). The first peak ($f \approx 0.11$Hz) is swell from the North Sea, the second peak ($0.4 \lesssim f \lesssim 0.6$Hz,) which is not present in the no-wind-case, is locally generated. Note however that the first peak calculated in SWAN at buoy 13, 15, and 16 is not visible in the measurements, so probably SWAN transports too much wave energy from the North Sea.

In runs s1e, s1f and s1g I experiment with the wind input to find out the influence on buoy 11 and 12 of the local wind and of the propagation of wave energy. The position of the (uniform) windfield used for the 'left-part-only-run' is given in fig. 4.7. No arrows means no wind. Without local wind SWAN calculates still some waves at buoy 11 and 12 (see fig. 4.9 and F-3).

	buoy19	buoy21	buoy11	buoy12	buoy13	buoy15	buoy16	SUM
meas. Hs	2.55	0.57	0.16	0.13	0.34	0.33	0.34	
u_{10}=8 Δ abs	-0.19	-0.25	+0.05	+0.14	+0.22	+0.01	+0.10	0.96
Δ %	7.45	43.9	31.3	107.7	64.7	3.03	29.4	287.4
vary. Δ abs	-0.19	-0.28	+0.03	+0.12	+0.23	+0.01	+0.11	0.97
Δ %	7.45	49.1	18.8	92.0	67.6	3.03	32.4	270.3
u_{10}=6 Δabs	-0.24	-0.32	+0.01	+0.08	+0.11	-0.06	+0.02	0.84
Δ %	9.41	56.1	6.25	61.5	32.4	18.2	5.88	189.7
left part only Δabs	-0.19	-0.33	-0.05	-0.04	+0.13	+0.01	+0.10	0.85
Δ %	7.45	57.9	31.3	30.8	39.4	3.03	29.4	199.3
u_{10}=0 Δabs	-0.17	-0.45	-0.13	-0.10	-0.06	-0.18	-0.19	1.28
Δ %	6.67	78.9	81.3	76.9	17.6	54.5	55.9	371.8

Table 4.5 influence wind on Hs. measurements and absolute errors (Δ abs = SWAN - measurement) in metre

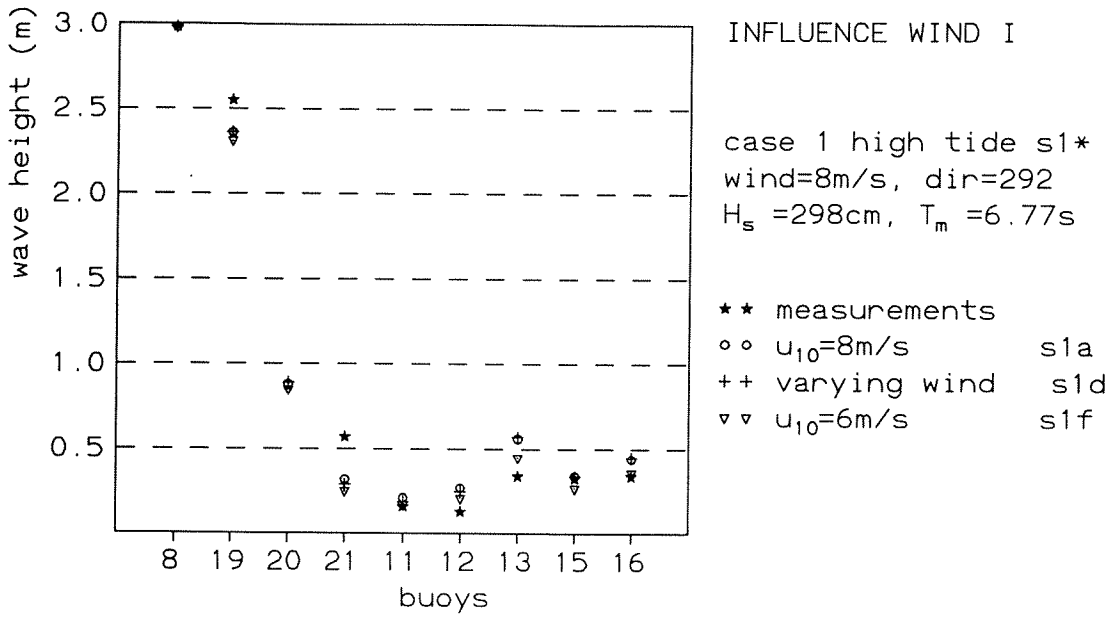

Fig. 4.8 influence wind on significant wave height I

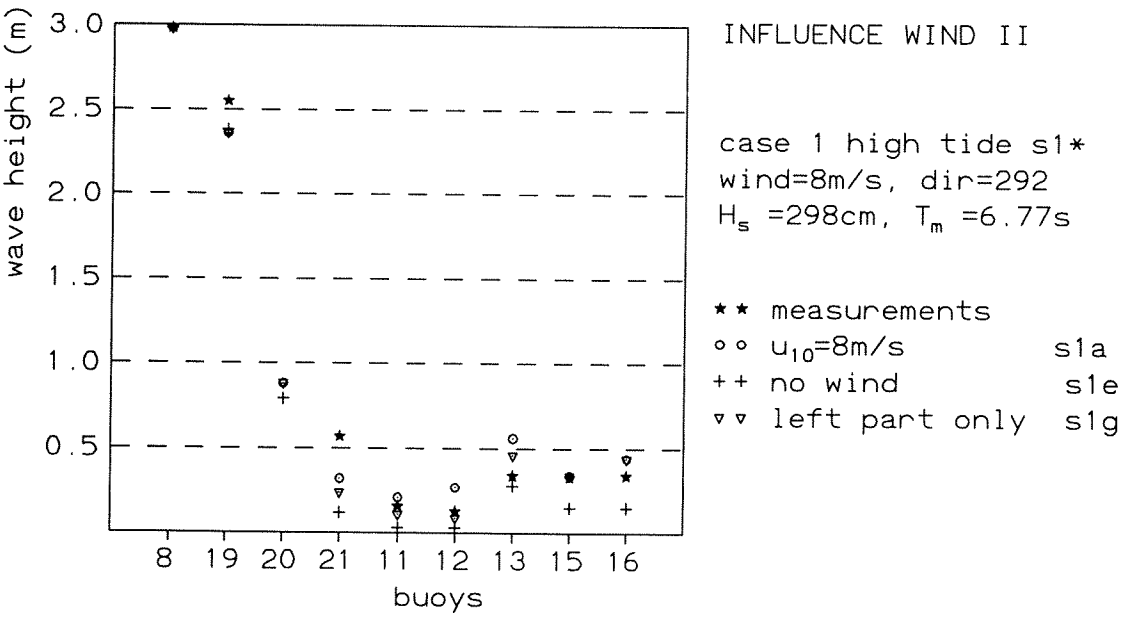

Fig. 4.9 influence wind on significant wave height II

- INFLUENCE TRIADS

As the quadruplets cannot be switched off, I only examine the influence of the triad interactions. The nonlinear three wave-wave interactions redistribute the wave energy over the frequencies in such a way that the first energy peak in the spectrum decreases and the second increases (or is generated). This is well noticeable for buoy 19, 20 and 13 in fig F-4. The extra available wave energy around f=0.3Hz for the run with activated triads (s1h) compared to the run without triads (s1a) at the position of buoy 11 seems very strange. The 'bulb' is not caused by the regeneration of wave energy within the spectrum though. Around buoy 11 the triads are not even active. The first peak is rather coming from buoy 21, whilst the second peak is locally generated by wind. So only indirectly the waves near buoy 11 are influenced by the triads. Fig. 4.10 shows that the wave heights calculated with triads are all larger than without triads. The over all absolute errors are equal.

	buoy19	buoy21	buoy11	buoy12	buoy13	buoy15	buoy16	SUM
meas. Hs	2.55	0.57	0.16	0.13	0.34	0.33	0.34	
triads off Δ abs	-0.19	-0.25	+0.05	+0.14	+0.22	+0.01	+0.10	0.96
Δ %	7.45	43.9	31.3	107.7	64.7	3.03	29.4	287.4
triads on Δ abs	-0.15	-0.19	+0.07	+0.14	+0.26	+0.03	+0.12	0.96
Δ %	5.88	33.3	43.8	107.7	76.4	9.09	35.3	311.47

Table 4.6 influence triads on Hs. measurements and absolute errors (Δ abs = SWAN - measurement) in metre

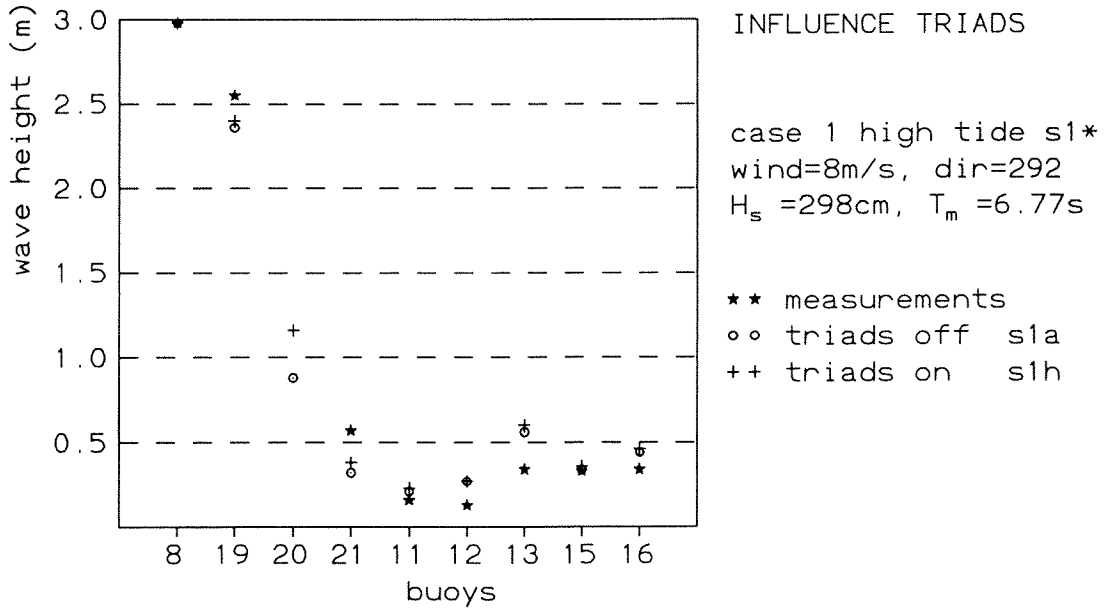

Fig. 4.10 influence triads on significant wave height

- INFLUENCE FRICTION

As can be expected the waves are bigger in case friction is switched off. This holds for all the buoy positions. The friction has mainly influence on the lower frequency waves (f≈0.1Hz) (see fig. F-5). Table 4.7 shows that it is unrealistic to do calculations without friction.

The friction formulation according to Putnam & Johnson (for which I used the default value for the wave induced friction coefficient cfw=0.01 and, because of lack of current, no current induced friction coefficient) dissipates the least amount of wave energy resulting in the highest waves (see fig.4.11 and F-6) Madsen's friction formulation gives at all buoy position the smallest waves. The absolute error between the measured wave heights and the calculated ones is smallest for the JONSWAP formulation, so this formulation comes out best.

	buoy19	buoy21	buoy11	buoy12	buoy13	buoy15	buoy16	SUM
meas. Hs	2.55	0.57	0.16	0.13	0.34	0.33	0.34	
Jonswap Δ abs	-0.19	-0.25	+0.05	+0.14	+0.22	+0.01	+0.10	0.96
Δ %	7.45	43.9	31.3	107.7	64.7	3.03	29.4	287.4
P&J Δ abs	-0.24	-0.25	+0.05	+0.19	+0.28	+0.03	+0.15	1.19
Δ%	9.41	43.9	31.3	146.2	82.4	9.09	44.0	366.3
Madsen Δ abs	-0.44	-0.26	+0.05	+0.14	+0.14	-0.02	+0.06	1.11
Δ%	17.3	45.6	31.3	107.7	41.2	6.06	17.6	266.8
friction off Δabs	+0.02	-0.24	+0.06	+0.26	+0.44	+0.07	+0.24	1.33
Δ%	0.78	42.1	37.5	200	129.4	21.2	70.6	501.6

Table 4.7 influence friction formulation on Hs. measurements and absolute errors (Δ abs = SWAN - measurement) in metre

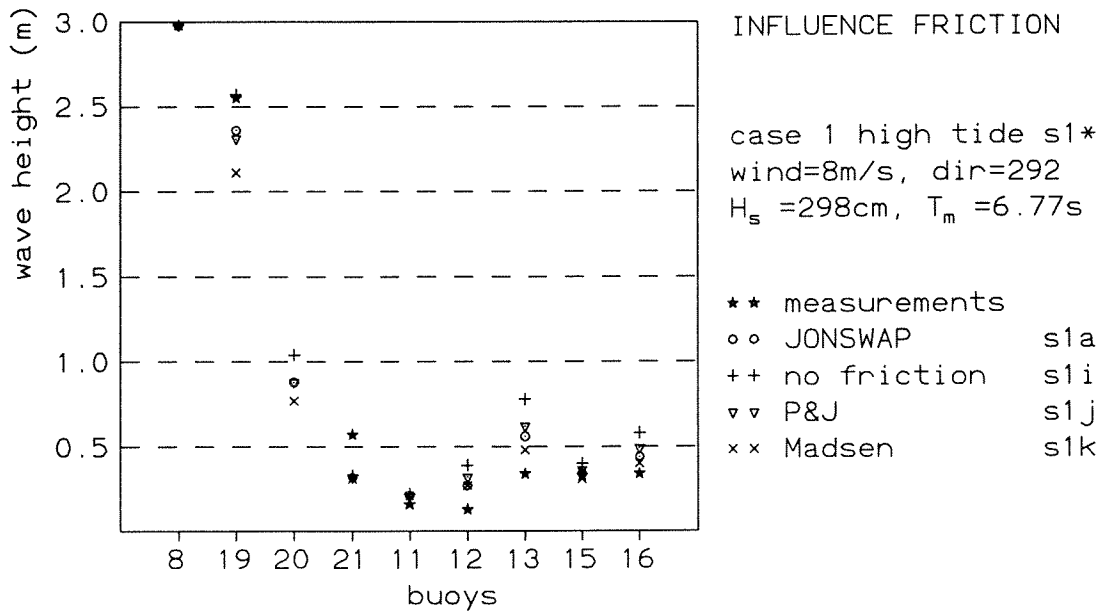

Fig. 4.11 influence friction on significant wave height

- INFLUENCE BREAKING

Switching off breaking is not very realistic. The dissipation due to breaking is of great importance for the wave height and the shape of the spectrum. Breaking influences mainly the low frequency waves (f≈0.1Hz) (see fig. F-7). The locally generated waves like the ones at the position of buoys 11 and 12 and the second peaks (f≈0.5Hz) of buoys 13, 15 and 16 show no considerable changes when breaking is either turned on or off.

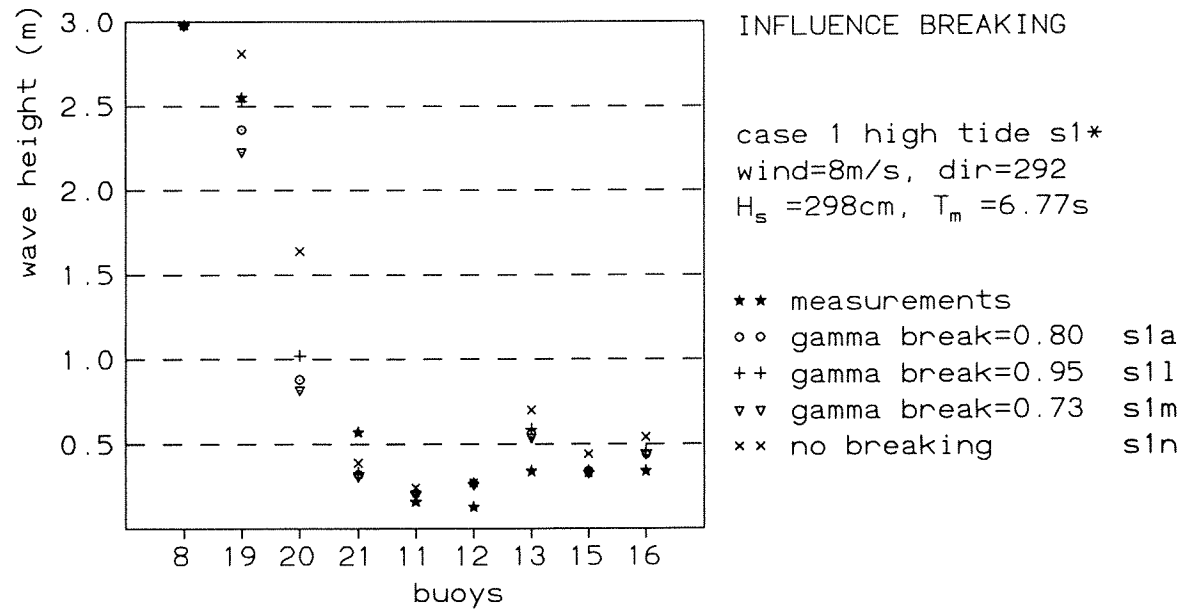

Fig. 4.12 influence breaking on significant wave height

The default value γ=0.80 gives too high waves on the Wadden Sea. In later SWAN versions the default value for γ is set equal to 0.73, giving better results in relative error. Although γ=0.95 mainly has the smallest overall absolute error because of the better performance at buoy 19, it is the best option here. The results of the calculations with different breaking coefficients can be found in fig. F-8 of appendix F and in fig. 4.12.

	buoy19	buoy21	buoy11	buoy12	buoy13	buoy15	buoy16	SUM
meas. Hs	2.55	0.57	0.16	0.13	0.34	0.33	0.34	
γ=0.80 Δ abs	-0.19	-0.25	+0.05	+0.14	+0.22	+0.01	+0.10	0.96
Δ %	7.45	43.9	31.3	107.7	64.7	3.03	29.4	287.4
γ=0.95 Δ abs	-0.02	-0.24	+0.06	+0.14	+0.25	+0.01	+0.12	0.84
Δ %	0.78	42.0	37.5	107.7	73.5	3.03	35.3	299.8
γ=0.73 Δ abs	-0.32	-0.26	+0.05	+0.13	+0.20	0	+0.10	1.06
Δ %	12.6	45.6	31.3	100.0	58.8	0	29.4	277.7
off break Δ abs	+0.26	-0.18	+0.08	+0.14	+0.36	+0.11	+0.21	1.34
Δ %	10.2	31.6	50.0	107.7	105.9	33.3	61.8	400.5

Table 4.8 Influence γbreak on Hs. measurements and absolute errors (Δ abs = SWAN - measurement) in metre

- INFLUENCE WHITECAPPING

In the third generation mode SWAN has two options representing the whitecapping dissipation; according to Komen and according to Janssen. Note that when using the Janssen formulation for whitecapping also the wind input formulation must be according to Janssen. The calculations with Janssen's whitecapping require more computational time because of the reaction of the roughness of the sea on the wind input.

From fig. 4.13 it can be seen that at every buoy position the calculations with whitecapping according to Janssen result in the smallest wave heights. Over all Janssen gives the best results. The results in spectral form can be found in fig. F-9 of the appendix.

	buoy19	buoy21	buoy11	buoy12	buoy13	buoy15	buoy16	SUM
meas. Hs	2.55	0.57	0.16	0.13	0.34	0.33	0.34	
Komen Δ abs	-0.19	-0.25	+0.05	+0.14	+0.22	+0.01	+0.10	0.96
Δ %	7.45	43.9	31.3	107.7	64.7	3.03	29.4	287.4
Janssen Δ abs	-0.21	-0.31	+0.02	+0.08	+0.13	-0.02	+0.04	0.81
Δ %	8.24	54.4	12.5	61.5	38.2	6.06	11.8	192.7

Table 4.9 influence whitecapping form. on Hs. measurements and absolute errors (Δ abs = SWAN - measurement) in metre

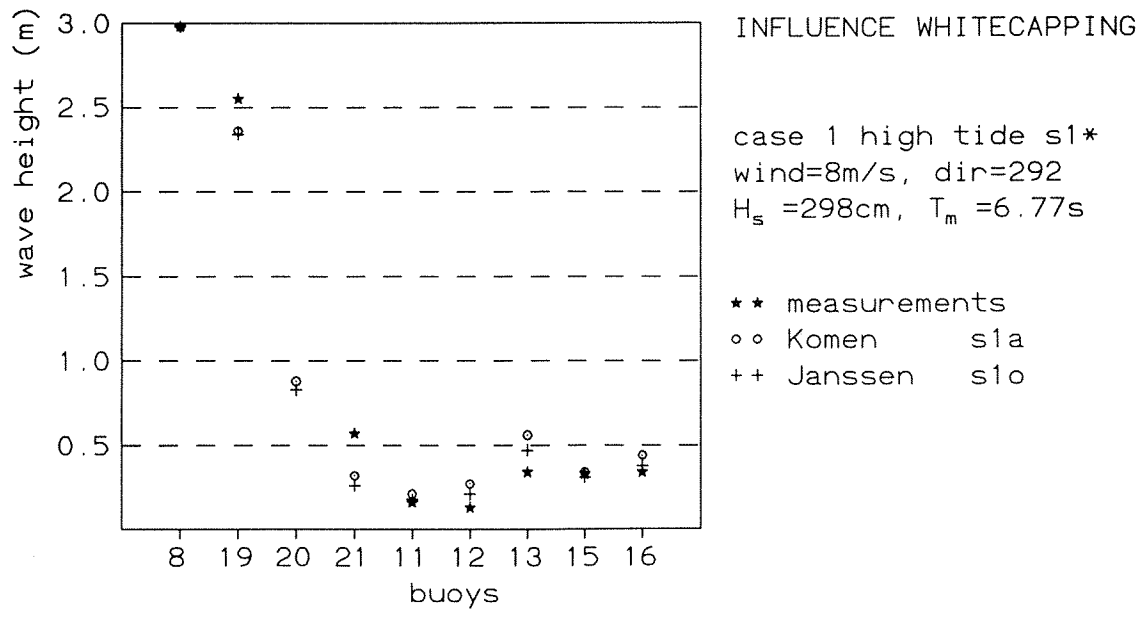

Fig. 4.13 influence whitecapping formulation on significant wave height

-INFLUENCE WATER LEVEL

Reducing the water level one metre (from the real 1.42m to 0.42m) gives considerably smaller wave heights, as can be seen in fig.4.14. The spectra at buoys 13, 15, and 16 in fig. F-10 show that the low frequency waves can not penetrate the Wadden Sea when the water level is reduced with one metre. This results in better approximations of the shape of the spectra and of the observed wave heights on the Wadden Sea.

	buoy19	buoy21	buoy11	buoy12	buoy13	buoy15	buoy16	SUM
meas. Hs	2.55	0.57	0.16	0.13	0.34	0.33	0.34	
w.l.=1.42 Δ abs	-0.19	-0.25	+0.05	+0.14	+0.22	+0.01	+0.10	0.96
Δ %	7.45	43.9	31.3	107.7	64.7	3.03	29.4	287.4
w.l.=0.42 Δ abs	-0.55	-0.29	+0.03	+0.07	+0.06	-0.07	-0.01	1.08
Δ %	21.6	50.9	18.75	53.8	17.6	21.2	2.94	186.8

Table 4.10 influence water level (w.l.) on Hs. measurements and absolute errors (Δ abs = SWAN - measurement) in metre

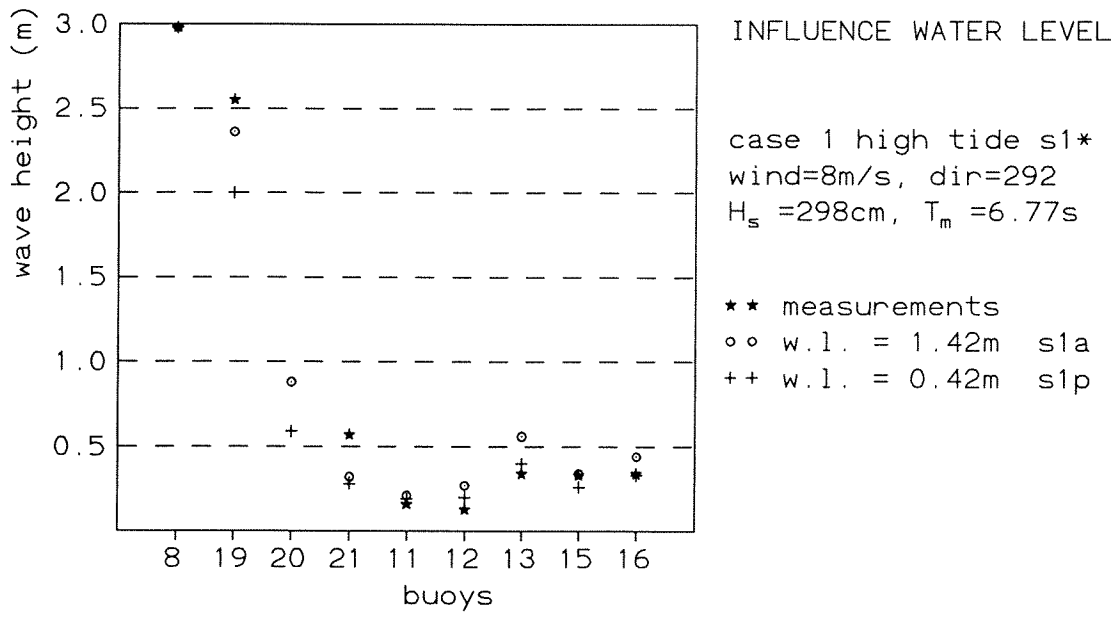

Fig. 4.14 influence water level on the significant wave height

- INFLUENCE INCOMING WAVE

The waves on the Wadden Sea do not seem to notice the 25%decrease in incoming wave height, as can be noticed from fig. 4.15. Only the waves at buoy 19 are affected by it. This implies that in this case it is not very important to know the incoming wave height exactly.

	buoy19	buoy21	buoy11	buoy12	buoy13	buoy15	buoy16	SUM
meas. Hs	2.55	0.57	0.16	0.13	0.34	0.33	0.34	
Hs_{in}=2.98 Δ abs	-0.19	-0.25	+0.05	+0.14	+0.22	+0.01	+0.10	0.96
Δ %	7.45	43.9	31.3	107.7	64.7	3.03	29.4	287.4
Hs_{in}=2.25 Δ abs	-0.44	-0.25	+0.05	+0.14	+0.22	0	+0.10	1.20
Δ %	17.3	43.9	31.3	107.7	64.7	0	29.4	294.3

Table 4.11 Influence incoming wave on Hs. measurements and absolute errors (Δ abs = SWAN - measurement) in metre

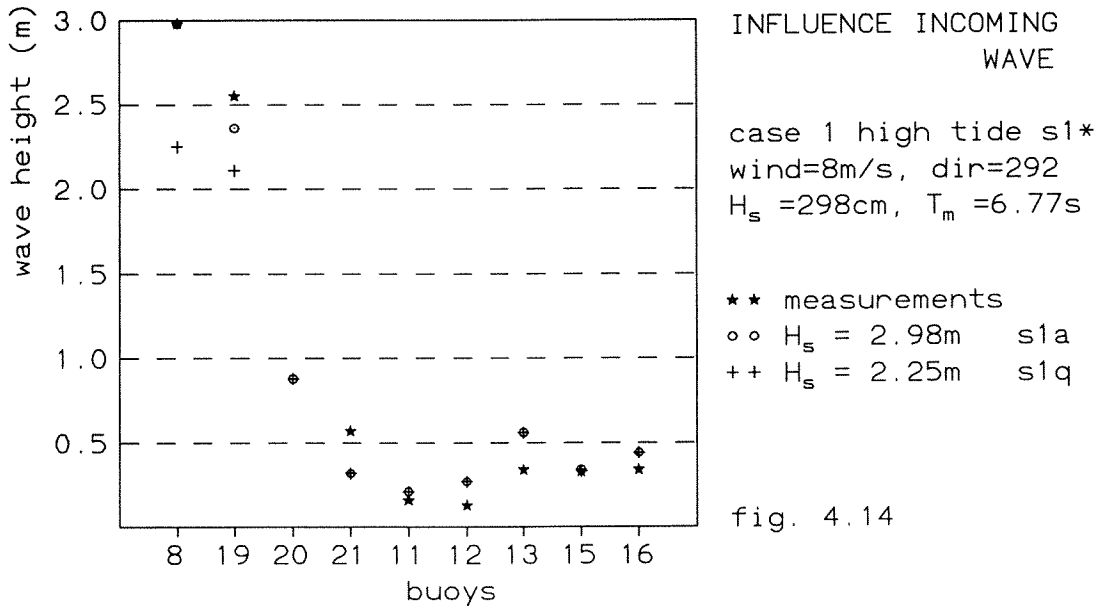

Fig. 4.15 influence incoming wave on the significant wave height

§ 4.2 HISWA Results Case 1 (high tide)

§ 4.2.1 HISWA Standard Run

The model options are described in the HISWA user manual (Booij *et al.*, 1995) The model input I used for the test cases will be given now.

- computational grid

  The origin of the computational grid is situated at (2566389 ; 5955613). The X-axis is rotated 197° anti-clockwise from the north so that it points in the direction of the main wave propagation (see fig. 4.1). In X-direction the area covers 190 meshes of 60m each and in Y-direction 125 meshes of 120m, giving an area of 11.4 x 15.0km^2. This is justified in appendix D. This computational grid does not fully correspond with the one in SWAN, because HISWA needs for the stability criterion a ratio of about 2 between the X-side of a mesh and the Y-side. In SWAN I did not use this grid because this criterion is not needed and I would rather give the bottom more or less equally well in both X- and Y-direction.

- spectral directions

  The spectral directions cover a segment of 120°, which is divided in 20 meshes of 6° .

- boundary

  The incoming waves, coming from buoy 8, are given along the seaward boundary of the computational grid in parametric form, so defined by Hs, Tm, mean wave direction and an energy distribution over the directions according to

$$D(\theta) = \cos^2(\theta)$$

  The incoming wave is assumed to be uniform along the seaward boundary

- numerical options

  For the numerical diffusion in Y-direction I add some diffusion by choosing cdn=0.5. The default value cdn=0.1, which has higher accuracy, makes the computation unstable. For the numerical diffusion in θ-direction I take the default value of cdd=0.1.

Standard run h1a, Case 1 (17.11.95 04:58)

- water level: 1.42m above N.N. (high tide)
- wind: u_{10}=8m/s, direction 292° (wind vector points 292° anti-clockwise from eastern direction)
- waves: Hs=2.98m
  T_{01}=6.77s
  mean wave direction=280°
- bottom friction: on. The coefficient for wave induced friction, cfw =0.01 (default). The bottom friction effects the mean wave frequency, and the coefficient for this has the default value bf=0.5.
- breaking: on. γ_s for shallow water breaking equals 0.8 (default) ($\gamma_s=H_{max}$/depth)
  γ_d for deep water breaking equals 1.0 (default) ($\gamma_d=H_{max}*k$)
  α (coefficient affecting the amount of dissipation due to breaking) =1.0 (default)
  frequency shift due to breaking not activated

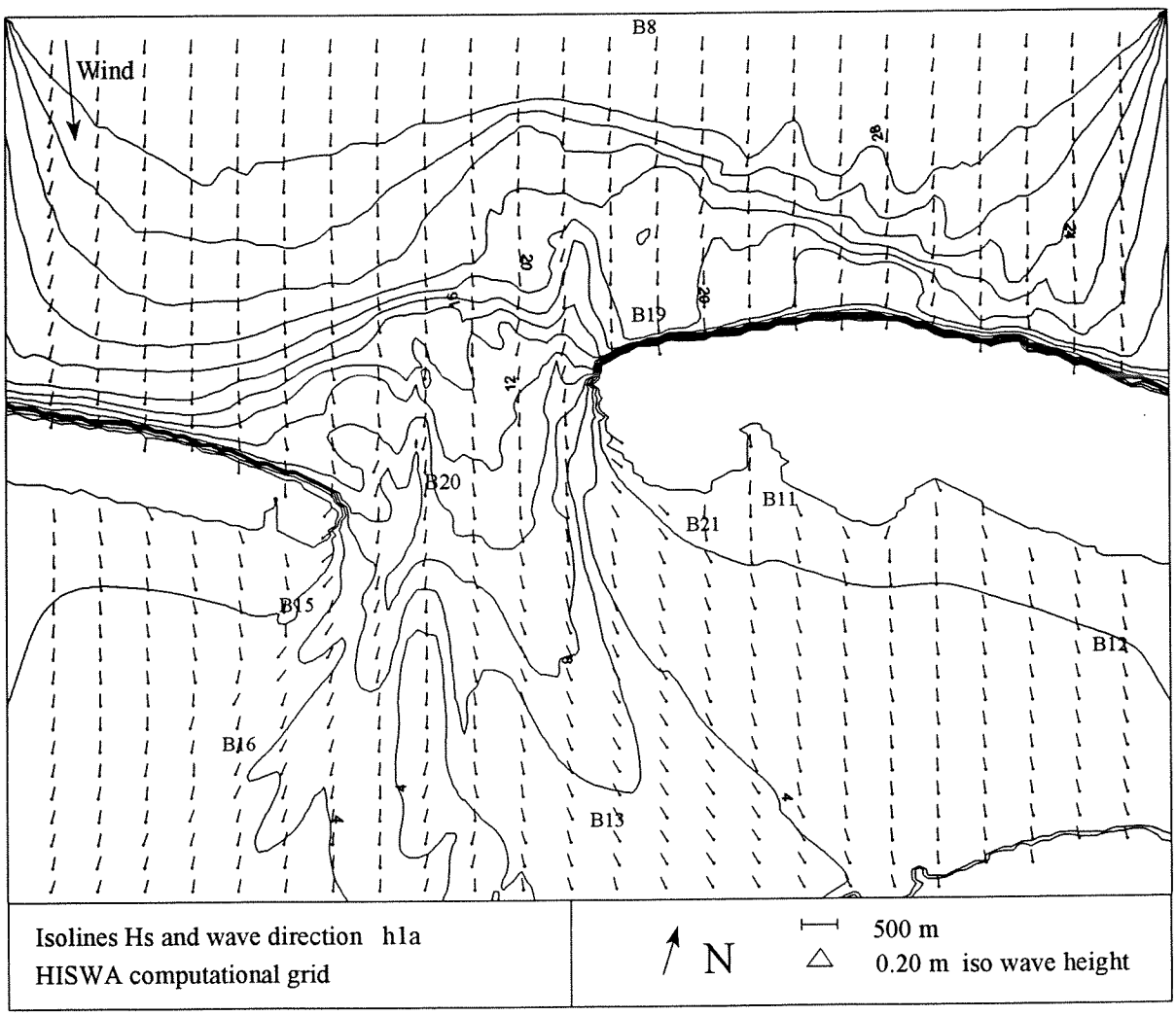

Fig 4.16 HISWA results case 1; iso wave height lines and wave direction on compgrid (values in dm)

Fig. 4.16 is a plot of the standard run showing the calculated wave heights and the direction in which the waves propagate. The decay of the waves as they propagate from the North Sea to the Wadden Sea is shown in fig. 4.17, where the significant wave height and the mean period of the standard run and the observations is plotted for the respective stations.

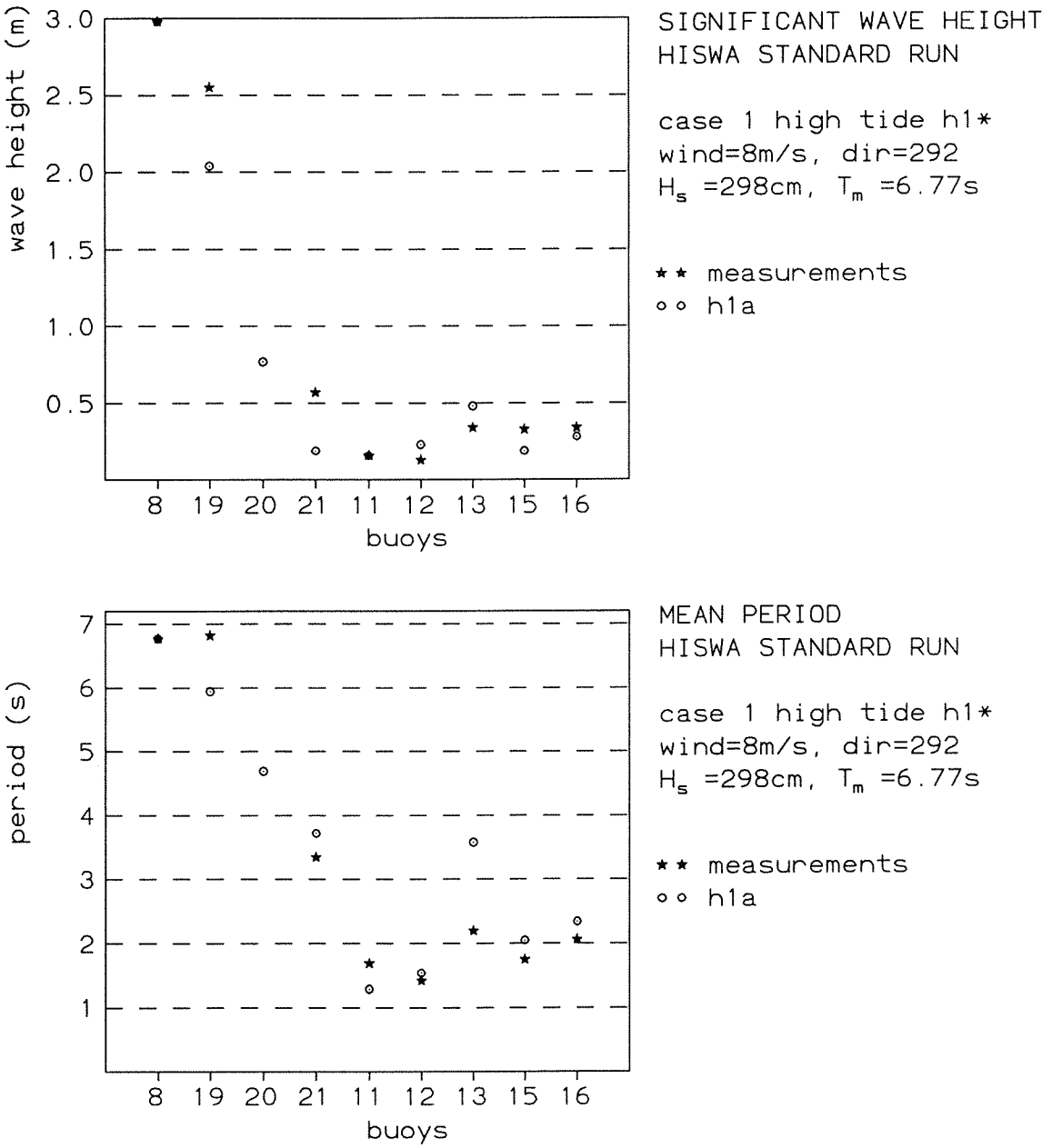

Fig. 4.17 significant wave height and period case 1

§ 4.2.2 HISWA Research Runs

As with SWAN a number of research runs has been carried out with HISWA. In each research run one input parameter is changed to find out its influence on the calculated results. Because the input options of SWAN are not the same as HISWA's input options, the research runs do not fully match either.
Table 4.12 gives an overview of the different HISWA runs that were carried out. The results can be found in table 4.13 (significant wave heights) and table 4.14 (mean periods). On the following pages the results of the research runs will be discussed.

run	wind [m/s] [°]	friction cfw	freq.shift fric /brea	$\gamma_{shallow}$	γ_{deep}	α	w.l [m]	H_s [m]	T_m [s]	dir [°]
h1a	8 292	0.01	on off	0.80	1.0	1.0	1.42	2.98	6.77	280
h1b	varying	0.01	on off	0.80	1.0	1.0	1.42	2.98	6.77	280
h1c	0.1 292	0.01	on off	0.80	1.0	1.0	1.42	2.98	6.77	280
h1d	6 292	0.01	on off	0.80	1.0	1.0	1.42	2.98	6.77	280
h1e	left part only	0.01	on off	0.80	1.0	1.0	1.42	2.98	6.77	280
h1f	8 292	0.005	on off	0.80	1.0	1.0	1.42	2.98	6.77	280
h1g	8 292	0	off off	0.80	1.0	1.0	1.42	2.98	6.77	280
h1h	8 292	0.01	off off	0.80	1.0	1.0	1.42	2.98	6.77	280
h1i	8 292	0.01	on on	0.80	1.0	1.0	1.42	2.98	6.77	280
h1j	8 292	0.01	on off	0.73	1.0	1.0	1.42	2.98	6.77	280
h1k	8 292	0.01	on off	0.95	1.0	1.0	1.42	2.98	6.77	280
h1l	8 292	0.01	on off	OFF	1.0	1.0	1.42	2.98	6.77	280
h1m	8 292	0.01	on off	0.80	20	1.0	1.42	2.98	6.77	280
h1n	8 292	0.01	on off	0.80	1.0	0.5	1.42	2.98	6.77	280
h1o	8 292	0.01	on off	0.80	1.0	1.0	0.42	2.98	6.77	280
h1p	8 292	0.01	on off	0.80	1.0	1.0	1.42	2.25	6.77	280

Table 4.12 HISWA runs case 1

run	buoy 19	buoy 20	buoy 21	buoy 11	buoy 12	buoy 13	buoy 15	buoy 16
meas.	2.55	1.04 ?	0.57	0.16	0.13	0.34	0.33	0.34
h1a	2.07	0.75	0.17	0.16	0.23	0.48	0.19	0.28
h1b	2.07	0.75	0.15	0.14	0.21	0.49	0.18	0.28
h1c	2.07	0.73	0.10	0.00	0.00	0.43	0.05	0.08
h1d	2.07	0.73	0.13	0.11	0.16	0.44	0.14	0.21
h1e	2.07	0.75	0.11	0.00	0.00	0.46	0.19	0.28
h1f	2.14	0.75	0.16	0.16	0.23	0.50	0.19	0.28
h1g	2.22	0.78	0.15	0.16	0.23	0.51	0.19	0.28
h1h	2.01	0.65	0.15	0.16	0.23	0.33	0.19	0.27
h1i	2.09	0.83	0.21	0.15	0.23	0.53	0.21	0.30
h1j	1.95	0.69	0.17	0.16	0.23	0.45	0.19	0.28
h1k	2.28	0.86	0.18	0.16	0.23	0.53	0.20	0.29
h1l	2.66	1.54	0.26	0.16	0.23	0.83	0.24	0.34
h1m	2.28	0.83	0.18	0.16	0.23	0.52	0.20	0.29
h1n	2.16	0.80	0.18	0.16	0.23	0.50	0.20	0.29
h1o	1.75	0.47	0.16	0.13	0.19	0.31	0.14	0.26
h1p	1.95	0.80	0.20	0.15	0.23	0.51	0.20	0.29

Table 4.13 HISWA results case 1; significant wave height in metre

run	buoy 19	buoy 20	buoy 21	buoy 11	buoy 12	buoy 13	buoy 15	buoy 16
meas.	6.85	?	3.35	1.69	1.42	2.20	1.75	2.06
h1a	5.94	4.69	3.72	1.29	1.54	3.58	2.05	2.34
h1b	5.94	4.69	4.15	1.24	1.47	3.53	2.13	2.38
h1c	5.94	4.69	4.88	0.06	0.06	3.67	4.50	4.31
h1d	5.94	4.69	4.26	1.12	1.34	3.65	2.24	2.46
h1e	5.94	4.69	4.66	0.00	∞	3.65	2.05	2.34
h1f	6.31	5.49	3.87	1.29	1.54	4.45	1.97	2.41
h1g	6.77	6.77	4.19	1.29	1.54	6.70	2.06	2.76
h1h	6.77	6.77	3.81	1.29	1.54	6.56	1.87	2.40
h1i	5.25	3.62	3.41	1.30	1.54	3.09	2.20	2.33
h1j	5.98	4.77	3.54	1.29	1.54	3.64	1.98	2.30
h1k	5.89	4.54	3.89	1.29	1.54	3.49	2.18	2.42
h1l	5.78	3.92	4.06	1.29	1.54	3.10	2.72	2.74
h1m	5.89	4.58	3.84	1.29	1.54	3.50	2.13	2.39
h1n	5.91	4.61	3.80	1.29	1.54	3.49	2.12	2.39
h1o	5.73	4.09	3.07	1.28	1.41	2.72	1.59	1.86
h1p	5.81	3.89	3.55	1.30	1.54	3.19	2.13	2.31

Table 4.14 HISWA results case 1; mean period* in second

*) Note that the mean period calculated by HISWA and buoys 8, 19, and 21 is T_{01}, whilst the mean period calculated by the buoys 11, 12, 13, 15 and 16 is T_{02}. For a narrow spectrum there is hardly any difference between these two. On the Wadden Sea where much energy is present in the higher frequencies T_{01} and T_{02} differ too much to compare them properly.

- INFLUENCE WIND

For the buoys on the North Sea hardly any difference is noticeable between the wave heights calculated with and without wind. From buoy 11 on the influence of the local wind becomes important, and from here on case h1c (no wind) comes out with clearly lower waves. HISWA has difficulties when no wind is given at all. Therefore I take the wind velocity 0.1m/s instead of zero. The difference in wave height between uniform and varying wind is surprisingly small. On the positions of buoy 11 and buoy 12, under the lee of the island of Norderney, the uniform wind velocity of 8m/s is 2m/s higher than the one according to the varying windfile. Still, this is hardly noticeable in the wave heights there. The absolute error is for the uniform wind run smaller than for the varying wind.

	buoy19	buoy21	buoy11	buoy12	buoy13	buoy15	buoy16	SUM
meas.Hs	2.55	0.57	0.16	0.13	0.34	0.33	0.34	
unifor.Δ abs	-0.48	-0.40	0	+0.10	+0.14	-0.14	-0.06	1.32
Δ%	18.8	70.2	0	76.9	41.2	42.4	17.6	267.1
varyin.Δ abs	-0.48	-0.42	-0.02	+0.08	+0.15	-0.15	-0.06	1.36
Δ%	18.8	73.7	12.5	61.5	44.1	45.5	17.6	253.6
u_{10}=6m/s	-0.48	-0.44	-0.05	+0.03	+0.10	-0.19	-0.13	1.42
Δ%	18.8	77.2	31.3	23.1	29.4	57.6	38.2	275.6
left part only	-0.48	-0.46	-0.16	-0.13	+0.12	-0.14	-0.06	1.55
Δ%	18.8	80.7	100	100	35.3	42.4	17.6	394.8

Table 4.15 influence wind on Hs. measurements and absolute errors (Δ abs =HISWA - measurement) in metre

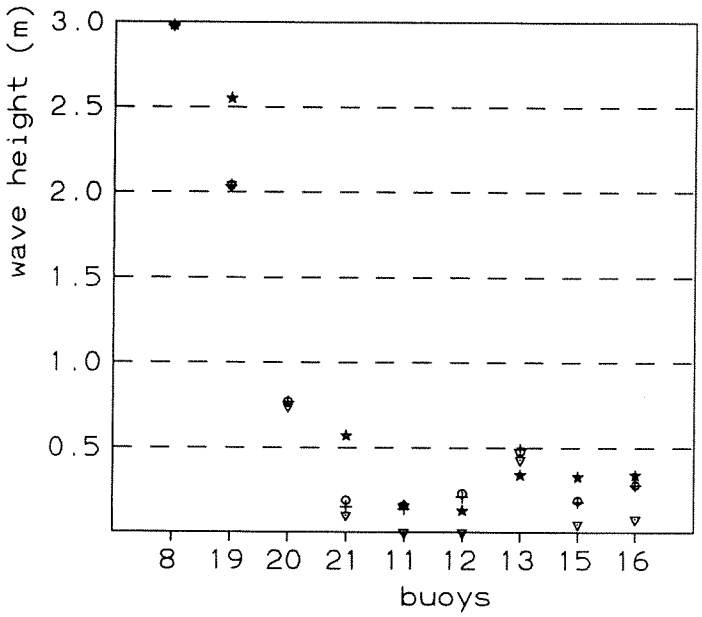

INFLUENCE WIND I

case 1 high tide h1*
wind=8m/s, dir=292
H_s =298cm, T_m =6.77s

** measurements
oo uniform wind h1a
++ varying wind h1b
▽▽ no wind h1c

fig. 4.18

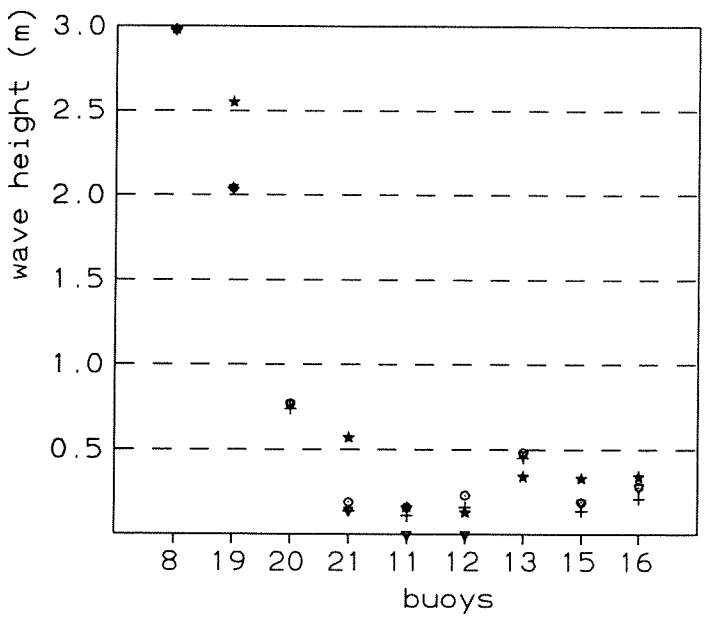

INFLUENCE WIND II

case 1 high tide h1*
wind=8m/s, dir=292
H_s =298cm, T_m =6.77s

** measurements
oo u_{10} = 8, h1a
++ u_{10} = 6, h1d
▽▽ left part only, h1e

fig. 4.19

- INFLUENCE FRICTION

Because the default value for cfw (=friction coefficient for waves) gives too low waves, I examined what would happen with respectively smaller cfw (less bottom dissipation) and no friction at all. The influence of the friction turns out to be small. Surprisingly enough at buoy21 the waves are higher in case the friction is stronger. Perhaps the waves in front of buoy 21 in case h1a (strong friction) might have been bigger, resulting in more breaking. The lower waves from case h1d and h1e just escape the breaking. The overall absolute error is smaller for the calculations with cfw=0.05. In case the frequency shift is not activated both the absolute and the relative error decreases. Especially the calculated wave height at the position of buoy 13 improves considerably.

	buoy19	buoy21	buoy11	buoy12	buoy13	buoy15	buoy16	SUM
meas.Hs	2.55	0.57	0.16	0.13	0.34	0.33	0.34	
cfw=0.01 Δ abs	-0.48	-0.40	0	+0.10	+0.14	-0.14	-0.06	1.32
Δ%	18.8	70.2	0	76.9	41.2	42.4	17.6	267.1
cfw=0.005 Δ abs	-0.41	-0.41	0	+0.10	+0.16	-0.14	-0.06	1.28
Δ%	16.6	71.9	0	76.9	47.1	42.4	17.6	272
freq.shift off Δ abs	-0.54	-0.42	0	+0.10	-0.01	-0.14	-0.07	1.28
Δ%	21.3	73.7	0	76.9	2.94	42.4	20.6	237.7

Table 4.16 influence friction on Hs. measurements and absolute errors (Δ abs = HISWA - measurement) in meter

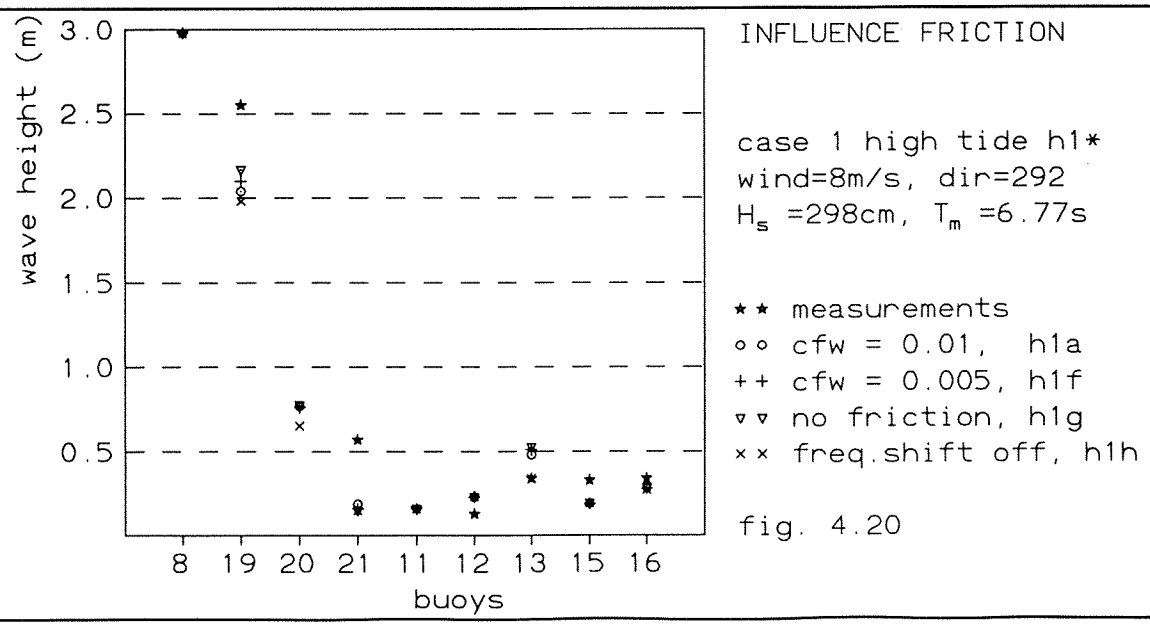

fig. 4.20

- INFLUENCE SHALLOW WATER BREAKING COEFFICIENT $\gamma_{shallow}$

Figure 4.21 shows that the default value for γ_s (=0.80) gives in general too low waves. γ_s =0.95 comes closer to the measurements. The influence of the frequency shift on the wave height is positive. In the table here below the run with frequency shift (h1g) uses γ_s =0.80

	buoy19	buoy21	buoy11	buoy12	buoy13	buoy15	buoy16	SUM
meas.Hs	2.55	0.57	0.16	0.13	0.34	0.33	0.34	
γ=0.80 Δ abs	-0.48	-0.40	0	+0.10	+0.14	-0.14	-0.06	1.32
Δ%	18.8	70.2	0	76.9	41.2	42.4	17.6	267.1
γ=0.73 Δ abs	-0.60	-0.40	0	+0.10	+0.11	-0.14	-0.06	1.41
Δ%	23.5	70.2	0	76.9	32.4	42.4	17.6	263
γ=0.95 Δ abs	-0.27	-0.39	0	+0.10	+0.19	-0.13	-0.05	1.13
Δ%	10.6	68.4	0	76.9	55.9	39.4	14.7	265.9
freq.shift on. Δ abs	-0.46	-0.36	-0.01	+0.10	+0.19	-0.12	-0.04	1.28
Δ%	18.0	63.2	0.4	76.9	55.9	36.4	11.8	262.6

Table 4.17 influence shallow breaking on Hs. measurements and absolute errors (Δ abs = HISWA - measurement) in metre

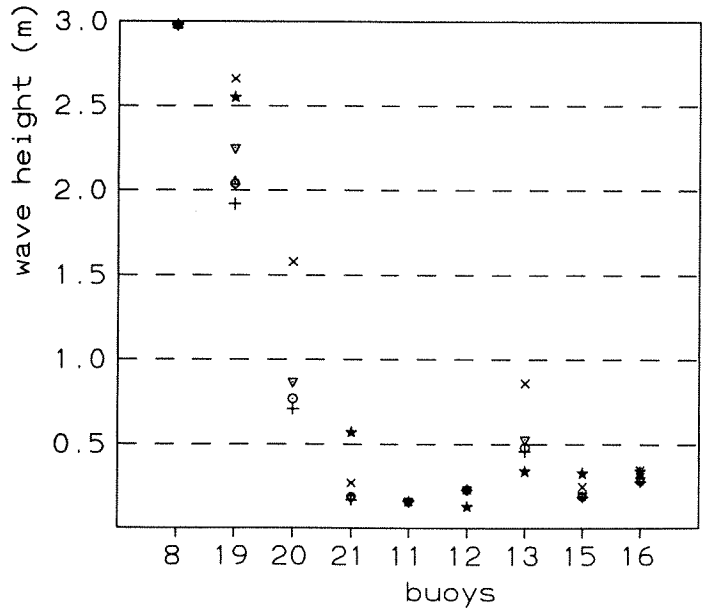

INFLUENCE GAMMA
SHALLOW BREAK (g_s)

case 1 high tide h1*
wind=8m/s, dir=292
H_s =298cm, T_m =6.77s

** measurements
oo g_s = 0.80 h1a
++ g_s = 0.73 h1j
▽▽ g_s = 0.95 h1k
×× no breaking h11
△△ frequency shift on h1i
fig. 4.21

- INFLUENCE DEEP WATER BREAKING COEFFICIENT γ_{deep}

By taking $\gamma_d = 20$ I turn off whitecapping (in case $\gamma_d = 20$ waves with lenghts as small as 4 metre still need heights of 80 metre or more before whitecapping occurs.). At buoy 9, buoy 20 and buoy 13, so in areas that can be reached by the waves that come from the North Sea, the influence of whitecapping is greatest. The table shows that too much wave energy is dissipated by the whitecapping mechanism and that the calculations without whitecapping approximate the measurements better.

	buoy19	buoy21	buoy11	buoy12	buoy13	buoy15	buoy16	SUM
meas.Hs	2.55	0.57	0.16	0.13	0.34	0.33	0.34	
γ_{deep}= 1 Δ abs	-0.48	-0.40	0	+0.10	+0.14	-0.14	-0.06	1.32
Δ%	18.8	70.2	0	76.9	41.2	42.4	17.6	267.1
γ_{deep}= 20 Δ abs	-0.27	-0.39	0	+0.10	+0.18	-0.13	-0.05	1.12
Δ%	10.6	68.4	0	76.9	52.9	39.4	14.7	264.9

Table 4.18 Influence deep breaking on Hs. measurements and absolute errors (Δ abs = HISWA - measurement) in metre

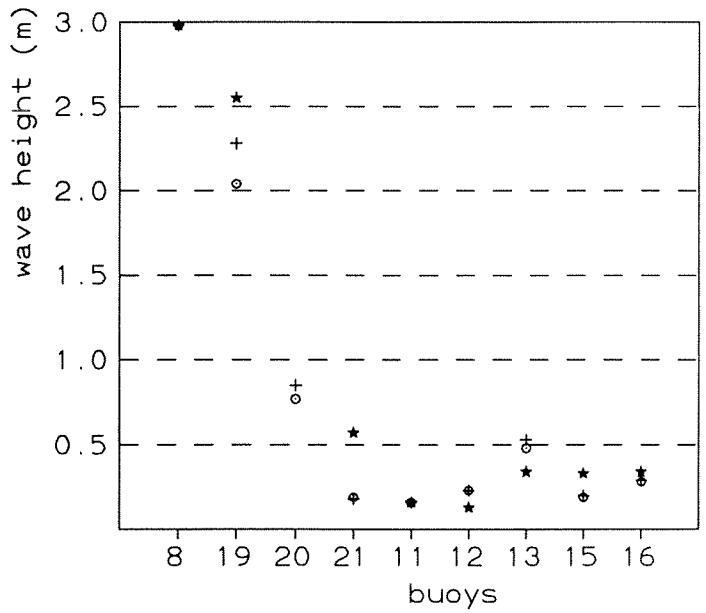

INFLUENCE GAMMA
DEEP BREAK (g_d)

case 1 high tide h1*
wind=8m/s, dir=292
H_s =298cm, T_m =6.77s

** measurements
oo g_d = 1.0 h1a
++ g_d = 20 h1m

fig. 4.22

- INFLUENCE ALPHA BREAK α

In HISWA one can influence the effect of breaking on wave height in three different ways. The first two ways are varying γ_s and γ_d, with which the maximum wave height before the waves break is influenced. The third manner is varying the amount of energy that is dissipated when the waves break.This can be done by changing α. A larger value of α corresponds to a larger rate of dissipation. Because the default value of α (=1.0) gave too low waves I halved α. This leads to higher waves, closer to the measurements .

	buoy19	buoy21	buoy11	buoy12	buoy13	buoy15	buoy16	SUM
meas.Hs	2.55	0.57	0.16	0.13	0.34	0.33	0.34	
α=1.0 Δ abs	-0.48	-0.40	0	+0.10	+0.14	-0.14	-0.06	1.32
Δ%	18.8	70.2	0	76.9	41.2	42.4	17.6	267.1
α=0.5 Δ abs	-0.39	-0.39	0	+0.10	+0.16	-0.13	-0.05	1.22
Δ%	15.3	68.4	0	76.9	47.1	39.4	14.7	261.8

Table 4.19 influence α breaking on Hs. measurements and absolute errors (Δ abs = HISWA - measurement) in metre

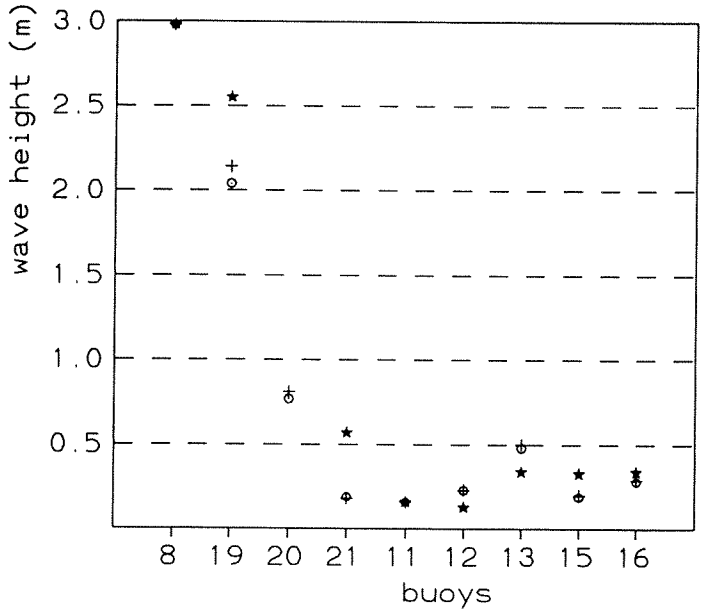

INFLUENCE ALPHA BREAK (a)

case 1 high tide h1*
wind=8m/s, dir=292
H_s =298cm, T_m =6.77s

** measurements
oo a = 1.0, h1a
++ a = 0.5, h1n

fig. 4.23

- INFLUENCE WATER LEVEL

From table 4.20 one can see that at some places a change in water depth influences the wave heights much more than at other places. The water depth is an important parameter, so effort should be made to have a good knowledge of bottom position and water level.

	buoy19	buoy21	buoy11	buoy12	buoy13	buoy15	buoy16	SUM
meas.Hs	2.55	0.57	0.16	0.13	0.34	0.33	0.34	
w.l = 1.42 Δ abs	-0.48	-0.40	0	+0.10	+0.14	-0.14	-0.06	1.32
Δ%	18.8	70.2	0	76.9	41.2	42.4	17.6	267.1
w.l.= 0.42 Δ abs	-0.80	-0.41	-0.03	+0.06	-0.03	-0.19	-0.08	1.60
Δ%	31.4	71.9	18.8	46.2	8.82	57.6	23.5	258.2

Table 4.20 influencewater level (=w.l.) on Hs. measurements and absolute errors (Δ abs = HISWA - measurement) in metre

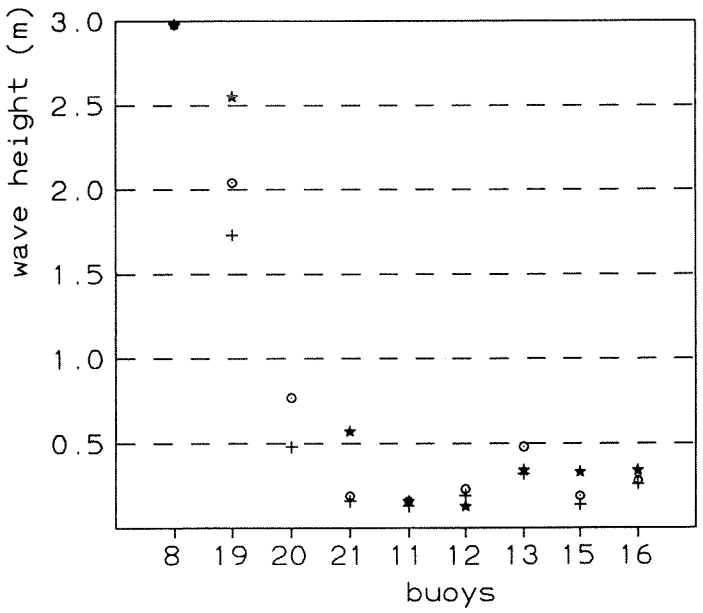

INFLUENCE WATER LEVEL

case 1 high tide h1*
wind=8m/s, dir=292
H_s =298cm, T_m =6.77s

** measurements
oo w.l. = 1.42m, h1a
++ w.l. = 0.42m, h1o

fig. 4.24

- INFLUENCE INCOMING WAVE

Only the waves at buoy 19 seem to notice the 25% decrease in wave height of the incoming wave. The waves on the Waden Sea are not affected by it. This implies that it is not necessary to know the incoming wave height exactly to obtain good results on the Wadden Sea.

	buoy19	buoy21	buoy11	buoy12	buoy13	buoy15	buoy16	SUM
meas.Hs	2.55	0.57	0.16	0.13	0.34	0.33	0.34	
Hs_{in}=2.98 Δ abs	-0.48	-0.40	0	+0.10	+0.14	-0.14	-0.06	1.32
Δ%	18.8	70.2	0	76.9	41.2	42.4	17.6	267.1
Hs_{in}=2.25 Δ abs	-0.60	-0.37	-0.01	+0.10	+0.14	-0.17	-0.05	1.43
Δ%	23.5	64.9	6.25	76.9	41.2	50.0	14.7	275.7

Table 4.21 influence incoming wave on Hs. measurements and absolute errors (Δ abs = HISWA - measurement) in metre

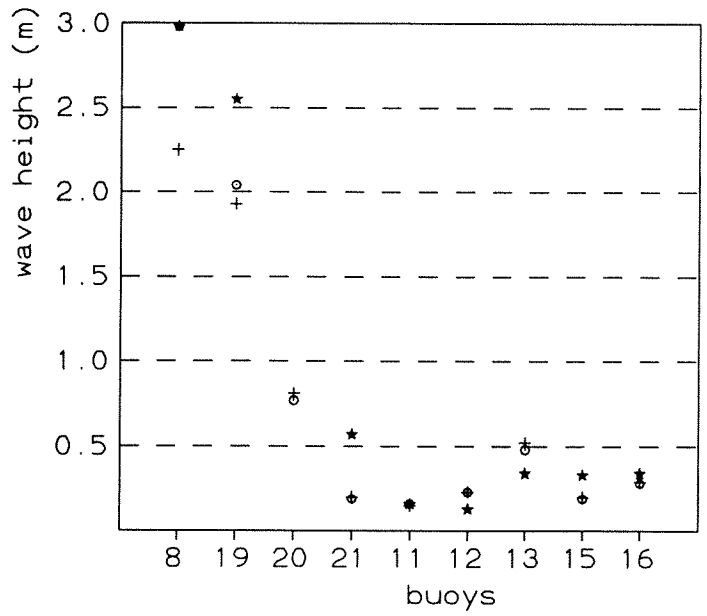

INFLUENCE INCOMING WAVE

case 1 high tide h1*
wind=8m/s, dir=292
H_s =298cm, T_m =6.77s

** measurements
oo Hs_{in} =2.98, h1a
++ Hs_{in} =2.25, h1p

fig. 4.25

Chapter 5

Results Case 2 (low tide)

... in which the actual modelling is reported for the low tide case. The input for both SWAN and HISWA is given and the results are presented and analysed.

Case 2 is the situation on November 16th 1995, at 22:58. The significant wave height at that time at the position of buoy 8 is 2.84m. The North-Eastern wind blows with a speed of u_{10}=13m/s. It is low tide so the tidal currents are expected to be small.
I varied several parameters in SWAN and HISWA to examine the influence on the wave heights and on the one dimensional spectrum (for SWAN only). § 5.1 deals with SWAN. First the standard run, next the research runs. HISWA comes up in § 5.2, also with standard run and research runs. The different runs have a three-character code. The first letter refers to SWAN (s) or HISWA (h). The second character refers to the case. In chapter 5 only case 2 can be found, whereas chapter 4 deals with case 1. The last character refers to the different runs (see table 5.1 and table 5.12).
The results of the research runs are handled as follows: In SWAN the 1D-spectra are produced (see appendix G). The computed significant wave height is compared with the measured significant wave height. Per buoy the absolute error is calculated and the relative error. Per research run these absolute errors are added and the relative errors too. The run with the smallest absolute error is considered best.

§ 5.1 SWAN Results Case 2 (low tide)

§ 5.1.1 SWAN Standard Run

The model options are described in the SWAN user manual (Ris *et al.*, 1995). Part of the model input I used is the same as for the high tide situation, e.g. the resolution and position of the computational grid, the frequency domain, the way the boundary is given, and the numerical options. For this information I refer to § 4.1.1. Starting from a standard run I will vary several parameters to find out how the model approximates the measurements best and to examine the influence of the parameters. The input for the standard run follows below. Except for γ_{break} the standard run uses default values where possible. I used a smaller value for γ_{break} than the default value of 0.8, because that resulted from the precalculations.

Standard run s2a, Case 2 (16.11.95 22:58)

- water level: 0.07m below N.N. (low tide)
- wind: u_{10}=13m/s, direction 315° (wind vector points 315° anti-clockwise from eastern direction)
- quadruplets: on (default)
- bottom friction: JONSWAP, Γ=0.067m^2/s^3 (default). Γ is the friction coefficient for wind sea conditions
- breaking: γ=0.60 (no default!) ($\gamma=H_{max}$/depth)
  α=1.0 (default) (α is a coefficient determining the rate of dissipation)
- wind input formulation: third generation, sny3 (default), with all default values.
  sny3 indicates a third generation wind input model according to Cavaleri and Malanotte-Rizzoli, 1981 and Snyder *et al.*, 1981 and Komen *et al.*, 1984
- whitecapping: formulation according to Komen (default), with all default values

Fig. 5.1 shows the calculated wave heights and the propagation direction of the waves. It is interesting to see how closely the isolines of the wave heights match the depth contour lines (see fig. 5.2) Within SWAN deeper channels allow the waves to propagate further down the Wadden Sea. The arrows, representing the wave direction, point in any direction (unlike HISWA, see fig. 5.14) Along the south coast of Norderney the waves refract towards the coast. The direction of the channel from buoy 21 to buoy 12 is followed well by the waves. Also some other bottom features can be recognized from the wave propagation direction, like the channel pointing south east from buoy20 and the one in the same direction halfway between buoy 11 and buoy 12.

In fig. 5.3 the observed and the calculated spectra are presented. When examining the spectra it is important to realise the difference in scale of the spectral density. To illustrate this, the observed spectra are presented in two ways: First, in fig. 5.3a on a scale that all plots have roughly the same height on the page; next, in fig. 5.3b all observed spectra together on one linear scale to show the huge decrease in wave energy from buoy 8 to the Wadden Sea buoys. The energy at the peak frequency of buoy 16 is approximately 2‰ of the energy at the peak frequency of buoy 8. The

decay of the waves as they propagate from the North Sea to the Wadden Sea is shown in fig. 5.4, where the significant wave height and the mean period of the standard run and the observations is plotted for the respective stations.

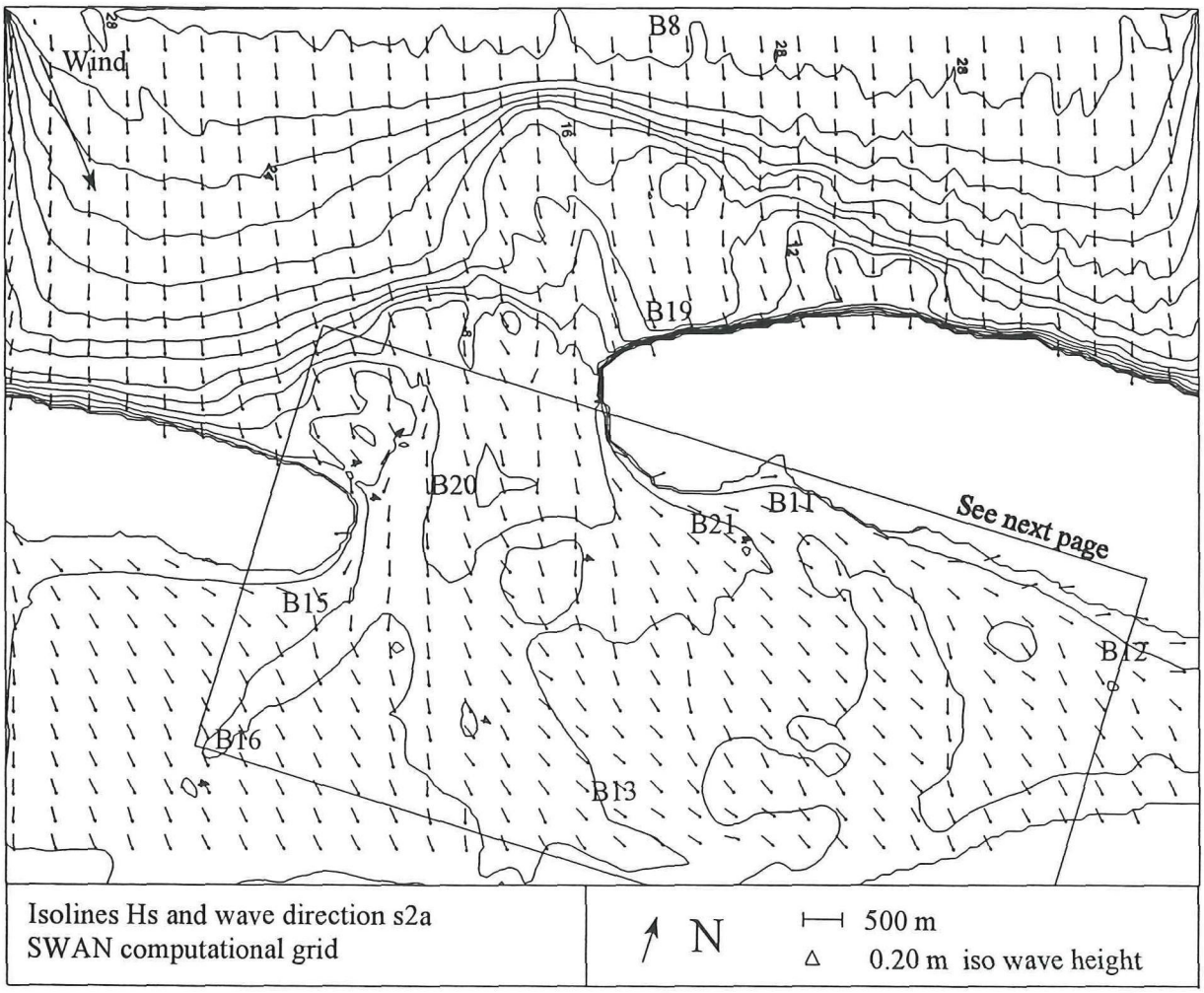

Fig. 5.1 SWAN results case 2; iso wave height lines and wave direction on compgrid (values in dm)

SWAN standard run case 2 (t2a) fig. 5.2

Wave height

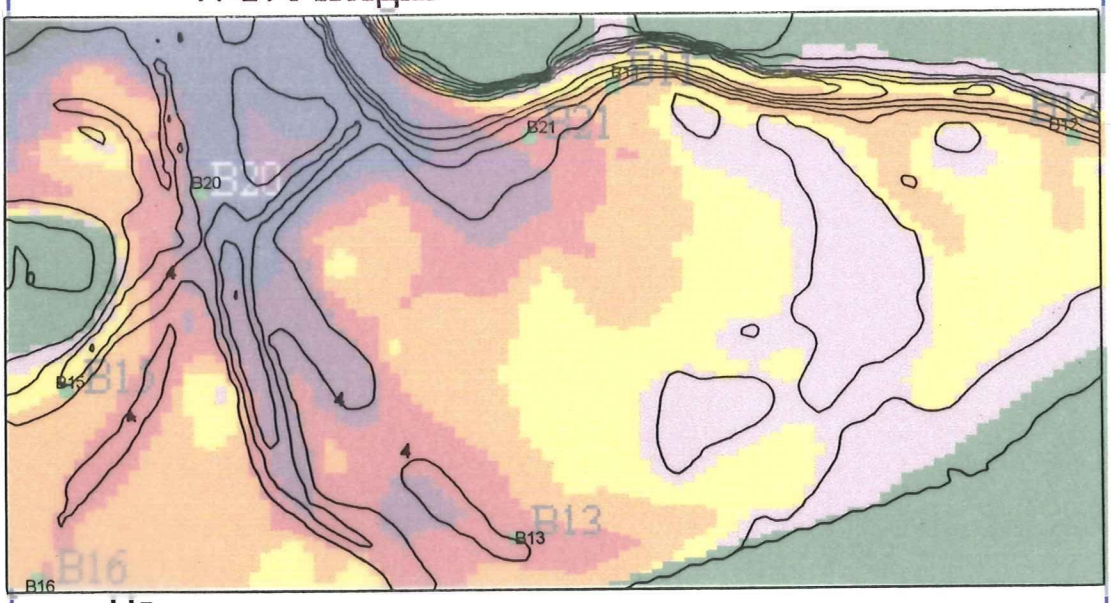

Hs
Land
0 - 0.2 m
0.2 - 0.3 m
0.3 - 0.4 m
0.4 - 0.5 m
0.5 - 0.6 m
0.6 - 0.8 m
0.8 - 1.0 m
1.0 - 2.26 m

N

1000 0 1000 2000
meter

Per
Land
0 - 1 s
1 - 1.4 s
1.4 - 1.7 s
1.7 - 2 s
2 - 2.5 s
2.5 - 3.5 s
3.5 - 6.3 s

Period

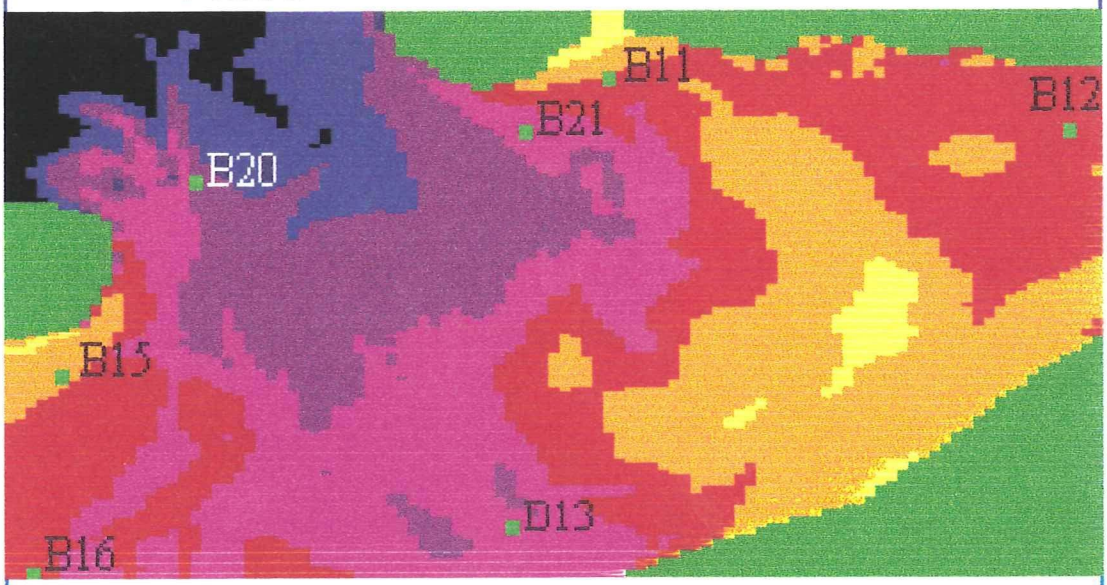

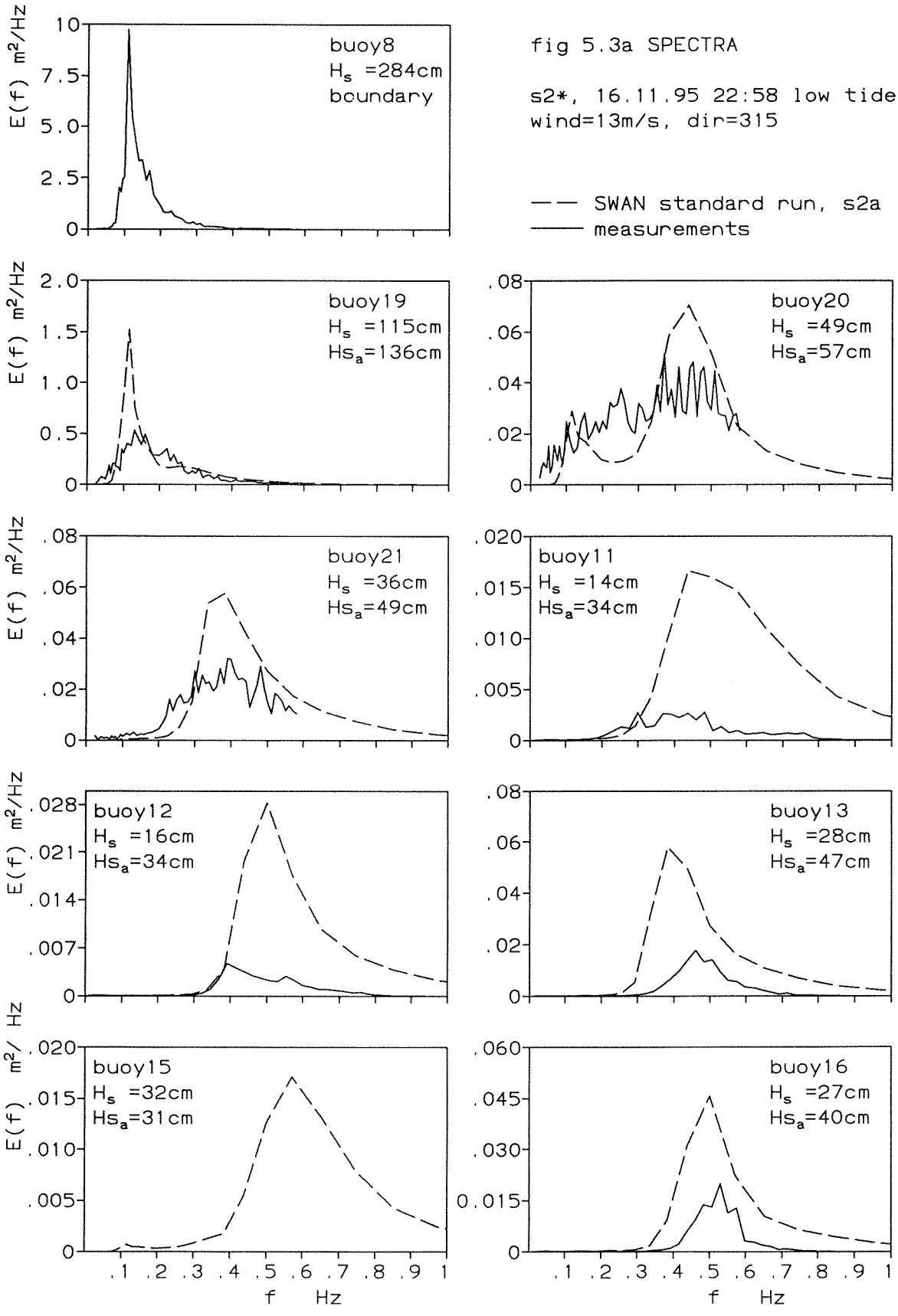

fig 5.3a SPECTRA

s2*, 16.11.95 22:58 low tide
wind=13m/s, dir=315

—— SWAN standard run, s2a
—— measurements

fig 5.3b SPECTRA

s2*, 16.11.95 22:58 low tide
wind=13m/s, dir=315

in decreasing order:
—— buoy 8, 19, 20, 21,
11, 12, 13 and 16

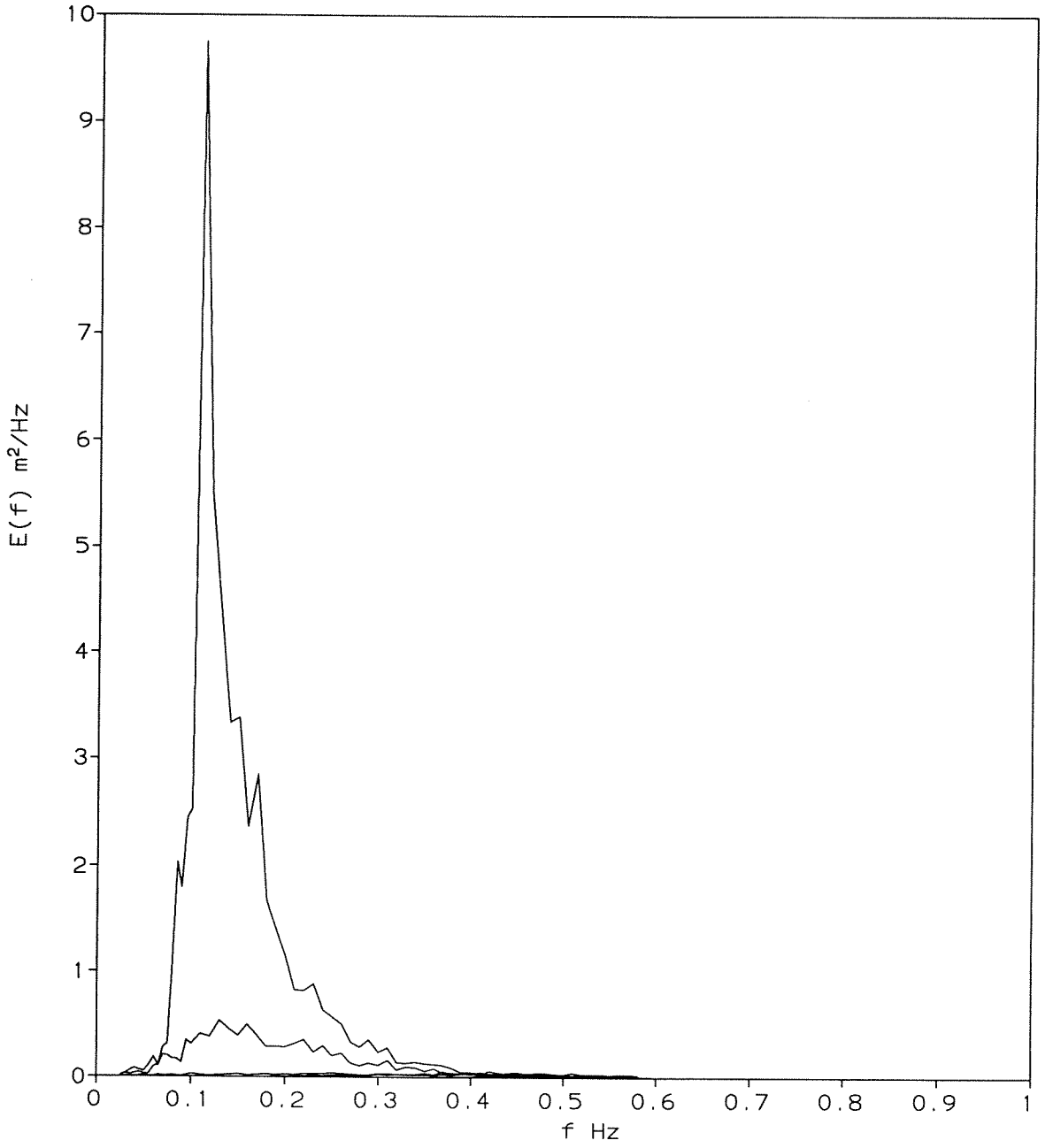

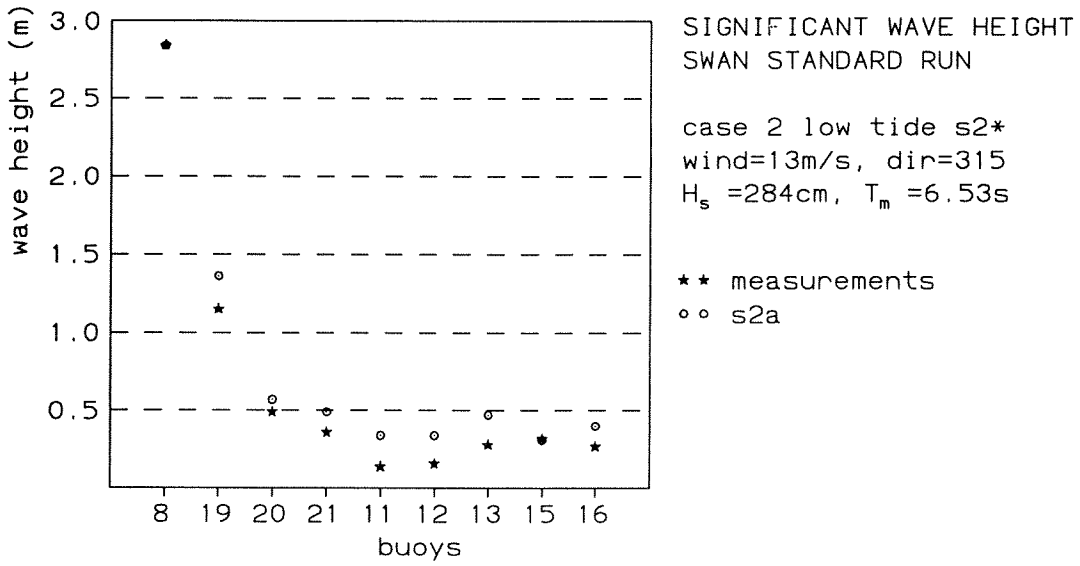

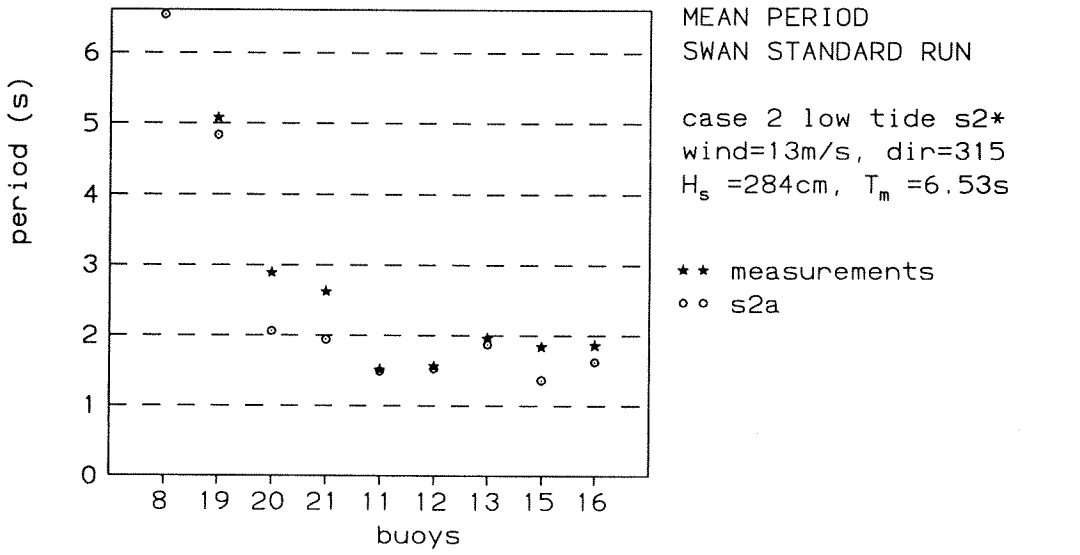

Fig. 5.4 significant wave height and period case 2

§ 5.1.2 SWAN Research Runs

As with the high tide case, also in the low tide case the standard run is followed by a number of research runs. The varying wind field was not available for case 2 so no experiment regarding varying wind is made. Concerning the breaking coefficient one more research run has been carried out in case 2, namely with a varying breaker coefficient γ_s. This γ_s is dependent on the bottom slope. For the rest, the research runs of case 2 correspond with those of case 1.
Table 5.1 gives an overview of the different SWAN runs I made. The results can be found in table 5.2 (significant wave height), table 5.3 (mean period), and in the figures on the following pages. The one dimensional spectra can be found in appendix G. In this paragraph I will take a closer look at the influence of the different parameters.

run	generation	wind [m/s]	[°]	triads	friction	γ break	whitecapp	w.level [m]	incoming waves
s2a	3rd (sny)	13	315	OFF	JONSWAP	0.60	Komen	-0.07	100%
s2b	2nd	13	315	OFF	JONSWAP	0.60	OFF	-0.07	100%
s2c	1st	13	315	OFF	JONSWAP	0.60	OFF	-0.07	100%
s2d	3rd (sny)	0	0	OFF	JONSWAP	0.60	Komen	-0.07	100%
s2e	3rd (sny)	10	315	OFF	JONSWAP	0.60	Komen	-0.07	100%
s2f	3rd (sny)	left part only		OFF	JONSWAP	0.60	Komen	-0.07	100%
s2g	3rd (sny)	13	315	ON	JONSWAP	0.60	Komen	-0.07	100%
s2h	3rd (sny)	13	315	OFF	OFF	0.60	Komen	-0.07	100%
s2i	3rd (sny)	13	315	OFF	P&J	0.60	Komen	-0.07	100%
s2j	3rd (sny)	13	315	OFF	Madsen	0.60	Komen	-0.07	100%
s2k	3rd (sny)	13	315	OFF	JONSWAP	0.80	Komen	-0.07	100%
s2l	3rd (sny)	13	315	OFF	JONSWAP	0.73	Komen	-0.07	100%
s2m	3rd (sny)	13	315	OFF	JONSWAP	gamvar	Komen	-0.07	100%
s2n	3rd (sny)	13	315	OFF	JONSWAP	OFF	Komen	-0.07	100%
s2o	3rd (jans)	13	315	OFF	JONSWAP	0.60	Janssen	-0.07	100%
s2p	3rd (sny)	13	315	OFF	JONSWAP	0.60	Komen	-1.07	100%
s2q	3rd (sny)	13	315	OFF	JONSWAP	0.60	Komen	-0.07	75%

Table 5.1 SWAN runs case 2

run	buoy19	buoy20	buoy21	buoy11	buoy12	buoy13	buoy15	buoy16
meas.	1.15	0.49	0.36	0.14	0.16	0.28	0.32	0.27
s2a	1.36	0.57	0.49	0.34	0.34	0.47	0.31	0.40
s2b	1.45	0.51	0.51	0.33	0.35	0.51	0.28	0.39
s2c	1.42	0.38	0.35	0.20	0.21	0.37	0.17	0.26
s2d	1.26	0.21	0.04	0.01	0.00	0.02	0.03	0.01
s2e	1.29	0.48	0.38	0.26	0.27	0.38	0.25	0.32
s2f	1.36	0.57	0.32	0.14	0.01	0.34	0.31	0.40
s2g	1.38	0.58	0.49	0.34	0.34	0.47	0.31	0.40
s2h	1.47	0.60	0.49	0.34	0.35	0.50	0.35	0.47
s2i	1.38	0.59	0.49	0.34	0.35	0.49	0.34	0.45
s2j	1.28	0.54	0.49	0.34	0.34	0.42	0.31	0.38
s2k	1.75	0.64	0.50	0.34	0.35	0.50	0.32	0.41
s2l	1.61	0.62	0.50	0.34	0.35	0.49	0.32	0.41
s2m	1.44	0.57	0.49	0.34	0.34	0.46	0.31	0.40
s2n	2.49	1.10	0.53	0.36	0.34	0.53	0.39	0.44
s2o	1.32	0.53	0.45	0.31	0.32	0.42	0.29	0.36
s2p	1.04	0.41	0.44	0.32	0.30	0.31	0.24	0.22
s2q	1.37	0.57	0.49	0.34	0.34	0.47	0.31	0.40

Table 5.2 SWAN results case 2; significant wave height in metre

run	buoy19	buoy20	buoy21	buoy11	buoy12	buoy13	buoy15	buoy16
meas.	5.08	2.89	2.62	1.51	1.56	1.96	1.84	1.86
s2a	4.84	2.06	1.94	1.49	1.52	1.87	1.36	1.62
s2b	4.94	2.18	2.15	1.59	1.60	2.07	1.34	1.68
s2c	5.53	2.55	2.28	1.69	1.66	2.23	1.48	1.81
s2d	7.46	6.81	4.79	3.60	6.51	5.07	6.41	5.06
s2e	5.35	2.01	1.76	1.33	1.37	1.75	1.26	1.48
s2f	4.85	2.06	2.14	1.77	0.80	1.89	1.36	1.62
s2g	4.23	2.10	1.94	1.50	1.52	1.88	1.37	1.62
s2h	5.21	2.25	1.93	1.49	1.54	2.00	1.50	1.82
s2i	4.89	2.15	1.95	1.49	1.53	1.96	1.46	1.76
s2j	4.53	1.96	1.93	1.49	1.51	1.74	1.35	1.55
s2k	5.62	2.29	1.97	1.52	1.52	1.94	1.39	1.63
s2l	5.40	2.21	1.96	1.51	1.52	1.92	1.38	1.63
s2m	5.03	2.08	1.94	1.49	1.52	1.86	1.36	1.62
s2n	6.65	4.57	2.03	1.52	1.48	2.01	1.59	1.68
s2o	5.07	2.05	1.92	1.43	1.49	1.86	1.35	1.59
s2p	3.93	1.60	1.79	1.43	1.41	1.47	1.15	1.20
s2q	4.74	2.07	1.94	1.49	1.52	1.88	1.37	1.62

Table 5.3 SWAN results case 2; mean period* in second

*) Note that the mean period calculated by SWAN and buoys 8, 19, 20 and 21 is T_{01}, whilst the mean period calculated by the buoys 11, 12, 13, 15 and 16 is T_{02}. For a narrow spectrum there is hardly any difference between these two. On the Wadden Sea where much energy is present in the higher frequencies T_{01} and T_{02} differ too much to compare them properly.

- INFLUENCE GENERATION

Fig. 5.5 shows that at almost all buoy positions the first generation run calculates the smallest wave heights, except for buoy 19. At the higher frequencies ($f \geq 0.8$) the order in wave height from big to small is always third generation, second generation, first generation. This can be seen in fig. G-1 of appendix G. Because of the lack of calculating a possible overshoot the first generation is smallest at the higher frequencies.

The measurements are approximated best by the run with first generation wind input formulation. This is somehow surprising because the third generation mode includes some processes which are not modelled in the first and second generation mode, but which are generally recognized to take place in reality. For instance the above-mentioned overshoot (because of the nonlinear interactions).

The second generation run often results in the highest waves. The reason for this is the fact that the saturation level (the amount of energy till which the spectrum may grow until an equilibrium level is reached) is not linearly dependent on a constant α as in the first generation, but this α varies with the total wave energy of the wind sea part of the spectrum. If α is high, the spectrum grows much bigger than the spectrum calculated with the first generation mode.

	buoy19	buoy20	buoy21	buoy11	buoy12	buoy13	buoy15	buoy16	SUM
meas.Hs	1.15	0.49	0.36	0.14	0.16	0.28	0.32	0.27	
3rd gen Δ abs	+0.21	+0.08	+0.13	+0.20	+0.18	+0.19	-0.01	+0.13	1.13
Δ %	18.3	16.3	36.1	142.9	112.5	67.9	3.13	48.1	445.2
2nd gen Δ abs	+0.30	+0.02	+0.15	+0.19	+0.19	+0.23	-0.04	+0.12	1.24
Δ %	26.1	4.08	41.7	135.7	118.8	82.1	12.5	44.4	465.4
1st gen Δ abs	+0.27	-0.11	-0.01	+0.06	+0.05	+0.09	-0.15	-0.01	0.75
Δ %	23.5	22.4	2.78	42.9	31.3	32.1	46.9	3.70	205.6

Table 5.4 influence generation on Hs. measurements and absolute errors (Δ abs= SWAN - measurement) in metre

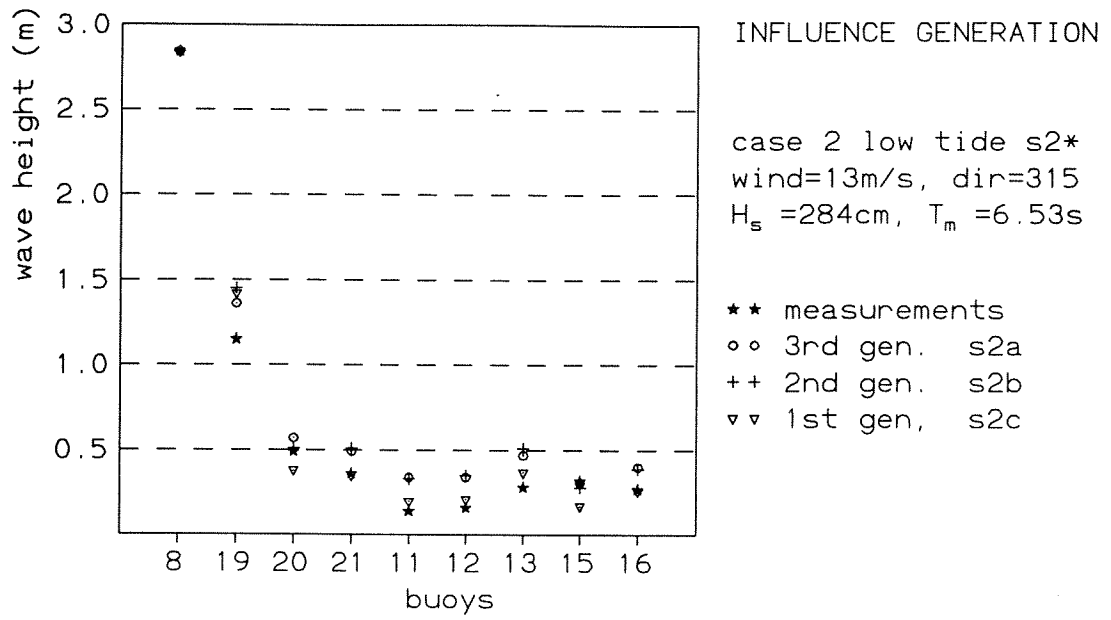

Fig. 5.5 influence generation on significant wave height

- INFLUENCE WIND

The calculations without wind are not realistic but they give an idea of the influence of the local wind. The results of these calculations can be found in fig. 5.6. Especially with low tide, the local wind is the main source for the waves on the Wadden Sea. The water is too shallow for the waves generated on the North Sea to enter the Wadden Sea (see fig G-2) unlike case 1 (see fig. F-2), where some waves can penetrate till buoy 13.

When decreasing the wind velocity with 25% (from u_{10}= 13m/s to u_{10}=10m/s) the calculated wave heights at all buoy positions decrease.

In the 'left-part-only-run' wind is just blowing over the left part of the computational grid (see fig.4.7), so no local wind is available for buoy 21, 11 and 12. This is done to examen to which extent the waves along the south coast of Norderney are generated by local wind or by the transportation of wave energy from the North Sea, within SWAN. The results can be found in fig. 5.7. Of the 34cm wave height at buoy 11 calculated in the standard run, 14cm are left over when the local wind is eliminated, and is thus coming from the North Sea. Looking at the spectrum of buoy 11 in fig. G-3, run s2f ('left-part-only') approximates the measured spectrum very well. This is somehow surprising, because during the measurements a quite severe wind was blowing, which I would expect to influence the waves there. For the waves at the position of buoy 12, the wind is clearly more important than at buoy 11. Firstly because buoy 12 is much further away from the Norderneyer Seegat, secondly because the fetch is larger. Here, only 1cm is left over in run s2f from the 34cm of run s2a.

Overall, SWAN seems to overestimate the wave heights not only because of too much transport of wave energy, but also because of too much local wave growth due to the wind.

	buoy19	buoy20	buoy21	buoy11	buoy12	buoy13	buoy15	buoy16	SUM
meas.Hs	1.15	0.49	0.36	0.14	0.16	0.28	0.32	0.27	
u_{10}=13 Δ abs	+0.21	+0.08	+0.13	+0.20	+0.18	+0.19	-0.01	+0.13	1.13
Δ %	18.3	16.3	36.1	142.9	112.5	67.9	3.13	48.1	445.2
U_{10}=10 Δ abs	+0.14	-0.01	+0.02	+0.12	+0.11	+0.10	-0.07	+0.05	0.62
Δ %	12.2	2.04	5.56	85.7	68.8	35.7	21.9	18.5	250.4
left part only abs	+0.21	+0.08	-0.04	0	-0.15	+0.06	-0.01	+0.13	0.68
Δ %	18.3	16.3	11.1	0	93.8	21.4	3.13	48.1	212.1
u_{10}=0 Δ abs	+0.11	-0.28	-0.32	-0.13	-0.16	-0.22	-0.29	-0.26	1.77
Δ %	9.57	57.1	88.9	92.9	100	78.6	90.6	96.3	614

Table 5.5 influence wind on Hs. measurements and absolute errors (Δ abs= SWAN - measurement) in metre

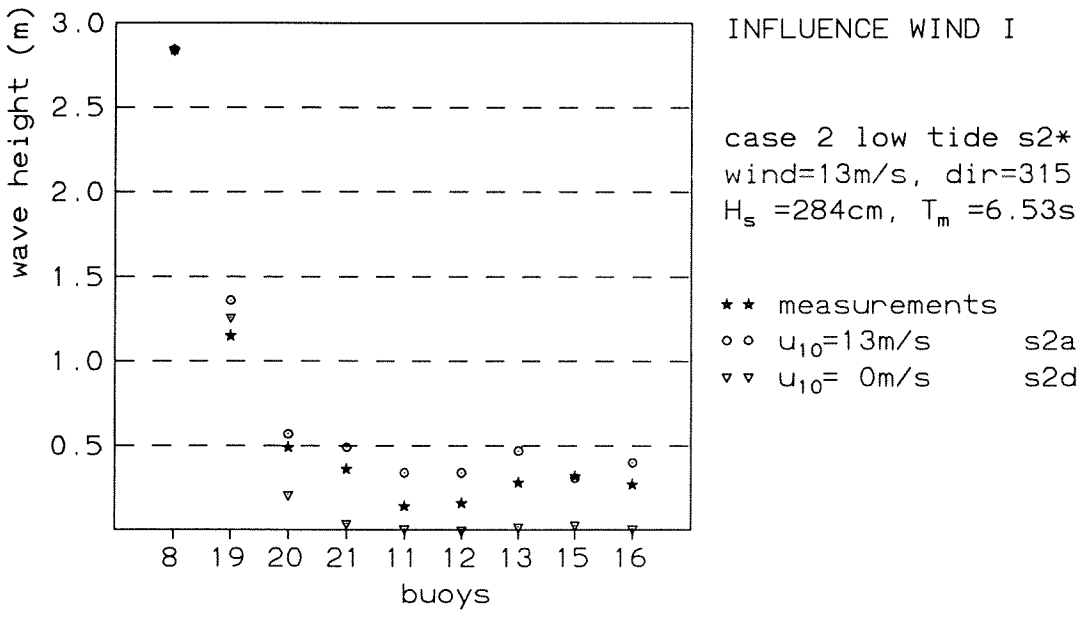

Fig. 5.6 influence wind on significant wave height I

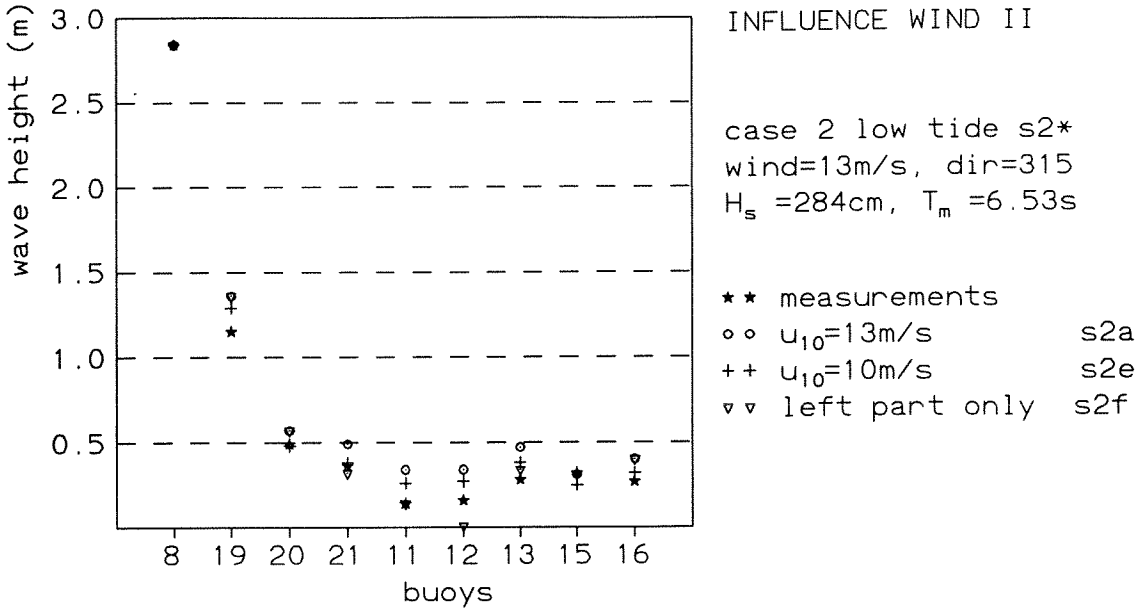

Fig. 5.7 influence wind on significant wave height II

- INFLUENCE TRIADS

On the Wadden Sea no difference is visible between the calculated spectrum with and without triads. However, buoys 19 and 20 (on the North Sea) in fig. G-4 of appendix G, show clearly the influence of the three wave-wave interactions. The first peak decreases and energy is shifted to the second peak. Looking at the spectra of fig. G-4 it is hard to say whether this energy shift also

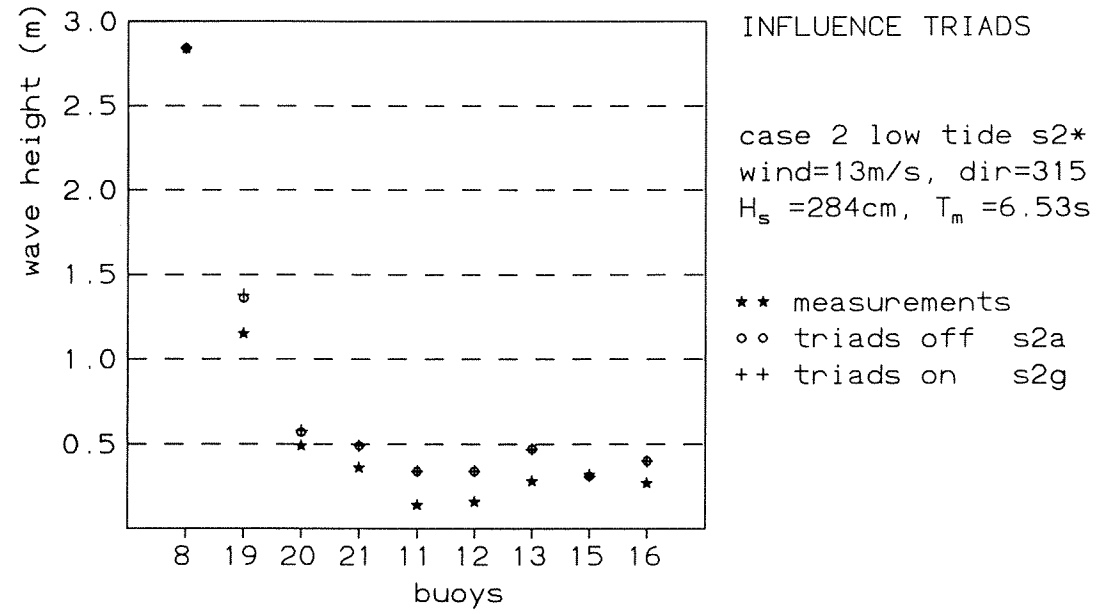

Fig. 5.8 influence triads on significant wave height

happens in the measured waves. It seems that the triads pump too much energy to the higher frequencies. Although the wave heights calculated with and without triads show hardly any differences (see fig. 5.8) the run without triads turns out to be slightly better.

	buoy19	buoy20	buoy21	buoy11	buoy12	buoy13	buoy15	buoy16	SUM
meas.Hs	1.15	0.49	0.36	0.14	0.16	0.28	0.32	0.27	
triads off Δ abs	+0.21	+0.08	+0.13	+0.20	+0.18	+0.19	-0.01	+0.13	1.13
Δ %	18.3	16.3	36.1	142.9	112.5	67.9	3.13	48.1	445.2
triads on Δabs	+0.23	+0.09	+0.13	+0.20	+0.18	+0.19	-0.01	+0.13	1.16
Δ %	20	18.4	36.1	142.9	112.5	67.9	3.13	48.1	449

Table 5.6 influence triads on Hs. measurements and absolute errors (Δ abs= SWAN - measurement) in metre

- INFLUENCE FRICTION

The friction has mainly influence on the low frequency waves (f≈0.1Hz). This is clearly visible in fig. G-5 for the position of buoy 20. With the friction formulation according to Madsen most energy is dissipated resulting in smallest waves. These waves come closest to the measured waves. The friction formulation according to Putnam and Johnson (=P&J) calculates the largest wave heights, and JONSWAP lies in between. This order holds for all buoy positions. The results concerning significant wave height are presented in fig. 5.9.

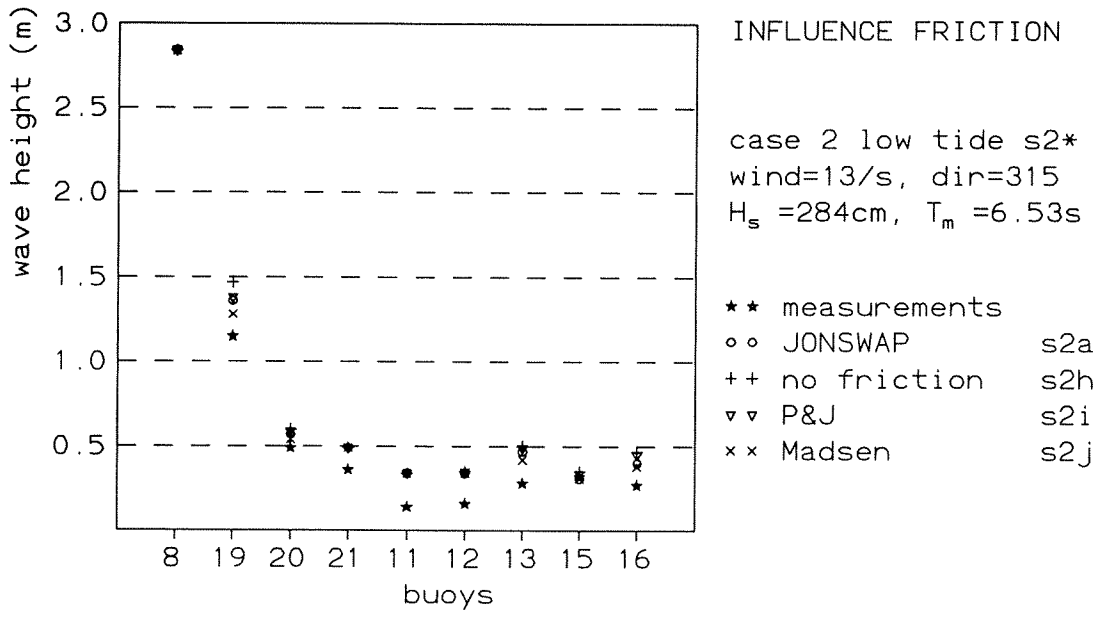

Fig. 5.9 influence friction on significant wave height

	buoy19	buoy20	buoy21	buoy11	buoy12	buoy13	buoy15	buoy16	SUM
meas.Hs	1.15	0.49	0.36	0.14	0.16	0.28	0.32	0.27	
JONSWAP Δ abs	+0.21	+0.08	+0.13	+0.20	+0.18	+0.19	-0.01	+0.13	1.13
Δ %	18.3	16.3	36.1	142.9	112.5	67.9	3.13	48.1	445.2
P&J Δ abs	+0.23	+0.10	+0.13	+0.20	+0.19	+0.21	+0.02	+0.18	1.26
Δ %	20.0	20.4	36.1	142.9	118.8	75.0	6.25	66.7	486.2
Madsen Δ abs	+0.13	+0.05	+0.13	+0.20	+0.18	+0.14	-0.01	+0.11	0.95
Δ %	11.3	10.2	36.1	142.9	112.5	50.0	3.13	40.7	406.8
friction off Δabs	+0.32	+0.11	+0.13	+0.20	+0.19	+0.22	+0.03	+0.20	1.40
Δ %	27.8	22.4	36.1	142.9	118.8	78.6	9.38	74.1	510.1

Table 5.7 influence friction on Hs. measurements and absolute errors (Δ abs= SWAN - measurement) in metre

- INFLUENCE BREAKING

The default value for γ_{break} is 0.80. In the standard run I used γ=0.60 because the default value made the waves too high compared to the measurements.

There is an option in SWAN which takes the influence of the bottom slope on the breaking coefficient into account. In the coastal area were the research takes place this varying γ gives the same results as a constant γ, except for buoy19's position, where the constant γ gives lower (here: better) wave heights.

Fig. 5.10 shows clearly for which buoy positions the breaking influence is important, and fig. G-8 for which frequencies within the spectrum. Breaking mainly dissipates energy from the low frequencies ($f \leq 0.2$Hz). Since the spectra at buoy 11 and 12 lack energy in the lower frequencies, breaking has hardly any influence on the waves there.

The measurements are best approximated by the calculations when a value of 0.6 is used for the breaking coefficient.

	buoy19	buoy20	buoy21	buoy11	buoy12	buoy13	buoy15	buoy16	SUM
meas.Hs	1.15	0.49	0.36	0.14	0.16	0.28	0.32	0.27	
γ=0.60 Δ abs	+0.21	+0.08	+0.13	+0.20	+0.18	+0.19	-0.01	+0.13	1.13
Δ %	18.3	16.3	36.1	142.9	112.5	67.9	3.13	48.1	445.2
γ=0.80 Δ abs	+0.60	+0.15	+0.14	+0.20	+0.19	+0.22	0	+0.14	1.64
Δ %	52.2	30.6	38.9	142.9	118.8	78.6	0	51.9	513.9
γ=0.73 Δ abs	+0.46	+0.13	+0.14	+0.20	+0.19	+0.21	0	+0.14	1.47
Δ %	40	26.5	38.9	142.9	118.8	75	0	51.9	494.0
vary γ Δ abs	+0.29	+0.08	+0.13	+0.20	+0.18	+0.18	-0.01	+0.13	1.18
Δ %	25.2	16.3	36.1	142.9	112.5	64.3	3.13	48.1	448.5
no break Δ abs	+1.34	+0.61	+0.17	+0.22	+0.18	+0.25	+0.07	+0.17	3.01
Δ %	116.5	124.5	47.2	157.1	112.5	89.3	21.9	63.0	732

Table 5.8 influence breaking on Hs. measurements and absolute errors (Δ abs= SWAN - measurement) in metre

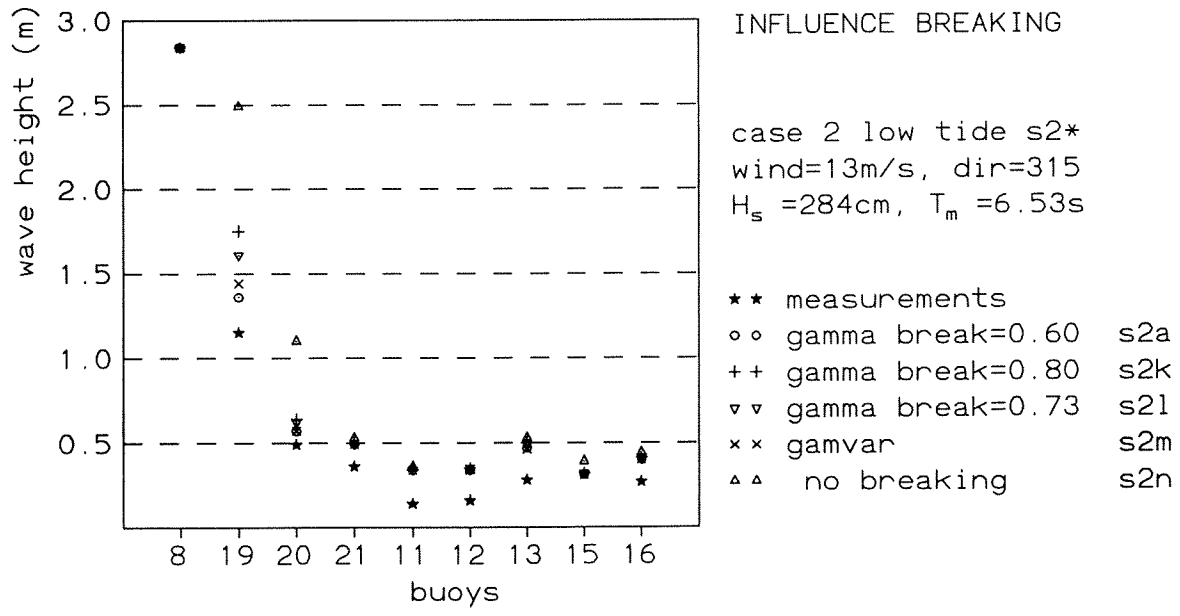

Fig. 5.10 influence breaking on significant wave height

- INFLUENCE WHITECAPPING

Janssen's whitecapping formulation results for all buoy positions in lower waves than calculations with the whitecapping formulation according to Komen (see fig.5.11). Using Janssen's whitecapping formulation implies also using Janssen's wind input formulation. Like Snyder's wind input formulation (necessary when using the whitecapping according to Komen), this is also a third generation formulation. The results according to Janssen turn out to be best.

	buoy19	buoy20	buoy21	buoy11	buoy12	buoy13	buoy15	buoy16	SUM
meas.Hs	1.15	0.49	0.36	0.14	0.16	0.28	0.32	0.27	
Komen Δ abs	+0.21	+0.08	+0.13	+0.20	+0.18	+0.19	-0.01	+0.13	1.13
Δ %	18.3	16.3	36.1	142.9	112.5	67.9	3.13	48.1	445.2
Janssen Δ abs	+0.17	+0.04	+0.09	+0.17	+0.16	+0.14	-0.03	+0.09	0.89
Δ %	14.8	8.16	25.0	121.4	100.0	50.0	9.38	33.3	362.0

Table 5.9 influence whitecapping on Hs. measurements and absolute errors (Δ abs= SWAN - measurement) in metre

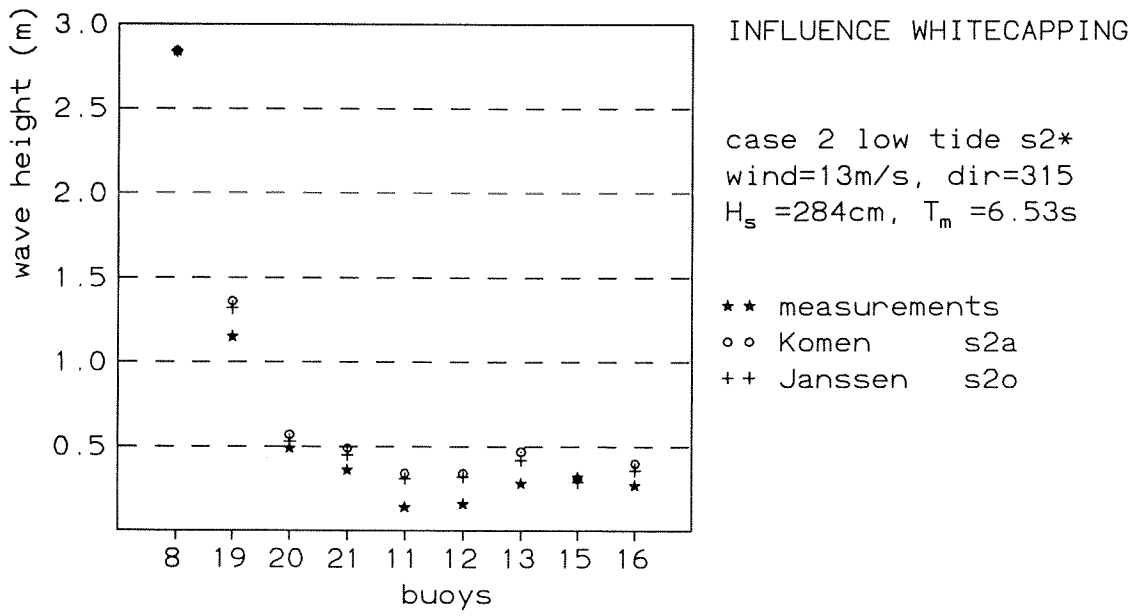

Fig. 5.11 influence whitecapping formulation on significant wave height

- INFLUENCE WATER LEVEL

What should have been an unrealistic research run - reducing the water level one metre - gives the smallest absolute error in wave height. This could lead to the conclusion that the used bottom file is not fully right. Another reason for the better performance with the smaller water depth might be that depth dependent processes (like surf breaking and friction) need to be more sensitively scaled. The results are presented in fig. 5.12 and fig. G-10 of appendix G.

	buoy19	buoy20	buoy21	buoy11	buoy12	buoy13	buoy15	buoy16	SUM
meas.Hs	1.15	0.49	0.36	0.14	0.16	0.28	0.32	0.27	
wl=-0.07 Δ abs	+0.21	+0.08	+0.13	+0.20	+0.18	+0.19	-0.01	+0.13	1.13
Δ %	18.3	16.3	36.1	142.9	112.5	67.9	3.13	48.1	445.2
wl=-1.07 Δ abs	-0.11	-0.08	+0.08	+0.18	+0.14	+0.03	-0.08	-0.05	0.75
Δ %	9.57	16.3	22.2	129.6	87.5	10.7	25.0	18.5	319.4

Table 5.10 influence water level on Hs. measurements and absolute errors (Δ abs= SWAN - measurement) in metre

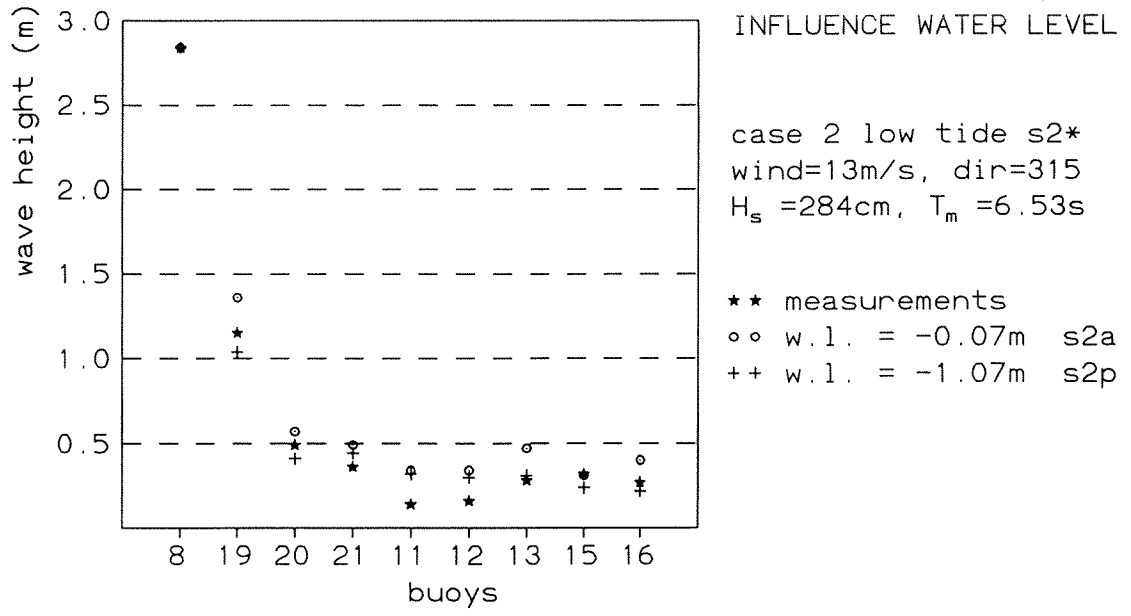

Fig. 5.12 influence water level on significant wave height

- INFLUENCE INCOMING WAVE

The influence of the wave height of the incoming wave is of minor importance to the waves on the Wadden Sea. A 25% decrease in height of the incoming wave is not found in the calculated wave heights at the positions of the buoys. Only buoy 19 is affected by the change, surprisingly enough resulting in higher waves. Note however that the minor influence holds especially for this case. When there is less wind, the incoming wave might become more important. The results are presented in fig. 5.13.

	buoy19	buoy20	buoy21	buoy11	buoy12	buoy13	buoy15	buoy16	SUM
meas.Hs	1.15	0.49	0.36	0.14	0.16	0.28	0.32	0.27	
Hs in =2.84 Δ abs	+0.21	+0.08	+0.13	+0.20	+0.18	+0.19	-0.01	+0.13	1.13
Δ %	18.3	16.3	36.1	142.9	112.5	67.9	3.13	48.1	445.2
Hs in =2.11 Δ abs	+0.22	+0.08	+0.13	+0.20	+0.18	+0.19	-0.01	+0.13	1.16
Δ %	19.1	16.3	36.1	142.9	112.5	67.9	3.13	48.1	446

Table 5.11 influence incoming wave on Hs. measurements and absolute errors (Δ abs=SWAN - measurement) in metre

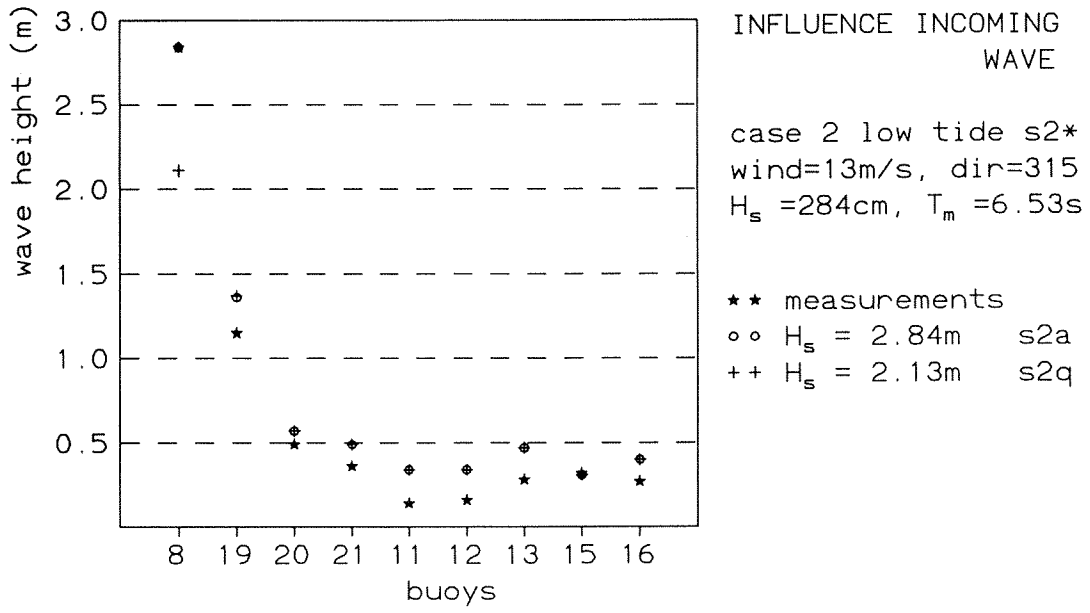

Fig. 5.13 influence incoming wave on significant wave height

§ 5.2 HISWA Results Case 2 (low tide)

§ 5.2.1 HISWA Standard Run

The model options are described in the HISWA user manual (Booij *et al.*, 1995). The model input for the low tide case is partly equal to the high tide case, like position and resolution of the computational grid, the spectral directions and the numerical options (see § 4.2.1). In the following the rest of the input for case 2 is given.

Standard run h2a, Case 2 (16.11.95 22:58)

- water level: 0.07m below N.N. (low tide)
- wind: u_{10}=13m/s, direction 315° (wind vector points 315° anti-clockwise from eastern direction)
- waves: Hs=2.84m
  Tm=6.53s
  mean wave direction=292°
- bottom friction: on. The coefficient for wave induced friction, cfw =0.01 (default). The bottom friction effects the mean wave frequency, and the coefficient for this has the default value bf=0.5.
- breaking: on. γ_s for shallow water breaking equals 0.6 (no default!) ($\gamma_s=H_{max}$/depth)
  γ_d for deep water breaking equals 1.0 (default) ($\gamma_d=H_{max}*k$)
  α (coefficient affecting the amount of dissipation due to breaking) =1.0 (default)
  frequency shift due to breaking not activated

Fig. 5.14 is a plot of the standard run showing the calculated wave heights and the direction in which the waves propagate. The wave direction looks pretty uniform. South of Juist (the western island) the wave direction equals the wind direction. All the waves are locally generated and hardly any wave energy from the North Sea can reach this area. Right between buoy 11 and buoy 12 waves propagate in southern direction instead of to the east like most arrows in that area point to. This is because of a deeper channel there which forces the waves in its direction.

The decay of the waves as they propagate from the North Sea to the Wadden Sea is shown in fig. 5.15, where the significant wave height and the mean period of the standard run and the observations is plotted for the respective stations.

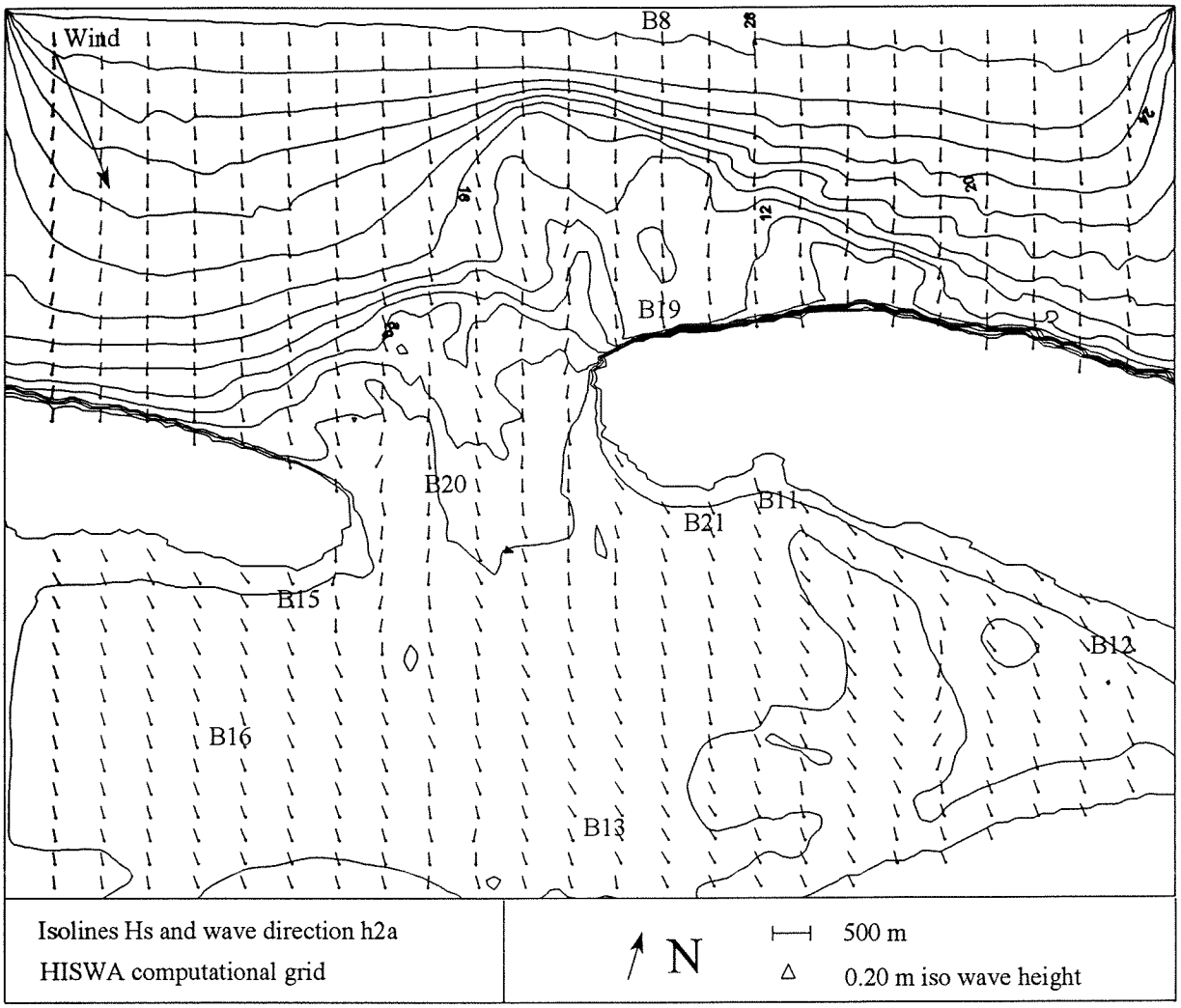

Fig. 5.14 HISWA results case2; iso wave height lines and wave direction on compgrid (values in dm)

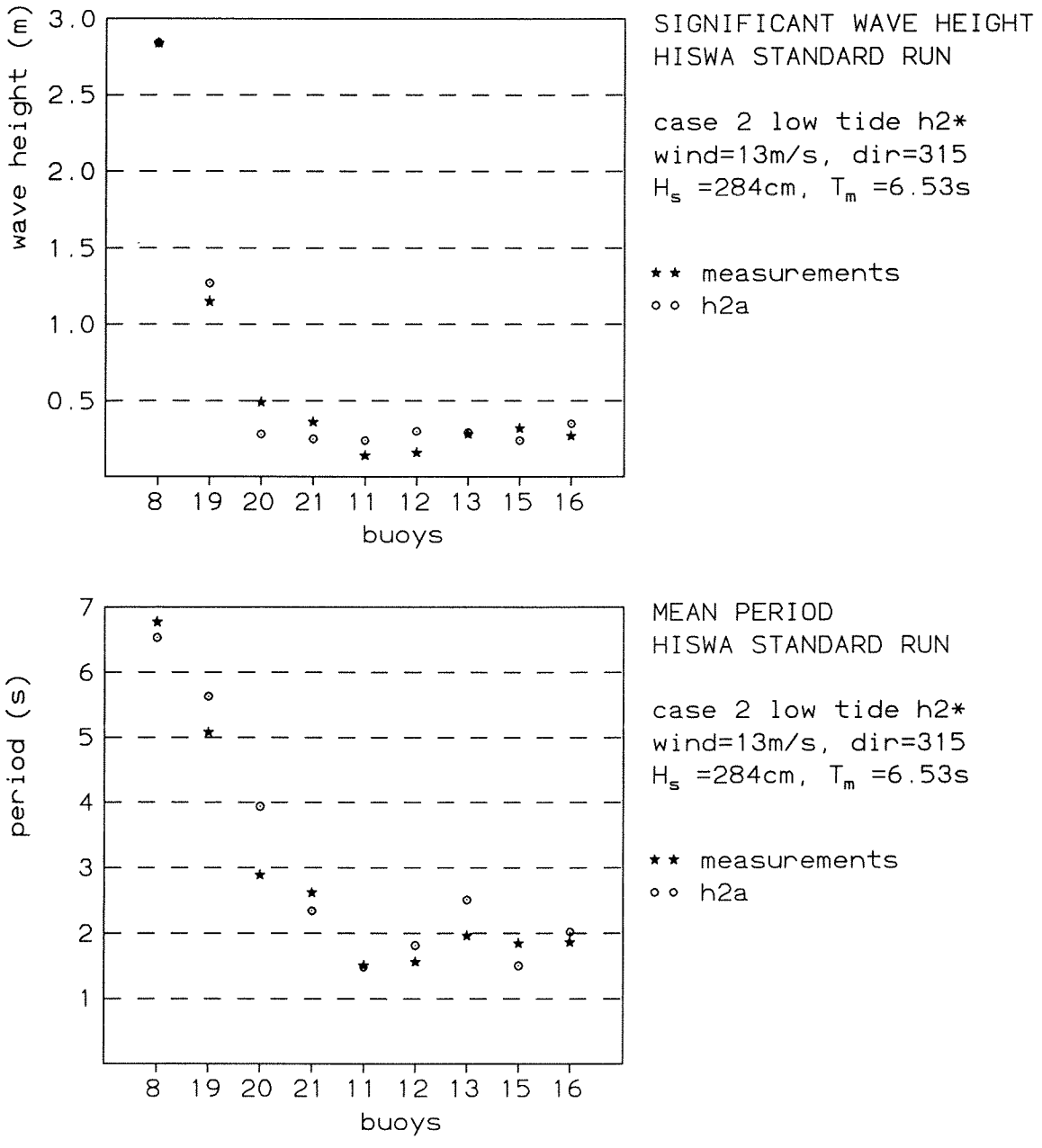

Fig. 5.15 significant wave height and period case 2

§ 5.2.2 HISWA Research Runs

Table 5.12 gives an overview of the different HISWA runs I made. The results can be found in table 5.13 (significant wave height) and table 5.14 (mean period), and in the figures on the following pages.

run	wind [m/s] [°]	friction cfw	freq.shift fric /brea	$\gamma_{shallow}$	γ_{deep}	α	w.l [m]	H_s [m]	T_m [s]	dir [°]
h2a	13 315	0.01	on off	0.60	1.0	1.0	-0.07	2.84	6.53	292
h2b	0.1 315	0.01	on off	0.60	1.0	1.0	-0.07	2.84	6.53	292
h2c	10 315	0.01	on off	0.60	1.0	1.0	-0.07	2.84	6.53	292
h2d	left part only	0.01	on off	0.60	1.0	1.0	-0.07	2.84	6.53	292
h2e	13 315	0.005	on off	0.60	1.0	1.0	-0.07	2.84	6.53	292
h2f	13 315	0	off off	0.60	1.0	1.0	-0.07	2.84	6.53	292
h2g	13 315	0.01	off off	0.60	1.0	1.0	-0.07	2.84	6.53	292
h2h	13 315	0.01	on on	0.60	1.0	1.0	-0.07	2.84	6.53	292
h2i	13 315	0.01	on off	0.80	1.0	1.0	-0.07	2.84	6.53	292
h2j	13 315	0.01	on off	0.50	1.0	1.0	-0.07	2.84	6.53	292
h2k	13 315	0.01	on off	OFF	1.0	1.0	-0.07	2.84	6.53	292
h2l	13 315	0.01	on off	0.60	20	1.0	-0.07	2.84	6.53	292
h2m	13 315	0.01	on off	0.60	0.6	1.0	-0.07	2.84	6.53	292
h2n	13 315	0.01	on off	0.60	1.0	1.5	-0.07	2.84	6.53	292
h2o	13 315	0.01	on off	0.60	1.0	1.0	-1.07	2.84	6.53	292
h2p	13 315	0.01	on off	0.60	1.0	1.0	-0.07	2.11	6.53	292

Table 5.12 HISWA runs case 2

run	buoy19	buoy20	buoy21	buoy11	buoy12	buoy13	buoy15	buoy 16
meas.	1.15	0.49	0.36	0.14	0.16	0.28	0.32	0.27
h2a	1.29	0.27	0.24	0.24	0.30	0.29	0.24	0.35
h2b	1.22	0.23	0.05	0.00	0.00	0.11	0.01	0.01
h2c	1.26	0.27	0.18	0.18	0.23	0.23	0.18	0.30
h2d	1.27	0.27	0.06	0.00	0.00	0.17	0.23	0.35
h2e	1.33	0.26	0.24	0.24	0.30	0.25	0.24	0.35
h2f	1.38	0.26	0.23	0.24	0.31	0.22	0.25	0.35
h2g	1.26	0.21	0.23	0.24	0.31	0.17	0.25	0.34
h2h	1.30	0.40	0.31	0.25	0.31	0.36	0.25	0.35
h2i	1.60	0.35	0.25	0.24	0.29	0.33	0.24	0.39
h2j	1.11	0.23	0.24	0.24	0.29	0.27	0.24	0.32
h2k	2.46	0.90	0.39	0.25	0.32	0.47	0.27	0.43
h2l	1.36	0.28	0.25	0.25	0.30	0.30	0.25	0.39
h2m	1.12	0.26	0.22	0.16	0.24	0.28	0.18	0.28
h2n	1.24	0.27	0.24	0.24	0.30	0.29	0.24	0.34
h2o	1.00	0.18	0.25	0.23	0.28	0.22	0.21	0.20
h2p	1.28	0.27	0.24	0.24	0.30	0.29	0.24	0.35

Table 5.13 HISWA results case 2; significant wave height in metre

run	buoy19	buoy20	buoy21	buoy11	buoy12	buoy13	buoy15	buoy 16
meas.	5.08	2.89	2.62	1.51	1.56	1.96	1.84	1.86
h2a	5.63	3.94	2.34	1.48	1.81	2.51	1.50	2.02
h2b	5.63	4.06	4.53	0.06	0.06	2.73	3.89	3.72
h2c	5.62	3.86	2.47	1.30	1.60	2.49	1.34	1.86
h2d	5.63	3.93	4.50	0.00	∞	2.60	1.51	2.02
h2e	6.03	4.89	2.23	1.48	1.81	3.12	1.49	2.06
h2f	6.54	6.54	2.17	1.48	1.79	5.67	1.50	2.11
h2g	6.54	6.54	2.09	1.48	1.79	5.02	1.50	2.10
h2h	3.92	2.65	2.29	1.48	1.79	2.26	1.56	1.92
h2i	5.47	3.61	2.56	1.48	1.81	2.43	1.53	2.03
h2j	5.73	4.17	2.21	1.48	1.81	2.58	1.49	2.00
h2k	5.10	2.83	3.00	1.49	1.80	2.34	1.74	2.06
h2l	5.59	3.88	2.36	1.49	1.81	2.48	1.52	2.04
h2m	5.70	4.02	2.35	1.42	1.74	2.56	1.46	1.98
h2n	5.65	3.97	2.31	1.48	1.81	2.52	1.50	2.01
h2o	5.37	2.48	2.06	1.44	1.71	1.86	1.35	1.52
h2p	5.67	3.95	2.33	1.48	1.81	2.51	1.50	2.02

Table 5.14 HISWA results case 2; mean period* in second

*) Note that the mean period calculated by HISWA and by buoys 8, 19, 20 and 21 is T_{01}, whilst the mean period calculated by the buoys 11, 12, 13, 15 and 16 is T_{02}. For a narrow spectrum there is hardly any difference between these two. On the Wadden Sea where much energy is present in the higher frequencies T_{01} and T_{02} differ too much to compare them properly.

- INFLUENCE WIND

Apart from buoys 19 and 20 the influence of the local wind is very important for all buoys. Without the wind there would hardly be any waves behind the islands (position of buoys 11, 12, 15 and 16). Also a decrease in wind velocity of 25% (from 13m/s to 10m/s) shows a considerable change in wave heights at all buoy positions.

In the 'left-part-only-run' wind is just blowing over the left part of the computational grid (see fig.4.7), so no local wind is available for buoy 21, 11 and 12. This is done to examen in which extent the waves along the south coast of Norderney are generated by wind or by the transportation of wave energy from the North Sea, within HISWA. It appears that HISWA lets no wave energy from the North Sea reach buoy 11 and 12, so the waves calculated in the standard run are fully generated by local wind. The results of these runs are presented in fig. 5.16 and 5.17.

	buoy19	buoy20	buoy21	buoy11	buoy12	buoy13	buoy15	buoy16	SUM
meas.Hs	1.15	0.49	0.36	0.14	0.16	0.28	0.32	0.27	
u_{10}=13 Δ abs	+0.14	-0.22	-0.12	+0.10	+0.14	+0.01	-0.08	+0.08	0.89
Δ%	12.2	44.9	33.3	71.4	87.5	3.57	25.0	29.6	307.5
u_{10}=10 Δ abs	+0.11	-0.22	-0.18	+0.04	+0.07	-0.05	-0.14	+0.03	0.66
Δ%	9.57	44.9	50.0	28.6	43.8	17.9	43.8	11.1	249.7
left part only Δabs	+0.12	-0.22	-0.30	-0.14	-0.16	-0.11	-0.09	+0.08	1.22
Δ%	10.4	44.9	83.3	100	100	39.3	28.1	29.6	435.6
u_{10}= 0.1 Δ abs	+0.07	-0.26	-0.31	-0.14	-0.16	-0.17	-0.31	-0.26	1.68
Δ%	6.09	53.1	86.1	100	100	60.7	96.9	96.3	599.2

Table 5.15 influence wind on Hs. measurements and absolute errors (Δ abs =HISWA - measurement) in metre

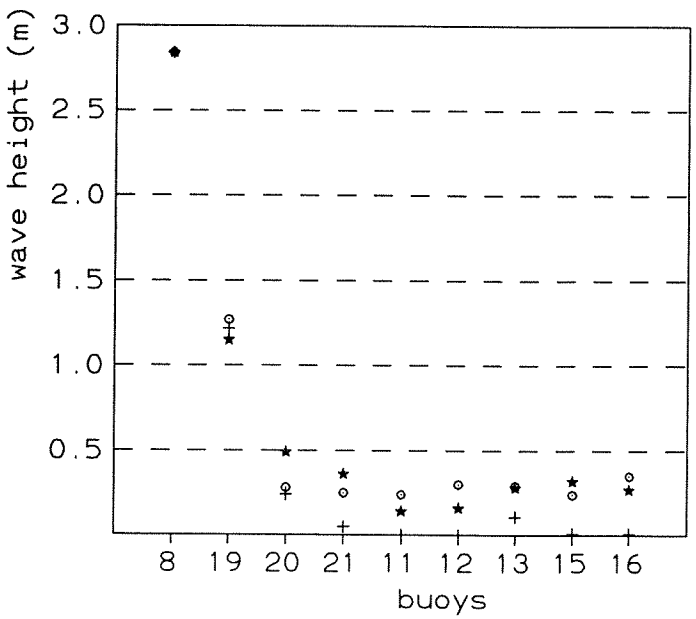

INFLUENCE WIND I

case 2 low tide h2*
wind=13m/s, dir=315
H_s =284cm, T_m =6.53s

** measurements
oo u_{10} = 13 , h2a
++ u_{10} = 0.1, h2b

fig 5.16

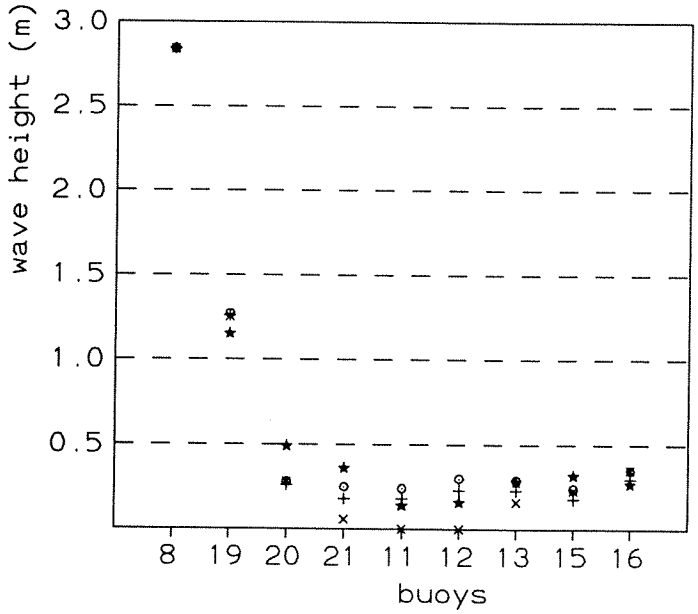

INFLUENCE WIND II

case 2 low tide h2*
wind=13m/s, dir=315
H_s =284cm, T_m =6.53s

** measurements
oo u_{10}=13, h2a
++ u_{10}=10, h2c
×× half area, h2d

fig 5.17

- INFLUENCE FRICTION

Higher waves are expected when friction is not activated. For buoy 19 this is confirmed but buoys 20, 21 and 13 show the opposite. This implies that one has to be careful when comparing different runs for one buoy. The wave heights on different positions are not fully independent of each other. So apart from the local influence of a certain parameter the calculated wave height depends also on the incoming wave which might be different for different runs. With incoming wave I do not mean the boundary, but the wave somewhat further 'downstream'.

The influence of the frequency shift is positive. The mean wave frequency per spectral wave direction is affected by bottom friction in HISWA, assuming that the wave energy dissipation due to bottom friction affects only the energy at low frequencies. Except for buoy 12 and 15 the frequency shift results in higher waves.

The friction coefficient for waves (cfw) has influence on the amount of energy that dissipates when friction occurs. A higher cfw results in more dissipation. The influence of halving cfw is small as can be seen in table 5.17. Here again at buoy 20, 21 and 13 the wave heights with cfw=0.01 are surprisingly larger than with cfw=0.005. The default value for cfw (=0.01) gives the smallest absolute error.

	buoy19	buoy20	buoy21	buoy11	buoy12	buoy13	buoy15	buoy16	SUM
meas.Hs	1.15	0.49	0.36	0.14	0.16	0.28	0.32	0.27	
cfw=0.01 Δ abs	+0.14	-0.22	-0.12	+0.10	+0.14	+0.01	-0.08	+0.08	0.89
Δ%	12.2	44.9	33.3	71.4	87.5	3.57	25.0	29.6	307.5
cfw=0.005 Δ abs	+0.18	-0.23	-0.12	+0.10	+0.14	-0.03	-0.08	+0.08	0.96
Δ%	15.7	46.9	33.3	71.4	87.5	10.7	25.0	29.6	320.1
freq.shift off Δ abs	+0.11	-0.28	-0.13	+0.10	+0.15	-0.11	-0.07	+0.07	1.02
Δ%	9.57	57.1	36.1	71.4	93.8	39.3	21.9	25.9	355.0
no friction Δ abs	+0.23	-0.23	-0.13	+0.10	+0.15	-0.06	-0.07	+0.08	1.05
Δ%	20	46.9	36.1	71.4	93.8	21.4	21.9	29.6	341.1

Table 5.16 influence friction on Hs. measurements and absolute errors (Δ abs =HISWA - measurement) in metre

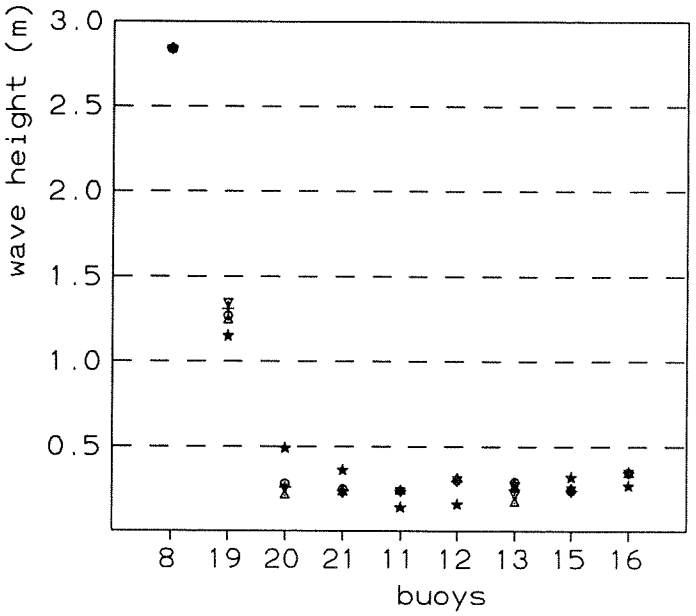

INFLUENCE FRICTION

case 2 low tide h2*
wind=13m/s, dir=315
H_s =284cm, T_m =6.53s

** measurements
oo cfw = 0.01 h2a
++ cfw = 0.005 h2e
▽▽ no friction h2f
△△ freq. shift off, h2g

fig 5.18

- INFLUENCE SHALLOW WATER BREAKING COEFFICIENT $\gamma_{shallow}$

Table 5.17 and fig. 5.19 show that the default value for γ_s (=0.80) gives fairly high waves. Using a smaller γ_s means that the waves break sooner, in greater depth. Run h2h (frequency shift on) shows that with activated frequency shift the measured wave heights are approximated better. Like friction, breaking also mainly affects the low frequencies.

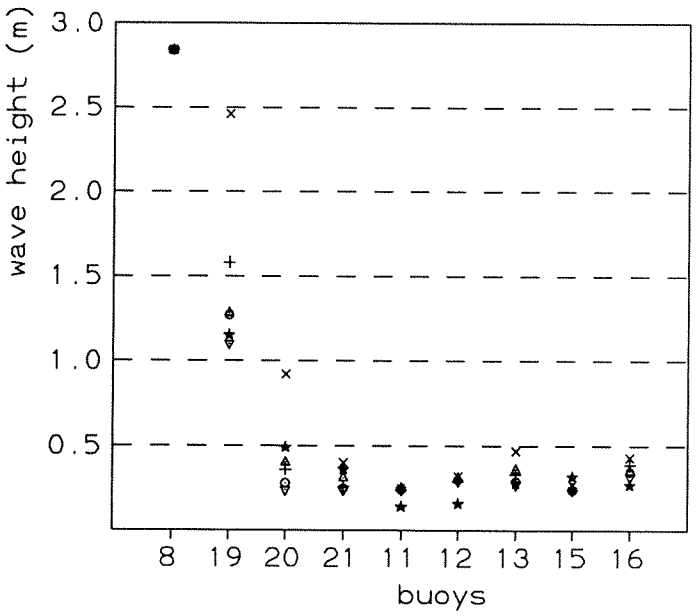

INFLUENCE GAMMA
SHALLOW BREAK (g_s)

case 2 low tide h2*
wind=13m/s, dir=315
H_s =284cm, T_m =6.53s

** measurements
oo g_s = 0.60, h2a
++ g_s = 0.80, h2i
▽▽ g_s = 0.50, h2j
×× no breaking, h2k
△△ frequency shift on, h2h
fig 5.19

	buoy19	buoy20	buoy21	buoy11	buoy12	buoy13	buoy15	buoy16	SUM
meas.Hs	1.15	0.49	0.36	0.14	0.16	0.28	0.32	0.27	
γ_s= 0.60 Δ abs	+0.14	-0.22	-0.12	+0.10	+0.14	+0.01	-0.08	+0.08	0.89
Δ%	12.2	44.9	33.3	71.4	87.5	3.57	25.0	29.6	307.5
γ_s= 0.80 Δ abs	+0.45	-0.14	-0.11	+0.10	+0.13	+0.05	-0.08	+0.12	1.18
Δ%	39.1	28.6	30.6	71.4	81.3	17.9	25.0	44.4	338.3
γ_s= 0.50 Δ abs	-0.04	-0.26	-0.12	+0.10	+0.13	-0.01	-0.08	+0.05	0.79
Δ%	3.48	53.1	33.3	71.4	81.3	3.57	25.0	18.5	289.7
freq.shift on Δ abs	+0.15	-0.09	-0.05	+0.11	+0.15	+0.08	-0.07	+0.08	0.78
Δ%	13.0	18.4	13.9	78.6	93.8	28.6	21.9	29.6	297.8
no break Δ abs	+1.31	+0.41	+0.03	+0.11	+0.16	+0.19	-0.05	+0.16	2.42
Δ%	113.9	83.7	8.33	78.6	100	67.9	15.6	59.3	527.3

Table 5.17 influence shallow breaking on Hs. measurements and absolute errors (Δ abs =HISWA-measurement) in metre

- INFLUENCE DEEP WATER BREAKING COEFFICIENT γ_{deep}

γ_d indicates at what steepness the waves break (if they are not broken yet by depth induced breaking). The default value for γ_d is 1.0. This means that the maximum wave height before the waves break because of steepness, equals the wave length ($H_{max}/L = 1.0$). Because this results in too high waves I decrease γ_d till 0.60; Whitecapping occurs already if H_{max} is only 0.6 times the wave length. Now the calculated wave heights come much closer to the measured values. Setting $\gamma_d = 20$ actually means switching off whitecapping. This is done just to see the influence on the wave height.

	buoy19	buoy20	buoy21	buoy11	buoy12	buoy13	buoy15	buoy16	SUM
meas.Hs	1.15	0.49	0.36	0.14	0.16	0.28	0.32	0.27	
γ_d=1.0 Δ abs	+0.14	-0.22	-0.12	+0.10	+0.14	+0.01	-0.08	+0.08	0.89
Δ%	12.2	44.9	33.3	71.4	87.5	3.57	25.0	29.6	307.5
γ_d=20 Δ abs	+0.21	-0.21	-0.11	+0.11	+0.14	+0.02	-0.07	+0.12	0.99
Δ%	18.3	42.9	30.6	78.6	87.5	7.14	21.9	44.4	331.3
γ_d=0.6 Δ abs	-0.03	-0.23	-0.14	+0.02	+0.08	0	-0.14	+0.01	0.65
Δ%	2.61	46.9	38.9	14.3	50.0	0	43.8	3.70	200.2

Table 5.18 influence deep breaking on Hs. measurements and absolute errors (Δ abs =HISWA - measurement) in metre

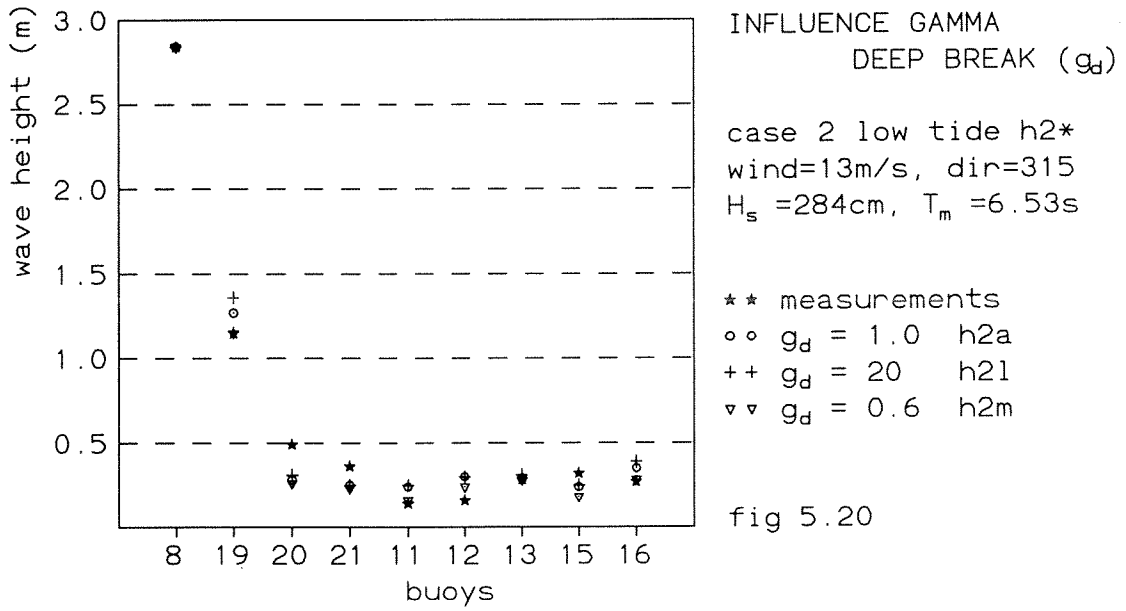

fig 5.20

- INFLUENCE ALPHA BREAK α

In HISWA one can influence the effect of breaking on wave height in three different ways. The first two ways are varying γ_s and γ_d, with which the maximum wave height before the waves break is influenced. The third manner is varying the amount of energy that is dissipated when the waves break. This can be done by changing α. A high value of α corresponds with much dissipation. Because the default value of α (=1.0) gave too high waves I increased its value to α=1.5. This leads to smaller waves, which approximate the measurements slightly better.

	buoy19	buoy20	buoy21	buoy11	buoy12	buoy13	buoy15	buoy16	SUM
meas.Hs	1.15	0.49	0.36	0.14	0.16	0.28	0.32	0.27	
α=1.0 Δ abs	+0.14	-0.22	-0.12	+0.10	+0.14	+0.01	-0.08	+0.08	0.89
Δ%	12.2	44.9	33.3	71.4	87.5	3.57	25.0	29.6	307.5
α=1.5 Δ abs	+0.09	-0.22	-0.12	+0.10	+0.14	+0.01	-0.08	+0.07	0.83
Δ%	7.83	44.9	33.3	71.4	87.5	3.57	25.0	25.9	299.4

Table 5.19 influence α break on Hs. measurements and absolute errors (Δ abs =HISWA - measurement) in metre

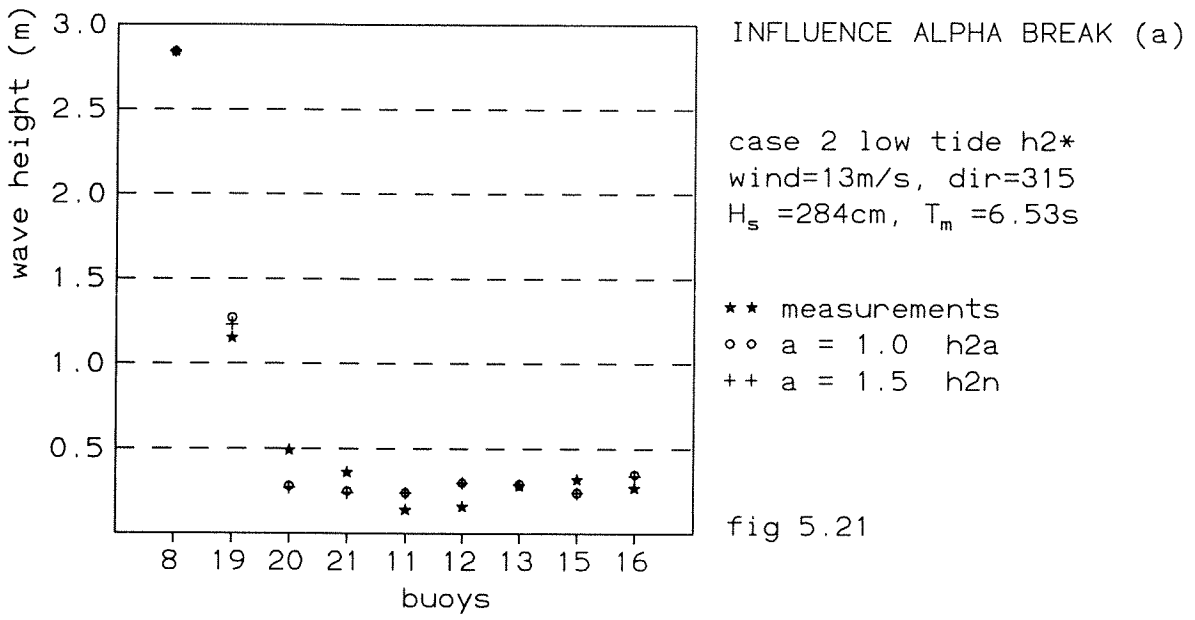

fig 5.21

- INFLUENCE WATER LEVEL

Table 5.20 and fig. 5.22 show that decreasing the depth with one metre leads to less high waves. At buoy 21, 11 and 12, where the calculated wave heights from the standard run differ much from the measured ones the influence of the depth is only very small. This implies that a more recent and detailed bottom file probably won't solve the problems at those buoys. At other places the differences are bigger, showing the sensitivity for the water depth.

	buoy19	buoy20	buoy21	buoy11	buoy12	buoy13	buoy15	buoy16	SUM
meas.Hs	1.15	0.49	0.36	0.14	0.16	0.28	0.32	0.27	
wl.=-0.07 Δ abs	+0.14	-0.22	-0.12	+0.10	+0.14	+0.01	-0.08	+0.08	0.89
Δ%	12.2	44.9	33.3	71.4	87.5	3.57	25.0	29.6	307.5
wl.=-1.07 Δ abs	-0.15	-0.31	-0.11	+0.09	+0.12	-0.06	-0.11	-0.07	1.02
Δ%	13.0	63.3	30.6	64.3	75.0	21.4	34.4	25.9	327.9

Table 5.20 influence water level on Hs. measurements and absolute errors (Δ abs =HISWA - measurement) in metre

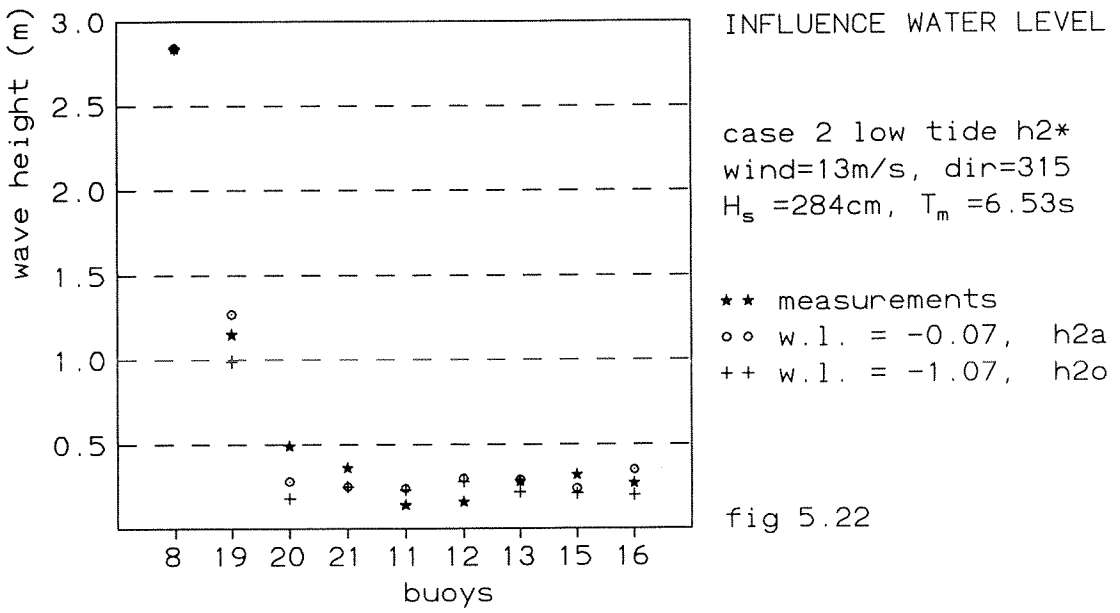

fig 5.22

- INFLUENCE INCOMING WAVE

In order to find out the importance of the exactness of the upwave boundary, a HISWA calculation is made in which the incoming wave height is 75% of the incoming wave from the standard run; so 2.11m instead of 2.84m. Table 5.21 shows that only buoy 19 is affected by this, with a decrease in wave height of a mere centimetre. The waves near the other buoys hardly feel the influence of the incoming wave height.

	buoy19	buoy20	buoy21	buoy11	buoy12	buoy13	buoy15	buoy16	SUM
meas.Hs	1.15	0.49	0.36	0.14	0.16	0.28	0.32	0.27	
Hs in=2.84 Δ abs	+0.14	-0.22	-0.12	+0.10	+0.14	+0.01	-0.08	+0.08	0.89
Δ%	12.2	44.9	33.3	71.4	87.5	3.57	25.0	29.6	307.5
Hs in=2.11 Δ abs	+0.13	-0.22	-0.12	+0.10	+0.14	+0.01	-0.08	+0.08	0.88
Δ%	11.3	44.9	33.3	71.4	87.5	3.57	25.0	29.6	306.6

Table 5.21 influence incoming wave on Hs. measurements and absolute errors (Δ abs =HISWA - measurement) in metre

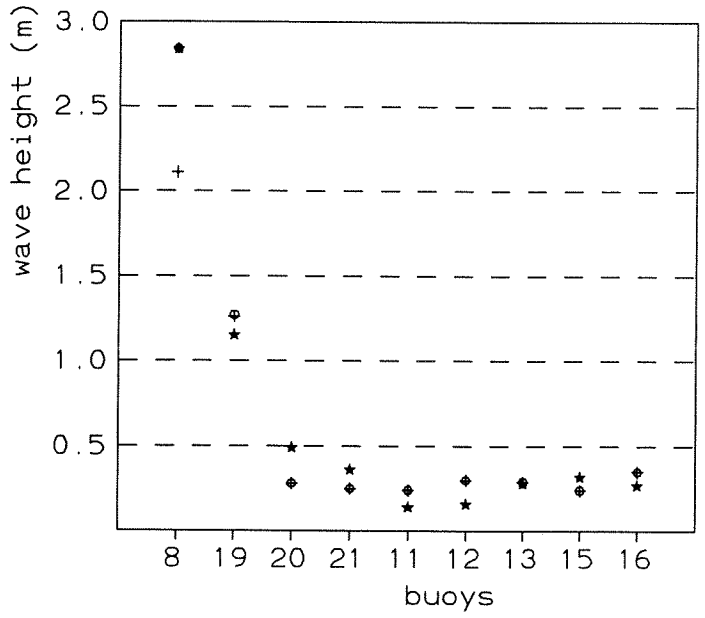

INFLUENCE INCOMING WAVE

case 2 low tide h2*
wind=13m/s, dir=315
H_s =284cm, T_m =6.53s

** measurements
oo Hs_{in} = 2.84, h2a
++ Hs_{in} = 2.13, h2p

fig 5.23

Chapter 6

Comparison SWAN and HISWA

... in which the results of the two models are compared with each other. Also 'best runs' are composed and case 3 is hindcasted.

In this chapter I will compare the results of SWAN with those of HISWA. In § 6.1 I will give some remarks derived from the plots showing the iso-Hs-lines of SWAN's and HISWA's standard runs (fig. 4.2 vs. 4.16, and 5.1 vs. 5.14). Next the models are compared on the basis of the research runs. In § 6.2 the performance indicator is introduced, indicating the performance of a model relative to the observed changes in wave height. It is an objective measure to compare the performance of wave models that have simulated different events. In § 6.2.1 a 'best run' is composed for case 1 and case 2 on the basis of the research runs, and the performance indicators belonging to them are determined. In § 6.2.2 a 'best run' is composed regardless the event that is simulated. With this set of input parameters the situation of case 3 (19th November 1995) is hindcasted.

§ 6.1 Remarks comparing SWAN and HISWA

At first sight the plots of the isolines of the significant wave heights and wave direction from SWAN and HISWA case 1 look quite similar. The isolines in both models have more or less the same pattern. Some other similarities that are represented by both models follow below:

- In case 2 the wave height patterns of both SWAN and HISWA follow the depth contours well in the area between Norderney and the mainland. Not only the isolines of the significant wave height say so, but also the arrows representing the wave propagation direction.

- South of Juist, on the left-hand side of the case-2-plot both SWAN and HISWA show that the wind is very important. The waves here propagate in the direction of the wind, not even changed by the channels pointing south. However, in case 1, according to SWAN and HISWA, the wave direction is not so much influenced by the local wind but rather by the channels which lie more or less from buoy 20 to buoy 15 and to buoy16.

But also differences can be observed:

- In general the waves calculated by SWAN are higher than those calculated by HISWA. This is not only the case on the North Sea but also on the Wadden Sea. The isolines from SWAN bend more around Norderney than those from HISWA. This is only partly because SWAN transports more wave energy around the west point of Norderney than HISWA. In HISWA all wave energy at buoy 11 is generated by the local wind, whereas SWAN also transports some energy from the North Sea to buoy 11 (see also s1g vs. h1e). Still, even without this transport SWAN comes out with higher waves than HISWA, but also higher than the observations, right behind Norderney. So it is probably not only too much propagation of wave energy from the incoming wave, but also the wind input formulation that overestimates the wave heights. Around the island of Juist SWAN's isolines also bend sharper than HISWA's. Unfortunately no proper observed wave spectrum is available here nor measurements concerning the direction of the waves, to make sure how much energy came from the incoming wave and how much from the local wind. Fact is that SWAN approximates the observed wave heights at buoy 15 in both cases very well, whilst HISWA underestimates them. In case the wind is turned off, more wave energy at buoy 15 is left over in SWAN than in HISWA. This implies that HISWA transports not enough energy from the incoming wave through the Norderneyer Seegat.

- The direction of the arrows representing the wave propagation direction varies in SWAN more than in HISWA. This is mainly because SWAN is spectral in frequencies and HISWA is not. Also SWAN's four sweep technique contributes to the variety in wave direction. HISWA calculates with one mean frequency per gridpoint whereas SWAN uses a range (in this research from 0.05 - 1.1Hz) of frequencies. The same water depth could be deep to high frequency waves and shallow to low frequency waves. So the low frequency part of the spectrum is more influenced by the bottom than the high frequency part. Because HISWA's mean frequency tends to be higher than the frequency below which the waves in SWAN are influenced by the bottom, the waves calculated with HISWA propagate rather in the direction of the wind than according to bottom features. A clear example is the Norderneyer Riffgat, the gully along the South coast of Norderney. The wave propagation direction computed by SWAN (especially for case 2) corresponds well with the gully which is situated there. Because of refraction the arrows point even perpendicular to the coast in case 2. This would never be possible in HISWA, but is very likely in reality.

- The isolines in SWAN are more jagged than in HISWA, because SWAN is more sensitive to bottom variations.

Next, SWAN and HISWA are compared on the basis of the research runs. Because the only research runs being equal for SWAN and HISWA concern wind, depth induced breaking, friction, incoming wave and water level, these items are discussed now.

- wind: The research runs where the wind is only present on the left part of the computational grid show that SWAN still calculates some wave height at buoys 11 and 12 whereas no wave energy is available in HISWA at these buoys. So behind the island of Norderney HISWA is totally dependent on the local wind. The decrease in wave heights in case the wind velocity is only 75% of what it used to be, is more or less equal for SWAN and HISWA.

- depth induced breaking: The shallow water wave breaking has more effect on the waves calculated by HISWA than on those calculated by SWAN. This holds for case 1 and for case 2. The γ-value with which the models perform best is the same for SWAN and HISWA; 0.95 for case 1 and 0.60 for case 2 (when frequency shift is activated).

- friction: The influence of friction on the wave heights is bigger in SWAN than in HISWA, and in case 1 more than in case 2. Switching off friction gives a total increase in wave height of 93cm in SWAN against 13cm in HISWA for case 1, and in case 2: 29cm for SWAN and 0cm for HISWA. This matches the supposition that higher waves experience more bottom friction.

- incoming wave: The two models react more or less similarly to the 25% decrease in incoming wave height. In case 1 it leads to smaller waves at buoy 19 for SWAN and HISWA. For the rest SWAN shows no change, HISWA small increases and decreases in wave height. In case 2 the change in incoming wave can hardly be noticed in the calculated wave height. At the positions of the buoys nothing changes except for buoy 19 where SWAN gains a centimetre in wave height and HISWA loses one.

- water level: The two models react more or less the same to the decrease in water level, namely with a decrease in wave height. In SWAN case 2 this leads to better approximations of the observations, for HISWA and the other case not.

§ 6.2 Performance Indicator

To judge each of the two models, I calculate the performance indicator, taken from Holthuijsen *et al.*, 1989, where it is called the performance rate). The performance indicator takes the difference between the measured waves and the upwave boundary into account. In the research area around the Norderneyer Seegat the buoys are positioned in such a way that they measure waves that are much smaller than the initial incoming waves. This makes it more difficult for a model to achieve good results than if the buoys were on the North Sea, close to the boundary. The performance indicator is defined as the performance of a perfect model (unity) minus the rms of the model relative to the rms of the observed changes (from the upwave boundary):

$$performance\ indicator = 1 - \frac{rms(error)}{rms(observed\ changes)}$$

The rms stands for the 'root-mean square' and is defined as:

$$rms = \sqrt{\frac{\sum_{i=1}^{n} H_i^2}{n}}$$

in which $H_i = H_{calculated} - H_{measured}$
i = 1..8, buoy 19, (20), 21, 11, 12, 13, 15, and 16

§ 6.2.1 Performance indicator standard runs and best runs

The performance indicator is given for the standard runs and for the so called 'best runs'. These best runs are composed with reference to the results of chapter 4 and chapter 5 respectively.

Best run SWAN (s1best): see s1a except for
- $\gamma = 0.95$
- wind input according to Janssen
- white capping according to Janssen

Best run HISWA (h1best): see h1a except for
- $\gamma_s = 0.95$
- $\gamma_d = 20$
- $\alpha = 0.5$
- frequency shift due to friction off

Best run SWAN (s2best): see s2a except for
- wind input according to Janssen
- white capping according to Janssen
- friction according to Madsen

Best run HISWA (h2best): see h2a except for
- $\gamma_d = 0.8$
- $\alpha = 1.5$
- frequency shift due to breaking activated

CASE 1	buoy 19	buoy 21	buoy 11	buoy 12	buoy 13	buoy 15	buoy 16	$\sqrt{[\Sigma H_i^2/n]}$
meas. Hs	2.55	0.57	0.16	0.13	0.34	0.33	0.34	
b8-b..	0.43	2.41	2.82	2.85	2.64	2.65	2.64	2.479 [1]
h1best Hs	2.39	0.16	0.16	0.23	0.36	0.19	0.27	
H_i	-0.16	-0.41	0	+0.10	+0.02	-0.14	-0.07	0.1807 [2]
h1a Hs	2.07	0.17	0.16	0.23	0.48	0.19	0.28	
H_i	-0.48	-0.40	0	+0.10	+0.14	-0.14	-0.06	0.2516 [2]
s1best Hs	2.54	0.27	0.18	0.21	0.50	0.33	0.40	
H_i	-0.01	-0.30	+0.02	+0.08	+0.16	0	+0.06	0.1342 [2]
s1a Hs	2.36	0.32	0.21	0.27	0.56	0.34	0.44	
H_i	-0.19	-0.25	+0.05	+0.14	+0.22	+0.01	+0.10	0.1600 [2]

Table 6.1 results best runs and standard runs SWAN and HISWA.
1) rms (bserved changes)
2) rms (error)

b8-b.. is difference between Hs at buoy8 and buoy considered. $H_i = H_{calculated} - H_{measured}$
all values in metre

CASE 2	buoy 19	buoy 20	buoy 21	buoy 11	buoy 12	buoy 13	buoy 15	buoy 16	$\sqrt{[\Sigma H_i^2/n]}$
meas.	1.15	0.49	0.36	0.14	0.16	0.28	0.32	0.27	
b8-b..	1.69	2.35	2.48	2.70	2.68	2.56	2.52	2.57	2.463 [1]
h2best Hs	1.17	0.36	0.29	0.22	0.30	0.34	0.23	0.31	
H_i	+0.02	-0.13	-0.07	+0.08	+0.14	+0.06	-0.09	+0.04	0.0877[2]
h2a Hs	1.29	0.27	0.24	0.24	0.30	0.29	0.24	0.35	
H_i	+0.14	-0.22	-0.12	+0.10	+0.14	+0.01	-0.06	+0.08	0.1235[2]
s2best Hs	1.24	0.50	0.44	0.31	0.32	0.39	0.29	0.34	
H_i	+0.09	+0.01	+0.08	+0.17	+0.16	+0.11	-0.04	+0.07	0.1047[2]
s2a Hs	1.36	0.57	0.49	0.34	0.34	0.47	0.31	0.40	
H_i	+0.21	+0.08	+0.13	+0.20	+0.18	+0.19	-0.01	+0.13	0.1553[2]

Table 6.2 results best runs and standard runs SWAN and HISWA
1) rms (observed changes)
2) rms (error)

b8-b.. is difference between Hs at buoy8 and buoy considered. $H_i = H_{calculated} - H_{measured}$
all values in metre

	s1a	s1best	h1a	h1best	s2a	s2best	h2a	h2best
performance indicator	0.94	0.95	0.90	0.93	0.94	0.96	0.95	0.96

Table 6.3 performance indicators case 1 and case 2

The values of the performance indicators in table 6.3 compare favourably with 0.91 for the significant wave height in the field test at the Haringvliet with HISWA (Holthuijsen *et al.*, 1989), or with 0.83 for the significant wave height from SWAN (run #3, high water) at the Friesche Zeegat (Dunsbergen, 1995). Case 1 is a little better simulated by SWAN. In case 2 the models perform equally well. It is positive that the performance indicators of the standard runs do not differ much from the 'best runs'. Someone without much experience can get good results using the default values.

§ 6.2.2 Performance Indicator Hindcast

When using a wave model in practise it is not good to have to distinguish between low tide and high tide for deciding which input parameters to choose. Therefore for each model I decide on a set of input parameters which have proven to be best according to this study. With this set (s3best and h3best), and with the default set (s3a and h3a), one more simulation run is made, hindcasting the situation on November the 19th (case 3, see § 3.2).

The input for SWAN, s3best, for case 3:
- water level: 1.75m above N.N. (high tide)
- wind: u_{10}=14m/s, direction 280° (wind vector points 280° anti-clockwise from eastern direction)
- quadruplets: on (default)
- bottom friction: JONSWAP, Γ=0.067m^2/s^3 (default)
- breaking: γ=0.77 (no default)
  α=1.0 (default)
- wind input formulation: third generation Janssen (no default), with all default values
- white capping: Janssen (no default) with all default values

For values of input options that are not mentioned here I refer to § 4.1.1.

The input for HISWA, h3best, for case 3:
- water level: 1.75m above N.N. (high tide)
- wind: u_{10}=14m/s, direction 280° (wind vector points 280° anti-clockwise from eastern direction)
- waves: Hs=3.46m
  Tm=6.56s
  mean wave direction=295°
- bottom friction: on,
  cfw (friction coefficient) = 0.01
  frequency shift due to bottom friction activated (no default)
- breaking:depth induced breaking: on, γ_s=0.78 (no default)

steepness induced breaking: on, γ_d=1.0 (default)
α=1.0 (default)
frequency shift due to breaking is not activated

For values of input options that are not mentioned here I refer to § 4.2.1.
The best runs and the standard runs differ in the underlined variables. The results are presented below:

CASE 3	buoy 19	buoy 20	buoy 21	buoy 11	buoy 12	buoy 13	buoy 15	buoy 16	$\sqrt{[\Sigma H_i^2/n]}$
meas	2.25	1.19	0.85	0.24	0.37	0.58	0.45	0.66	
b8-b..	1.21	2.27	2.61	3.22	3.09	2.88	3.01	2.80	2.705 [1]
h3best Hs	2.14	0.85	0.31	0.30	0.41	0.70	0.33	0.50	
H_i	-0.11	-0.34	-0.54	+0.06	+0.04	+0.12	-0.12	-0.16	0.245 [2]
h3a Hs	2.17	0.81	0.30	0.30	0.41	0.61	0.29	0.47	
H_i	-0.08	-0.38	-0.55	+0.06	+0.04	+0.03	-0.16	-0.19	0.255 [2]
s3best Hs	2.35	1.12	0.46	0.34	0.44	0.90	0.54	0.72	
H_i	+0.10	-0.07	-0.39	+0.10	+0.07	+0.32	+0.09	+0.06	0.192 [2]
s3a Hs	2.50	1.14	0.48	0.35	0.46	0.92	0.56	0.75	
H_i	+0.25	-0.05	-0.37	+0.11	+0.09	+0.34	+0.11	+0.09	0.212 [2]

Table 6.4 results SWAN and HISWA case 3
1) rms (observed changes)
2) rms (error)
b8-b.. is difference between Hs at buoy8 and buoy considered. $H_i = H_{calculated} - H_{measured}$
all values in meter

	h3a	h3best	s3a	s3best
performance indicator	0.91	0.91	0.92	0.93

Table 6.5 performance indicators case 3

Case 3 shows similar performance indicators as case 1 and 2; SWAN turns out to be slightly better than HISWA, and not much difference occurs between the standard runs and the best runs.

Chapter 7

Conclusions & Recommendations

...in which the conclusions following this study are presented. Also recommendations are given to improve the models and for future studies.

The conclusions of this study are divided in conclusions for both models together, for SWAN, and for HISWA. In § 7.2 the recommendations are presented.

§ 7.1 Conclusions

BOTH MODELS
- The models both have a good performance indicator (>90%).
- The 'best runs' (composed with reference to the research runs) and their results differ only little from the standard run.
- Changing the wave height of the incoming wave does not result in considerable changes of the wave heights at the positions of the buoys.
- The wave heights are to a large extent determined by the wind and by breaking.
- The breaking coefficient for depth induced breaking (γ_s) which gives the best results for low tide differs substantially from the one for high tide (0.60 and 0.95).

SWAN
- In general SWAN overestimates the wave heights. During high tide the calculated wave heights on the North Sea are too low but on the Wadden Sea, and also during low tide on the North Sea, the wave heights are overestimated.
- Both local wind and the propagation of wave energy from the North Sea lead to an overestimation of the wave heights.
-The wind input formulation according to Janssen gives best results.
- In the low tide case the first generation run is best, probably because of the high wind velocity.
- The influence of triads during low tide is nil.
- In SWAN the waves follow the tidal channels more than in HISWA.

HISWA
- In the high tide case HISWA underestimates the wave heights, except for the positions of buoy 11, 12 and 13. In the low tide case at most buoys waves are overestimated.
- In HISWA not enough wave energy is propagated from the North Sea to the Wadden Sea.
- Activating the frequency shift due to friction has a positive effect on the calculated wave heights.
- HISWA requires much less time than SWAN for comparable calculations.

§ 7.2 Recommendations

SWAN
- The regeneration of waves by wind should be decreased.
- The low frequency waves are not enough affected by dissipation processes like bottom friction and wave breaking. These processes should be tuned more sharply.

RESEARCH
- It would be better to simulate a storm event which causes higher waves on the Wadden Sea than the waves that were available for this study. Now the waves were so small that a disturbance may easily lead to errors in the measurements.
- The buoys should preferably not be located in places where strong bottom gradients occur, because then the observed wave heights are too much place-dependent. More concretely: Buoy 11 and 21 had better be placed right in the tidal channel than on its slope.
- The times for which the buoys record the data should match.

List of Symbols

Roman Symbols

a	wave amplitude	[L]
A	linear term in wind input	
B	exponential term in wind input	
c	phase velocity	[L/T]
c_g	group velocity	[L/T]
c_θ	rate of change of wave direction	[°/T]
c_σ	rate of change of frequency	[rad/T^2]
C_d	drag coefficient	
E	energy density spectrum	[L^{2}T]
f	frequency	[1/T]
f_m	peak frequency	[1/T]
$\tilde{F}$	dimensionless fetch	
g	gravitational acceleration = 9.81	[L/T^2]
h	depth	[L]
$\tilde{H}$	dimensionless wave height	
H_i	$H_{calculated}$ - $H_{observed}$	[L]
H_{max}	maximun wave height	[L]
H_{rms}	root mean square wave height	[M]
H_s	significant wave height	[L]
i	discrete dummy index	
k	wave number	[1/L]
$\underline{k}$	wave number vector	[1/L]
L	wave length	[L]
m	space coordinate perpendicular to propagation direction θ	[L]
m_n	nth moment of the spectrum	
n	number of observations	
N	action density	[L^2/T^2]
N_0	zeroth order moment of the action density spectrum	
N_1	first order moment of the action density spectrum	
s	space coordenate in propagation direction θ	[L]
S	general symbol for source term	[L^2]
t	time	[T]
$\tilde{t}$	dimensionless duration	
$\tilde{T}$	dimensionless period	
T_0	parametrized source functions for m_0	[L^{2}T]
T_1	parametrized source functions for m_1	[L^2]
T_0	zero down crossing wave period	[T]
T_{m01}	mean wave period	[T]
T_p	peak period	[T]
u_*	friction velocity	[L/T]

U	wind velocity	[L/T]
$\underline{U}$	current velocity vector	[L/T]
U_{10}	wind velocity at 10m	
z_0	roughnes length	[L]
z_e	effective roughness length	[L]

Greek Symbols

α	phase	
α_{PM}	scale parameter of Pierson-Moskowitz spectrum	
α_{ch}	Charnock constant	
β	Miles constant	
γ_d	deep water breaking coefficient (whitecapping)	
γ_s	shallow water breaking coefficient	
Γ	bottom friction coefficient	$[L^2/T^3]$
η	elevation of water surface	[L]
θ	wave direction	
κ	von Karman constant	
μ_H	mean wave height	[L]
ω	angular frequency	[rad/T]
π	pi, 3.14159....	
ρ	density	$[M/L^3]$
τ	wave stress	$[M/T^2L]$
σ	relative frequency	[rad/T]
Σ	summation	

Other Symbols

∇_X	$(\partial/\partial x, \partial/\partial y)$

List of References

Adel, J.D. den, H.D. Niemeyer, A.F.Franken, N. Booij, J. Dekker, and J.A. Vogel, (1990) *Wave Model Application in a Wadden Sea Area*, Coastal Engineering 1990

Barber, N. F. And F. Ursell (1948), *The generation and propagation of ocean waves and swell: Part I, periods and velocities*, Phil. Trans. Royal Soc. London, A, 240, p.527-560

Battjes, J.A. and P.A.E.M. Janssen (1978) *Energy loss and set-up due to breaking of random waves*, Proc. 16th Int. Conf. Coastal Eng., Hamburg, 569-587

Booij, N and H.L. Holthuijsen,(1995) *HISWA user manual*

Cavaleri, L. and P. Malanotte-Rizzoli (1981) *Wind wave prediction in shallow water: Theory and applications*. J. Geophys. Res., 86, No. C11, 10, 961-10, 973

Dunsbergen, D.W. (1995) *Validation of SWAN 20.51 against field measurements in the Friesche Zeegat*

Hasselmann, K. et al. (1973) *Measurements of wind-wave growth and swell decay during the Joint North Sea Wave Project (JONSWAP)*, Dtsch. Hydrogr. Z. Suppl. A, No.12

Holthuijsen, L.H., N. Booij and T.H.C. Herbers (1989) *A prediction model for stationary, short-crested waves in shallow water with ambient currents*. Coastal Engineering, 13, 23-54

Holthuijsen, L.H., N. Booij and R.C. Ris (1993) *A spectral wave model for the coastal zone*

Janssen, P.A.E.M. (1989) *Wave induced stress and the drag of air flow over sea waves*, J. Phys. Oceanography., 19, 745-754

Janssen, P.A.E.M. (1991) *Quasi-linear theory of wind-wave generaton applied fo wave forecasting*, J.Phys. Oceanography, 21, 1631-1642

Komen, G.J., L.Cavaleri, M. Donelan, K.Hasselmann, S.Hasselmann and P.A.E.M. Janssen (1994) *Dynamics and Modelling of Ocean Waves*, Cambridge University Press

Madsen, O.S., Y.K. Poon and H.C. Graber (1988) *Spectral wave attenuation by bottom friction* Theory. Abstracts book 21st Int. Conf. Coastal Eng., Malaga, 185-186

Neumann, G. (1953) *On ocean wave spectra and a new method of forecasting wind-generated sea*, Beach Erosion Board, Corps of Engineers, Department of the Army, Techn. Memo No. 43.

Niemeyer, H.D. (1983) *Über den Seegang an einer inselgeschützten Wattküste*

Niemeyer, H.D. et al (1992) *Anwendung des mathematischen seegangsmodells HISWA auf*

Wattenmeerbereiche

Otta, A.K., G.Ph. Van Vledder, L.H. Holthuijsen and R.C.Ris, 1995: *Validation of SWAN against field and experimental data*

Phillips, O.M. (1957) *On the generation of waves by turbulent wind*, Journal of Fluid Mechanics, Vol.4, No.4, p426-434

Pierson, W.J. and L. Moskowitz (1964) *A proposed spectral form for fully developed wind seas based on the similarity theory of S.A. Kitaigorodskii*, J. of Geophysical Research, Vol. 69, No.24, p 5181-5190

Putnam, J.A. and J.W. Johnson (1949) *The dissipation of wave energy by bottom friction*, EOS Trans. AGU, 30 (1), 67-74

Ris, R.C., N. Booij and L.H.Holthuijsen (1995) *SWAN user manual*

Ris, R.C., N. Booij and L.H.Holthuijsen (1996) *SWAN user manual*

Snyder, R.L., F.W. Dobson, J.A. Elliott and R.B. Long (1981) *Array measurements of atmospheric pressure fluctuations above surface gravity waves*, J. Fluid Mech., 102, 1-59

Sverdrup, H.U. and W.H. Munk (1946) *Emperical and theoretical relations between wind, sea, and swell*, Trans. Am. Geoph. Union, Vol. 27, No. 6, blz. 823-827

Vogel, J.A., A.C. Radder and J.H. de Reus (1989) *Verification of numerical wave propagation projects in tidal inlets*

Young, I.R., and L.A. Verhagen (1996) *The Growth of Fetch Limited Waves in Water of Finite Depth*

Secondary literature

Anonymus (1980) *Reisefibel* Forschungsstelle für Insel- und Kuestenschutz der Niedersaechsischen Wasserwirtschaftsverwaltung

Arcilla, A.S.and C.M. Lemos (1990) *Surf-Zone Hydrodynamics*

Battjes, J.A. (1992) *Windgolven*, lecture notes B78

Bishop, J.M. (1984) *Applied Oceanography*

Dingemans, M.W. (1983) *Verification of numerical wave propagation models with field*

measurements, Delft Hydraulics report W488, part 1a, 1b, 1c

Endt, M.J. van (1996) *Comparison of SWAN and HISWA in the Friesche Zeegat*

Holthuijsen, L.H. (1980) *Methoden voor golfvoorspelling*, Rapport Technische Adviescommissie voor de Waterkeringen

Luo, W (1995) *Wind Wave Modelling in Shallow Water*, PhD thesis, Department of Civil Engineering K.U.Leuven, Belgium

Ris, R.C., L.H. Holthuijsen and N. Booij, 1994: *A Spectral Model for Waves in the Near Shore Zone*, Coastal Engineering 1994

Verhagen, C.M., P.L. Gerritzen; J.G.A. van Breugel, *Operation and Service Manual for Waverider*, Datawell bv Haarlem

APPENDIX A: BUOYS

The Operation of the Buoys

-The Waverider

The waverider is a buoy which, following the movements of the water surface, measures waves by measuring the vertical acceleration of the buoy. This is done by means of a accelerometer placed on a gravity stabilised platform. This platform is formed by a disk which is suspended in a fluid within a plastic sphere placed at the bottom of the buoy. From the electronic point of view the accelerometer is a potentiometer. The buoy accelerations cause a change in voltage. The out-of-balance voltage is amplified, phase sensitive rectified and twice integrated resulting in a wave height signal. This signal is converted into an fm signal which is sent to shore. Fig A-1 is an example of the registration of the surface elevation. Out of this registration the spectrum and some statistical wave parameters are calculated. A vertical mooring line keeps the buoy on its place. The wave heights that can be measured vary from 0.02 m to 40 m, and the frequency range is from 0.033 Hz to 0.60 Hz (1.6 - 30 sec). The buoy itself has a diameter of 0.7 m and weights 100 kg.

-The Directional Waverider

The directional waverider is a spherical (diameter 0.9 m) buoy which determines wave heights and wave directions by measuring the water level fluctuations.

The principle of the vertical acceleration measurements is the same as by the above mentioned waverider. The horizontal acceleration is measured in x and y direction, with two fixed accelerometers. For the measuring of the pitch and roll angles two vertical coils are wound around the plastic sphere and one small horizontal coil is placed on the gravity stabilized platform, all in the buoy. By determinig the fluxes of the magnetic fields generated by the coils, the sine of the angles between the coil axes (x and y axes) and the horizontal plane (the platform) can be found. A fluxgate compass measures the components of the earth magnetic field in the x, y, z directions to determine the orientation of the buoy. Now a transformation matrix can be determined to give the relation between vector components in buoy coordinates and fixed coordinates. With help of the transformation matrix and these measured accelerations, the accelarations in direction north-south and west-east can be calculated. All three accelerations (vertical, north-south and west-east) are then digitally integrated to displacement. The direction measurement is based on the translational principle which means that horizontal motion instead of wave slopes are measured. As a consequence the measurement is independent of buoy roll motions and therefor a relative small spherical buoy can be used. Every 90 minutes a complete spectrum is calculated and transmitted derived from 8 time series of 200 seconds, using Fast Fourier Transform. From the spectrum the significant wave heights and mean periods are calculated:

$$M_n = \int f^n E(f) df$$

$$H_s = 4\sqrt{M_0}$$

$$T_z = T_{02} = \sqrt{\frac{M_0}{M_2}}$$

$$T_{01} = \frac{M_0}{M_1}$$

Abridged Specification Waverider Buoy

Heave range: -20m - +20m
resolution: 1cm
scale accuracy: 3%
period time in free floating condition: 1.6sec-30sec
moored condition: 1.6sec-20sec
resolution: 0.005Hz for 0.025Hz < f < 0.1Hz
0.01 Hz for 0.1 Hz < f < 0.60 Hz

(for directional waverider only:)
Direction range: 0°- 360°
resolution: 1.5°
buoy heading error: 0.5°- 2° depending on latitude

The directional waveriders have an anti-spin triangle to reduce the hazard of spinning caused by passing ships or rolling during transport.

The discrepancy between vertical movement of the waverider and the movement of the sea surface is small. When a moored buoy follows the waves the force of the mooring line will change. This force is produced by the changing immersion of the buoy, resulting in an error of max. 1.5%. With decreasing wavelength the buoy will not follow the wave amplitude if the wavelength is less than 5m (wave period below 1.8sec). If the wavelength is less than 2.5m (wave period 1.25sec) the response of the buoy decreases fast with increasing frequency.

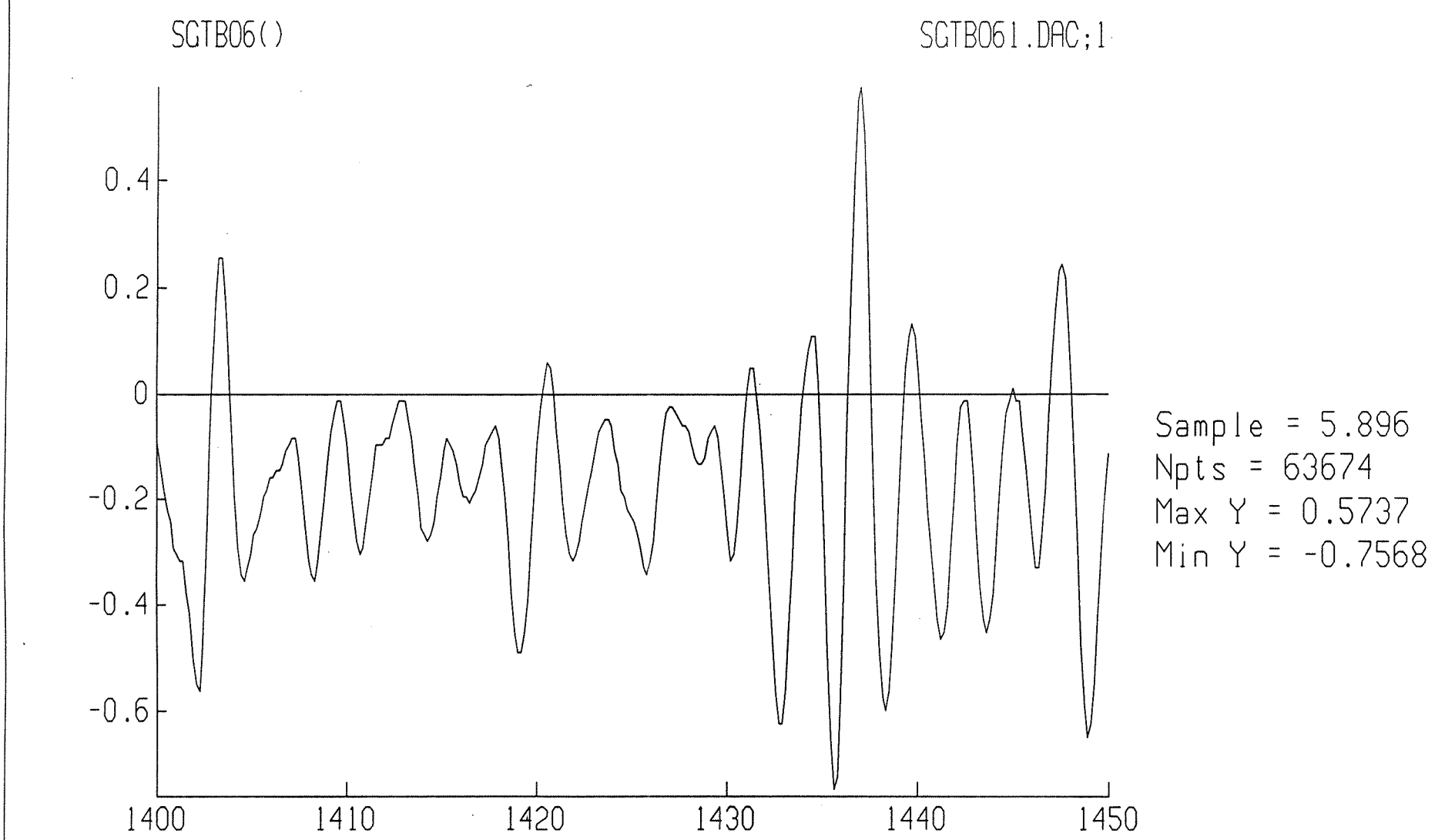

Plot of data page 1

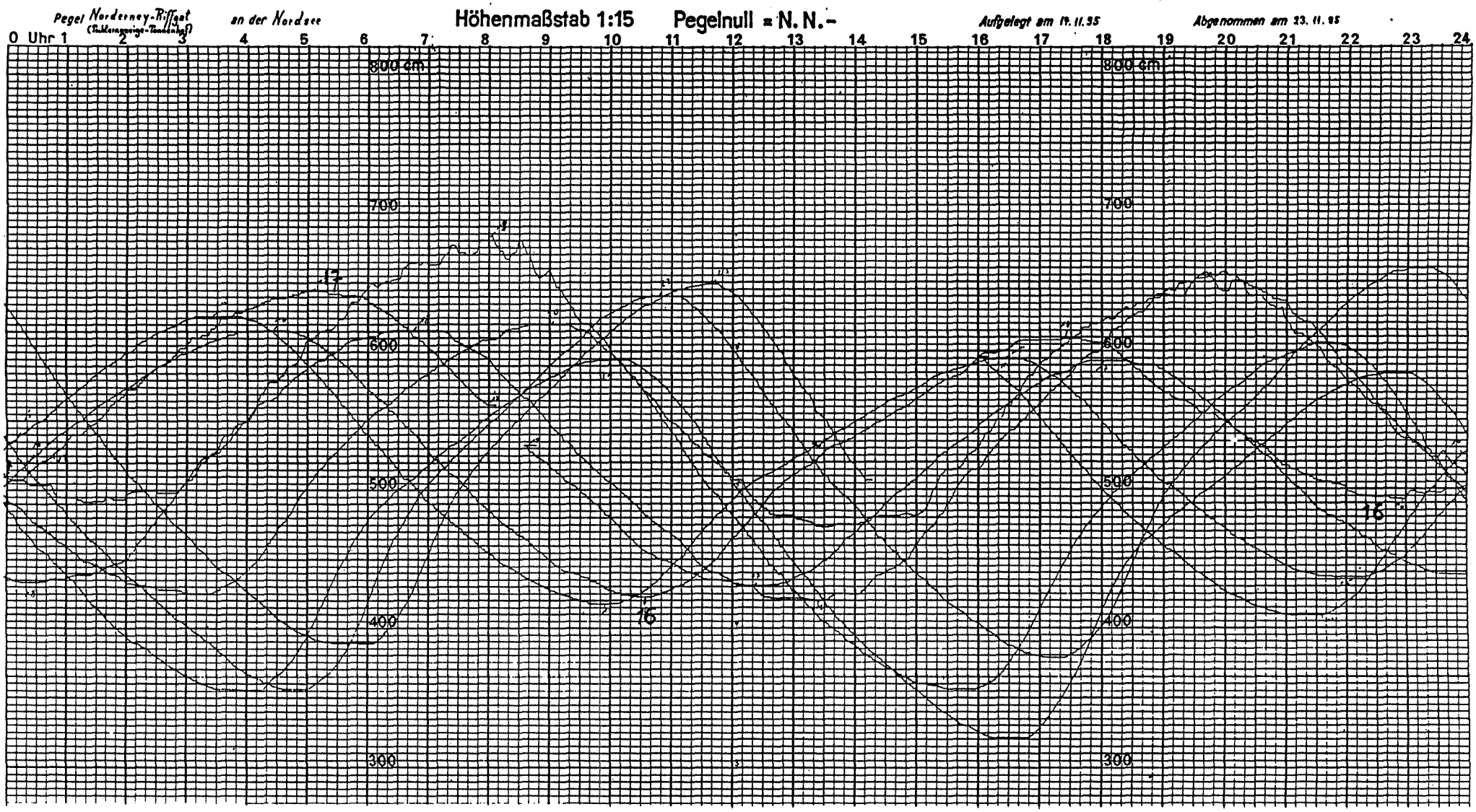

Fig.B1 water level record

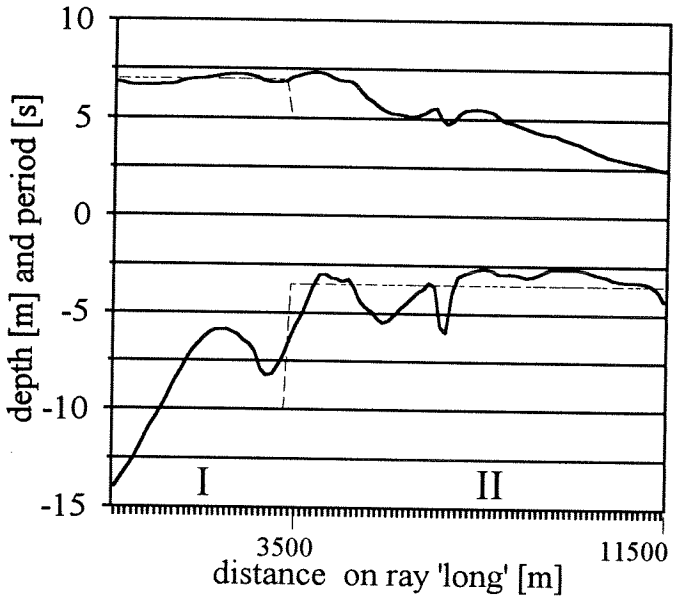

Fig.B-2a Depth and period on ray 'long'

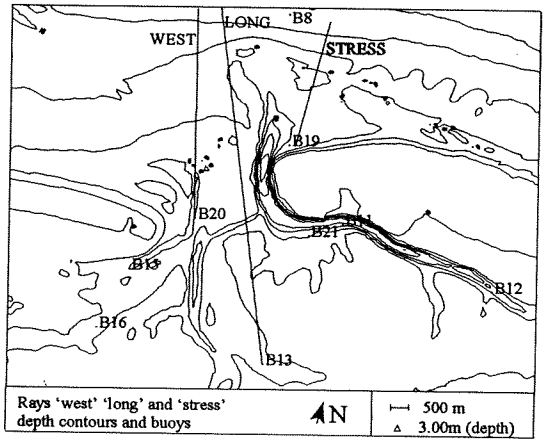

Fig.B-2b position of rays 'west' 'long' and 'stress'

WIND SET UP

As wind blows over the water surface, shear stresses will occur, resulting in a gradient in the water level.

$F_1 = c_1 \rho_1 u^2 \Delta s$
$F_2 = \rho_w g h i \Delta s$

Neglecting the bottom stress leads to $F_1=F_2$ and $i=c\, u^2/gd$

c_1= friction coefficient
ρ_1= density of the air [kg/m^3]
ρ_w= desity of the water [kg/m^3]
d = water depth [m]
i = water level gradient
c = coefficient 3.5 a 4 x 10^{-6}
u = wind velocity [m/s]

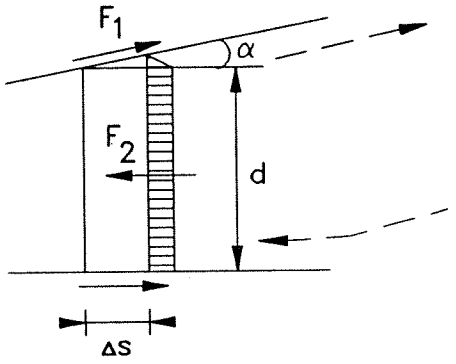

Fig. B-3 wind set up

APPENDIX B: WATER LEVEL

Fig.B1 shows a typical example of the water level records as they come from the tide gauge. The reference level for the gauge is PN, Pegelnull, which is 5.00 m below NN, Normalnull. NN corresponds to the Dutch NAP.
Some statistical information: The highest high water level was measured at 16-2-1962: 912cm above PN (so 412 cm above NN), the lowest low water was on 16-2-1900, being 161 cm above PN (339 cm below NN).
The next paragraphs examine whether the assumption that the water level is stationairy and uniform is permissible.

-Travelling time for the waves

To calculate the time needed for the waves to travel the width of the computational grid on ray 'long', I divide the journey of the waves in two parts. See fig. B-2.
The first 3800m (referring to with subscript I) in which the depth decreases from 14 till 6m, I schematize as having a depth of 10m. The second part (subscript II), some 7600m in which the depth varies from about 6 to 2.5m I schematize with a depth of 3.5m. Also the period I take constant to simplify the calculation.

$c = c_o * \tanh kh$

$(c_0)_I = gT_I/2\pi = 9.8*7/2\pi = 10.9\text{m/s}$

$(L_0)_I = gT_I^2/2\pi = 9.8*49/2\pi = 76.3\text{m}$

$h_I = 10\text{m}$

$h_I/(L_0)_I = 0.13$

$\tanh (kh)_I = 0.7804$

$c_I = 10.9*0.78 = 8.5\text{m/s}$

A distance of 3800m with a velocity of 8.5m/s takes 7.45 min.

$(c_0)_{II} = gT_{II}/2\pi = 9.8*5/2\pi = 7.8\text{m/s}$

$(L_0)_{II} = gT_{II}^2/2\pi = 9.8*25/2\pi = 39\text{m}$

$h_{II} = 3.5\text{m}$

$h_{II}/(L_0)_{II} = 0.090$

$\tanh (kh)_{II} = 0.6808$

$c_{II} = 7.8*0.68 = 5.3\text{m/s}$

A distance of 7600m with a velocity of 5.3m/s takes 23.90 min.

Total travel time approximately 31 minutes.
In 31 min the water level changes so little that we can assume it to be constant (see also fig B-1).
This also applies to the wind; for only half an hour it can be taken constant.

Roughly I take c= 4.0×10^{-6}
u= 14 m/s
g= 9.8 m/s^2
d= 6 m/s
This makes i= 1.3×10^{-5}. On a distance of 11000m (approximately the width of the computational grid) this will give a difference in water level of 14cm. This is too small too take into account.

WAVE SET UP/ SET DOWN

Gradients in radiation stress may cause a change in water level along a profile perpendicular to the coast. Outside the surf zone - neglecting the energy dissipation - the water level decreases in the direction to the coast (set down), inside the surf zone the water level increases (set up).

With a rough calculation I examined whether the influence of the radiation stress on the water level for ray 'stress' (see fig. B-2b) is negligible.

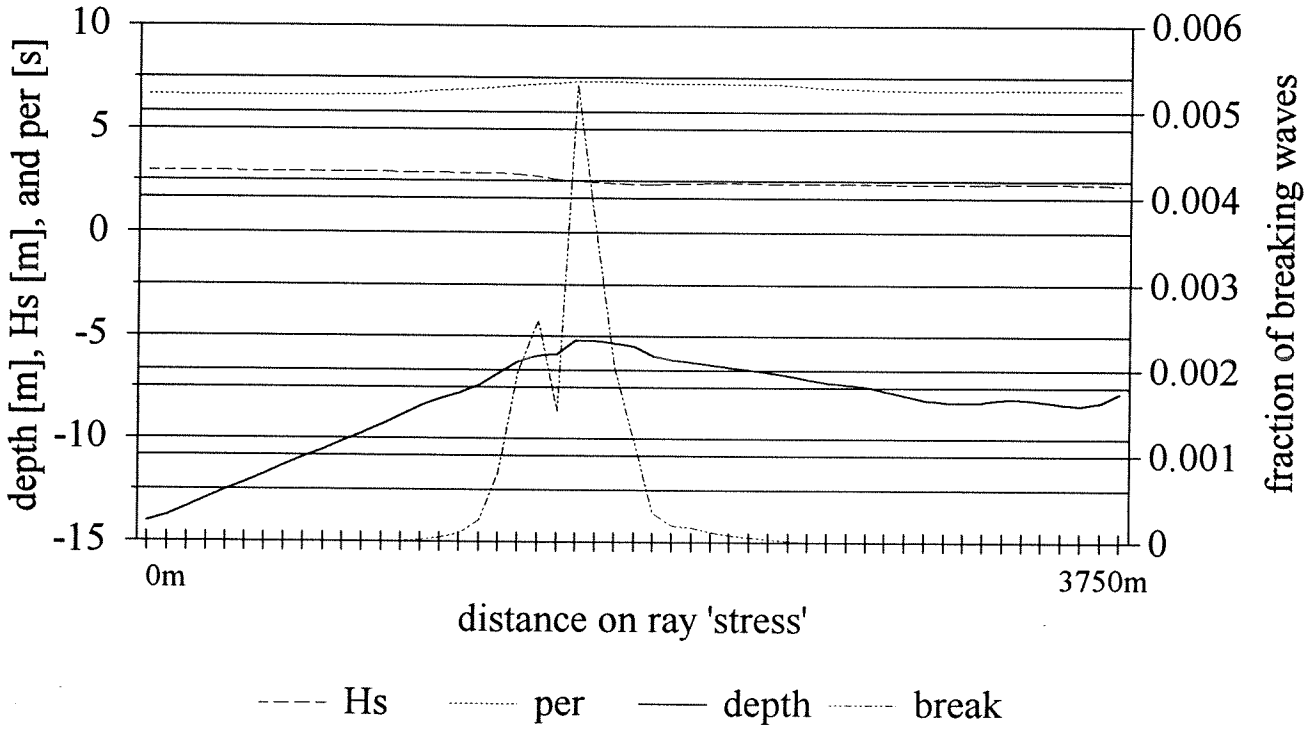

Fig B-4 wave parameters on ray 'stress'

$S_{xx} = (2n-½)E$
$\Delta S_{xx} = (2n-½) \cdot 0.125 \cdot \rho \cdot g \cdot (\Delta H^2)$

S_{xx}: radiation stress[N/m']
n: ratio c_g to c [-]

E: wave energy [J/m^2]
ρ: water density [kg/m^3]
ΔH^2: $H_0^2 - H_1^2$ [m^2]

The change in water level is: $-\Delta S_{xx} / \rho g h$ in which h is the water depth [m]

Assumptions: uniform depth = 10m
uniform period = 7s
$H_0 = 3m$
$H_1 = 2.3m$
the surf zone begins some 1500m from the beginning of ray 'stress', where the depth is approximately 5.5m. Because the water depth increases again after this point, wave set up won't occur there. Behind buoy 19, on the shore wave set up might become dominant but that won't affect the waves at the position of buoy 19.
$L_0 = gT^2/2\pi$ (table → n=..)

$L_0 = 9{,}8 \cdot 49 / 2\pi = 76.43$
$h/L_0 = 10 / 76.43 = 0.13 \rightarrow n = 0.76$
$\Delta S_{xx} = 1.02 \cdot 0.125 \cdot 1025 \cdot 9.8 \cdot 3.71 = 4752 N/m$
$-\Delta S_{xx} / \rho g h = -(4752 / 1025 \cdot 9.8 \cdot 10) = -0.047m$

A decrease in water level of 5cm can be neglected.

Considering the travelling time for the waves in relation to the tide, the wind set up and the influence of the wave stress on the water level, I conclude that the stationary and uniform water level is justified.

buoy	time	Hs	time	Hs	time	Hs
8			**04:58**	**2.98**	06:28	2.27
19			**04:46**	**2.55**	06:16	2.05
20	03:40	0.98				
21			**05:02**	**0.57**	06:32	0.52
11	04:51	0.16	**05:19**	**0.16**	05:39	0.15
12	04:51	0.13	**05:19**	**0.13**	05:39	0.12
13	04:51	0.34	**05:19**	**0.34**	05:39	0.29
15	04:51	0.33	**05:19**	**0.33**	05:39	0.30
16	04:51	0.34	**05:19**	**0.34**	05:39	0.27

Table C-1 observed wave heights on 17th of November 1995 (case1)

buoy	time	Hs	time	Hs	time	Hs
8	21:28	2.06	**22:58**	**2.84**		
19			**22:46**	**1.15**	00:16	1.78
20			**22:40**	**0.49**	00:10	0.55
21			**22:34**	**0.36**	00:02	0.36
11			**23:04**	**0.14**	23:24	0.11
12			**23:04**	**0.16**	23:24	0.15
13			**23:04**	**0.28**	23:24	0.25
15			**23:04**	**0.32**	23:24	0.29
16			**23:04**	**0.27**	23:24	0.21

Table C-2 observed wave heights on 16th of November 1995 (case 2)

APPENDIX D: COMPUTATIONAL GRIDS SWAN AND HISWA

SWAN

In SWAN the user can choose the position, size, orientation and resolution of the computational grid.

- Position and Size: The size must be larger than the area where reliable output is required, because the boundary condition is given in on one side. Along the other sides no boundary conditions are known and no waves are assumed. This is not realistic, and unfortunately this error is even transported into the computational area. For this reason the results on the sides are not realiable. In the case of the Norderneyer Seegat the islands Juist and Norderney reduce the size of the disturbed area as can be seen in for instance fig. 4.2.
- Orientation: The orientation is chosen such that it corresponds with HISWA. HISWA needs the X-axis in the same direction as the mean wave propagation direction.
- Resolution: The spatial resolution of the computational grid should be sufficient to resolve relevant details of the wave field. A very high resolution costs considerable computational effort and time, a low resolution misses for instance important bottom features. Fig D-1 shows the influence of the grid size on the bottom position and to a surprisingly less extent on the wave height at ray west (see fig.C-2b for the position of ray 'west'). It has to be added that the calculation with grids from 200m*200m needs 21 min, whilst the one with gridsize 60m*90m needs 126 min. In this research I use a grid size of 70m*95m.

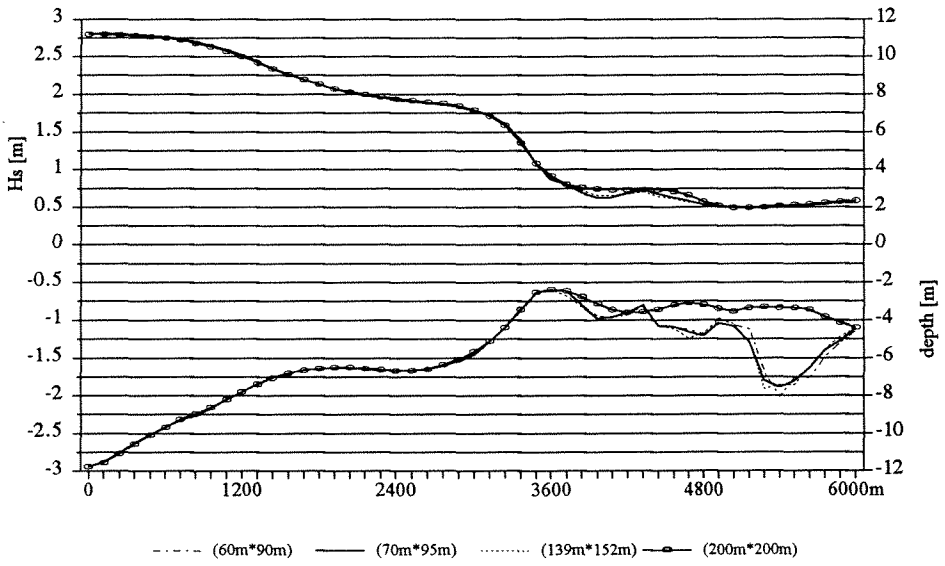

Fig D-1 SWAN resolution test on ray west, mesh size computational grid

HISWA

Concerning the computational grid the user has less latitudes in HISWA than in SWAN. The same restrictions hold as for SWAN (see here above) but there are more things to take into account. Firstly, the X-axis must more or less point into the direction of the wave propagation. Secondly, for reasons of numerical stability the resolution in X-direction should be a factor 2 or 3 smaller than in Y-direction. To find out what resolution to use for the computational grid in HISWA I did some tests with varying grid sizes. The difference between the resolutions is most obvious in the lines for the bottom position in fig D-2 (see fig C-2b for the position of ray 'west'). But also for the wave height the differences are clear. I decided to use a gridsize of 60m*120m because there is not much difference in result, allthough the calculations with the finer grid take longer. Moreover it is not wise to use a resolution for the computational grid that is much higher than the resolution for the bottom grid.This would presume an accuracy which is not really present.

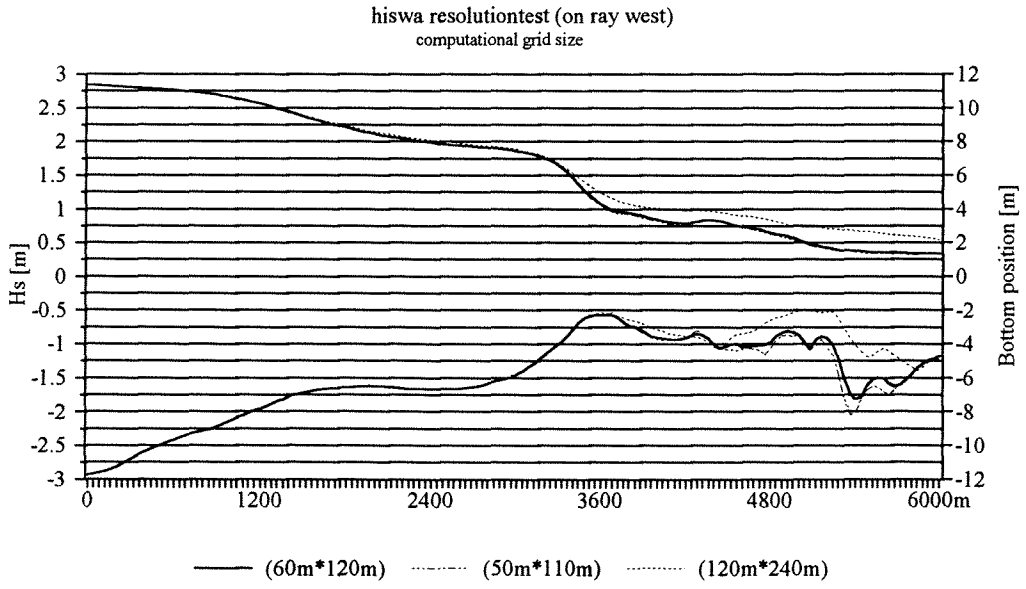

fig. D-2 HISWA resolution test on ray west, mesh size computational grid

APPENDIX E: FREQUENCY DOMAIN SWAN

The incoming wave spectrum at buoy 8 which I use as boundary for the models is measured over 65 (non uniform) frequency steps, going from 0.025Hz until 0.58Hz. In SWAN I use a larger frequency domain, from 0.045Hz until 1.11Hz to make sure that the waves with periods below 1.7s that mainly occur on the Wadden Sea will also be counted for. The domain is logarithmically divided in 24 frequency steps. Fig E-1 shows that this schematization approximates the measured spectrum well.
Also the triad wave-wave interactions require a certain frequency domain. The triads are modelled in such a way that the enery going with a certain frequency is pumped to a frequency twice as high as the initial one. For good scaling behaviour the frequency domain should be chosen so that $f2/f1 \approx 2$, in which f1 is the peak frequency, and f2 the higher harmonic of f1. In case the lowest period is 0.9s and the highest 22s, the ratio is 1.95. This is close enough to one to satisfy the good scaling criterium.

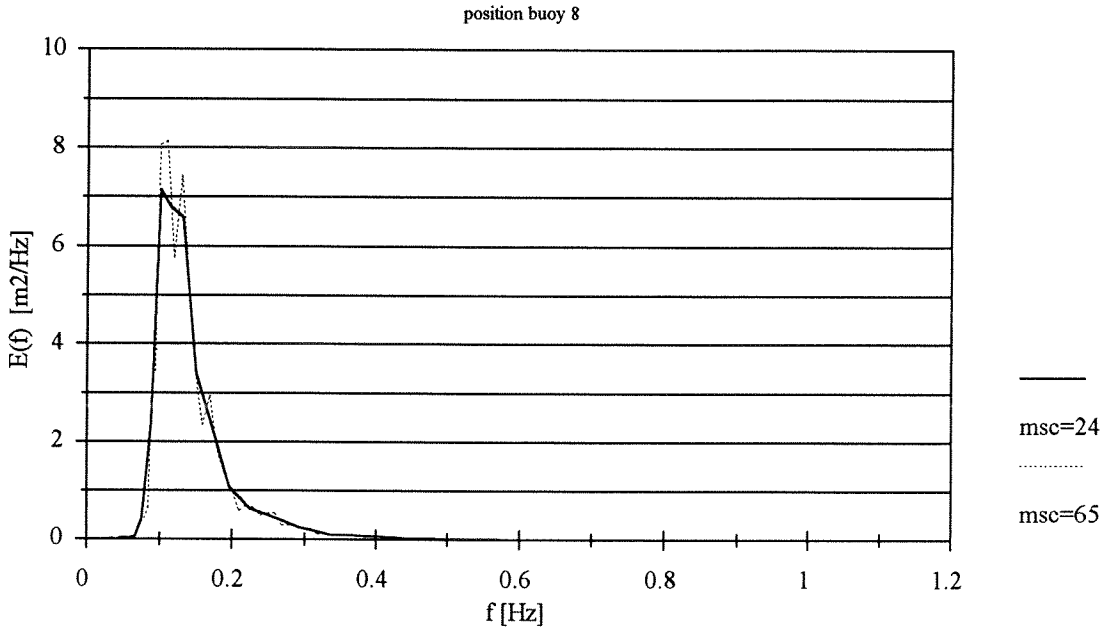

Fig. E-1 frequency resolution

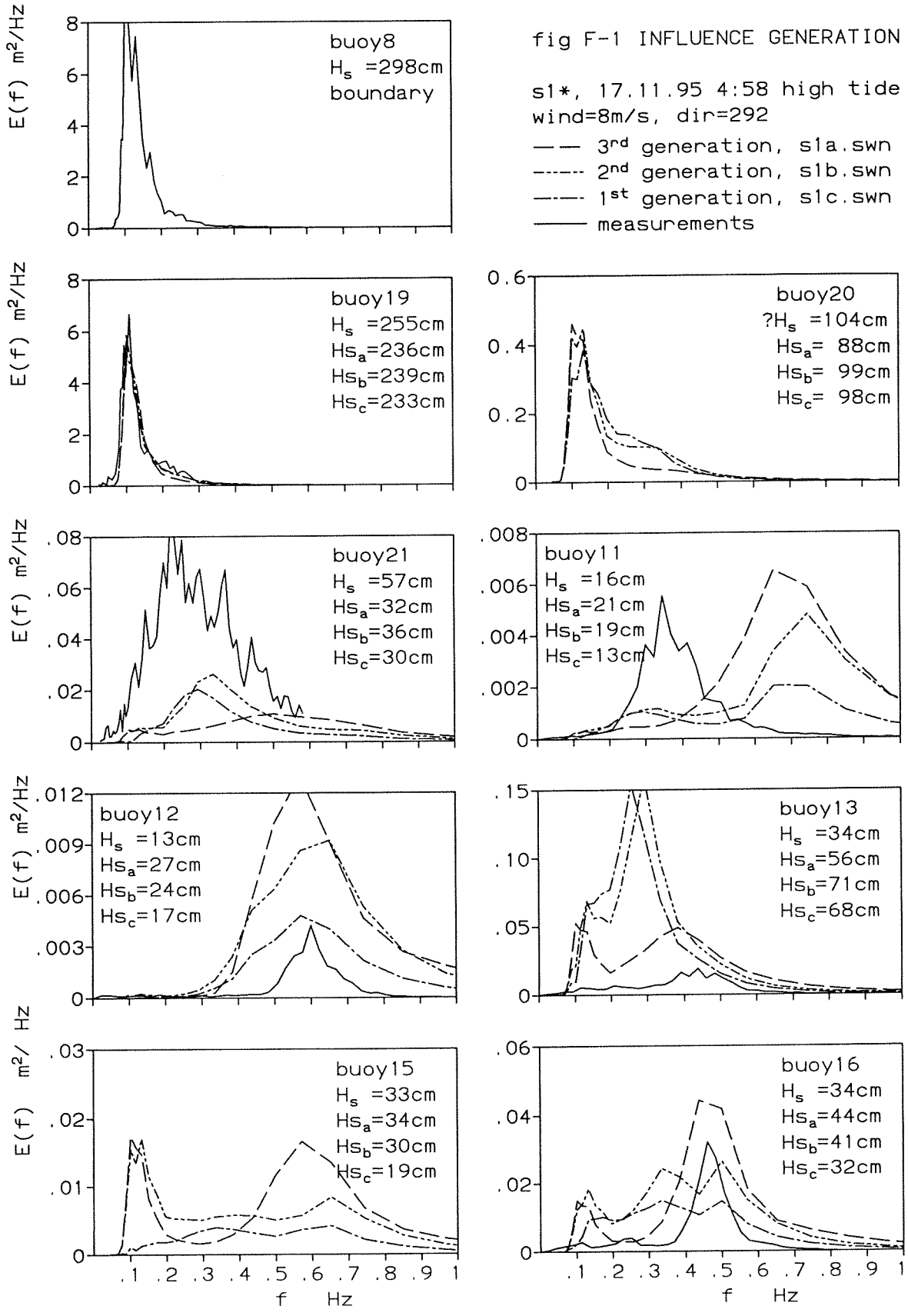
E(f) m²/Hz
buoy8
Hs =298cm
boundary
fig F-1 INFLUENCE GENERATION
s1*, 17.11.95 4:58 high tide
wind=8m/s, dir=292
3rd generation, s1a.swn
2nd generation, s1b.swn
1st generation, s1c.swn
measurements
buoy19
Hs =255cm
Hsa=236cm
Hsb=239cm
Hsc=233cm
buoy20
?Hs =104cm
Hsa= 88cm
Hsb= 99cm
Hsc= 98cm
buoy21
Hs =57cm
Hsa=32cm
Hsb=36cm
Hsc=30cm
buoy11
Hs =16cm
Hsa=21cm
Hsb=19cm
Hsc=13cm
buoy12
Hs =13cm
Hsa=27cm
Hsb=24cm
Hsc=17cm
buoy13
Hs =34cm
Hsa=56cm
Hsb=71cm
Hsc=68cm
E(f) m²/ Hz
buoy15
Hs =33cm
Hsa=34cm
Hsb=30cm
Hsc=19cm
buoy16
Hs =34cm
Hsa=44cm
Hsb=41cm
Hsc=32cm
f Hz
f Hz

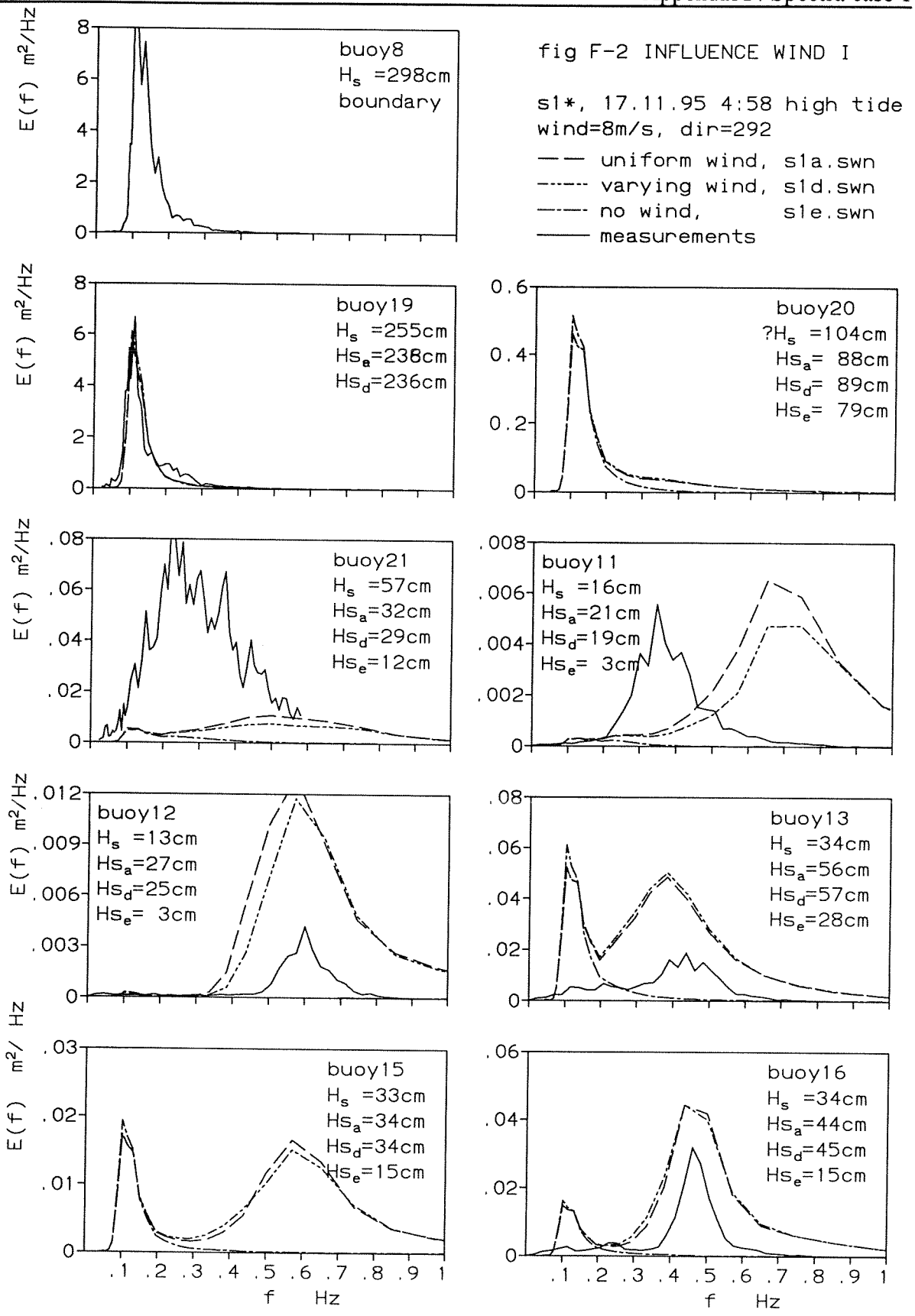
fig F-2 INFLUENCE WIND I
s1*, 17.11.95 4:58 high tide
wind=8m/s, dir=292
uniform wind, s1a.swn
varying wind, s1d.swn
no wind, s1e.swn
measurements
buoy8
Hs =298cm
boundary
buoy19
Hs =255cm
Hse=238cm
Hsd=236cm
buoy20
?Hs =104cm
Hsa= 88cm
Hsd= 89cm
Hse= 79cm
buoy21
Hs =57cm
Hsa=32cm
Hsd=29cm
Hse=12cm
buoy11
Hs =16cm
Hsa=21cm
Hsd=19cm
Hse= 3cm
buoy12
Hs =13cm
Hsa=27cm
Hsd=25cm
Hse= 3cm
buoy13
Hs =34cm
Hsa=56cm
Hsd=57cm
Hse=28cm
buoy15
Hs =33cm
Hsa=34cm
Hsd=34cm
Hse=15cm
buoy16
Hs =34cm
Hsa=44cm
Hsd=45cm
Hse=15cm
E(f) m²/Hz
f Hz

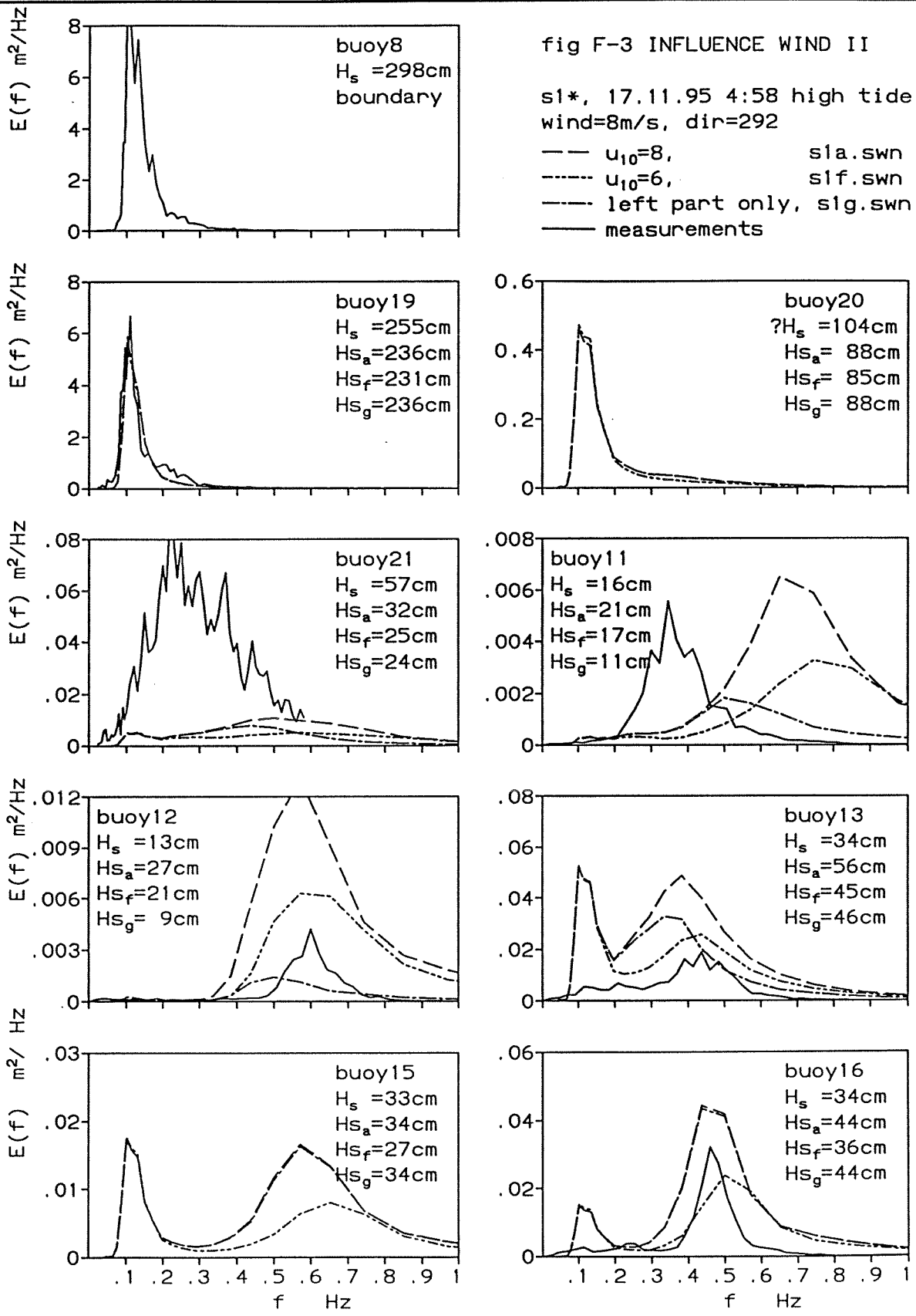
fig F-3 INFLUENCE WIND II
s1*, 17.11.95 4:58 high tide
wind=8m/s, dir=292
u10=8, s1a.swn
u10=6, s1f.swn
left part only, s1g.swn
measurements
buoy8
Hs =298cm
boundary
buoy19
Hs =255cm
Hsa=236cm
Hsf=231cm
Hsg=236cm
buoy20
?Hs =104cm
Hsa= 88cm
Hsf= 85cm
Hsg= 88cm
buoy21
Hs =57cm
Hsa=32cm
Hsf=25cm
Hsg=24cm
buoy11
Hs =16cm
Hsa=21cm
Hsf=17cm
Hsg=11cm
buoy12
Hs =13cm
Hsa=27cm
Hsf=21cm
Hsg= 9cm
buoy13
Hs =34cm
Hsa=56cm
Hsf=45cm
Hsg=46cm
buoy15
Hs =33cm
Hsa=34cm
Hsf=27cm
Hsg=34cm
buoy16
Hs =34cm
Hsa=44cm
Hsf=36cm
Hsg=44cm
E(f) m²/Hz
E(f) m²/ Hz
f Hz

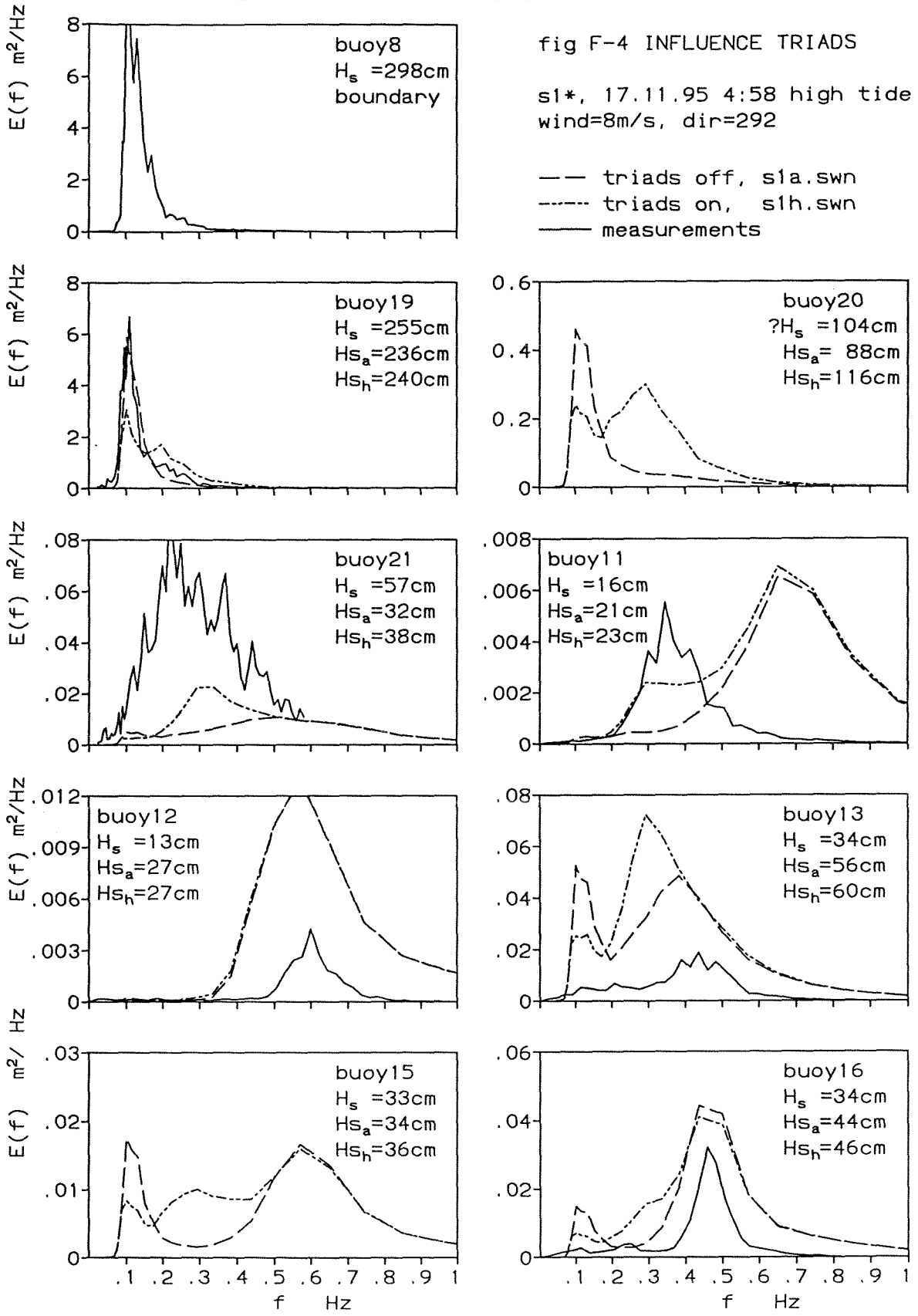
fig F-4 INFLUENCE TRIADS
s1*, 17.11.95 4:58 high tide
wind=8m/s, dir=292
—— triads off, s1a.swn
------ triads on, s1h.swn
—— measurements
buoy8
Hs =298cm
boundary
buoy19
Hs =255cm
Hsa=236cm
Hsh=240cm
buoy20
?Hs =104cm
Hsa= 88cm
Hsh=116cm
buoy21
Hs =57cm
Hsa=32cm
Hsh=38cm
buoy11
Hs =16cm
Hsa=21cm
Hsh=23cm
buoy12
Hs =13cm
Hsa=27cm
Hsh=27cm
buoy13
Hs =34cm
Hsa=56cm
Hsh=60cm
buoy15
Hs =33cm
Hsa=34cm
Hsh=36cm
buoy16
Hs =34cm
Hsa=44cm
Hsh=46cm
E(f) m²/Hz
E(f) m²/ Hz
f Hz

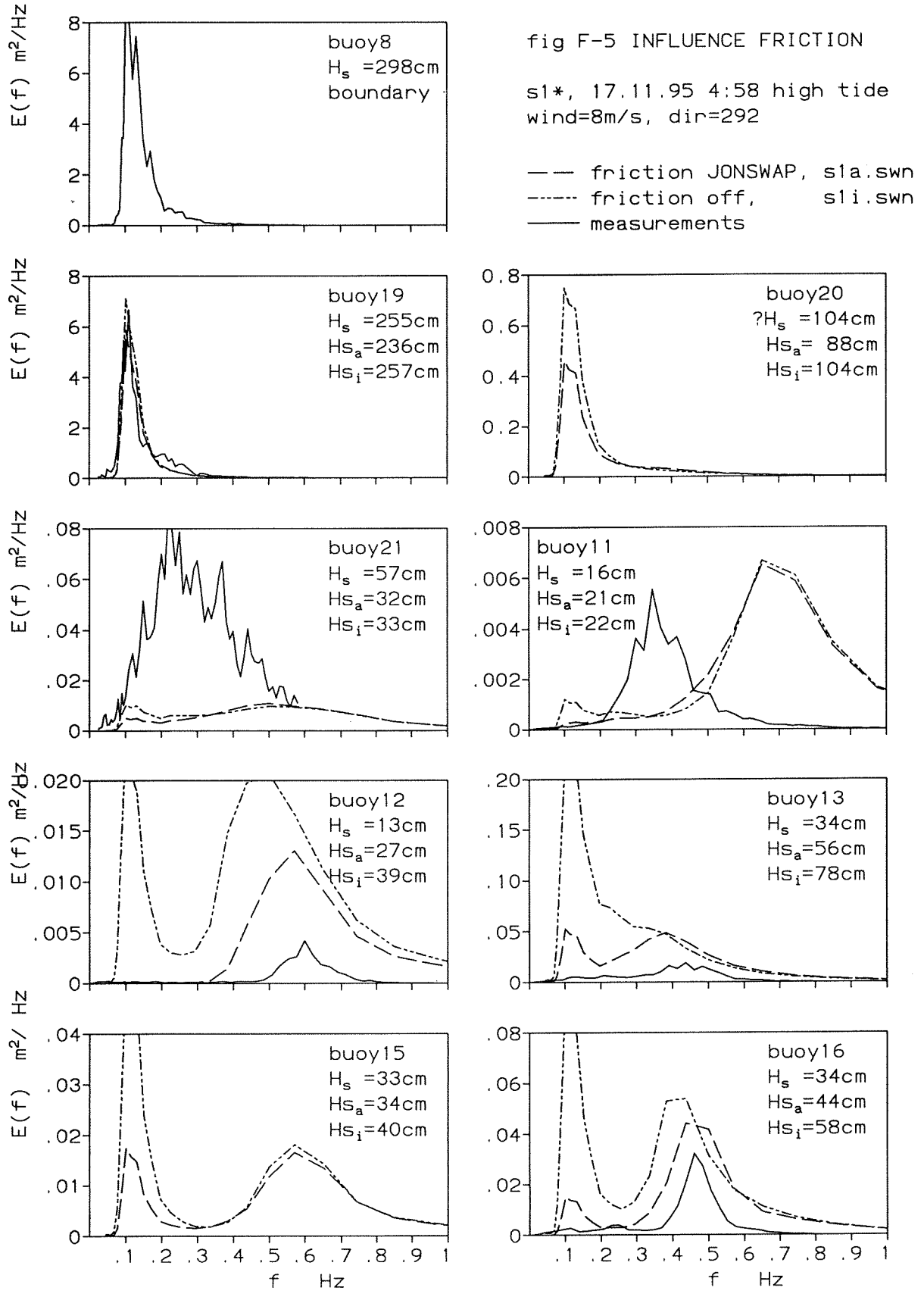
fig F-5 INFLUENCE FRICTION
s1*, 17.11.95 4:58 high tide
wind=8m/s, dir=292
friction JONSWAP, s1a.swn
friction off, s1i.swn
measurements
buoy8
Hs =298cm
boundary
buoy19
Hs =255cm
Hsa=236cm
Hsi=257cm
buoy20
?Hs =104cm
Hsa= 88cm
Hsi=104cm
buoy21
Hs =57cm
Hsa=32cm
Hsi=33cm
buoy11
Hs =16cm
Hsa=21cm
Hsi=22cm
buoy12
Hs =13cm
Hsa=27cm
Hsi=39cm
buoy13
Hs =34cm
Hsa=56cm
Hsi=78cm
buoy15
Hs =33cm
Hsa=34cm
Hsi=40cm
buoy16
Hs =34cm
Hsa=44cm
Hsi=58cm
E(f) m²/Hz
E(f) m²/ Hz
f Hz

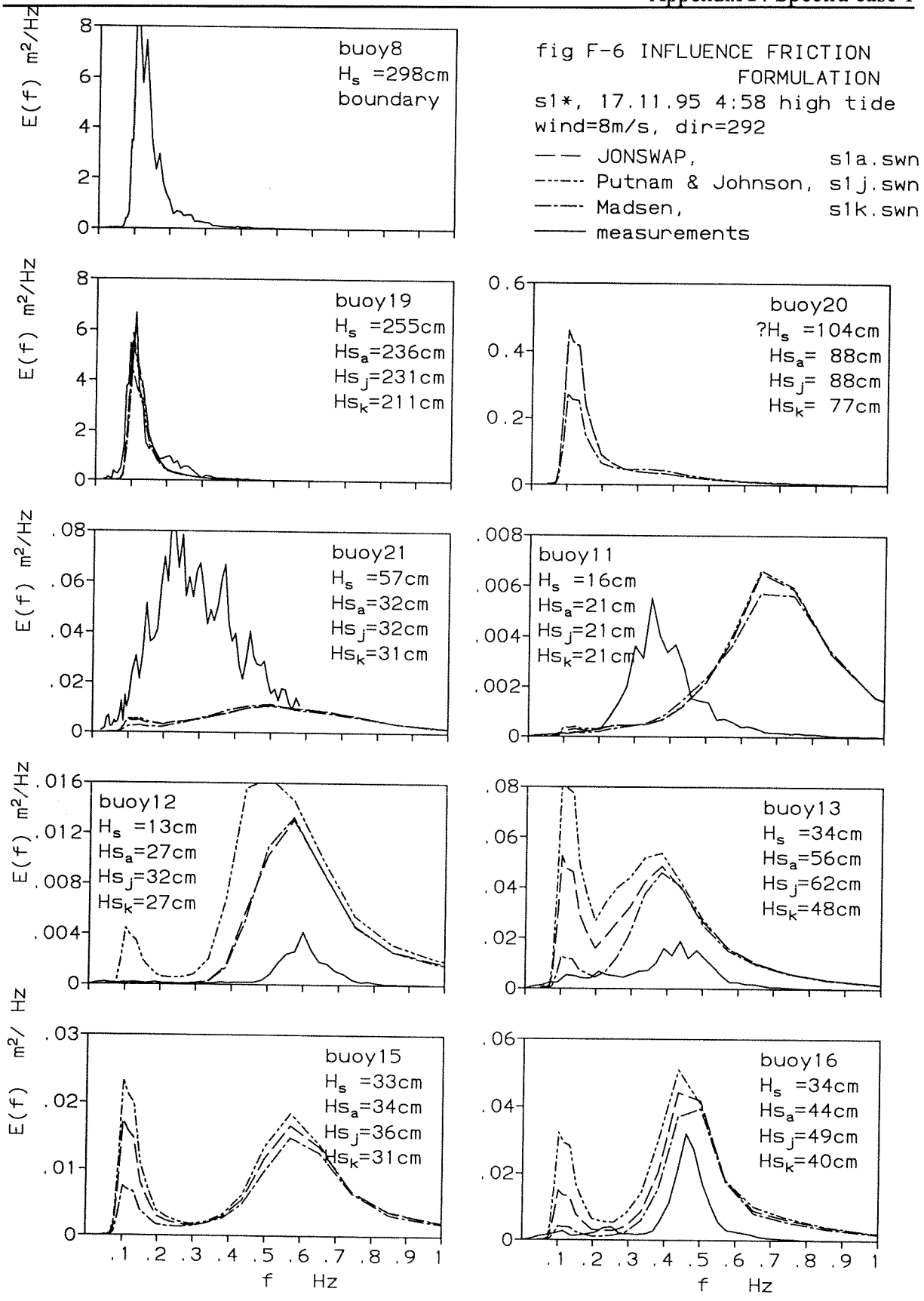
fig F-6 INFLUENCE FRICTION FORMULATION
s1*, 17.11.95 4:58 high tide
wind=8m/s, dir=292
JONSWAP, s1a.swn
Putnam & Johnson, s1j.swn
Madsen, s1k.swn
measurements
buoy8
Hs =298cm
boundary
buoy19
Hs =255cm
Hsa=236cm
Hsj=231cm
Hsk=211cm
buoy20
?Hs =104cm
Hsa= 88cm
Hsj= 88cm
Hsk= 77cm
buoy21
Hs =57cm
Hsa=32cm
Hsj=32cm
Hsk=31cm
buoy11
Hs =16cm
Hsa=21cm
Hsj=21cm
Hsk=21cm
buoy12
Hs =13cm
Hsa=27cm
Hsj=32cm
Hsk=27cm
buoy13
Hs =34cm
Hsa=56cm
Hsj=62cm
Hsk=48cm
buoy15
Hs =33cm
Hsa=34cm
Hsj=36cm
Hsk=31cm
buoy16
Hs =34cm
Hsa=44cm
Hsj=49cm
Hsk=40cm
E(f) m²/Hz
E(f) m²/ Hz
f Hz

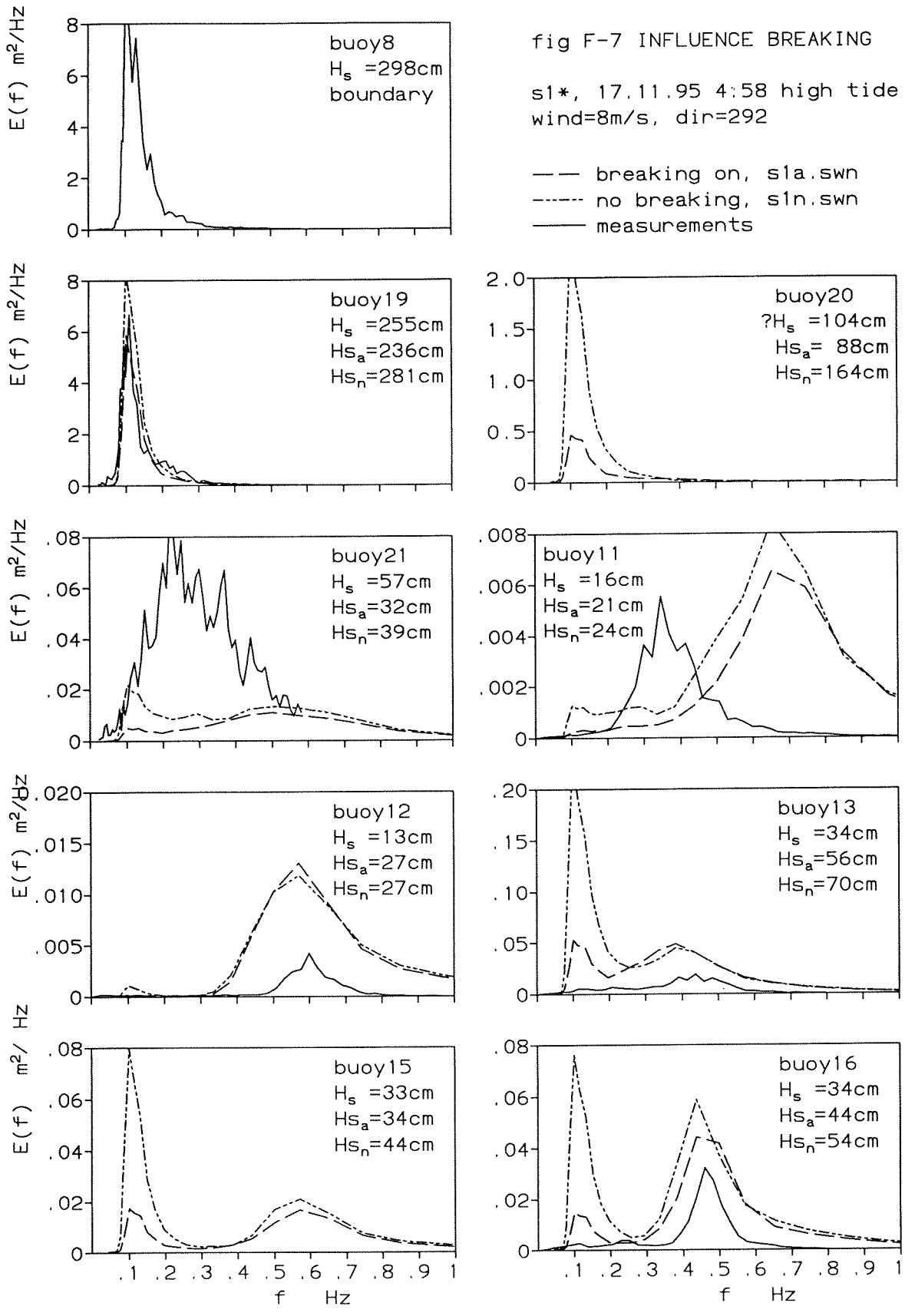
fig F-7 INFLUENCE BREAKING
s1*, 17.11.95 4:58 high tide
wind=8m/s, dir=292
breaking on, s1a.swn
no breaking, s1n.swn
measurements
buoy8
Hs =298cm
boundary
buoy19
Hs =255cm
Hsa=236cm
Hsn=281cm
buoy20
?Hs =104cm
Hsa= 88cm
Hsn=164cm
buoy21
Hs =57cm
Hsa=32cm
Hsn=39cm
buoy11
Hs =16cm
Hsa=21cm
Hsn=24cm
buoy12
Hs =13cm
Hsa=27cm
Hsn=27cm
buoy13
Hs =34cm
Hsa=56cm
Hsn=70cm
buoy15
Hs =33cm
Hsa=34cm
Hsn=44cm
buoy16
Hs =34cm
Hsa=44cm
Hsn=54cm
E(f) m²/Hz
E(f) m²/ Hz
f Hz

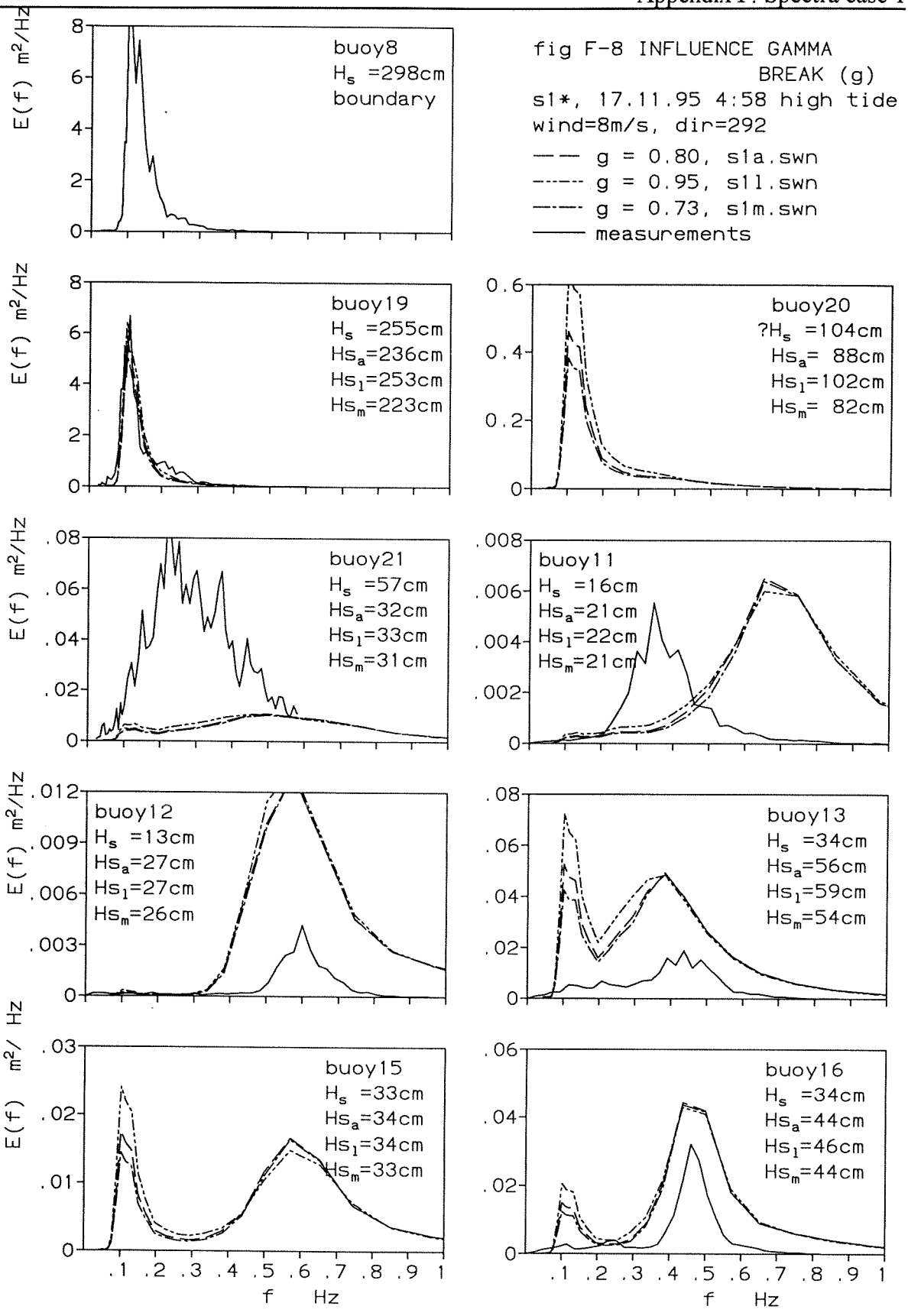
fig F-8 INFLUENCE GAMMA
BREAK (g)
s1*, 17.11.95 4:58 high tide
wind=8m/s, dir=292
g = 0.80, s1a.swn
g = 0.95, s1l.swn
g = 0.73, s1m.swn
measurements
E(f) m²/Hz
buoy8
Hs =298cm
boundary
buoy19
Hs =255cm
Hsa=236cm
Hs1=253cm
Hsm=223cm
buoy20
?Hs =104cm
Hsa= 88cm
Hs1=102cm
Hsm= 82cm
buoy21
Hs =57cm
Hsa=32cm
Hs1=33cm
Hsm=31cm
buoy11
Hs =16cm
Hsa=21cm
Hs1=22cm
Hsm=21cm
buoy12
Hs =13cm
Hsa=27cm
Hs1=27cm
Hsm=26cm
buoy13
Hs =34cm
Hsa=56cm
Hs1=59cm
Hsm=54cm
E(f) m²/ Hz
buoy15
Hs =33cm
Hsa=34cm
Hs1=34cm
Hsm=33cm
buoy16
Hs =34cm
Hsa=44cm
Hs1=46cm
Hsm=44cm
f Hz

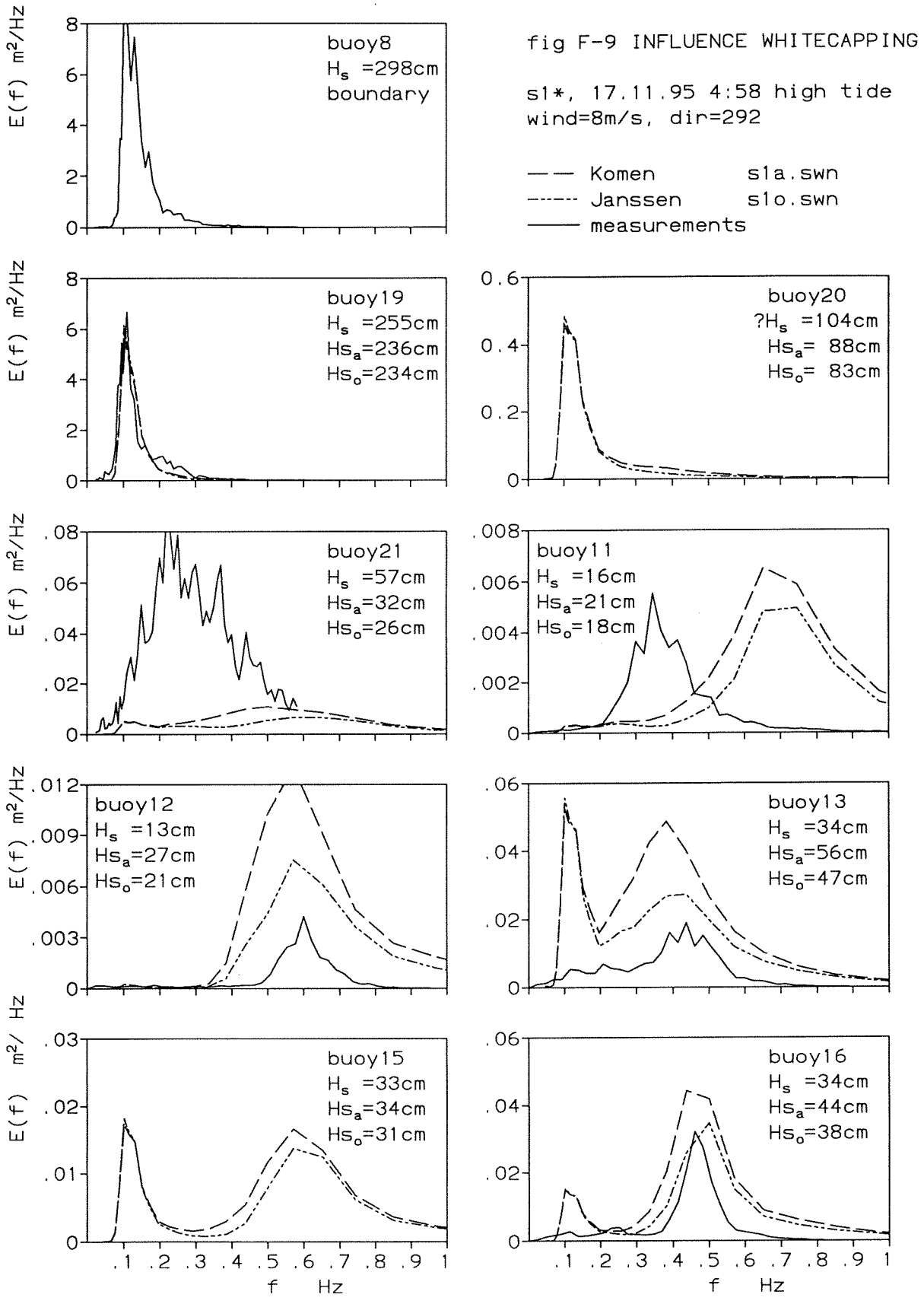
fig F-9 INFLUENCE WHITECAPPING
s1*, 17.11.95 4:58 high tide
wind=8m/s, dir=292
Komen s1a.swn
Janssen s1o.swn
measurements
buoy8
Hs =298cm
boundary
buoy19
Hs =255cm
Hsa=236cm
Hso=234cm
buoy20
?Hs =104cm
Hsa= 88cm
Hso= 83cm
buoy21
Hs =57cm
Hsa=32cm
Hso=26cm
buoy11
Hs =16cm
Hsa=21cm
Hso=18cm
buoy12
Hs =13cm
Hsa=27cm
Hso=21cm
buoy13
Hs =34cm
Hsa=56cm
Hso=47cm
buoy15
Hs =33cm
Hsa=34cm
Hso=31cm
buoy16
Hs =34cm
Hsa=44cm
Hso=38cm
E(f) m²/Hz
f Hz

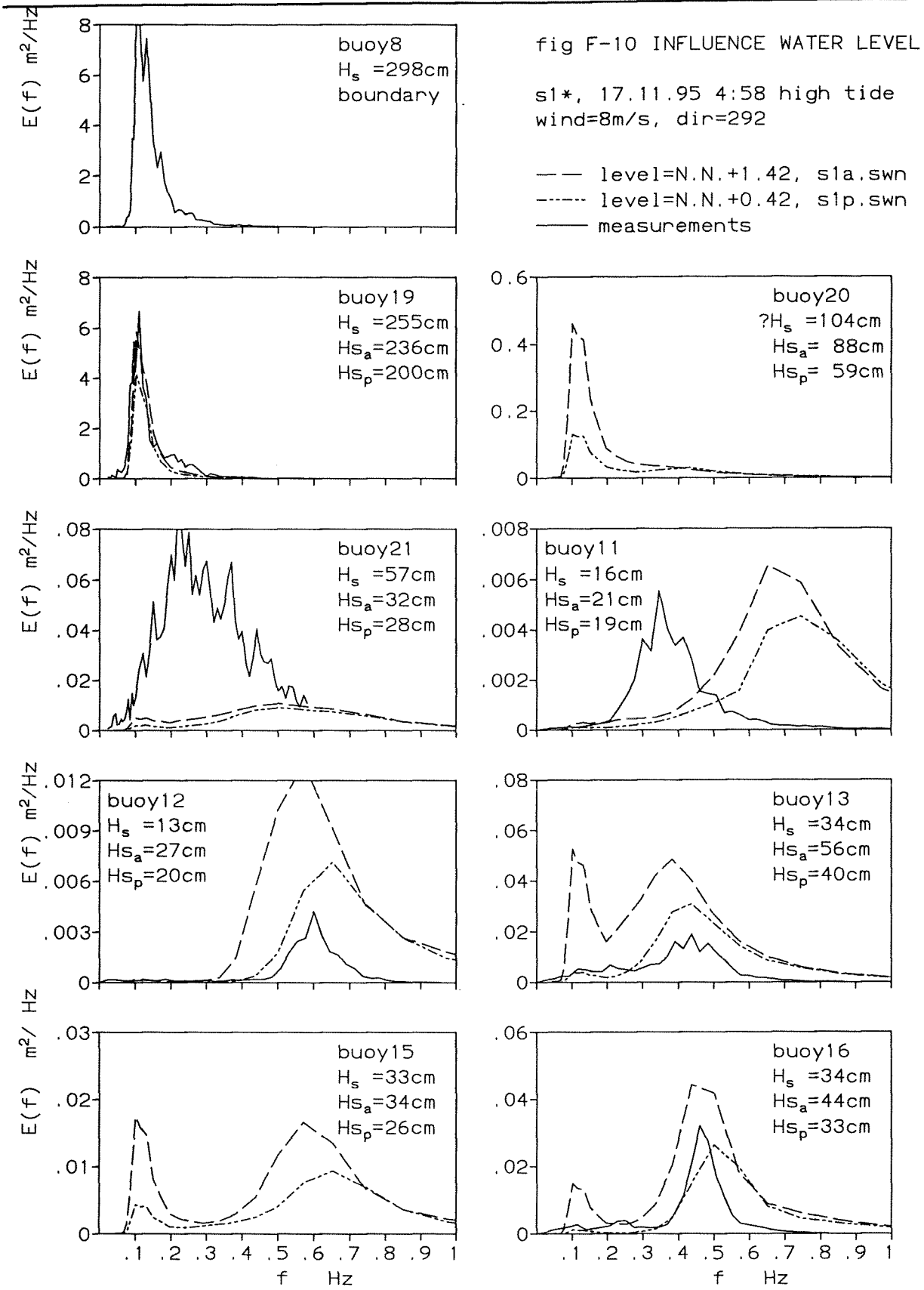
fig F-10 INFLUENCE WATER LEVEL
s1*, 17.11.95 4:58 high tide
wind=8m/s, dir=292
level=N.N.+1.42, s1a.swn
level=N.N.+0.42, s1p.swn
measurements
buoy8
Hs =298cm
boundary
buoy19
Hs =255cm
Hsa=236cm
Hsp=200cm
buoy20
?Hs =104cm
Hsa= 88cm
Hsp= 59cm
buoy21
Hs =57cm
Hsa=32cm
Hsp=28cm
buoy11
Hs =16cm
Hsa=21cm
Hsp=19cm
buoy12
Hs =13cm
Hsa=27cm
Hsp=20cm
buoy13
Hs =34cm
Hsa=56cm
Hsp=40cm
buoy15
Hs =33cm
Hsa=34cm
Hsp=26cm
buoy16
Hs =34cm
Hsa=44cm
Hsp=33cm
E(f) m²/Hz
E(f) m²/ Hz
f Hz

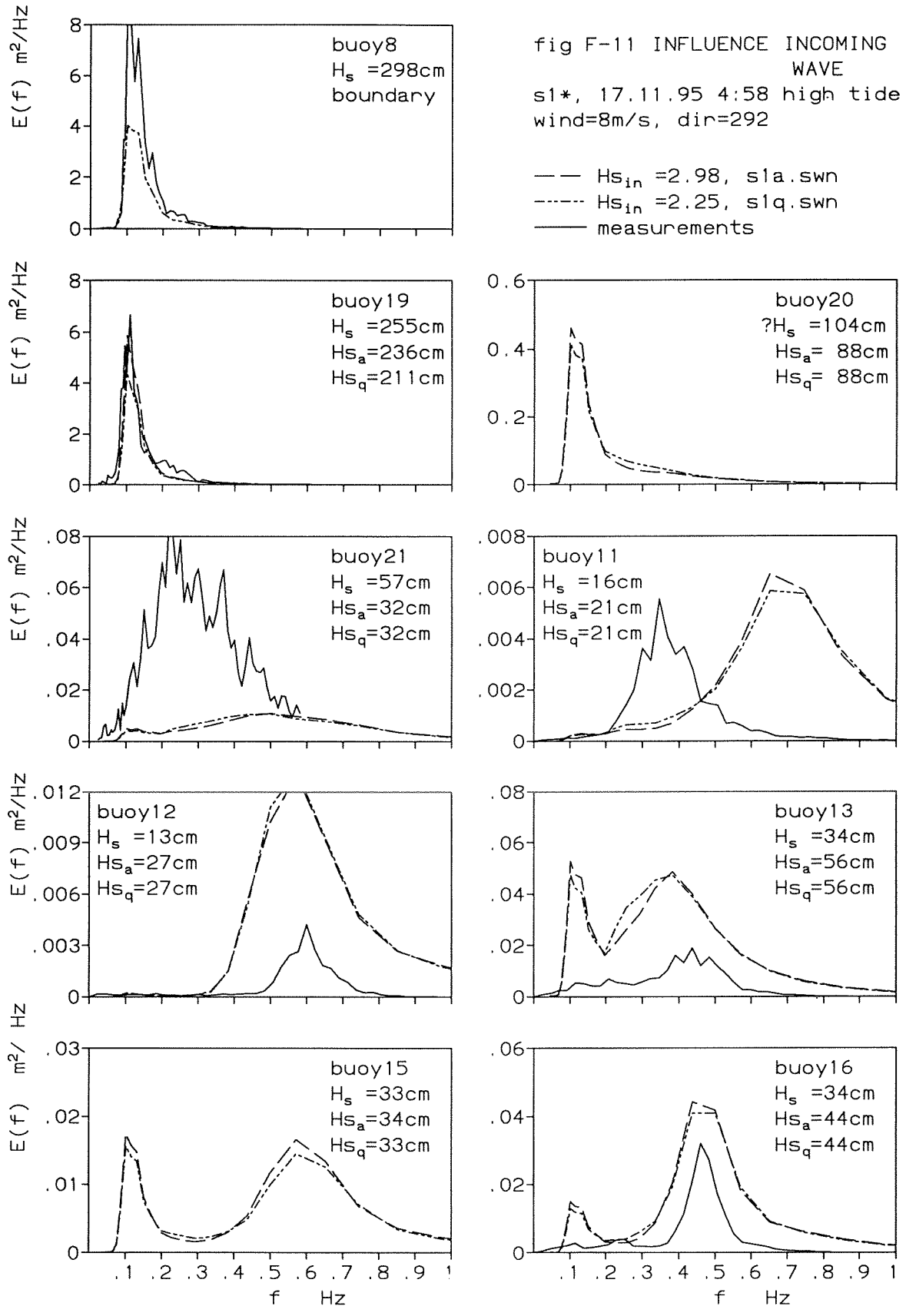
fig F-11 INFLUENCE INCOMING WAVE
s1*, 17.11.95 4:58 high tide
wind=8m/s, dir=292
Hs_in =2.98, s1a.swn
Hs_in =2.25, s1q.swn
measurements
E(f) m²/Hz
buoy8
Hs =298cm
boundary
buoy19
Hs =255cm
Hsa=236cm
Hsq=211cm
buoy20
?Hs =104cm
Hsa= 88cm
Hsq= 88cm
buoy21
Hs =57cm
Hsa=32cm
Hsq=32cm
buoy11
Hs =16cm
Hsa=21cm
Hsq=21cm
buoy12
Hs =13cm
Hsa=27cm
Hsq=27cm
buoy13
Hs =34cm
Hsa=56cm
Hsq=56cm
buoy15
Hs =33cm
Hsa=34cm
Hsq=33cm
buoy16
Hs =34cm
Hsa=44cm
Hsq=44cm
f Hz

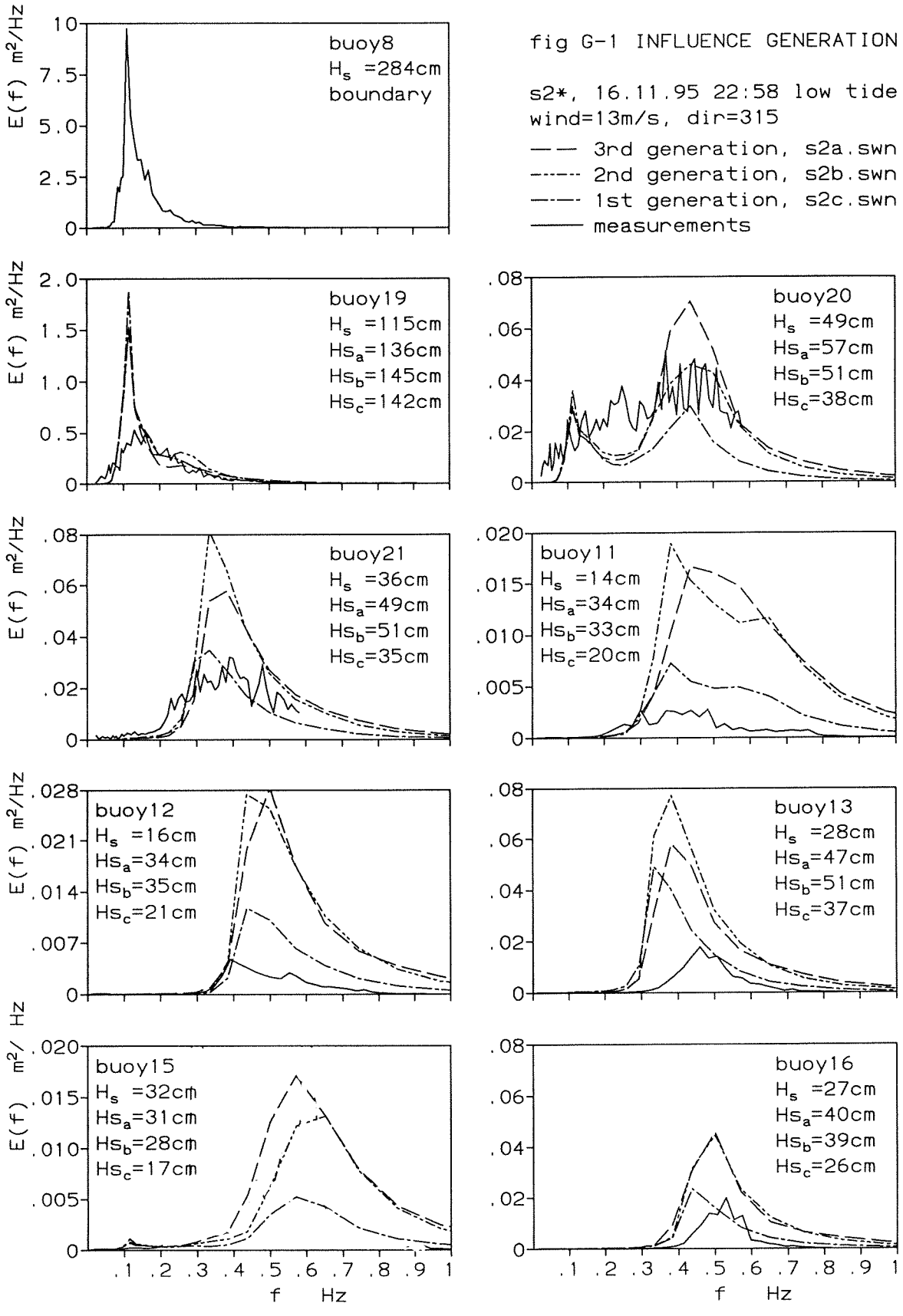
fig G-1 INFLUENCE GENERATION
s2*, 16.11.95 22:58 low tide
wind=13m/s, dir=315
3rd generation, s2a.swn
2nd generation, s2b.swn
1st generation, s2c.swn
measurements
E(f) m²/Hz
buoy8
Hs =284cm
boundary
buoy19
Hs =115cm
Hsa=136cm
Hsb=145cm
Hsc=142cm
buoy20
Hs =49cm
Hsa=57cm
Hsb=51cm
Hsc=38cm
buoy21
Hs =36cm
Hsa=49cm
Hsb=51cm
Hsc=35cm
buoy11
Hs =14cm
Hsa=34cm
Hsb=33cm
Hsc=20cm
buoy12
Hs =16cm
Hsa=34cm
Hsb=35cm
Hsc=21cm
buoy13
Hs =28cm
Hsa=47cm
Hsb=51cm
Hsc=37cm
buoy15
Hs =32cm
Hsa=31cm
Hsb=28cm
Hsc=17cm
buoy16
Hs =27cm
Hsa=40cm
Hsb=39cm
Hsc=26cm
f Hz

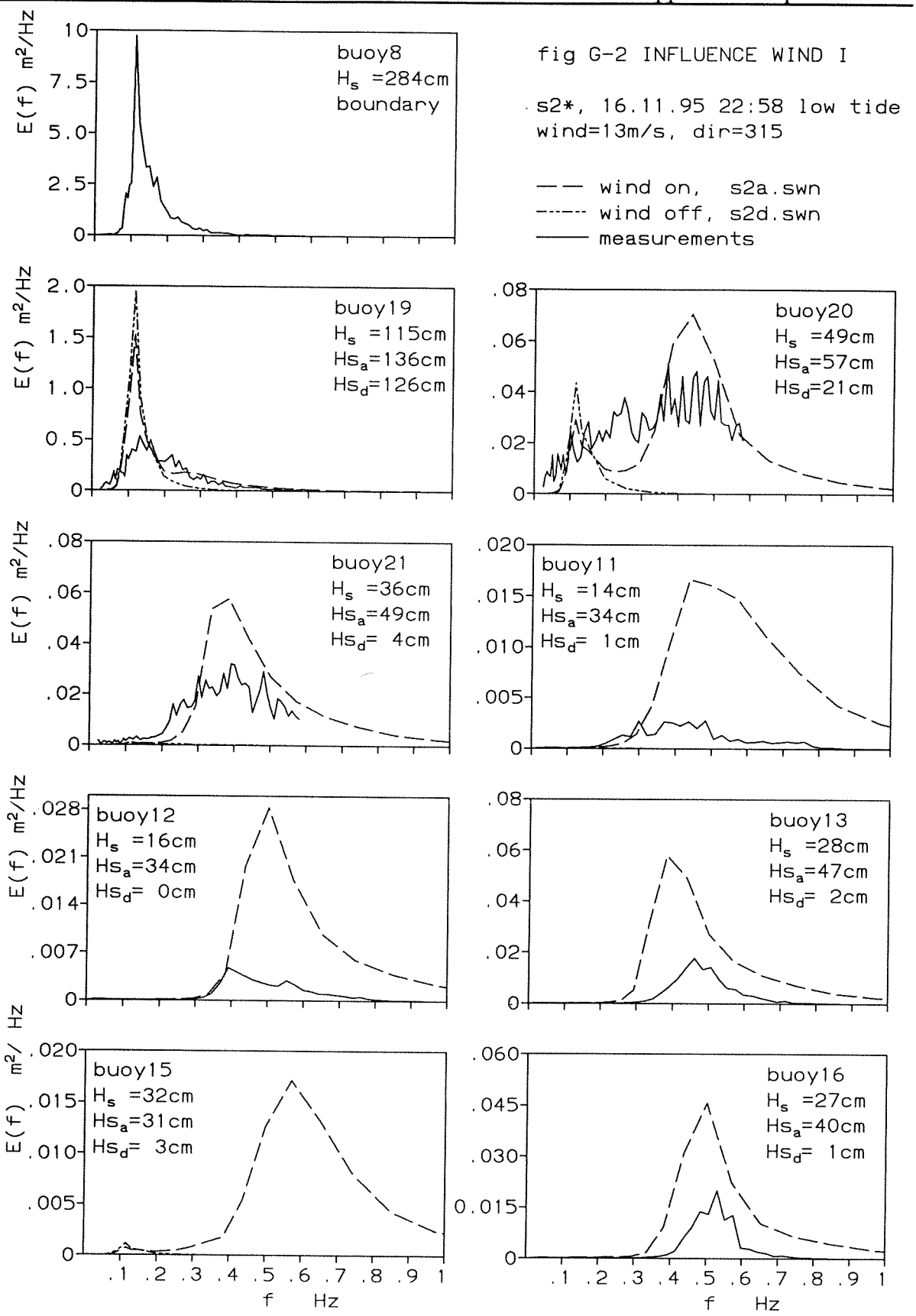
fig G-2 INFLUENCE WIND I
s2*, 16.11.95 22:58 low tide
wind=13m/s, dir=315
wind on, s2a.swn
wind off, s2d.swn
measurements
buoy8
Hs =284cm
boundary
buoy19
Hs =115cm
Hsa=136cm
Hsd=126cm
buoy20
Hs =49cm
Hsa=57cm
Hsd=21cm
buoy21
Hs =36cm
Hsa=49cm
Hsd= 4cm
buoy11
Hs =14cm
Hsa=34cm
Hsd= 1cm
buoy12
Hs =16cm
Hsa=34cm
Hsd= 0cm
buoy13
Hs =28cm
Hsa=47cm
Hsd= 2cm
buoy15
Hs =32cm
Hsa=31cm
Hsd= 3cm
buoy16
Hs =27cm
Hsa=40cm
Hsd= 1cm
E(f) m²/Hz
f Hz

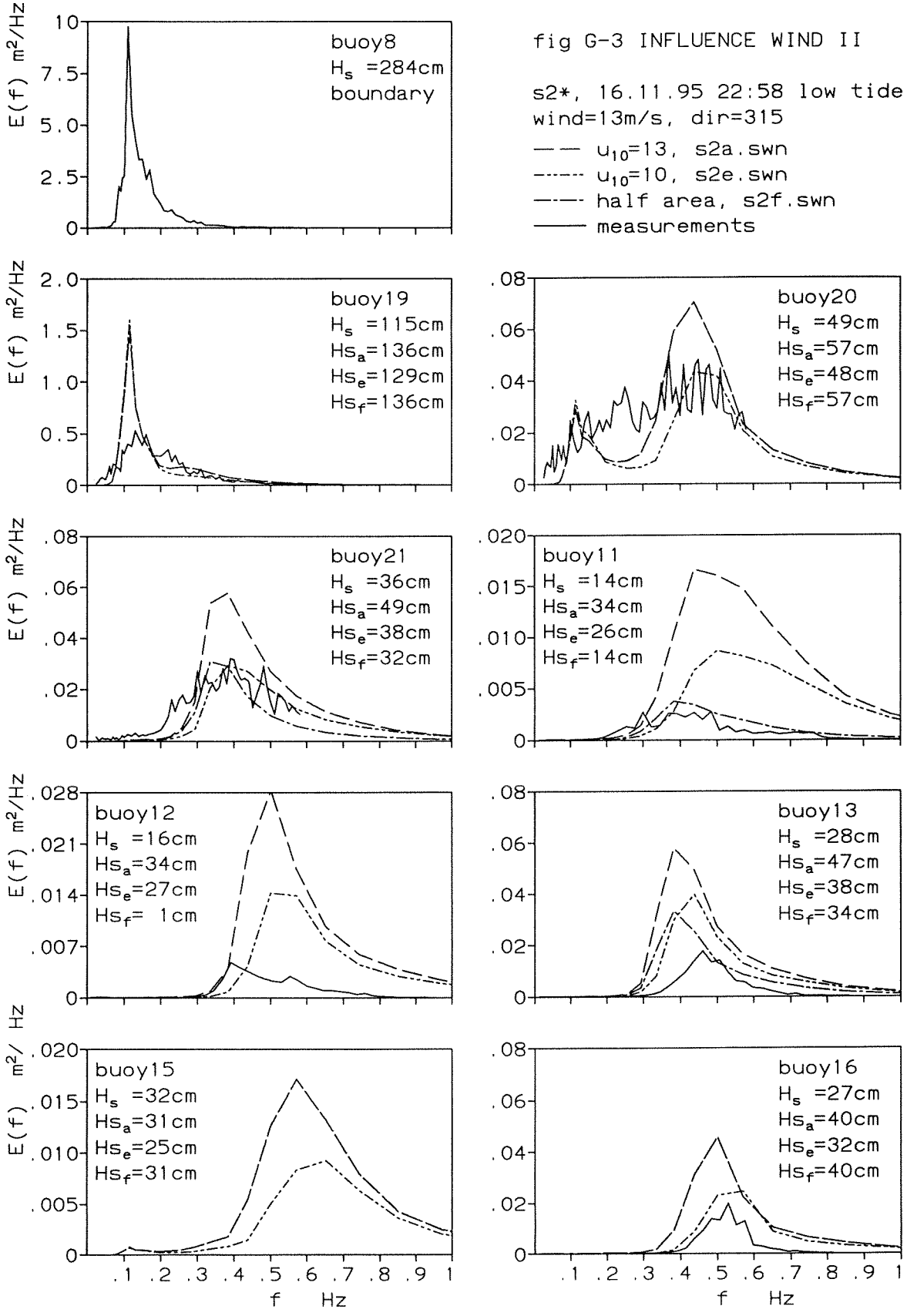
fig G-3 INFLUENCE WIND II
s2*, 16.11.95 22:58 low tide
wind=13m/s, dir=315
u10=13, s2a.swn
u10=10, s2e.swn
half area, s2f.swn
measurements
buoy8
Hs =284cm
boundary
buoy19
Hs =115cm
Hsa=136cm
Hse=129cm
Hsf=136cm
buoy20
Hs =49cm
Hsa=57cm
Hse=48cm
Hsf=57cm
buoy21
Hs =36cm
Hsa=49cm
Hse=38cm
Hsf=32cm
buoy11
Hs =14cm
Hsa=34cm
Hse=26cm
Hsf=14cm
buoy12
Hs =16cm
Hsa=34cm
Hse=27cm
Hsf= 1cm
buoy13
Hs =28cm
Hsa=47cm
Hse=38cm
Hsf=34cm
buoy15
Hs =32cm
Hsa=31cm
Hse=25cm
Hsf=31cm
buoy16
Hs =27cm
Hsa=40cm
Hse=32cm
Hsf=40cm
E(f) m²/Hz
f Hz

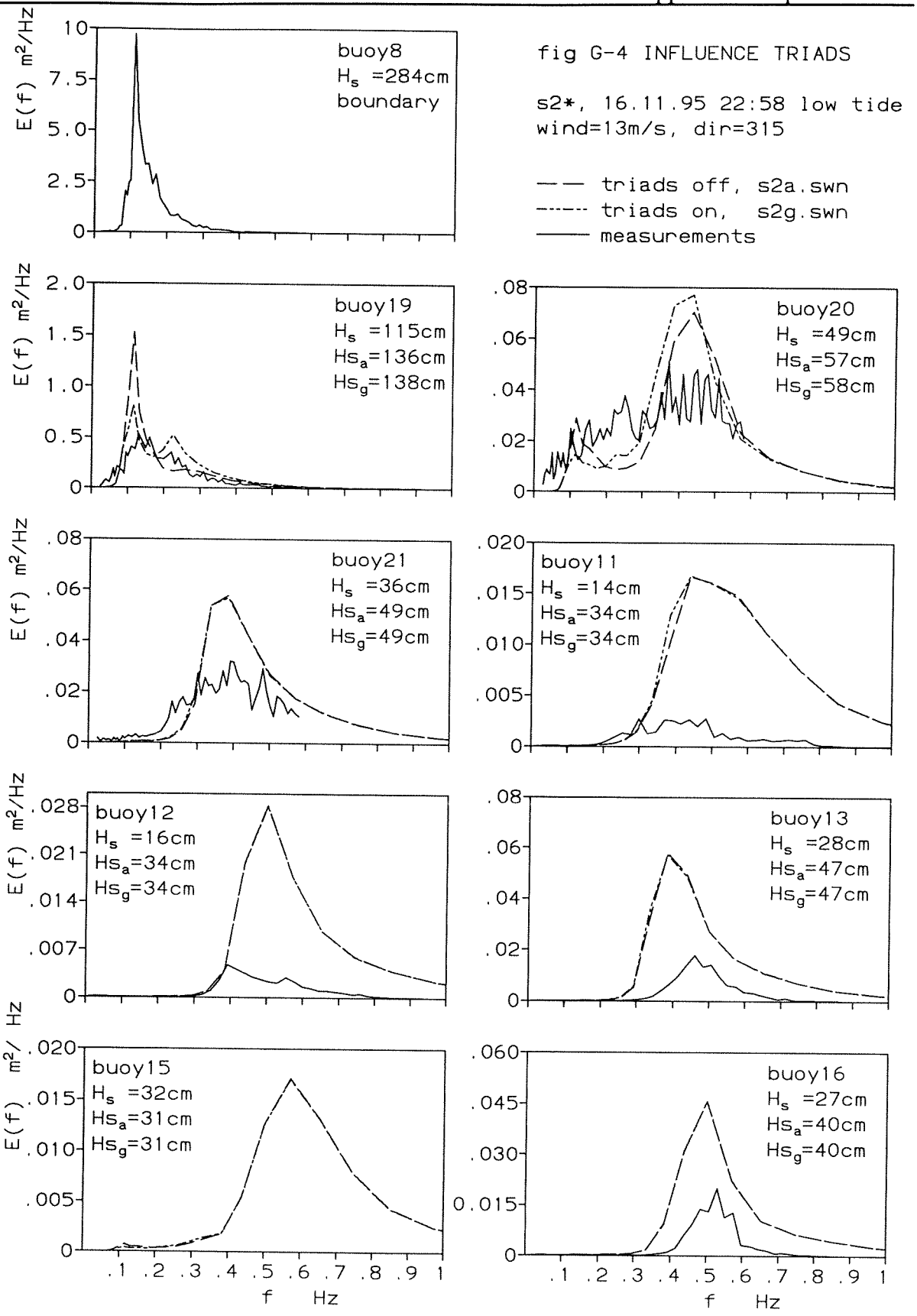
fig G-4 INFLUENCE TRIADS
s2*, 16.11.95 22:58 low tide
wind=13m/s, dir=315
triads off, s2a.swn
triads on, s2g.swn
measurements
buoy8
Hs =284cm
boundary
buoy19
Hs =115cm
Hsa=136cm
Hsg=138cm
buoy20
Hs =49cm
Hsa=57cm
Hsg=58cm
buoy21
Hs =36cm
Hsa=49cm
Hsg=49cm
buoy11
Hs =14cm
Hsa=34cm
Hsg=34cm
buoy12
Hs =16cm
Hsa=34cm
Hsg=34cm
buoy13
Hs =28cm
Hsa=47cm
Hsg=47cm
buoy15
Hs =32cm
Hsa=31cm
Hsg=31cm
buoy16
Hs =27cm
Hsa=40cm
Hsg=40cm
E(f) m²/Hz
E(f) m²/ Hz
f Hz

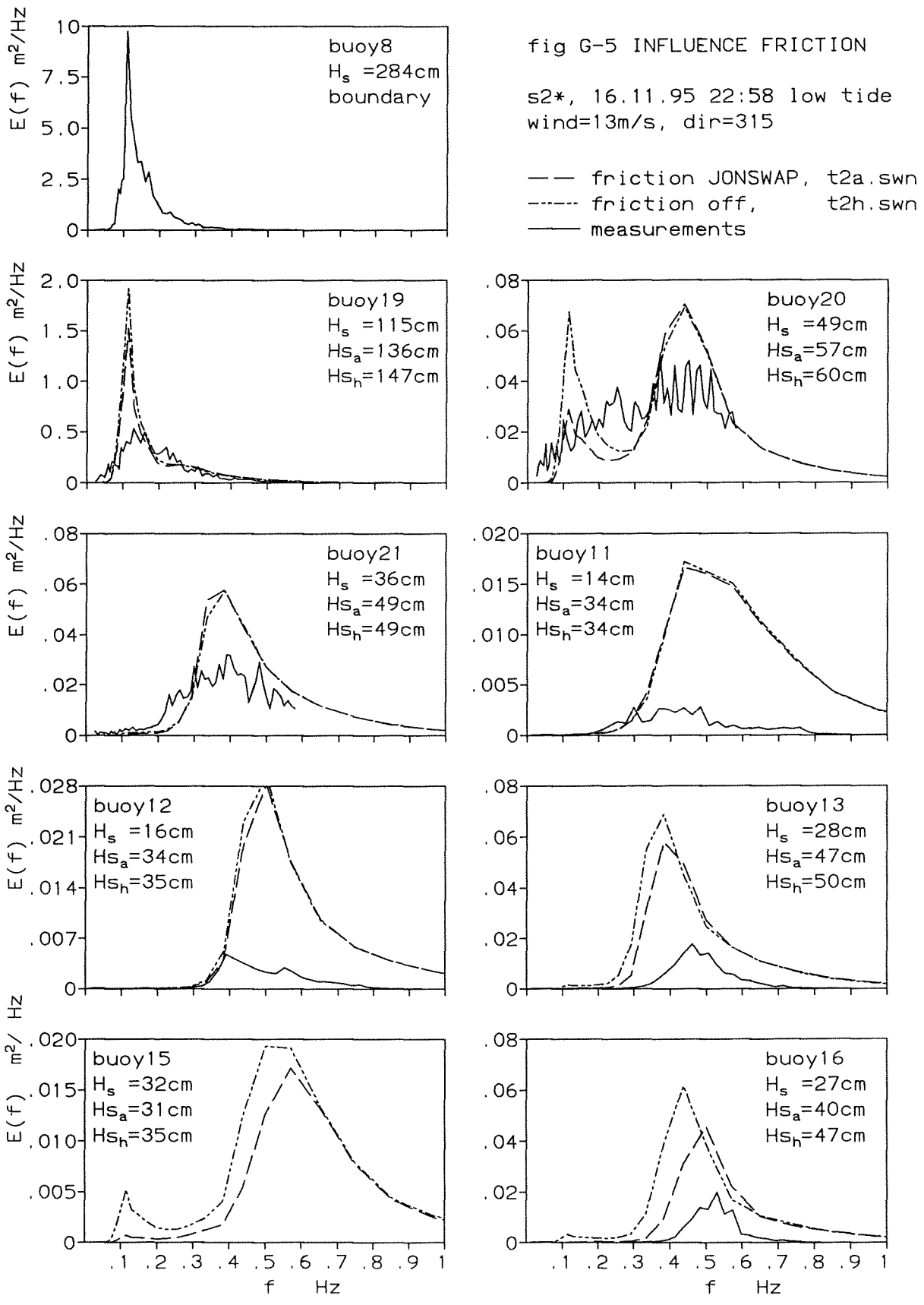
fig G-5 INFLUENCE FRICTION
s2*, 16.11.95 22:58 low tide
wind=13m/s, dir=315
friction JONSWAP, t2a.swn
friction off, t2h.swn
measurements
buoy8
Hs =284cm
boundary
buoy19
Hs =115cm
Hsa=136cm
Hsh=147cm
buoy20
Hs =49cm
Hsa=57cm
Hsh=60cm
buoy21
Hs =36cm
Hsa=49cm
Hsh=49cm
buoy11
Hs =14cm
Hsa=34cm
Hsh=34cm
buoy12
Hs =16cm
Hsa=34cm
Hsh=35cm
buoy13
Hs =28cm
Hsa=47cm
Hsh=50cm
buoy15
Hs =32cm
Hsa=31cm
Hsh=35cm
buoy16
Hs =27cm
Hsa=40cm
Hsh=47cm
E(f) m²/Hz
E(f) m²/ Hz
f Hz

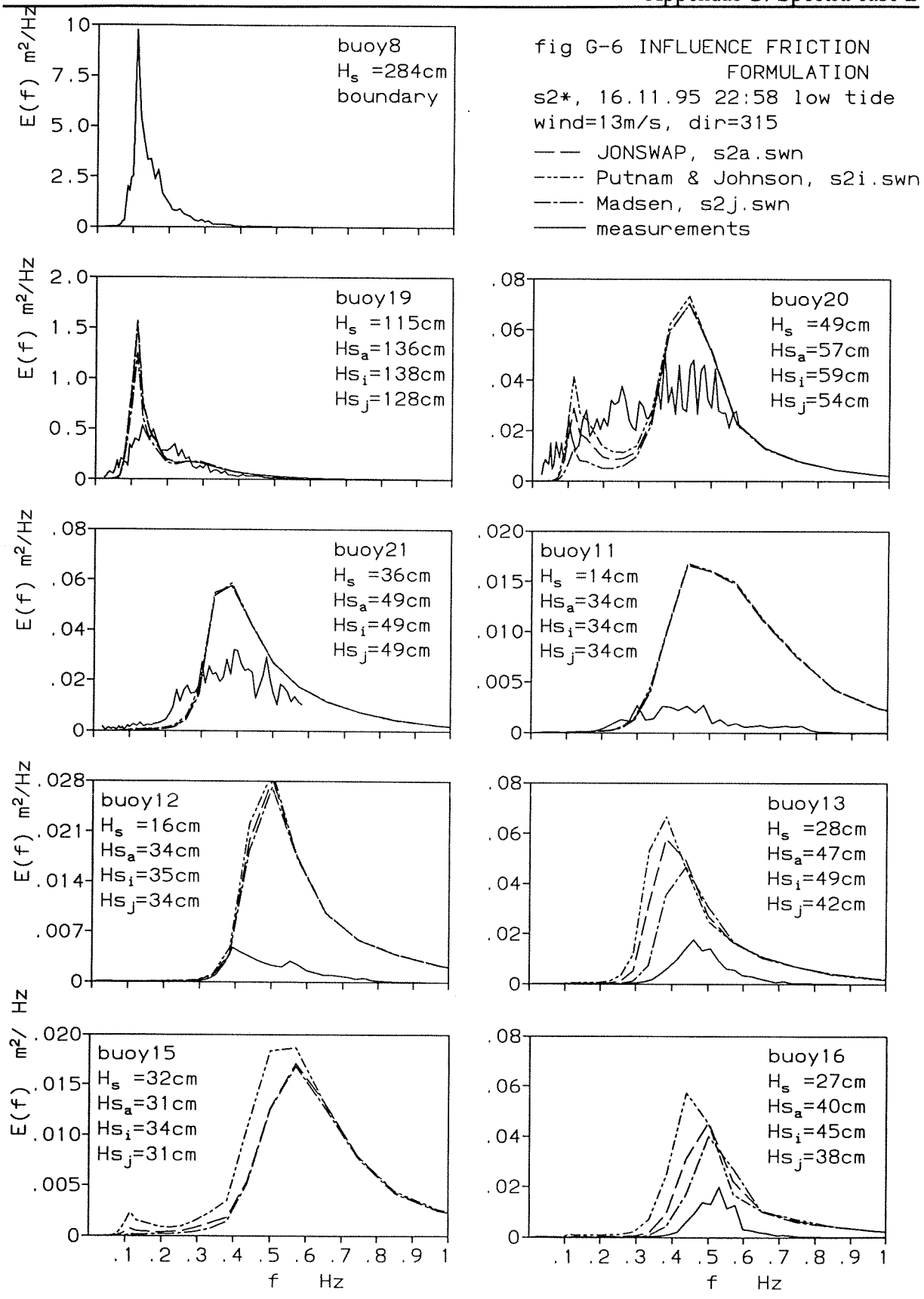
E(f) m²/Hz
buoy8
Hs =284cm
boundary
fig G-6 INFLUENCE FRICTION FORMULATION
s2*, 16.11.95 22:58 low tide
wind=13m/s, dir=315
JONSWAP, s2a.swn
Putnam & Johnson, s2i.swn
Madsen, s2j.swn
measurements
buoy19
Hs =115cm
Hsa=136cm
Hsi=138cm
Hsj=128cm
buoy20
Hs =49cm
Hsa=57cm
Hsi=59cm
Hsj=54cm
buoy21
Hs =36cm
Hsa=49cm
Hsi=49cm
Hsj=49cm
buoy11
Hs =14cm
Hsa=34cm
Hsi=34cm
Hsj=34cm
buoy12
Hs =16cm
Hsa=34cm
Hsi=35cm
Hsj=34cm
buoy13
Hs =28cm
Hsa=47cm
Hsi=49cm
Hsj=42cm
E(f) m²/ Hz
buoy15
Hs =32cm
Hsa=31cm
Hsi=34cm
Hsj=31cm
buoy16
Hs =27cm
Hsa=40cm
Hsi=45cm
Hsj=38cm
f Hz

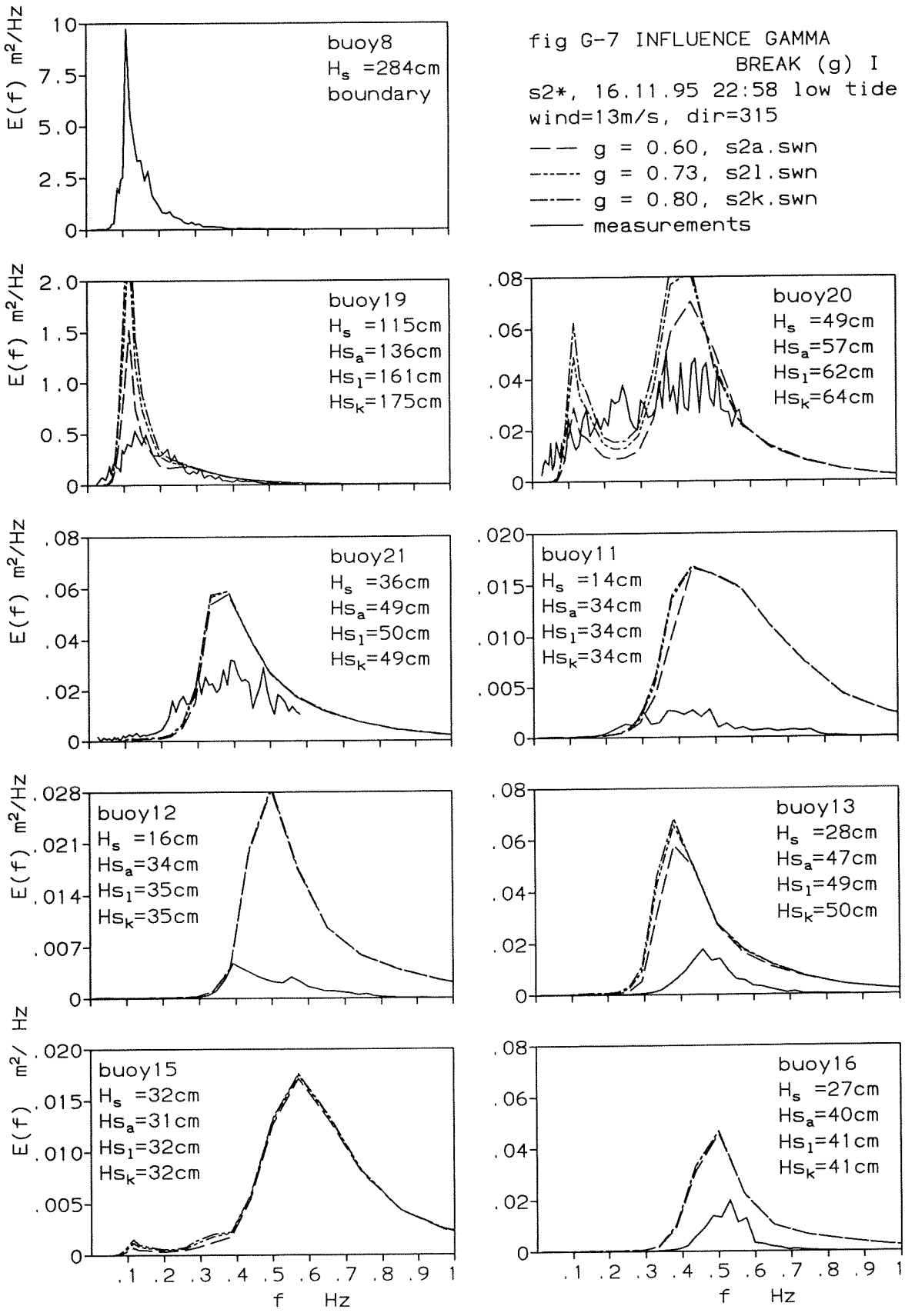
fig G-7 INFLUENCE GAMMA
BREAK (g) I
s2*, 16.11.95 22:58 low tide
wind=13m/s, dir=315
g = 0.60, s2a.swn
g = 0.73, s21.swn
g = 0.80, s2k.swn
measurements
buoy8
Hs =284cm
boundary
buoy19
Hs =115cm
Hsa=136cm
Hs1=161cm
Hsk=175cm
buoy20
Hs =49cm
Hsa=57cm
Hs1=62cm
Hsk=64cm
buoy21
Hs =36cm
Hsa=49cm
Hs1=50cm
Hsk=49cm
buoy11
Hs =14cm
Hsa=34cm
Hs1=34cm
Hsk=34cm
buoy12
Hs =16cm
Hsa=34cm
Hs1=35cm
Hsk=35cm
buoy13
Hs =28cm
Hsa=47cm
Hs1=49cm
Hsk=50cm
buoy15
Hs =32cm
Hsa=31cm
Hs1=32cm
Hsk=32cm
buoy16
Hs =27cm
Hsa=40cm
Hs1=41cm
Hsk=41cm
E(f) m²/Hz
f Hz

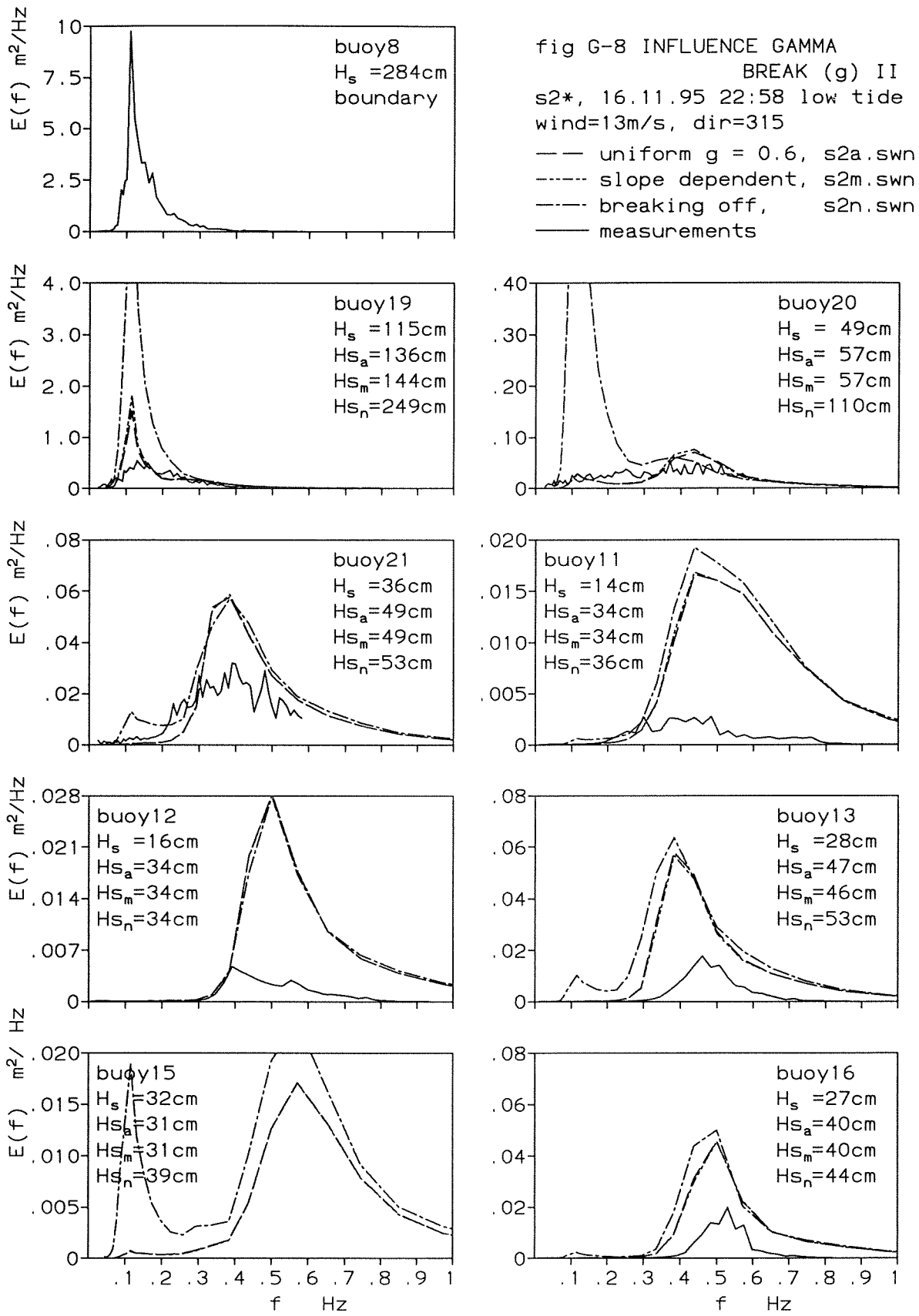
fig G-8 INFLUENCE GAMMA
BREAK (g) II
s2*, 16.11.95 22:58 low tide
wind=13m/s, dir=315
—— uniform g = 0.6, s2a.swn
------ slope dependent, s2m.swn
-·-·- breaking off, s2n.swn
—— measurements
E(f) m²/Hz
buoy8
Hs =284cm
boundary
buoy19
Hs =115cm
Hsa=136cm
Hsm=144cm
Hsn=249cm
buoy20
Hs = 49cm
Hsa= 57cm
Hsm= 57cm
Hsn=110cm
buoy21
Hs =36cm
Hsa=49cm
Hsm=49cm
Hsn=53cm
buoy11
Hs =14cm
Hsa=34cm
Hsm=34cm
Hsn=36cm
buoy12
Hs =16cm
Hsa=34cm
Hsm=34cm
Hsn=34cm
buoy13
Hs =28cm
Hsa=47cm
Hsm=46cm
Hsn=53cm
buoy15
Hs =32cm
Hsa=31cm
Hsm=31cm
Hsn=39cm
buoy16
Hs =27cm
Hsa=40cm
Hsm=40cm
Hsn=44cm
f Hz

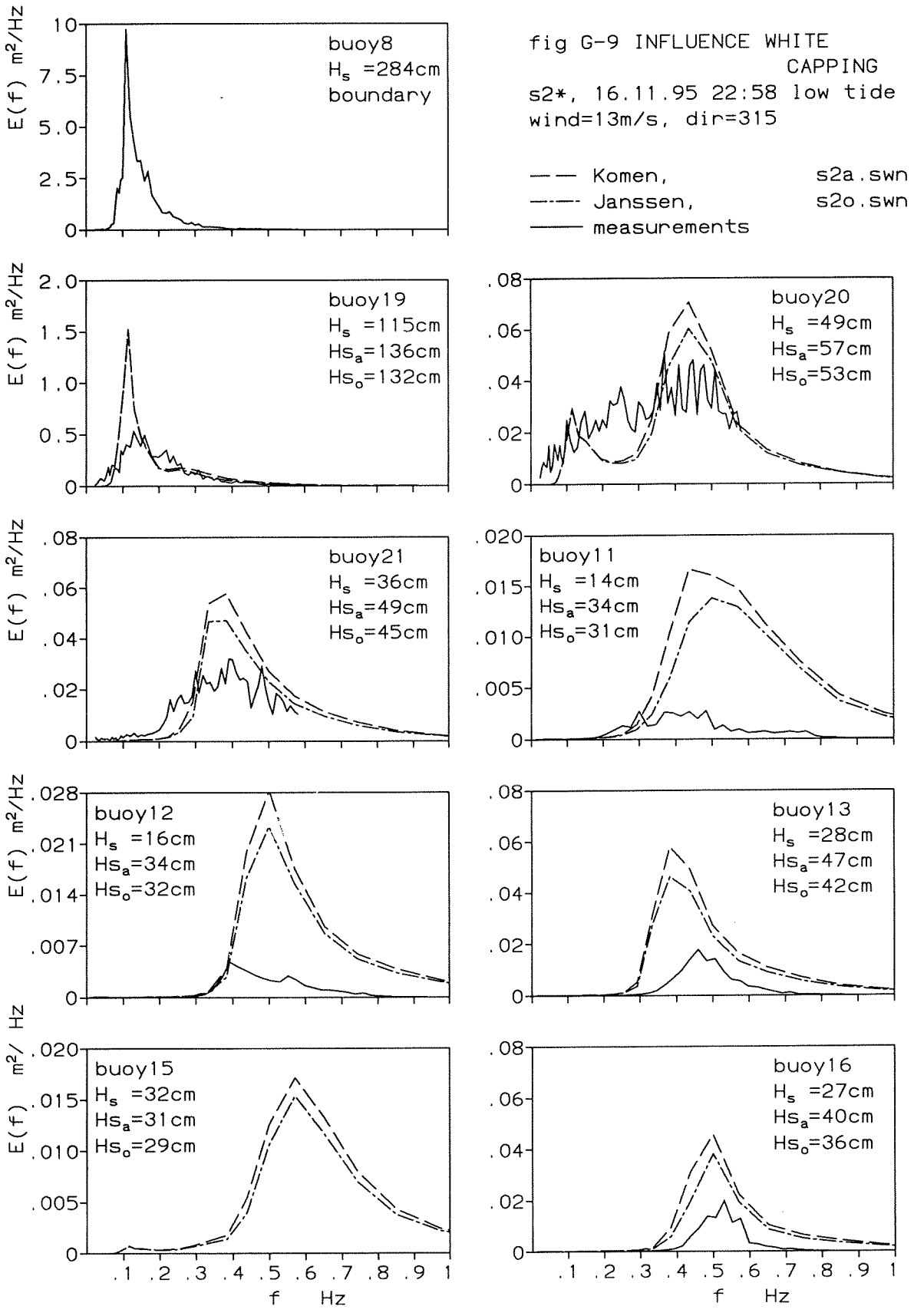
fig G-9 INFLUENCE WHITE CAPPING
s2*, 16.11.95 22:58 low tide
wind=13m/s, dir=315
Komen, s2a.swn
Janssen, s2o.swn
measurements
buoy8
Hs =284cm
boundary
buoy19
Hs =115cm
Hsa=136cm
Hso=132cm
buoy20
Hs =49cm
Hsa=57cm
Hso=53cm
buoy21
Hs =36cm
Hsa=49cm
Hso=45cm
buoy11
Hs =14cm
Hsa=34cm
Hso=31cm
buoy12
Hs =16cm
Hsa=34cm
Hso=32cm
buoy13
Hs =28cm
Hsa=47cm
Hso=42cm
buoy15
Hs =32cm
Hsa=31cm
Hso=29cm
buoy16
Hs =27cm
Hsa=40cm
Hso=36cm
E(f) m2/Hz
E(f) m2/ Hz
f Hz

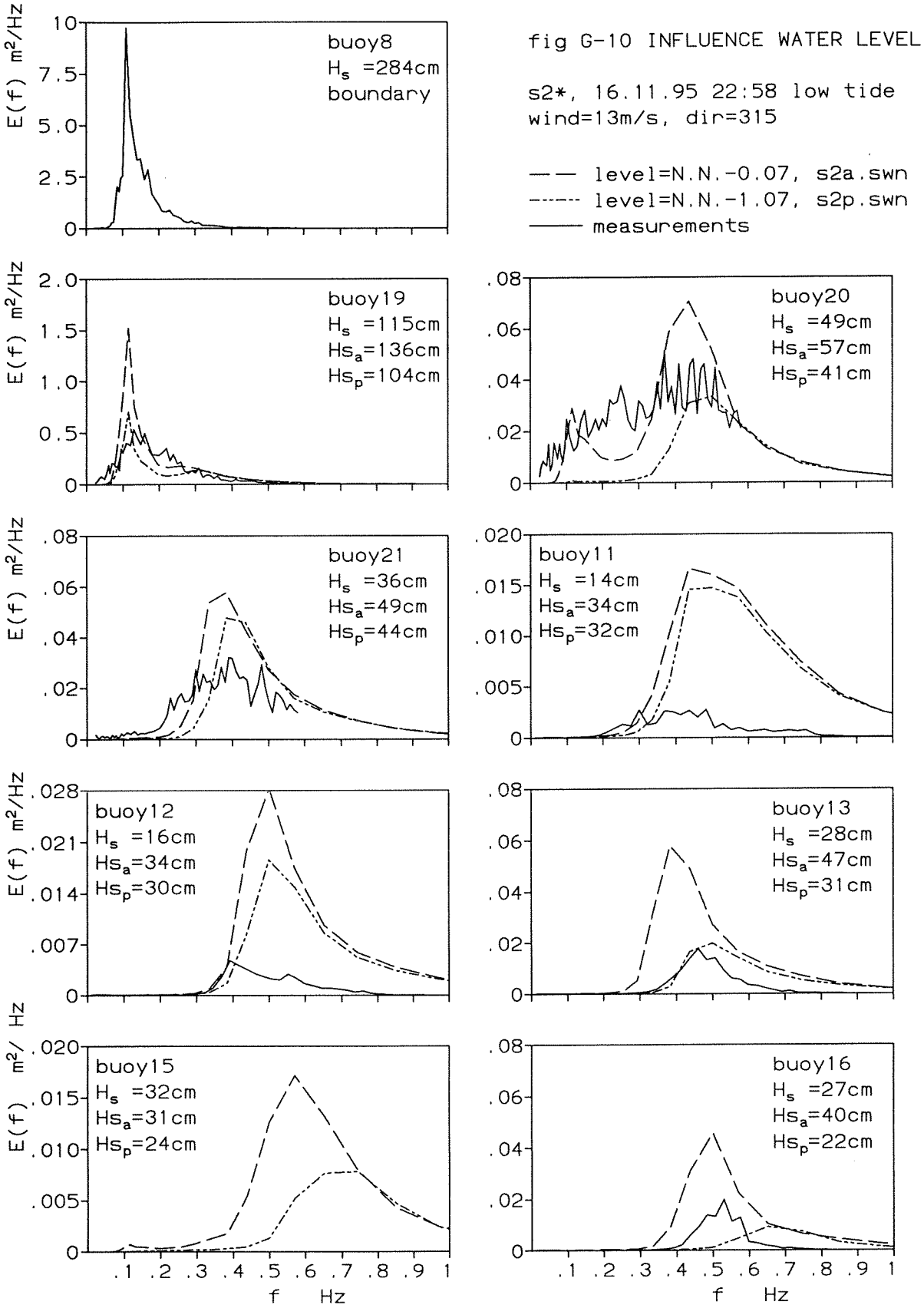
fig G-10 INFLUENCE WATER LEVEL
s2*, 16.11.95 22:58 low tide
wind=13m/s, dir=315
level=N.N.-0.07, s2a.swn
level=N.N.-1.07, s2p.swn
measurements
E(f) m²/Hz
buoy8
Hs =284cm
boundary
buoy19
Hs =115cm
Hsa=136cm
Hsp=104cm
buoy20
Hs =49cm
Hsa=57cm
Hsp=41cm
buoy21
Hs =36cm
Hsa=49cm
Hsp=44cm
buoy11
Hs =14cm
Hsa=34cm
Hsp=32cm
buoy12
Hs =16cm
Hsa=34cm
Hsp=30cm
buoy13
Hs =28cm
Hsa=47cm
Hsp=31cm
buoy15
Hs =32cm
Hsa=31cm
Hsp=24cm
buoy16
Hs =27cm
Hsa=40cm
Hsp=22cm
f Hz

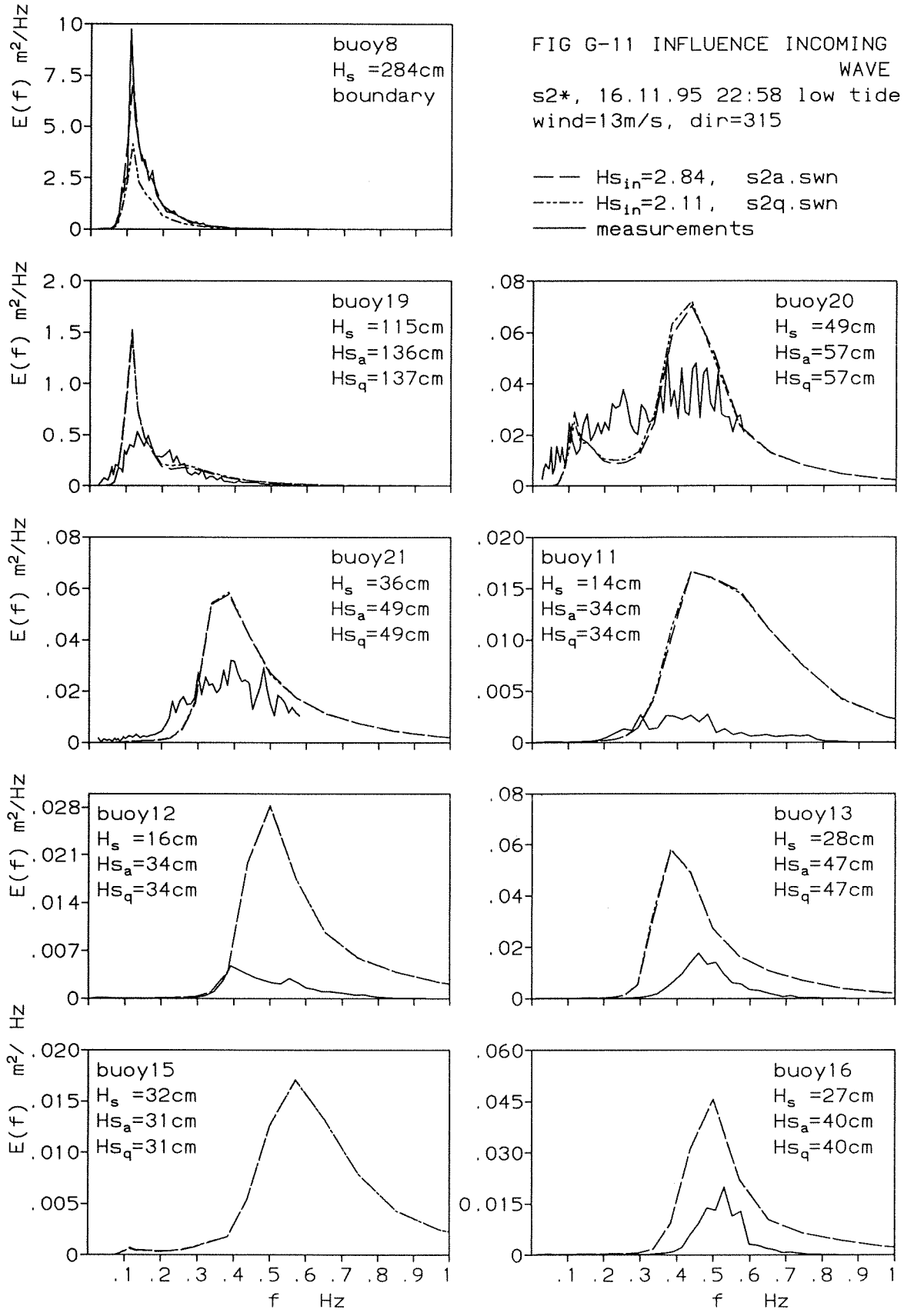
FIG G-11 INFLUENCE INCOMING WAVE
s2*, 16.11.95 22:58 low tide
wind=13m/s, dir=315
Hs_in=2.84, s2a.swn
Hs_in=2.11, s2q.swn
measurements
buoy8
Hs =284cm
boundary
buoy19
Hs =115cm
Hsa=136cm
Hsq=137cm
buoy20
Hs =49cm
Hsa=57cm
Hsq=57cm
buoy21
Hs =36cm
Hsa=49cm
Hsq=49cm
buoy11
Hs =14cm
Hsa=34cm
Hsq=34cm
buoy12
Hs =16cm
Hsa=34cm
Hsq=34cm
buoy13
Hs =28cm
Hsa=47cm
Hsq=47cm
buoy15
Hs =32cm
Hsa=31cm
Hsq=31cm
buoy16
Hs =27cm
Hsa=40cm
Hsq=40cm
E(f) m2/Hz
f Hz